

Synthesis of modular folate derivatives for tumor targeting

Dissertation

a thesis submitted for the degree of Doctor rer. nat.

Natalija Peric

Department of Chemistry, Institute of Pharmacy

Pharmaceutical and Medicinal Chemistry

University of Hamburg

Hamburg

2019

The practical part of this thesis is done between 2015 and 2019 at the Institute of Pharmacy and Medicinal Chemistry, University of Hamburg under the supervision of Prof. Dr. Wolfgang Maison.

The disputation (oral defense) of this thesis took place at 05.04.2019 in Hamburg.

1. Academic supervisor: Prof. Dr. Wolfgang Maison
2. Academic supervisor: Prof. Dr. Chris Meier

Focus creates reality

Acknowledgements

First of all, I would like to immensely thank to my supervisor Prof. Dr. Wolfgang Maison for giving me the chance to do my PhD here in Germany. I am beyond grateful for your guidance, for all the knowledge and experience that I gained through this journey in your working group. Thank you for trusting in me and giving me such a challenging task to fulfill, and for always being there when I needed help.

Prof. Dr. Chris Meier, thank you for kindly accepting to be a second supervisor of this thesis. I would also like to thank to all the technical services, especially NMR, MS and IT service who helped throughout my whole PhD. Thank you Kathleene, Anette and Rainer for always helping us with all the technical necessities and for all your kind help!

A special thank you to all of my students who were part of my PhD journey, helping me to achieve this goal together. Thank you Patrick, David, Eili, Ann-Kathrin, Oumeyma, Lara and Berk. You all contributed so much to this thesis. And a very very special thank you is for my former master student and now my dear colleague Sarah. Without your great help I wouldn't have dared to figure out Buchwald-Hartwig chemistry and expand my topic. Thank you for your time, for always being kind and for all the fun hours out of lab.

A massive thank you goes to Malte. From the very beginning you were there to teach me the basics of chemistry and MS, and how to have fun in lab with loud hip hop music. Thank you for your immense effort and help on my topic, for all the coupled substances and countless days on figuring out how to evaluate them. And lastly, thank you for proof reading this thesis and helping me to make best out of it.

Silke, Serge, Tom, Moritz, Eric, Tim, Flo, Jasper, Steffen, Pia, Ella, Franzl, Marci, Fabi, Claudia thank you for such an amazing time, for all the help, coffee breaks, fun evenings and conversations. It was the biggest pleasure working with you guys. Also I want to thank AK Lemcke, AK Wicha and AK Schützenmeister for great atmosphere at our Institute!

Serge, thank you so much for being a great office mate in the writing stage of our thesis, for always being there for my boring questions and still having patience. Thank you for your kindness and all the help with writing.

Also to all of my dear friends from Serbia thank you for still being by my side, for encouraging me and sharing our dreams together. Even though we are physical apart it never felt like that!

I want to thank from all of my heart to my family. Thank you for your unconditional love and support, for always believing me and helping me to make my dreams come true. Without you my journey would never be so happy and blessed. Thank you for helping me to spread my wings.

And the final and biggest thank you is for Mathias. Thank you for being the best partner in life. For your unconditional help, guidance and support. I have learned so much from you and I know that finishing my thesis wouldn't be possible without you. Thank you for being with me on this journey, and making me happy every single day. I am beyond grateful to have you in my life.

Content

1	Introduction	1
1.1.	Folic acid	1
1.1.1.	Folate receptors	3
1.1.2.	Antifolates	4
1.2.	PSMA	5
1.2.1	PMSA ligands.....	8
1.3	Folate based imaging agents.....	14
1.3.1	Folates for PSMA targeting.....	19
2	Aims and Objectives	21
3	Results and Discussion.....	23
3.1.	Docking studies	23
3.2.	Folate-GPI hybrid with different heteroaromatic groups	25
3.2.1.	Synthesis of secondary amines	26
3.2.2.	Synthesis of tertiary benzylamines	27
3.2.3.	Synthesis of GPI.....	41
3.2.4.	Coupling of the tertiary amine with GPI	42
3.2.5.	Coupling with DOTA	45
3.3.	Simplified folate-GPI conjugates with modified aryl linker	46
3.3.1.	Docking studies of the simplified folate-GPI conjugates with modified aryl linker	48
3.3.2.	Synthesis plan.....	53
3.3.3.	Synthesis of the secondary amines	54
3.3.4.	Coupling with GPI.....	55
3.3.5.	Coupling of simplified folate-GPI conjugates with DOTA.....	56
3.4.	TRIS-GPI derivatives	57
3.4.1.	Synthesis of TRIS-GPI derivatives with different linker groups.....	61
3.4.2.	Coupling of TRIS-GPI derivatives with DOTA.....	63
3.5.	Biological evaluation.....	64
5	Conclusion.....	66
6	Experimental part	69
6.1.	General conditions.....	69
6.2.	Chromatography.....	69
6.2.1.	TLC	69
6.2.2.	Flash chromatography	69
6.3.	Analytics.....	69
6.3.1.	Melting points.....	69

6.3.2. NMR Spectroscopy	69
6.3.3. Infrared spectroscopy	70
6.3.4. Mass spectroscopy.....	70
8 Appendix	112
NMR.....	112
9 Literature	162
10 Hazard materials.....	169

List of abbreviations

ACAIR	aminoimidazole carboxamide ribonucleotide
aq.	aqueous
BINAP	2,2'-bis(diphenylphosphino)-1,1'-binaphthyl
Boc	<i>tert</i> -butyloxycarbonyl
BSA	bis(trimethylsilyl)acetamide
Cbz	benzyloxycarbonyl
CNS	central nervous system
CyJohnPhos	(2-biphenyl)dicyclohexylphosphine
CT	computed tomography
δ	chemical shift
d	duplet (NMR)
DavePhos	2-dicyclohexylphosphino-2'-(<i>N,N</i> -dimethylamino)biphenyl
dd	doubled duplet (NMR)
ddd	tripled duplet (NMR)
DFO	deferoxamine
DHF	dihydrofolate
DHFR	dihydrofolatereductase
DME	1,2-dimethoxyethan
DMF	<i>N,N</i> -dimethylformamide
DMSO	dimethylsulfoxid
DOTA	1,4,7,10- <i>Tetraazacyclododecane-1,4,7,10-tetraacetic acid</i>
dppf	1,1'-ferrocenediyl-bis(diphenylphosphine)
dt	doubled triplet (NMR)
EDC	1-ethyl-3-(3-dimethylaminopropyl)carbodiimid
EDG	electron-donating group(s)

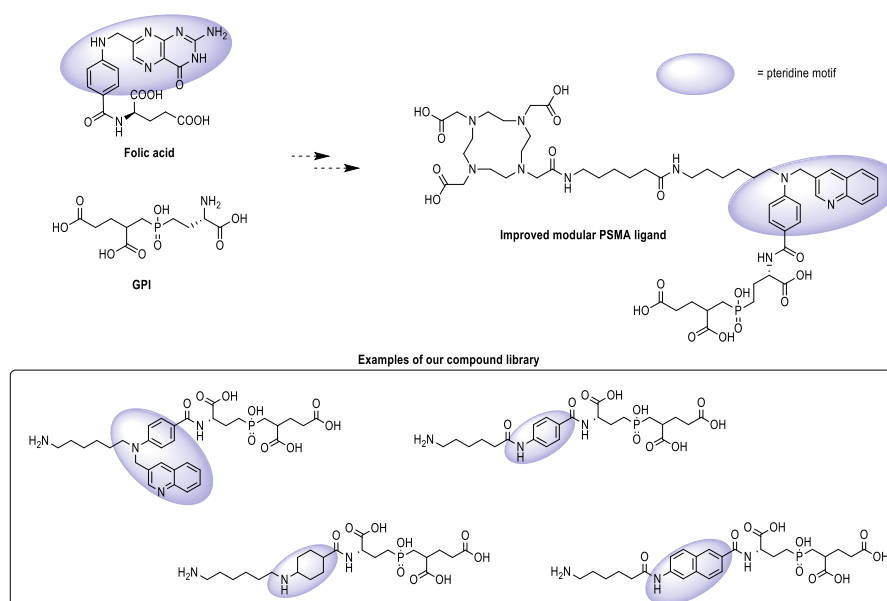
EEDQ	EEDQ
ESI	electron-spray ionisation
et al.	and others
EtOAc	ethyl acetate
equiv.	equivalents
EWG	electron-withdrawing group(s)
FA	formic acid
FDA	Food and Drug Administration
FOLH	folate hydrolase
FPGS	folylpolyglutamate synthase
FR	folate reductase
GCP	glutamate carboxypeptidase
h	hour(s)
HetAr	heteroaromatic
HMBC	heteronuclear multiple bond correlation (NMR)
HO-Su	<i>N</i> -hydroxysuccinimid
HRMS	HRMS
HSQC	heteronuclear single quantum correlation (NMR)
Hz	Hertz
IR	infrared spectroscopy
IUPAC	International Union of Pure and Applied Chemistry International Union of Pure and Applied Chemistry
<i>J</i>	coupling constant
JohnPhos	(2-biphenyl)di-tert-butylphosphine
LC-MS	liquid chromatography–mass spectrometry
m	multiplet
MeOH	methanol
MHz	Megahertz

mmol	millimole
μmol	micromole
MRI	magnetic resonance imaging
MTHFR	methylen-tetrahydrofolat-reductase
MTR/MTRR	methionine synthase/methionine synthase reductase
5-MTHF	5-methyltetrahydrofolate
MTX	methotrexate
NAAG	<i>N</i> -acetylaspartylglutamic acid
NAALADase	<i>N</i> -acetyl-L-aspartyl-L-glutamate peptidase
<i>N</i> -Boc	<i>N</i> - <i>tert</i> -butyloxycarbonyl
NIXantPhos	4,6-bis(diphenylphosphino)-10 <i>H</i> -phenoxazine
NHS	<i>N</i> -Hydroxysuccinimid
NMR	nuclear magnetic resonance
PBS	phosphate-buffered saline
PCFT	proton-coupled folate transporter
PCy ₃	tricyclohexylphosphine
PEG	polyethylenglycol
PET	positron emission tomography
2-PMPA	2-(phosphonomethyl)-pentandioic acid
PPh ₃	tricyclophenylphosphine
ppm	parts per million
PSMA	prostate specific membrane antigene
quant.	quantitative
quint	quintet (NMR)
<i>R_f</i>	ratio of fronts
RFC	reduced folate carrier
r.t.	room temperature room temperature

RuPhos	2-dicyclohexylphosphino-2',6'-diisopropoxybiphenyl
RP	reversed-phase
s	singlet (NMR)
SAH	S-adenosylhomocysteine
SAM	S-adenosylmethionine
SnAr	nucleophilic aromatic substitution
SPECT	single photon emission computed tomography
SPhos	2-dicyclohexylphosphino-2',6'-dimethoxybiphenyl
t	triplet (NMR)
TBS	tris-buffered saline
<i>t</i> BuXPhos	2-di-tert-butylphosphino-2',4',6'-triisopropylbiphenyl
TEA	triethylamine
TFA	trifluoroacetic acid
THF	tetrahydrofolate
TLC	thin layer chromatography
TMG	1,1,3,3-tetramethylguanidine
TRIS	tris(hydroxymethyl)aminomethane
TS	thymidylate synthetase
UV	ultra violet
v/v	volume per volume
XantPhos	4,5-bis(diphenylphosphino)-9,9-dimethylxanthene
XPhos	2-dicyclohexylphosphino-2',4',6'-triisopropylbiphenyl

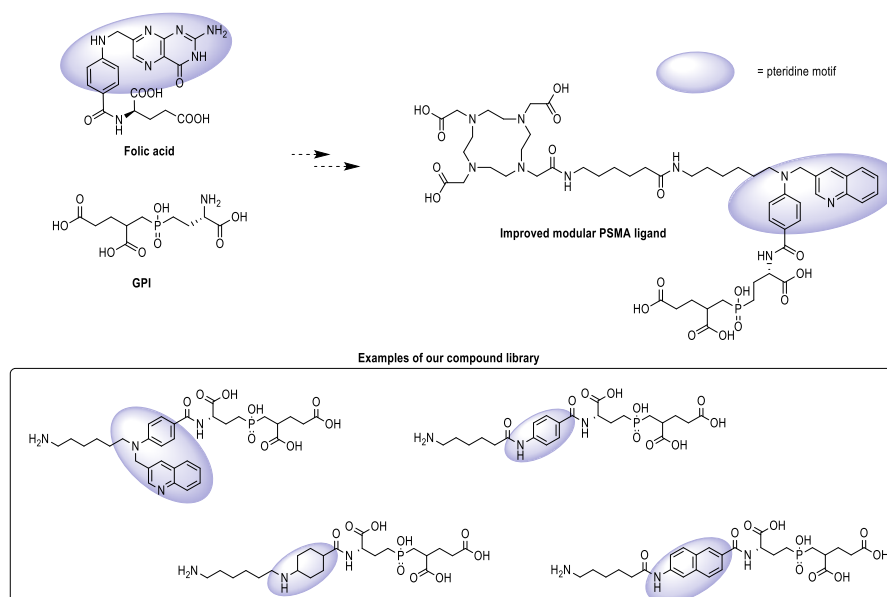
Abstract

Folates are essential cofactors in the *de novo* biosynthesis of pyridine and pyrimidines. Moreover, antifolates are key components in cancer therapy. Targeting tumor specific cell surface epitopes, so called tumor markers, with small molecules can lead to improved tools for cancer diagnosis and therapy. Elevated levels of prostate specific membrane antigen (PSMA) are used as a tumor marker for prostate cancer. PSMA is a glycosylated type-II membrane protein that is present in high density on the surface of malignant prostate cancer cells. Its expression increases with clinical stage, thus making it an extremely useful tumor marker. Phosphinic acids like GPI, for example, can be used as modular ligands for the targeting of prostate cancer. GPI binds with nanomolar affinity to PSMA and permits conjugation of effector molecules like dyes without altering the binding properties. However, GPI has suboptimal binding properties *in vivo* and needs to be improved for imaging applications in animals or humans. GPI has been developed as a transition state analogue of the native PSMA substrate *N*-acetylaspartylglutamate (NAAG). In addition, PSMA has been found to act as a folate hydrolase and does thus recognize folylpolyglutamates in the same binding pocket as NAAG. We have combined properties of the known ligand GPI with structural elements of folates and a conjugation site for effector molecules (in our case DOTA). This work highlights the design and synthesis of improved modular PSMA ligands. With this compound library we would like to evaluate the impact of different aromatic moieties as pteridine analogues, their spacing from GPI and the role of geometry and aromaticity of the spacer via *in vitro* assays using LNCaP (PSMA-positive) and PC3 (PSMA negative) cell lines and PSMA-617 as positive control.



Zusammenfassung

Erhöhte Spiegel von prostataspezifischem Membranantigen (PSMA) werden als Tumormarker für Prostatakrebs verwendet. PSMA ist ein glykosyliertes Typ-II-Membranprotein, das auf der Oberfläche von malignen Prostatakrebszellen in hoher Dichte vorliegt. Seine Expression nimmt mit dem klinischen Stadium zu und ist somit ein äußerst nützlicher Tumormarker. Phosphinsäuren wie GPI können beispielsweise als modulare Liganden zur Bekämpfung von Prostatakrebs eingesetzt werden. GPI bindet mit nanomolarer Affinität an PSMA und ermöglicht die Konjugation von Effektormolekülen wie Farbstoffen, ohne die Bindungseigenschaften zu verändern. GPI weist jedoch in vivo suboptimale Bindungseigenschaften auf und muss für Bildgebungsanwendungen bei Tieren oder Menschen verbessert werden. GPI wurde als Übergangszustandsanalogon des nativen PSMA-Substrats *N*-Acetylaspartylglutamat (NAAG) entwickelt. Darüber hinaus wirkt PSMA als Folat-Hydrolase und erkennt somit Folylpolyglutamate in derselben Bindungstasche wie NAAG. Wir haben die Eigenschaften des bekannten Liganden GPI mit Strukturelementen von Folaten und einer Konjugationsstelle für Effektormoleküle (in unserem Fall DOTA) kombiniert. Diese Arbeit beleuchtet das Design und die Synthese verbesserter modularer PSMA-Liganden. Mit dieser Substanzbibliothek möchten wir die Auswirkung verschiedener aromatischer Einheiten als Pteridinanaloge, ihren Abstand von GPI und die Rolle der Geometrie und Aromatizität des Spacers mithilfe von In-vitro-Assays unter Verwendung von LNCaP (PSMA-positiv) und PC3 (PSMA-negativ) bewerten. Zelllinien und PSMA-617 als positive Kontrolle.



1 Introduction

Folates and folate derivatives play an important role in medicinal chemistry and are present in various pharmaceutically relevant compounds.¹ Folic acid is a crucial factor for cell growth and development and plays a vital role in DNA metabolism, as an essential cofactor in the *de novo* biosynthesis of purines and pyrimidines.² In the human metabolism folate is required to deliver a C1-fragment for methylation reactions³ and nucleic acid synthesis.⁴ Moreover, folates are also crucial for conversion of homocysteine to methionine.⁵ Folate deficiency is directly correlated to hindrance of DNA synthesis and cell division, thus affecting the cells with highest frequency of cell division such as hematopoietic cells.⁴ Therefore, folate derivatives are often key components in cancer therapy.⁵ Due to their vital role in cell division, folates are essential during infancy and pregnancy, as it is known that deficiency can lead to infant's disorders such as *neural tube defects (spina bifida)*⁶ and brain defects (*anencephaly*).⁷ Furthermore, folic acid deficiency can negatively affect the production of red blood cells (*erythropoiesis*)⁸, and consequently induce megaloblastic anemia.⁹ It has also been shown in some clinical studies that folates can play a complex role in prostate cancer.^{10,11}

1.1. Folic acid

Folic acid is not *per se* available in its active form in the human body and through several metabolic reactions it gets converted into different structures. The active forms of folic acid are tetrahydrofolic acid, methyltetrahydrofolate (MTHFR), methenyltetrahydrofolate, folinic acid, and folacin.^{2,12} As shown in Figure 1 the metabolic cycle of folic acid includes conversion of dietary folate to dihydrofolate (DHF) and subsequently to tetrahydrofolic acid. In this metabolic cycle, tetrahydrofolic acid is converted through an enzymatic cascade to 5-methyl tetrahydrofolic acid, and functions as substrate for the methionine synthase/methionine synthase reductase (MTR/MTRR) system to tetrahydrofolic acid and methionine.³ Additionally, 5-methyl tetrahydrofolic acid is involved in purine synthesis. Through the metabolic cycle methionine is converted to S-adenosyl-methionine (SAM), S-adenosyl-homocysteine (SAH) and homocysteine. Furthermore, SAM and SAH play a vital role in choline metabolism.¹³ SAM is also involved in the methylation of DNA, RNA, proteins, and phospholipids.¹²

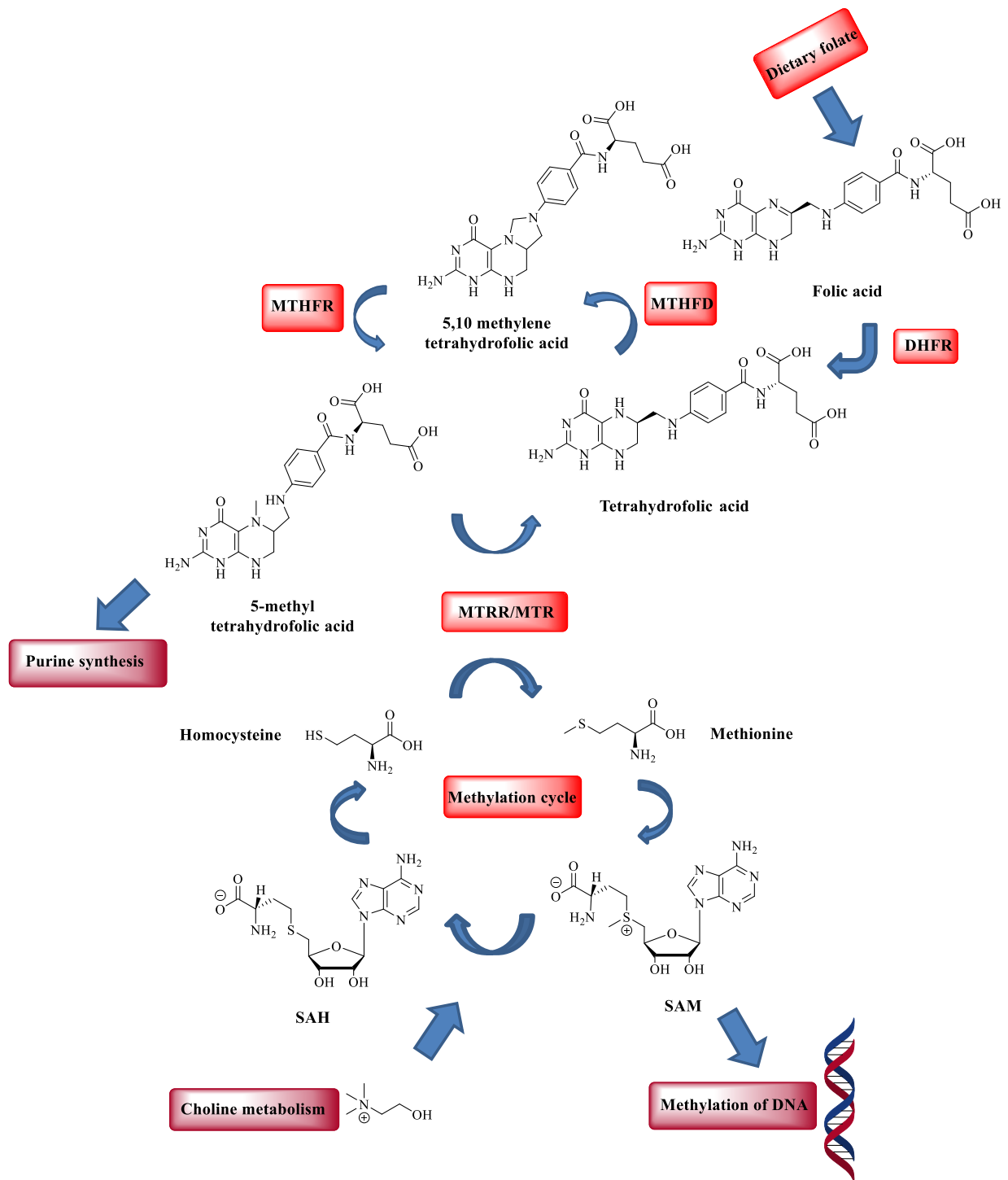


Figure 1: Metabolic cycle of folic acid.

1.1.1. Folate receptors

Folate transport through the cell membrane occurs *via* several pathways. The main folate pathway is through the reduced folate carrier (RFC), which takes up dietary folate.¹⁴ The second essential pathway is through the proton-coupled folate transporter (PCFT), which transports folate into the cells.¹⁵ Additionally, there are four important folate receptors expressed on the cell membrane responsible for folate transport: FR α , FR β , FR γ and FR δ .^{16,17} Folate receptors are well-known tumor markers since they are highly expressed in ovarian¹⁸, breast¹⁹, lung²⁰ and colorectal²¹ cancer. A clinically relevant example is the folate receptor α (FR α) which carries and coordinates the transport of the active form of folate (5-MTHF). Furthermore, it has been shown that FR α can be useful as a target for cancer treatment or diagnosis since it is overexpressed in solid tumors like ovarian^{16, 22} and lung cancers.^{23, 24}

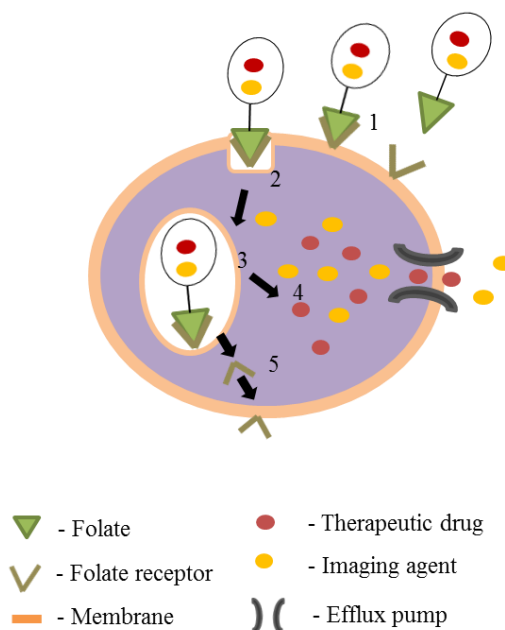


Figure 2: Receptor-mediated endocytosis of a drug conjugated to folate. (1) The drug–folate conjugate binds to folate receptors (2) Internalisation. (3) Lysosome load release (4) Released drug and imaging agent in the cytosol. (5) The folate receptor can be recycled and returned to the cell membrane.²⁵

Targeting folate receptors is a very effective tool for delivery of radiopharmaceuticals for imaging and radiation therapy.²⁶ This targeting strategy involves the use of small molecules such as folate itself or derivatives and the use of FR α -binding antibodies, antibody-like fragments or other antibody-like binding moieties.^{22,27,28} It is also common to use folate-conjugates with cytotoxic agents for anticancer therapy such as carboplatin analogs, paclitaxel-loaded dendrimer nanodevices²⁹, 5-FU analogs³⁰, rhaponticin³¹ and vinblastine analogs.^{27, 32}

1.1.2. Antifolates

Antifolates have played a crucial role in the treatment of a broad spectrum of diseases such as microbial and parasitic infections and chronic inflammatory diseases² in the past. Therefore, antifolates are often key components in cancer therapy.³³ The general mechanism of antifolates is the competitive inhibition of DHFR. In 1948 Fiber *et al.* discovered the first antifolate – aminopterin and observed improved health condition of children with acute lymphoblastic leukemia after treatment with this novel drug.³⁴ After these positive results, the scientific community was encouraged to treat other malignant diseases with this promising chemotherapeutic. However, several cases showed unpredictable toxicity of aminopterin and it was consequently replaced in 1950 with methotrexate (MTX).³⁵ MTX is also a competitive inhibitor of DHF and therefore often applied as a cytostatic in malignant diseases such as lymphoblastic leukemia³⁶, breast cancer³⁷ and osteosarcoma.³⁸ In a lower dose it is used as an antirheumatic drug for rheumatoid arthritis.³⁹

It was discovered that antifolates in their polyglutamate forms can directly inhibit further enzymes of the metabolic cycle of folic acid such as TS and aminoimidazole carboxamide ribonucleotide formyltransferase (AICAR transformylase).^{40,41} Due to major side effects of MTX, observed over decades of clinical application, raltitrexed was introduced by AstraZeneca as a new chemotherapeutic (Figure X).⁴² In its polyglutamate form raltitrexed can additionally inhibit TS which makes this drug more attractive in the clinical circles compared to MTX.⁴³ Raltitrexed was the first new drug developed for colorectal cancer in 35 years. Until now it represents an important part of colorectal cancer treatment. In 2003 pemetrexed appeared as a new drug of choice for the treatment of non-small cell lung cancer⁴⁵ and breast cancer.⁴⁴ Pemetrexed can also be found under the name multitargeted antifolate (MTA) because it inhibits *de novo* pyrimidine and purine pathways by TS, DHFR, glycinamide ribonucleotide formyltransferase, and AICAR transformylase.⁴⁴⁻⁴⁹ Another antifolate in the row with higher affinity for RFC and polyglutamatisation is pralatrexate.⁵⁰⁻⁵² This drug is applied during treatment of cutaneous T-cell lymphoma together with folate supplementation.⁵³⁻⁵⁵

Figure 3 shows the structures of the most important antifolates in therapy and highlights their chemical similarities. Aminopterin is a derivative of folic acid substituted with an amino group at the pteridine ring (N4-position). Compared to aminopterin MTX has an additional methyl group at the N10 position. In pralatrexate and pemetrexed the nitrogen in the N4 position is

replaced by a carbon atom. This shows that modifications of folic acid in N-4 position play an important role in the inhibition of DHFR.

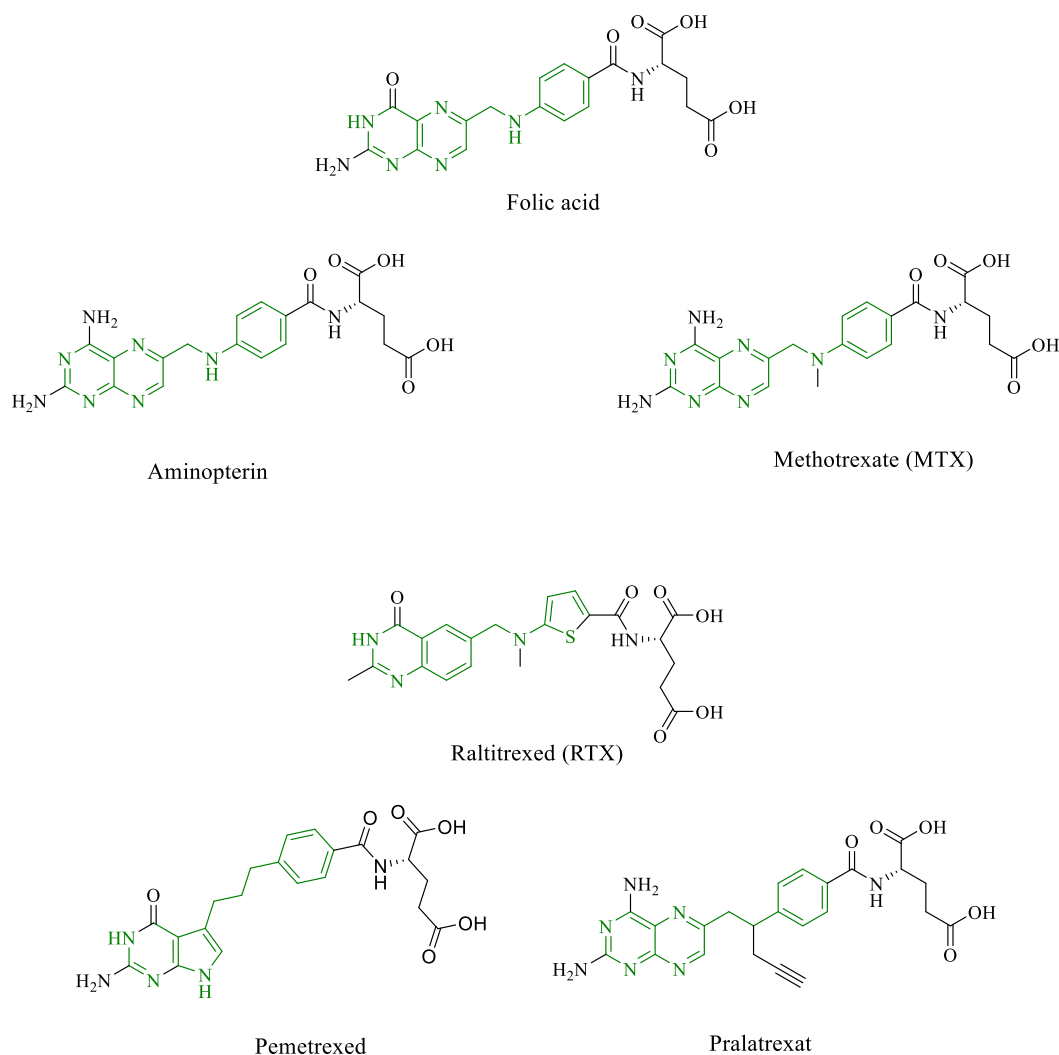


Figure 3: Examples of clinically important antifolates.

1.2. PSMA

Prostate cancer is the most common tumor found in men in Germany and the second most frequently encountered cancer in males in the western world.⁵⁶ Early diagnosis is essential for the effective treatment considering that prostate tumor is slow-growing cancer but becomes potentially lethal when it comes close to the metastatic stage. The most common tools for early diagnosis consider functional imaging, namely MRI (magnetic resonance imaging)⁵⁷, SPECT (single-photon-emission tomography)⁵⁸, PET (positron emission tomography)⁵⁹, and ¹⁸F-choline PET/CT.⁶⁰ The prostate tumor is highly hormone-dependent and one of the common treatments is radical prostatectomy and / or radiotherapy.⁶¹ These clinical treatments usually

are not appropriate for patients with metastasis since the majority of men develop hormone-refractory disease often within a year.

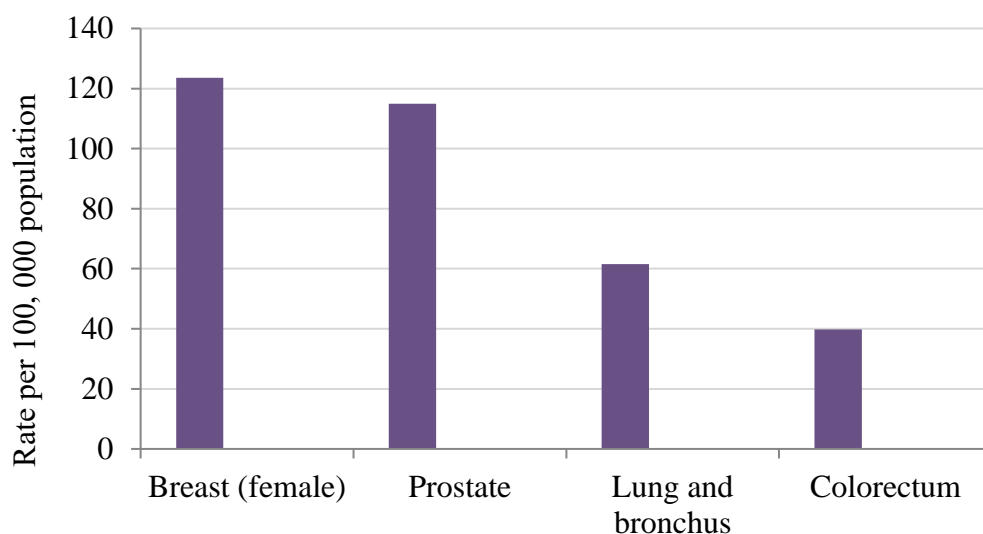


Figure 4: Incidence rate of selected cancer types, 2010-2014 by North American Association of Central Cancer Registries (NAACCR), 2017.

Prostate specific membrane antigen (PSMA) is a folate hydrolase that is used as a tumor marker for prostate cancer.⁶² PSMA is a membrane glycoprotein that is usually present on healthy prostate cells and in high density on the surface of malignant prostate cancer cells.⁶³ It is also present in other tissues such as liver⁶⁴, brain⁶⁵, kidney^{66,67}, proximal small intestine⁶⁸, colon⁶⁹ and salivary glands.⁶⁹ PSMA is a type II integral membrane glycoprotein and consists of 750 amino acids. It consists of three different parts: 24 amino acids are localized in the cell membrane, 707-amino acids are located in the extracellular region and 19 amino acids are placed in the cytoplasmic tail.^{68,70} The crystal structure of PSMA showed that the extracellular part of the enzyme has three main domains: protease (Figure 5, pink), apical (Figure 5, yellow) and C-terminal domain (Figure X, orange). These parts play a vital role in substrate recognition.^{63,71} It was also discovered that the active site contains two zinc ions (Figure 5, shown as two grey spheres) and it is connected with the extracellular domain through a ~20 Å deep tunnel.⁶³ Zinc atoms in the active site are further coordinated with different amino acids: histidine, terminal aspartate or glutamate, and a bridged aspartate. Finally, the whole catalytic center is surrounded by water molecules.^{72,56} Determination of all these features was essential for further development of PSMA ligands in the treatment and diagnosis of prostate cancer.

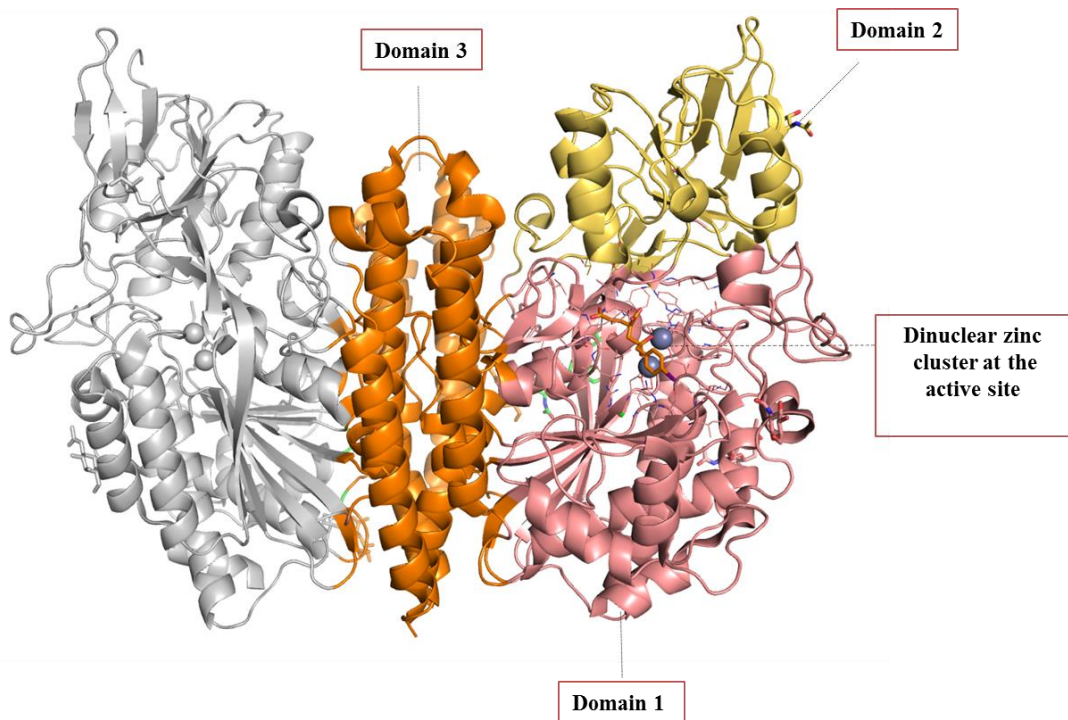


Figure 5: Crystal structure of PSMA-GPI 18431-complex.⁶³ Three-dimensional structure of the dimer. One subunit is shown in gray, while the other is colored according to organization into domains. Domain 1, light pink; domain 2, yellow; domain 3, orange. dinuclear zinc cluster at the active site is indicated by grey spheres.

PSMA plays also a role in other metabolic reactions such as glutamatergic neurotransmission⁶⁵ and folate absorption.⁶² Because of its versatile functions, PSMA is often found under different names in literature such as glutamate carboxypeptidase II (GCPII)⁶⁴ or NAALADase, since PSMA is vital for the metabolism of *N*-acetyl aspartyl glutamate (NAAG) in the central nervous system.^{62,73} PSMA catalyzes the hydrolysis of NAAG to NAA and L-glutamate (Figure 6). Additionally, PSMA hydrolyses folylpolyglutamates in the small intestine and therefore it is also named folate hydrolase (FOLH1).^{62,74,75}

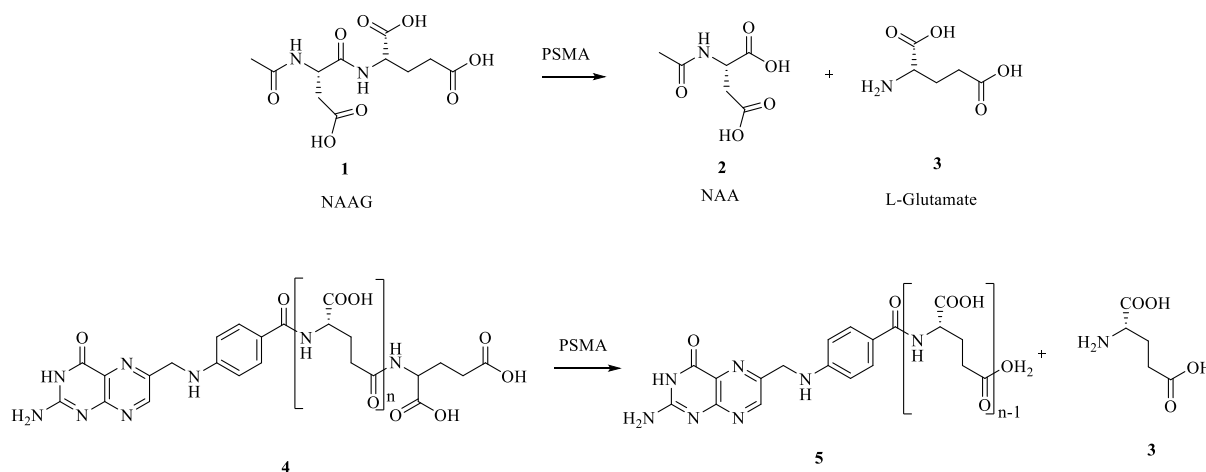


Figure 6: Hydrolytic activity of PSMA.

PSMA is part of the cocatalytic zinc metallopeptidase family M28 which is directly correlated to PSMA's enzymatic activity.^{71,76} PSMA recognizes folylpolyglutamates in the same binding pocket as NAAG and hydrolyses poly- γ -glutamated folates released from dead and dying tumor cells to folate and glutamate (Figure 6).⁶² In the following step, folate is taken up by the living tumor cells *via* the folate receptor or reduced folate carrier. As soon as folate enters the cell, it converts into its polyglutamated form again and in that form is further used for metabolic reactions in tumor cells, which supports their proliferation.⁷⁶

It is reported that in the patients with a slightly elevated prostate-specific antigen level PSMA-targeted PET/CT is able to detect and localize the prostate cancer lesions that normally were not detectable by CT, MRI, or ¹⁸F-choline PET/CT.⁷⁷ Expression of PSMA increases within the clinical stage significantly, especially in the hormone-refractory and metastatic stage of the disease.⁶⁸ Therefore, PSMA is an attractive target for therapeutic agents in the treatment of the prostate cancer.

1.2.1 PSMA ligands

The identification of NAALADase activity of PSMA in CNS led to the proposal that NAAG may serve as a storage form of synaptic glutamate.⁷³ In order to further ascertain the exact role of NAALADase and NAAG in the CNS, a number of *in vitro* and *in vivo* studies have been conducted. It was shown that elevated levels of NAAG play a significant role in neurodegenerative processes in CNS leading to epilepsy⁷⁸, schizophrenia⁷⁹ and Alzheimer's disease.⁸⁰ Moreover, a series of small molecules were designed for the purpose of inhibiting

NAALDase. In 1995, Jackson *et al.* reported the first synthesis of a highly active NAALADase inhibitor, 2-PMPA (Figure 7).⁷³ This compound showed a very high binding affinity having a K_i of 0.275 nM, thus confirming that glutamate-like moieties are essential for good binding. 2-PMPA is very often used as a reference substance in biological evaluation of the binding affinities.^{73,81,82} However, small substances like 2-PMPA that bear three negative charges show rather non-favorable pharmacokinetic characteristics for the design of lead compounds because the penetration through the blood-brain barrier would be hindered.^{83,84}

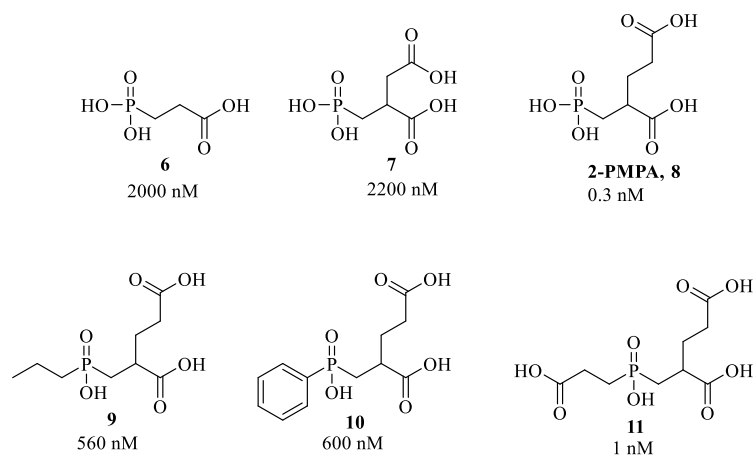


Figure 7: Structures and IC_{50} of phosphinic acid derivatives with different substituents.^{81,85}

In further studies, there have been many attempts to design a NAALADase inhibitor with similar affinity to 2-PMPA and lower polarity.⁸⁵ The first compounds were prepared by altering the γ -acid (**6** and **7**, Figure 7). The acidic functionality, however, appears necessary for potent inhibition of the enzyme. Therefore, it was investigated if the substitution of hydroxyl-group of phosphinic acid with different aromatic moieties and alkyl chains may increase affinity (**9** and **10**, Figure 7).⁸¹ Introducing additional acidic moiety through the substitution of hydroxyl group (**11**, Figure 7) showed a good affinity (1nM), however, none of these ligands could outperform the binding affinity of 2-PMPA. Based on this knowledge, a series of PSMA ligands with different functionalities were designed over the last decade. In addition, it was discovered that newly designed ligands can address PSMA in prostate cancer cells and therefore can be used for PET⁵⁹ and SPECT imaging.⁸⁶ Consequently, the research focus was moving away from the design of PSMA ligands for treatment of brain diseases to ligands for prostate cancer imaging. Elevated expression of PSMA is directly correlated with the progression of the prostate tumor, thus making it an extremely useful tumor marker.^{82,87-89} The key components of newly designed PSMA ligands for prostate cancer imaging include a targeting vector (small molecule or antibody) which can allow coupling with effector molecules (radiometal chelators, fluorescent dyes) *via* spacer moiety (Figure 8).

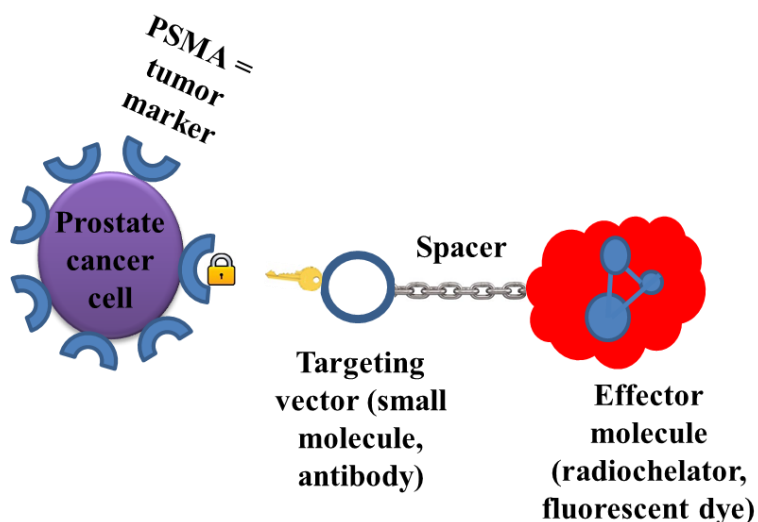


Figure 8: Key components of prostate tumor targeting: PSMA serves as a tumor marker. A targeting vector, coupled with an effector molecule via a spacer, selectively binds to the tumor marker.

There are three main groups of small molecules for PSMA targeting, including thiols **12**, phosphonates **13** and ureas **14** (Figure 9).⁵⁶ Each of these molecules contains a glutamate mimic for PSMA recognition, as well as different functionalities for interaction with a zinc ion in the active site of the enzyme (highlighted in blue, Figure 9).

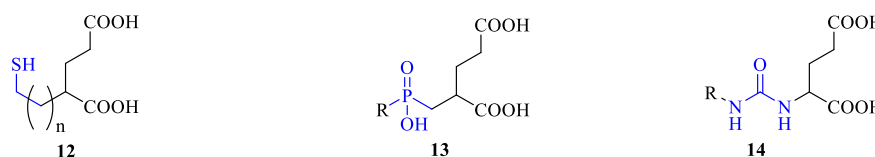


Figure 9: The three groups of small molecules for PSMA targeting include: thiols **12**, phosphonates **13** and ureas **14**.⁵⁶ The core structures important for interaction with the active site of PSMA are highlighted in blue.

It was observed that the affinity and tumor uptake increase depending on the applied radiolabel, chelator, and spacer.⁵⁶ Spacer has an important impact on the modularity of a ligand because it can allow functionalization with effector molecules. Further development of new derivatives focused on decreasing polarity and altering the length and nature of spacer groups (Figure 10). Chen *et al.* evaluated PSMA ligands with different linker lengths (**15-17**, Figure 10) and conjugated with different NIR dyes (IRDye800CW, IRDye800RS, Cy5.5, Cy7).⁹⁰ The length of the spacer group is important because it should allow conjugation with effector molecule without compromising the binding in the active site of PSMA. Huang *et al.* also showed that implementation of longer spacer chains can allow conjugation of bulky chelated metals. These

bulky chelators are on this example situated outside the active site and will not interfere with binding (**18** and **19**, Figure **10**).⁹¹⁻⁹³.

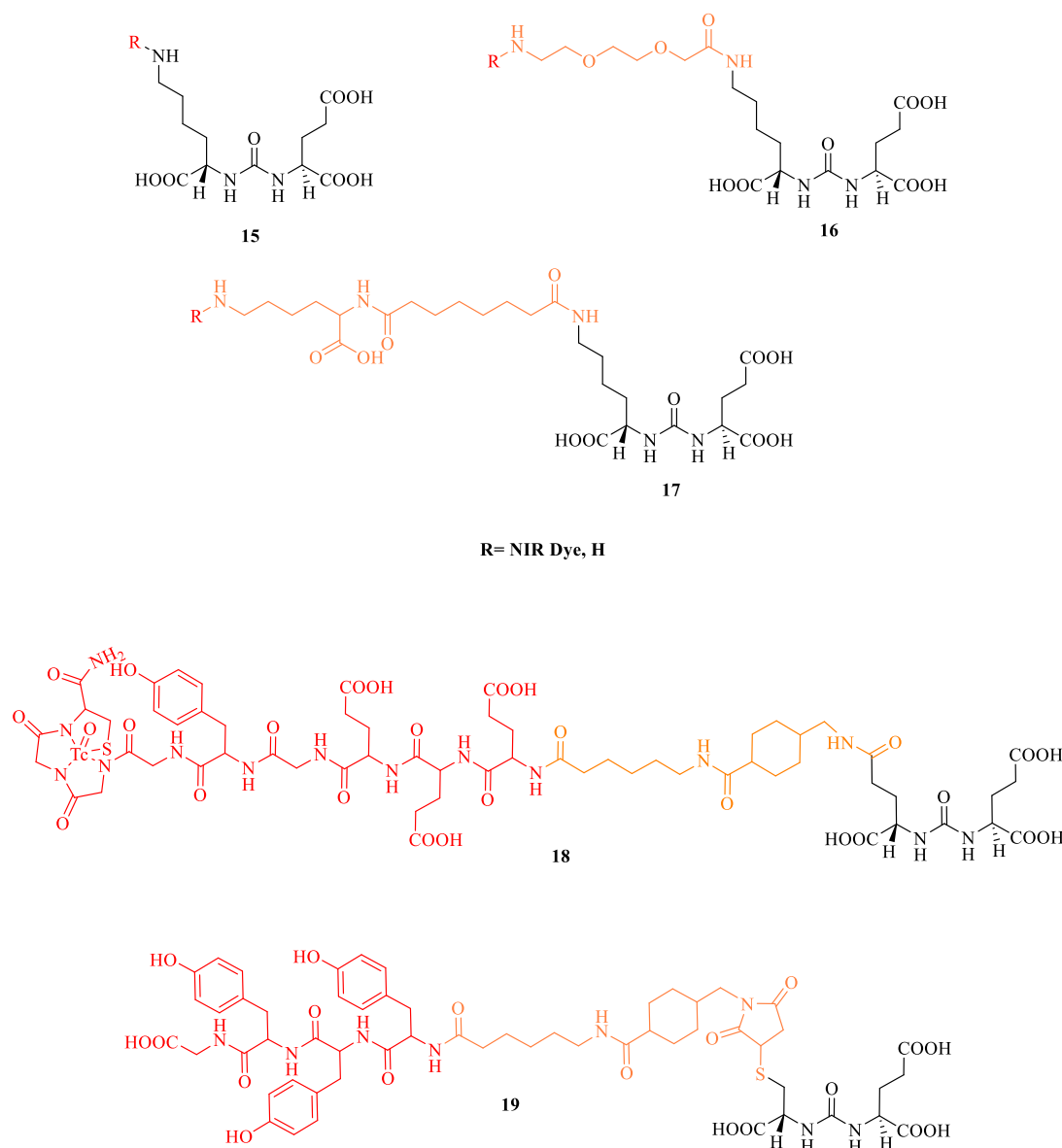


Figure 10: PSMA ligands with different spacer lengths and effector molecules.^{90,92}

Coward *et al.* together with Guilford Pharmaceuticals synthesized and evaluated a new PSMA ligand termed GPI 11254-36 (GPI)⁹⁴ in 2001. GPI is a phosphinic acid derivative that revealed very high binding affinity to PSMA with a $K_i = 9.0$ nM. The advantage of GPI is that it has a highly modular structure in comparison to 2-PMPA since it contains a free amino group that allows conjugation to different types of effector molecules. However, the major drawback of GPI is the low binding affinity in phosphate containing buffers and in serum. In order to increase the binding affinity of GPI, Maison *et al.* designed multivalent Adamantan-GPI conjugates

(Figure 11).⁹⁵ This concept led to an improved binding affinity of the AdamGPI trimer ($K_d = 3.0$ nM in serum, 0.5 nM in PBS buffer and 0.4 nM in TBS buffer).

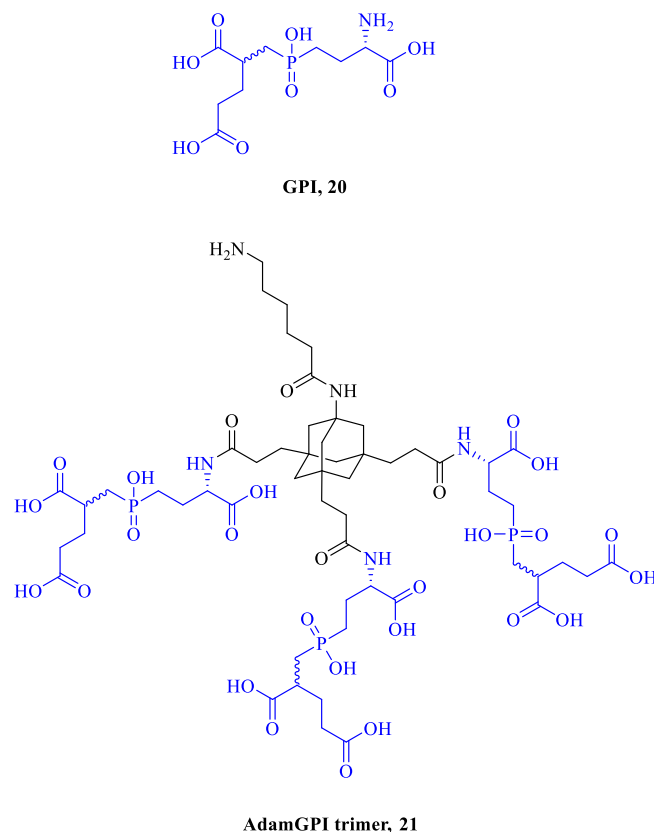
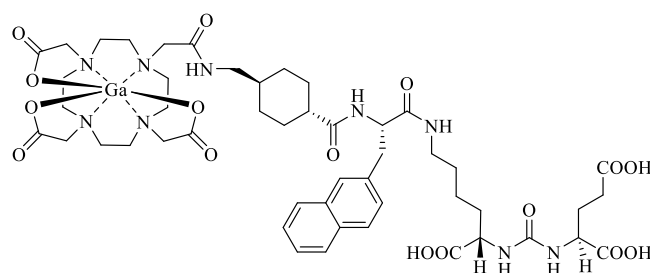


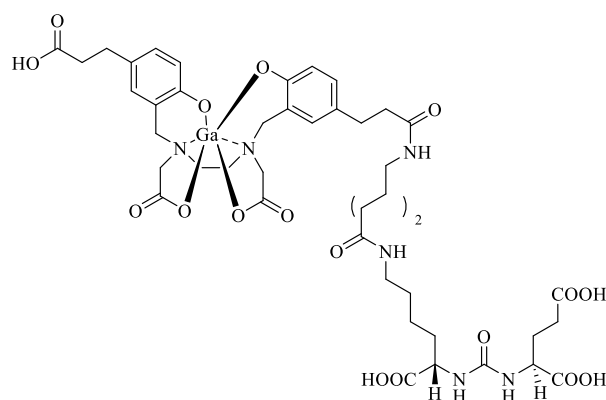
Figure 11: Structures of GPI (highlighted in blue) and multivalent Adamantan-GPI conjugates.⁹⁵

Synthesis and *in vitro* evaluation of very potent urea-based PSMA ligands was published by Benesova *et al.* in 2015.⁹⁶ They described the synthesis and *in vitro* binding of a new ^{68}Ga -labeled, urea-based PSMA inhibitor, (PSMA-617, **22**) as well as the biodistribution and *in vivo* imaging studies. In this study, DOTA was used as a multi-dentate chelator, which can be labeled with diagnostic (^{68}Ga , ^{177}Lu) or therapeutic radionuclides. The design of a structure is based on three building blocks, namely: a PSMA targeting moiety, a linker, and a chelator for ^{68}Ga . The study also showed that the role of the linker bearing a naphthalene side chain plays a big role for binding affinity and pharmacokinetics. PSMA-617 is one of the most promising PSMA ligands due to its strong binding affinity ($K_i = 2.34$ nM) to PSMA and high rate of internalization in prostate cancer cells. Biological properties of PSMA-617 were significantly improved in comparison with already clinically evaluated ^{68}Ga -PSMA-11 (**23**), which was previously reported by Eder *et al.* in 2012.⁹⁷ Clinical studies in patients showed that ^{68}Ga -

PSMA-617 detects lesions of prostate cancer with high imaging quality and minimal radiation exposure.⁹⁸



⁶⁸Ga-PSMA-617, 22



⁶⁸Ga-PSMA-11, 23

Figure 12: Structures of potent PSMA ligands ⁶⁸Ga-PSMA-617 and ⁶⁸Ga-PSMA-11.^{96,97}

Another group of PSMA ligands includes-antibody based tumor vectors coupled to the effector molecules such as radiometal chelators. The first FDA-approved imaging agent for PSMA was ¹¹¹In-capromab pendetide (ProstaScint®), established by Cytogen Corporation. This capromab is functionalized with the chelator diethylenetriaminepentaacetic acid (DTPA) and labeled with ¹¹¹In to obtain ¹¹¹In-7E11-C5.⁹⁹ Additionally, this antibody binds to the intracellular site of PSMA, which is accessible on necrotic tumors only and it is used for SPECT imaging in patients with hormone-refractory tumors after prostatectomy.^{100,101} The group of Bander *et al.* designed another antibody - J591¹⁰² binding to an extracellular site of PSMA, thus enhancing the sensitivity for detection of bone metastasis. J591 has been functionalized with different types of chelators, such as DOTA and DFO and labeled with ^{99m}Tc, ¹¹¹In, ⁸⁹Zn, ⁶⁴Cu, ¹⁷⁷Lu, ⁹⁰Y for SPECT and PET imaging.¹⁰²⁻¹¹¹ Recently, the concept of Bander *et al.* was adapted and altered. Namely, J591 has been humanized and genetically engineered to a minibody ⁸⁹Zr- Df-IAB2M,

having the advantage of drastically smaller size in comparison to the J591 antibody.¹¹² The drawback of treatments with antibodies mainly comes from their size and consequently very long half-time in blood circulation, the bad signal-to-noise ratio in imaging and poor tumor penetration. Also, there is always a certain probability of an immune response to the applied treatment. Furthermore, the costs of introducing antibodies in therapy are much higher in comparison to the application of small molecules obtained by chemical synthesis.^{113,114} The need for more favorable pharmacokinetic characteristics triggered the development of PSMA-binders with low molecular weight.¹¹⁴ A major advantage of these PSMA-ligands is faster clearance that leads to lower toxicity, no immune response and lower signal to noise ratio.

1.3 Folate based imaging agents

Over the last two decades, a major effort was invested in the development of folate-based radiotracers for nuclear imaging of folate receptor (FR)-positive tumors using SPECT.^{26,115,116} There are several groups of folate agents that have been designed and preclinically evaluated, including [¹⁸F]fluorofolate radiotracers, deferoxamine-folate, and DOTA-folates. Fluorofolate radiotracers represent a group of folate precursors designed with the pendent approach, which means they are constituted out of ¹⁸F-labeled prosthetic group conjugated to a folate. Further examples of interest include: [¹⁸F]fluoro-benzylamine-folate and [¹⁸F]fluoro-benzene-folates. The first *in vivo* application of these types of imaging agents was reported by Bettio *et al.*¹¹⁷ In 2006, Al Jammaz *et al.* used a similar radiosynthesis strategy to develop [¹⁸F]fluorobenzene- and [¹⁸F]fluoropyridinecarbohydrazide-folates (**24-28**, Figure **13**).¹¹⁸ Additionally, they used methotrexate instead of folic acid as ¹⁸F-labeled prosthetic group. However, *in vitro* tests showed that the methotrexate analogs were binding with lower affinity in comparison to folates.

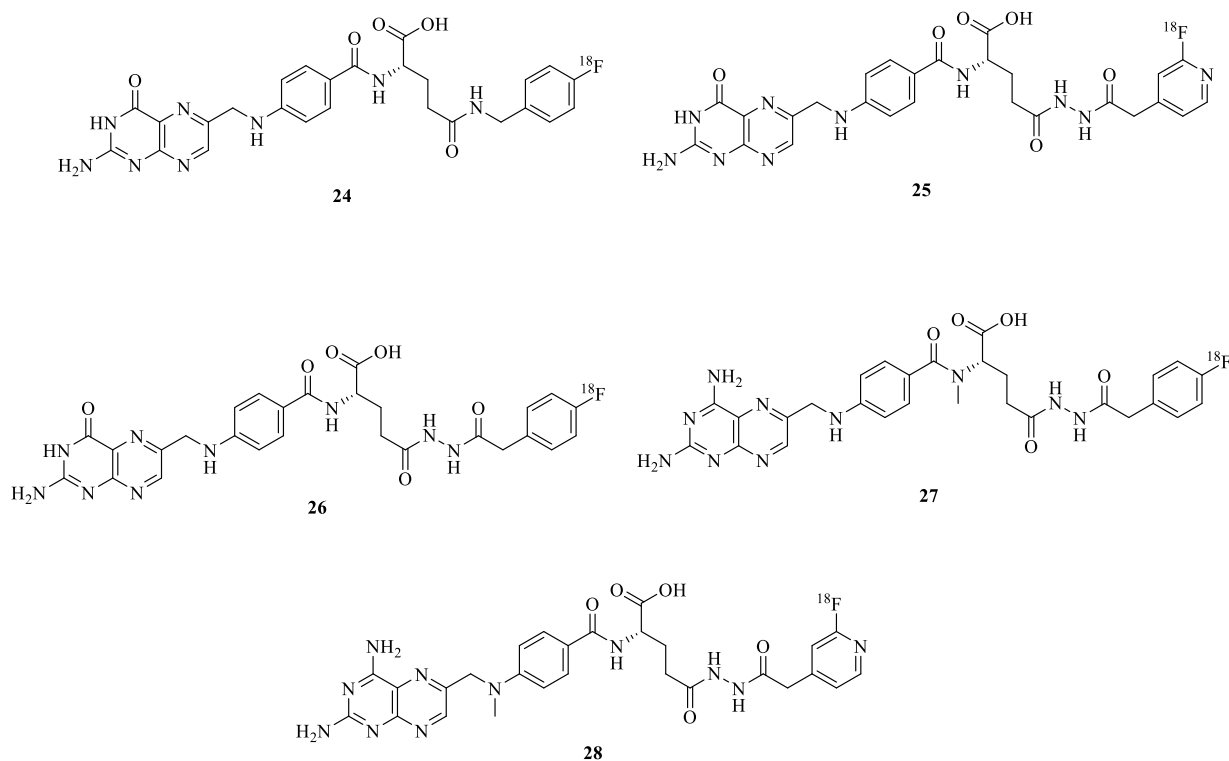


Figure 13: [^{18}F]fluorobenzene- and [^{18}F]fluoropyridinecarbohydrazide- folates for imaging applications.^{117,118}

In order to increase the modularity of folate radiotracers Ross *et al.*, developed an ^{18}F fluoro-click-folate **31**.¹¹⁹ The synthesis included coupling of azide-functionalized folate precursor (**29**) and 6- [^{18}F]fluoro-1-hexyne (**30**) *via* copper-catalyzed click reaction. Unfortunately, increasing hydrophobicity led to a higher uptake of fluoro-click-folate in the bile and feces indicating its hepatobiliary excretion. However, retention in the kidneys was comparatively low.

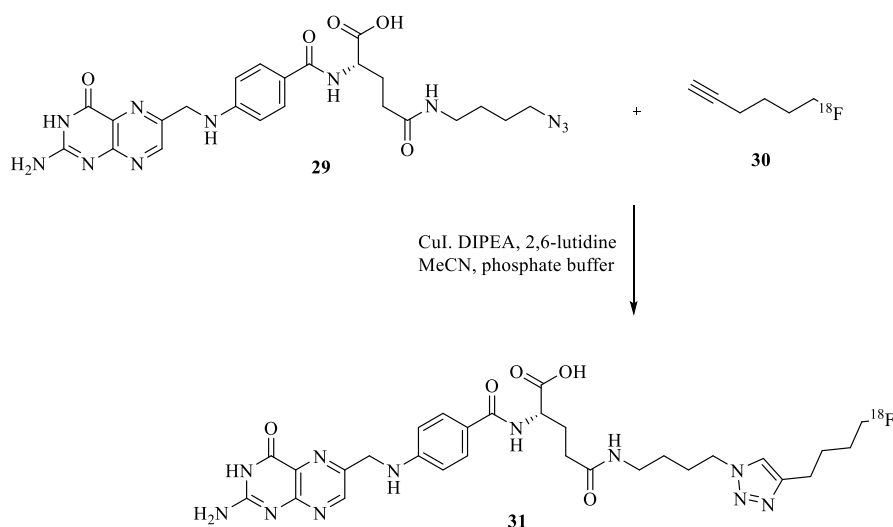


Figure 14: Synthesis of ^{18}F fluoro-click-folate via click chemistry.¹¹⁹

Noticing that the high hepatobiliary excretion of new derivatives can lead to the accumulation in the abdominal vicinity, which may limit their potential as radiotracers for PET imaging of the folate receptor-positive tumors, Al Jammaz *et al.* reported a synthesis of fluoro-folate conjugates with different sugars.¹²⁰ In order to achieve better pharmacokinetic properties, hydrophilic sugar moiety (fluoro-deoxy-glucose) was coupled to folate (Figure 15). This work also showed a short and rapid synthesis, with high purity and radionuclide yield, which makes these folate-analogs good candidates for large-scale production. Besides, biodistribution studies revealed a rapid blood clearance with excretion primarily by the urinary and hepatobiliary systems. Significant tumor uptake and favorable pharmacokinetics over other radioconjugates were also demonstrated.

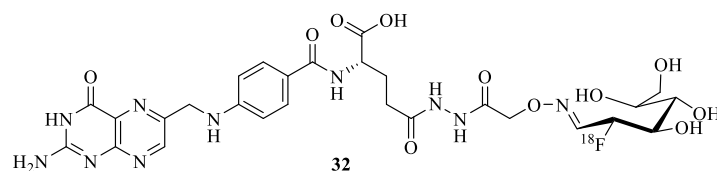


Figure 15: Fluoro-deoxy-glucose-folate.¹²⁰

The same year Fisher *et al.* published the fluoro-deoxy-glucose-folates derivatives using click-chemistry to introduce a sugar moiety (Figure 16).¹²¹ The authors claimed that these results were clearly outperforming [¹⁸F]fluoro-click-folate, previously synthesized by Ross *et al.*

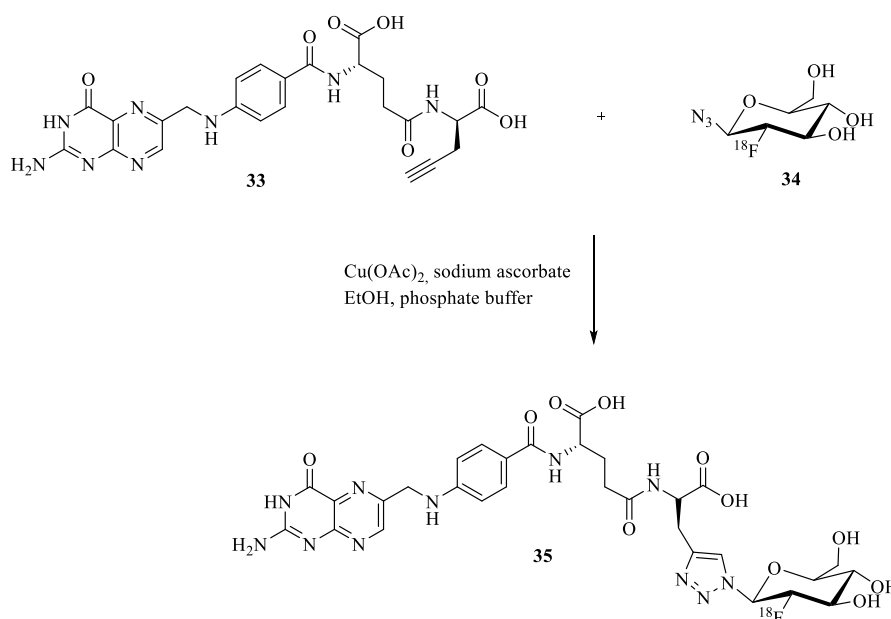


Figure 16: Synthesis of fluoro-glucose-folates via click chemistry.¹²¹

Development of folate radiotracer moved further to the functionalization of folic acid with different types of acyclic and macrocyclic chelators such as DFO and DOTA. Fani *et al.* synthesized several DOTA- and DFO-folate conjugates with selective targeting of FR and good tumor to background ratio (Figure 17).¹²² They also introduced a shorter 1,2-diaminoethane linker (36) as well as longer PEG spacer (37) between folate and DOTA as potential pharmacokinetic modifiers. The substitution of DFO with DOTA, as well as the length of the spacer did not have a huge impact on the binding affinity and biodistribution of these radiotracers.

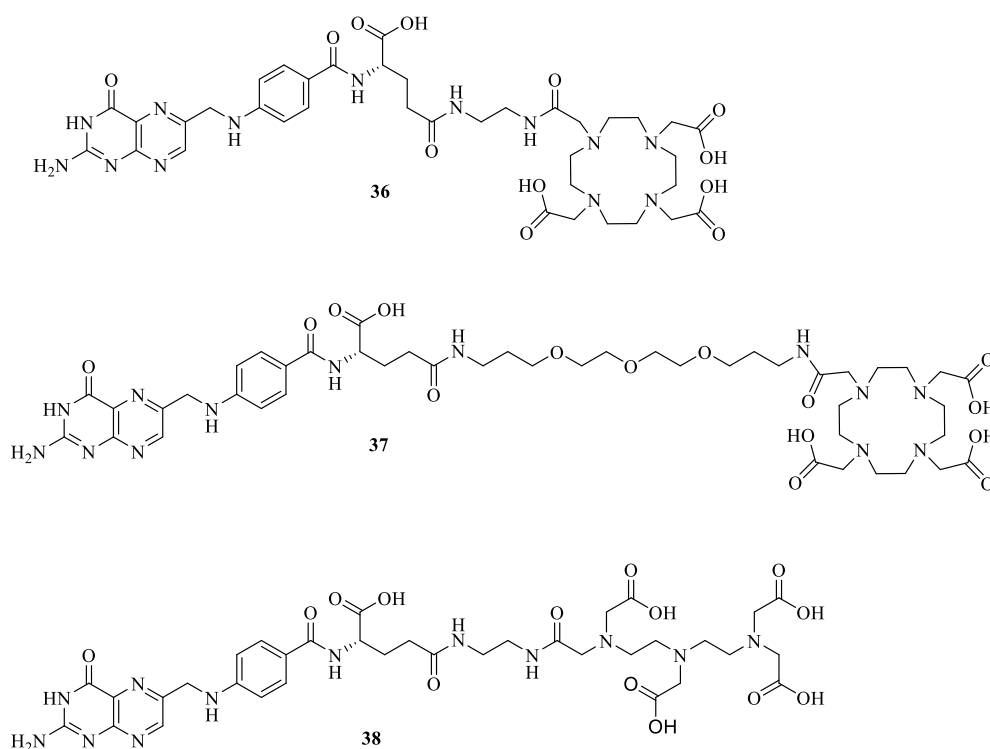


Figure 17: DOTA and DFO - Folate conjugates.¹²²

In 2012, Müller *et al* reported first in vivo tests of new DOTA-folate conjugates with ¹⁵²Tb and ¹⁷⁷Lu-labeled versions.^{123,124} These radiotracers contained an additional functionality that is able to bind serum albumin with μM - affinity (Figure 18). The albumin binding group was introduced into the backbone of the DOTA-folate molecule, thus enhancing the blood circulation time of ¹⁷⁷Lu-folate-DOTA conjugate. Another outcome was the increased tumor uptake of 39 and lower renal accumulation compared to other ¹⁷⁷Lu-labeled DOTA-folate without an albumin binding entity.

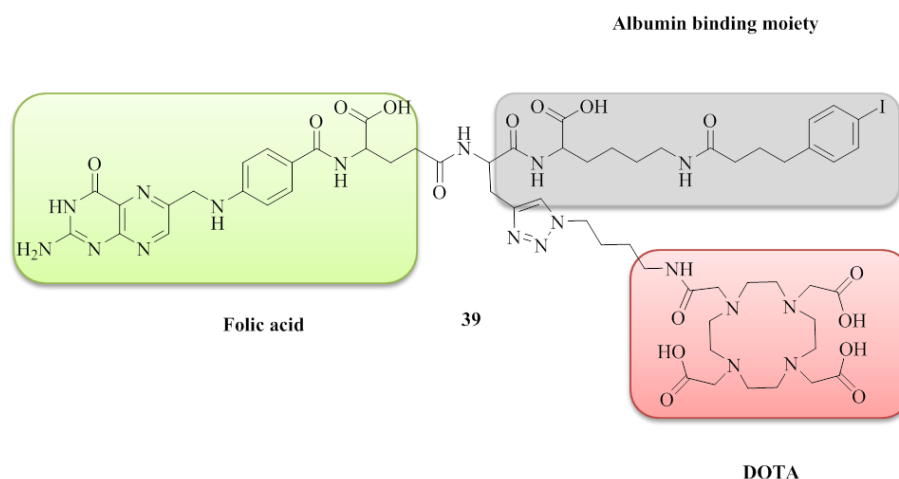


Figure 18: Chemical structure of DOTA-folate conjugated with albumin binding moiety.¹²³

Furthermore, in 2017 Siwowska together with Müller investigated further the role of albumin binding moiety as well as the spacer between it and folic acid.¹²⁵ They evaluated the two compounds with different types of spacer: compound **41** with longer PEG-11 chain, and compound **40** with a short alkane chain. These studies revealed that the spacer length plays a critical role in terms of tissue distribution of the folate conjugate. The compound containing the alkyl chain showed increased albumin binding interactions in comparison to PEG derivative. The studies also confirmed a general high tumor uptake and *in vitro* stability of all the albumin-binding entities compared with the reference compound without albumin binder.¹²⁵

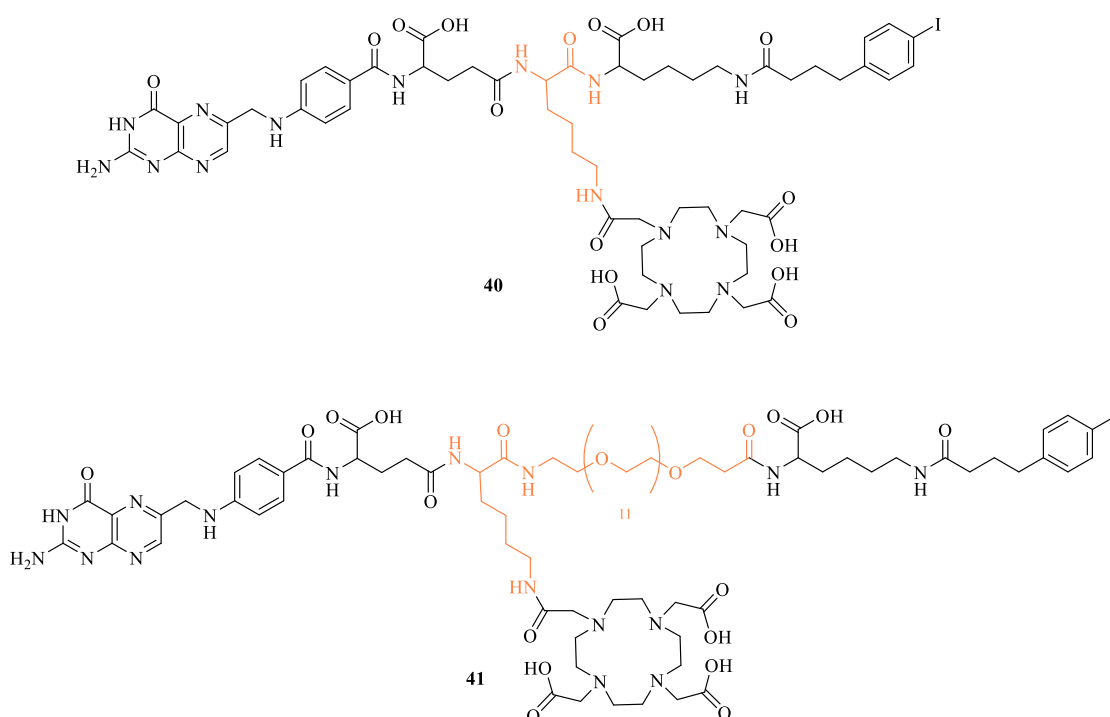
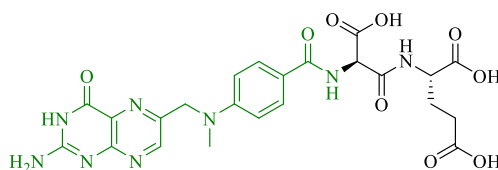


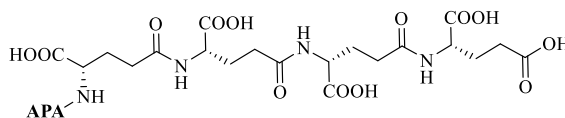
Figure 19: DOTA-folate conjugates with shorter (**40**) and longer (**41**) spacer groups.¹²⁵

1.3.1 Folates for PSMA targeting

Mhaka *et al.* combined the receptor and enzyme function of PSMA in the prostate tissue, and developed a folate-based PSMA ligand.^{126,127} They used the prodrug concept which is composed of a chemotherapeutic methotrexate fragment AMPte (green, Figure 20) coupled with a peptide chain that can be activated exclusively by the hydrolysis *via* the enzymatic activity of PSMA.



AMPte-Asp- α -Glu, 42



AMPte-Glu- γ -Glu- γ -Glu- γ -Glu, 43

Figure 20: Folate-based analogs for PSMA targeting.^{126,127}

Small NAAG-like α -dipeptides (Asp- α -Glu), as well as poly- γ -Glu peptides, were coupled to AMPte in order to find the optimal substrate for PSMA. The advantage of this system is that AMPte is commercially available and inexpensive in large quantities. Besides, hydrolysis of peptides can be followed by HPLC since this compound contains UV active groups. The outcome was that compounds with very long peptide chains were not significantly hydrolyzed to AMPte-Glu by PSMA. This was explained by the fact that these folate analogs were transported into the cells *via* folate-specific uptake that is independent of PSMA hydrolysis. It was also hypothesized that the potential PSMA ligands should contain additional acidic amino acids (glutamic or aspartic), thus providing a charged molecule that shouldn't cross the cell membrane before hydrolysis of the peptide by PSMA.

Coward *et al.* reported synthesis of a folate-GPI derivative that inhibits FPGS.¹²⁸ However, as PSMA recognizes GPI, this model can serve for further development of folate analogs for PSMA targeting. In this structure, the scaffold of folic acid is mimicked by AMPte (green,

Figure 21), and polyglutamate with GPI (blue, Figure 21). This concept allowed the inhibition of FPGS with $IC_{50} = 0.12 \text{ nM}$.¹²⁹ In addition, this work reports a first stereoselective synthesis of GPI, as well as coupling to known heterocyclic inhibitors of FPGS.

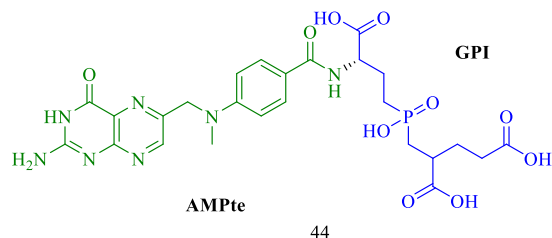


Figure 21: Structure of folate-GPI analog by Coward *et al.*¹²⁸ NUMBER BOLD

2 Aims and Objectives

Targeting tumor-specific cell surface epitopes, so-called tumor markers, with small molecules can lead to improved tools for cancer diagnosis and therapy. Elevated levels of PSMA are used as a tumor marker for prostate cancer diagnosis.⁶³ PSMA has been found to act as a folate hydrolase and thus can recognize folylpolyglutamates.⁶² GPI (shown in blue, Figure 22) binds selectively to PSMA^{95,130} and imitates the polyglutamate sequence (highlighted also in blue, Figure 22) of folic acid. The aim of this thesis is the development of new folate-GPI derivatives to generate high-affinity modular PSMA binders for tumor targeting. As mentioned before, thorough investigations of GPI and its specific binding affinities are the key to the target-driven treatment of prostate cancer. However, sole GPI shows poor binding affinity *in vivo*.^{95,130} In order to overcome these limitations of GPI there is a need for modular ligand systems with functional groups that provide additional interactions in the active site of PSMA. In this work, synthesis of a modular ligand system combines structural features of folates (green, Figure 22) with the known ligand GPI (blue, Figure 22) and a spacer with a conjugation site for effector molecule. These structures were supposed to combine favorable binding characteristics of both structural elements and could thus overcome known limitations of GPI for *in vivo* applications. The core of new PSMA ligands is a hybrid structure folate-GPI. An important design criteria of these hybrid structures was modularity to allow functionalization with effector molecules such as chemotherapeutics for targeted cancer therapy, fluorescent dyes or metal chelators for targeted cancer imaging. As already shown in the literature, conjugation of spacer group in glutamate part of the PSMA ligands leads to decreased binding affinity. Therefore, in this work, the spacer unit is conjugated *via* amino group of an aminobenzoic acid part and is terminated by a primary amine which allows the conjugation with effector molecules. There are three main tasks in order to address the hypothesis of this thesis. Firstly, docking studies have to be pursued in order to find the optimal structures that can fit into the PSMA binding site. The selected substances have to be further synthesized and analyzed. The last step is the binding affinity evaluation of all the synthesized substances, *via* biological assays. For that purpose, the folate-GPI hybrid has to be conjugated with a metal chelator DOTA as an effector molecule.

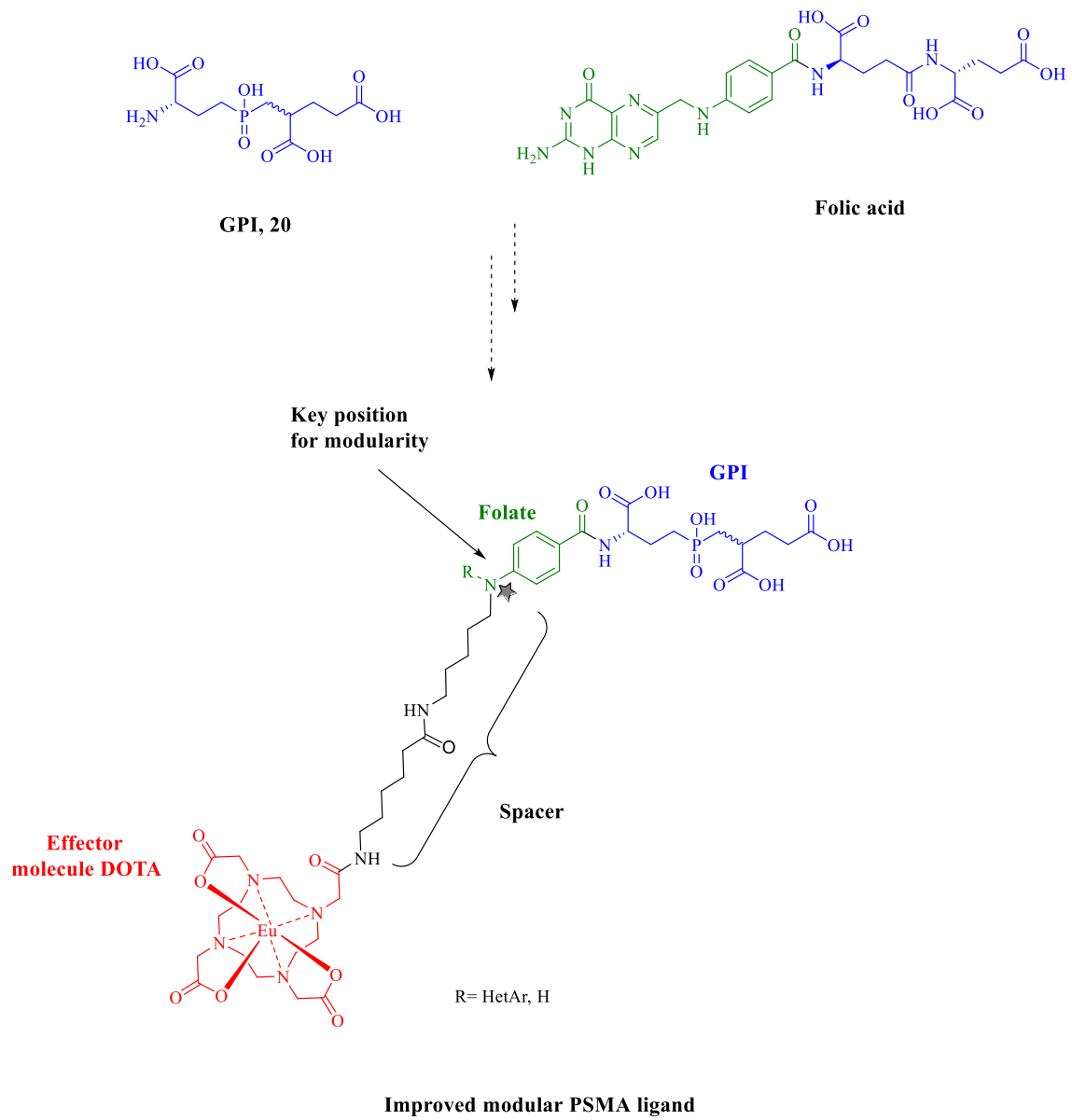
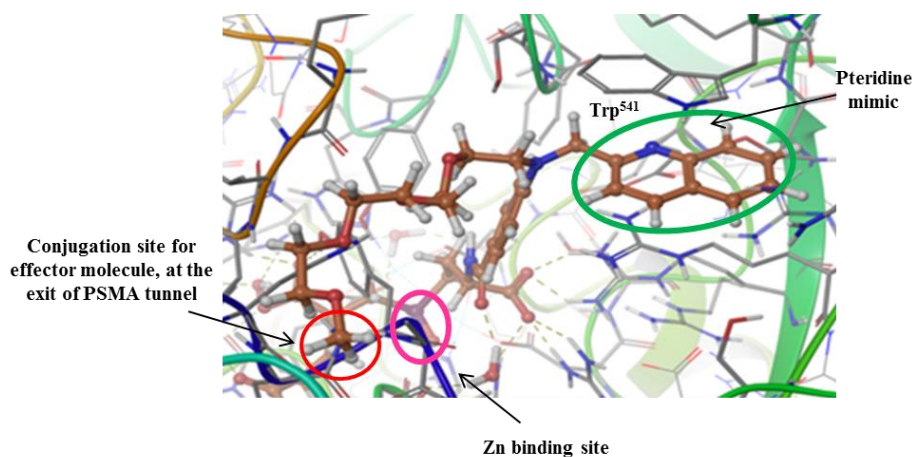


Figure 22: Design of novel folate-GPI derivatives.

3 Results and Discussion

3.1. Docking studies

The design of new hybrid targeting vectors is firstly verified through docking studies. As already mentioned these vectors contain a folate scaffold, a NAAG mimic derived from the known PSMA ligand GPI and contain a linker moiety terminated by a primary amine for the conjugation of effector molecules such as radiometal chelators, dyes or cytotoxic moieties (Figure 23). Docking analysis of known modular PSMA binders suggested the aniline nitrogen as a good anchor group for attachment of linkers to the effector molecule without compromising the binding affinity to PSMA.^{95,130} Molecular modeling studies in cooperation with Dr. Thomas Lemcke, showed that the binding affinity of GPI can be improved by conjugating structural elements of folate, thus enabling additional π stacking in a hydrophobic pocket of PSMA with Trp⁵⁴¹. A suggested scaffold for these modifications is a hybrid structure 45, shown in Figure 23. Chinoline derivatives are well-known mimics of the pteridine structure motive found in folate derivatives (circled in green, Figure 23).⁴³ These heteroaromatic moieties can additionally be conjugated with effector molecules at the end of the spacer unit (encircled in red) to form modular ligand systems. Earlier modifications of folic acid derivatives were mostly performed *via* functionalization of carboxylic groups in glutamate rest, which compromises binding affinity.^{115,117,120,121,131} However, this work focuses on aniline nitrogen (highlighted with grey star, Figure 23) as a key position for further structure modification.



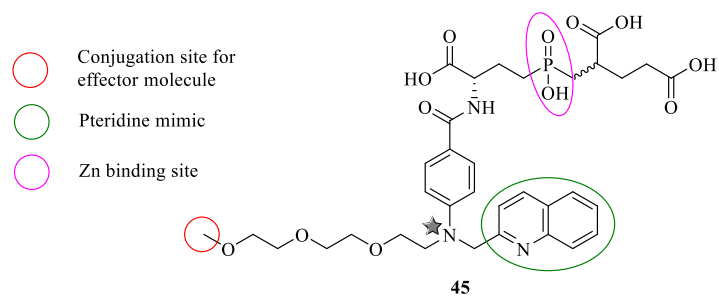


Figure 23: Molecular modeling of folate mimic **45** with key interactions and functional groups.

3.2. Folate-GPI hybrid with different heteroaromatic groups

Based on the docking studies of GPI the proposed scaffold of improved PSMA binders includes GPI as glutamate mimetic (blue), folate mimetic (green) and a spacer unit terminated by a primary amine (red) that allows further conjugation with effector molecule (Figure 24). For a detailed study of structure-activity relationships of hybrids **46**, general short synthesis is needed, which would allow structural variation to build up a small library of test compounds. There are two main parts of the structure that can be varied. The aniline nitrogen is a good anchor group for attachment of variable heteroaromatic moieties, as well as a spacer unit. Simple heteroaromatic residues like chinolyl or pyridyl are suitable pteridine replacements for the synthesis of folate mimics, due to their structural similarity and their commercial availability. Despite indications that functionalization of the benzylamine in folate may improve binding affinity to PSMA, only a few examples of these type of PSMA-ligands are known (most of them *N*-methylated derivatives).^{128,132} Another part of folate-GPI hybrid that can be altered is *p*-aminobenzoic acid. There are several references in the literature for this type of modification.^{92,133-135}

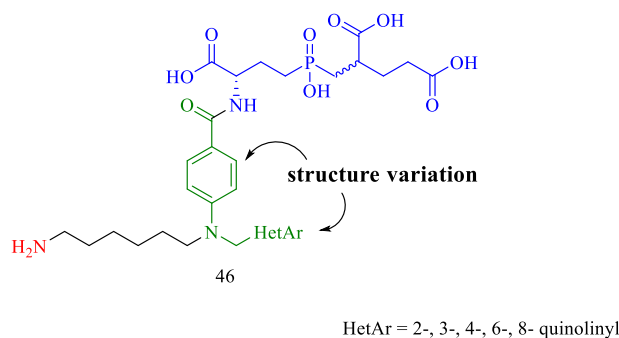


Figure 24: Proposed scaffold of new folate mimetics. **Bold number**

The retrosynthetic concept to the tailored folate analog, shown in Figure 25, involves the formation of the secondary amine **50** in the first step, which would be assembled from a suitable and commercially available primary amine **51** and a heteroaromatic aldehyde **52** *via* reductive amination. The following step involves an arylation of the secondary amine **50** with 4-bromobenzoic methyl ester **49**. This step is crucial since it builds the core for a modular ligand system. Moreover, this step is also very challenging because the complex nature of heteroaryl-substituted secondary amines can cause lower reactivity for this reaction. Subsequent

deprotection of methylester **48** allows further coupling with GPI **20**. The coupling of GPI **20** with tertiary amine **47** also represents another synthesis challenge. Carboxyl groups of glutamate rest are essential for the binding in PSMA active site. Therefore, the primary amine of GPI **20** has to be coupled to free carboxylic acid of **47**. Using GPI with protected carboxyl groups for the coupling with **47** would consider hydrolysis of all protecting groups in the final step. The hydrolysis of protected GPI goes under harsh conditions (6M HCl), which is incompatible with the highly functionalized folate-GPI conjugate. Therefore, the coupling reaction has to proceed with the unprotected GPI. Lastly, Boc deprotection of primary amine allows further conjugation with effector molecule.

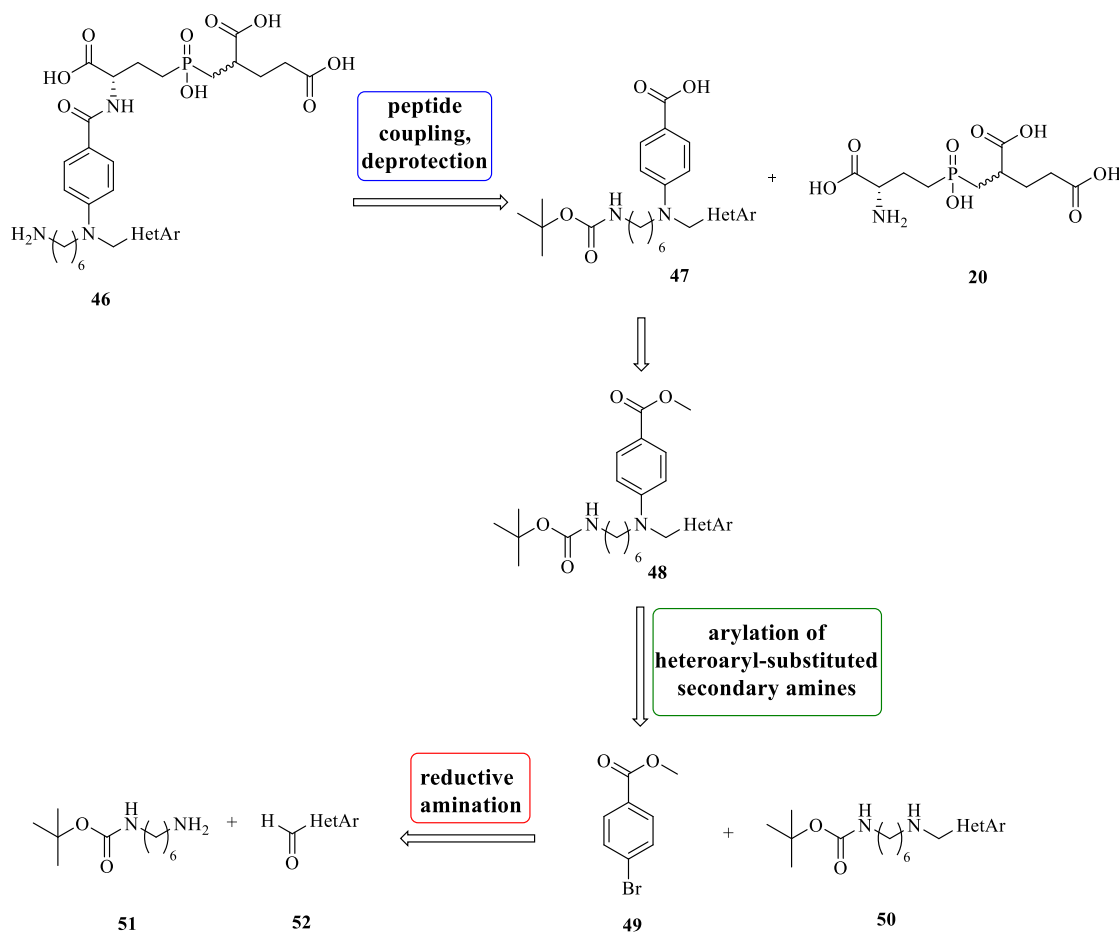


Figure 25: Retrosynthesis design of novel folate mimics. **20 bold!**

3.2.1. Synthesis of secondary amines

Secondary amines with different heteroaromatic moieties (**50a-f**) were obtained *via* reductive amination of suitable aldehydes (**52**) and primary amine (**51**) following the protocol of Nasr *et al.*¹³⁶ The commercially available primary amine **51** and the aldehyde **52** were stirred under

reflux for 48 h in methanol, to ensure complete conversion to the imine. In the following step, the formed imine was reduced with NaBH₄ to the corresponding secondary amine. Figure 26 shows a general reaction scheme for this synthesis and the obtained yields for each derivative.

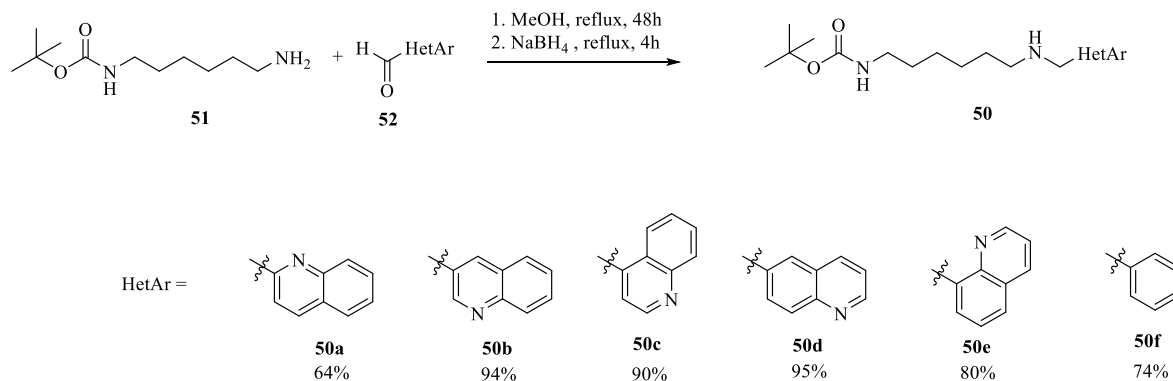


Figure 26: Synthesis of secondary amines via reductive amination.

3.2.2. Synthesis of tertiary benzylamines

Synthetic routes to the required tertiary *N*-aryl benzylamine **48** include arylation of secondary benzylamines. Traditional approaches consider nucleophilic aromatic substitution (S_NAr)¹³⁷, the Cu-catalyzed Ullmann-coupling reaction and reductive amination. All of these methods require harsh conditions and show low substrate scope that often leads to low region selectivity and low reactivity.¹³⁸

First attempts involved nucleophilic displacements or reductive aminations of secondary anilides, but both approaches were either impaired by the low nucleophilicity of the secondary anilides or the lack of appropriate precursors. These findings forced a switch of the synthetic strategy to a late stage introduction of the central aniline motif by a Pd-catalyzed (Buchwald-Hartwig) arylation of intermediate secondary benzylamines.

Transition metal-catalyzed cross-coupling and particularly Pd-catalyzed reactions such as the Buchwald-Hartwig arylation are among the most attractive approaches in this field. The mild conditions and the broad reaction scope, combined with good functional group tolerance, make these conversions attractive in academia and pharmaceutical industry.¹³⁹⁻¹⁴² The mechanism of this type of reactions described by Hartwig is shown in Figure 27.¹⁴³ The first step in the catalytic cycle is the oxidative addition of Pd(0) species to the aryl halide (**a**). Two different reaction pathways are suggested starting from the Pd(II) species. The first pathway postulates addition of the amine (**b**) which results in the formation of the Pd(II) arylamine complex (**c**).

The last step of this pathway includes deprotonation followed by reductive elimination. In the second pathway, the base is added after the analogous oxidative addition and leads to the complex **b'**. In the following step, the amine is deprotonated by the Pd-coordinated base and added to a Pd-Ar complex. Finally, complex **c** is obtained again, as in the previously described pathway.

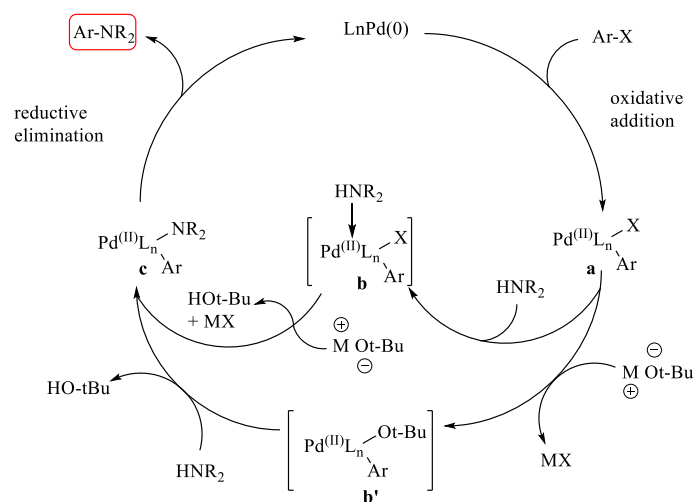


Figure 27: General mechanism for Pd-catalyzed N-arylation.¹⁴³

A very frequent side reaction can occur during the reductive elimination, where the amine undergoes β -hydride elimination to generate an imine and a Pd(II) aryl hydride. A major problem if sterically hindered secondary amines are used as starting materials is the formation of the reduced arene and regenerated Pd(0) (Figure 28).¹⁴³ Bulky bidentate Pd-ligands like XPhos, DavePhos and SPhos are known to accelerate the overall rate of arylation and enhance reductive elimination relative to β -hydride elimination.¹⁴⁴

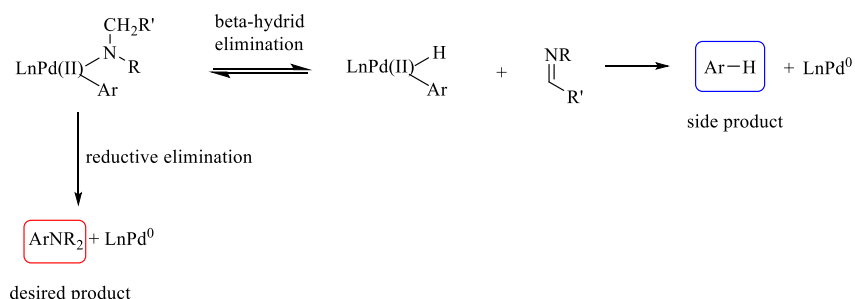


Figure 28: β -Hydride elimination as a side reaction to reductive elimination.^{143,145}

In 1997 Buchwald *et al.* published one of the first procedures for the cross-coupling of a wide range of amines and aryl bromides. Standard conditions use a Pd source such as Pd(OAc)₂, BINAP as a ligand and a suitable base, most commonly Cs₂CO₃ (Figure 29).¹⁴⁴

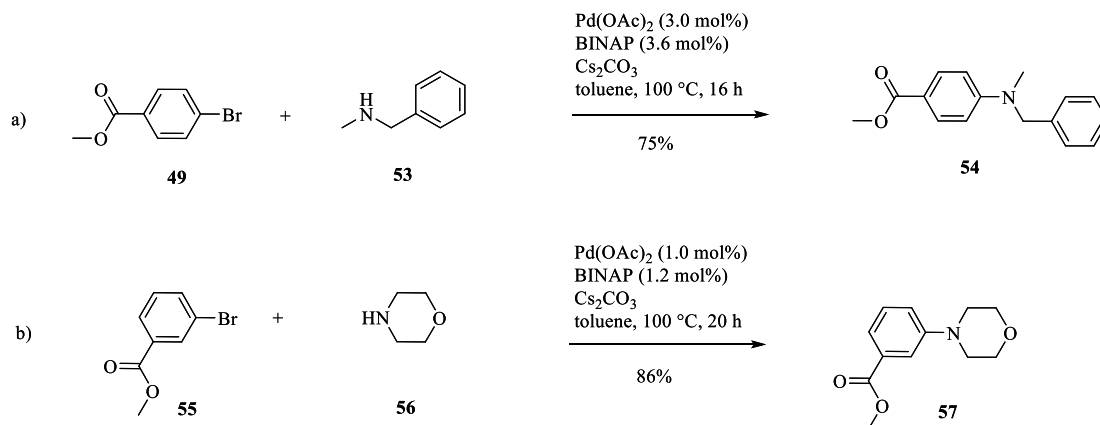


Figure 29: One of the first practical protocols for the coupling of amines with aryl halides by Buchwald *et al.*¹⁴⁴

Based on these results, the “first-generation” of Buchwald-Hartwig catalyst systems were soon established and over the last decade expanded to more sophisticated phosphine ligands. Whereas “first-generation” conditions for primary amine alkylation were based on chelating ligands such as BINAP (**L6**) or DPPF (**L5**) which occasionally lead to imine byproducts, the focus shifted to simple PR₃ (**L4**, **L6**) or PAr₃ (**L5**, **L7**) ligands (Figure 30).^{143,146}

The third generation of ligands are dialkylbiarylphosphine ligands (**L8-L14**). They can be strongly varied by different alkyl groups on the phosphorus atom and substituents on the biaryl system and thus offer highly tailored catalyst systems.¹⁴⁷

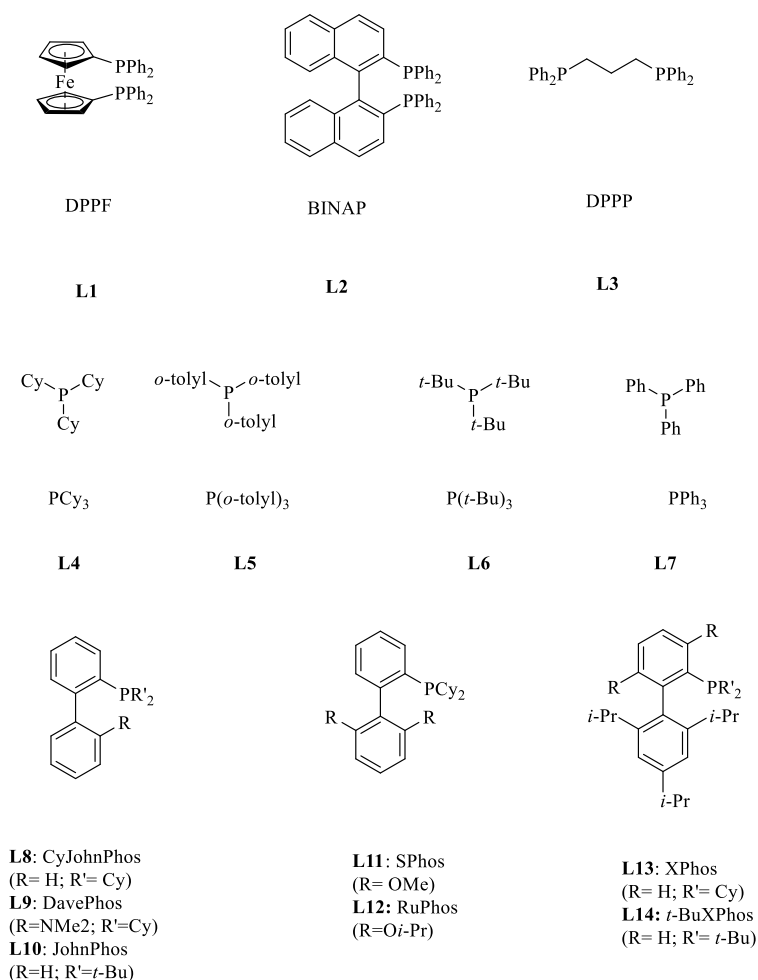


Figure 30: Most prominent phosphine ligands for Pd-catalyzed Buchwald-Hartwig cross-coupling reactions.

The latest generation consists of precatalysts, which are activated under the normal reaction conditions, e.g. through the added base (Figure 31).¹⁴⁸⁻¹⁵⁵ Buchwald *et al.* designed precatalysts that require lower temperatures, less catalyst loading and shorter reaction times for arylation than comparable catalyst systems. A list of frequently used precatalysts (**P1-4**) is shown below:

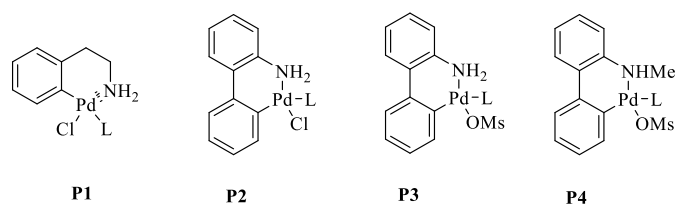


Figure 31: The latest generation of Buchwald-Hartwig catalyst systems.

In this work, the Buchwald-Hartwig arylation has been utilized for the synthesis of multifunctional tertiary amines **48**. The general scheme of the reaction conditions is shown in Figure 32.

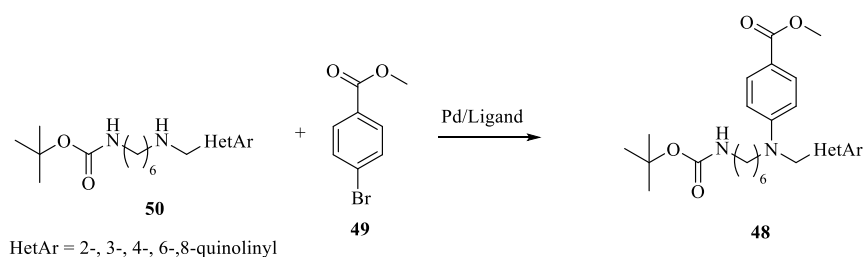


Figure 32: General conditions of Buchwald-Hartwig reaction for the synthesis of folate mimics.

The synthesis of multifunctional tertiary amines bearing a benzylic position and a heteroaromatic system *via* Pd-catalyzed cross-coupling reactions has not been reported in the literature. Based on the experience that secondary benzylamines are highly challenging substrates for Buchwald-Hartwig arylations, numerous conditions were examined to obtain the desired tertiary *N*-aryl benzylamine. The secondary amine **50a-f** were submitted to Pd-catalyzed arylation with aryl bromide **49** under typical Buchwald-Hartwig conditions.^{140,156} The outcome of these initial attempts was quite poor with a low conversion of starting amines **50a-f**. In addition, rather complex mixtures of products were obtained in many cases. A representative example is shown in Figure **33** with the conversion of secondary amine **50a**. The reaction process was found to be unselective and we observed an incomplete conversion of starting materials resulting in the formation of rather complex product mixtures.

Next to expectable side products such as benzoic acid ethyl ester (dehalogenated arylbromide) or degradation products, derived from β -hydride elimination, we identified three different arylation products **58-60**. Besides the desired *N*-arylated product **58**, the regioisomeric products (*N*-Boc arylated) **59** and a *C*-arylated product **60** were also identified and characterized.

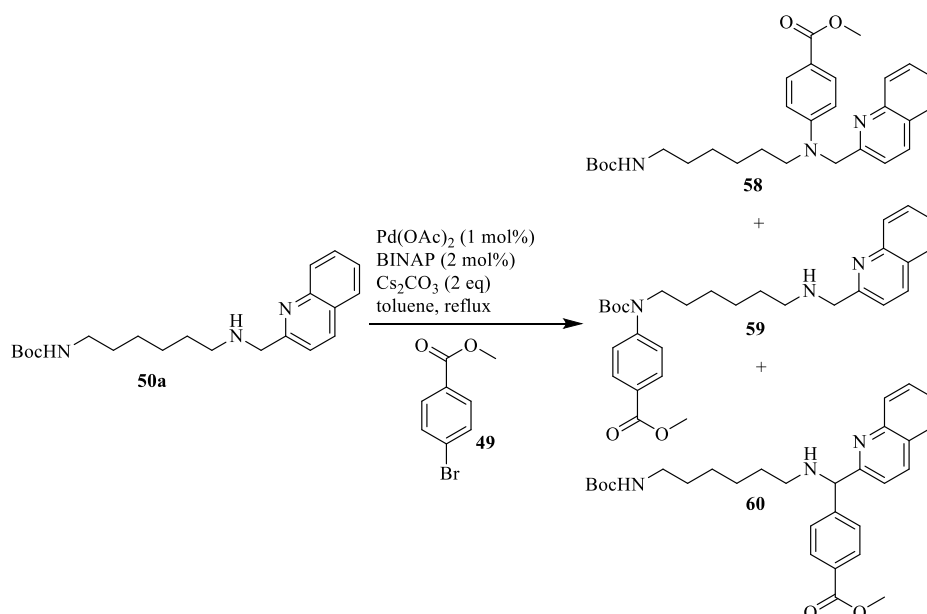
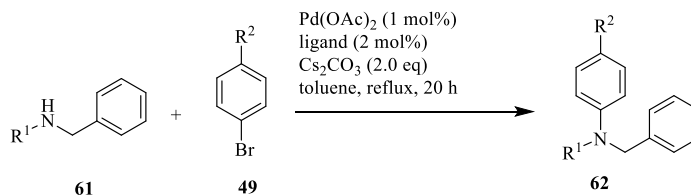


Figure 33: The observed mixture of products with secondary amines **50**.

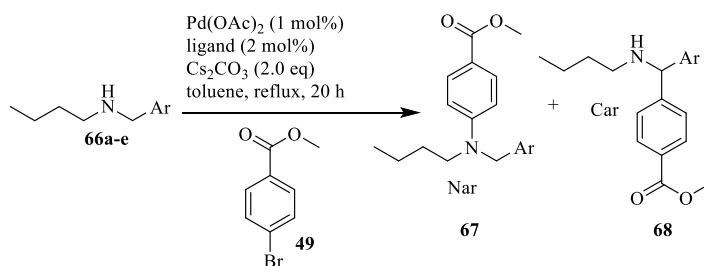
In order to clarify the role of the structural elements in arylation substrates **50a-f** for chemoselectivity of the arylation reaction, the structural complexity of the starting materials was reduced to simple benzylamines **61**. For this purpose, Sarah Chandralingam was investigating new reaction conditions. The standard reaction conditions were used for Pd-catalyzed arylation of secondary amines with different Pd-ligands (Table 1).¹⁴⁴ As shown in Table 1, the reactions with different ligands proceeded smoothly and the *N*-arylated products **62** were obtained with good yields (entries 1-8). Moreover, the arylations of bulky secondary amines such as *N*-benzylbutan-1-amine were still clean, but show a rather slow conversion of starting materials. A conversion of 66% was observed after 20 h of reflux in toluene to give **62d** in 55% yield (entry 4). The application of more recent ligands such as XPhos, CyJohnPhos, DavePhos, and SPhos (entries 1 and 5-8) showed particularly clean conversions due to a significant reduction of the main side reaction (β -elimination). These bulky, monodentate ligands are known to accelerate the overall rate of arylation and enhance reductive elimination relative to β -hydride elimination.¹⁵⁷ It is notable, that only *N*-arylation was observed and no *C*-arylation in benzylic position in this set of experiments.

Table 1. Pd-catalyzed arylation of benzyl amines **61**.

Entry	R ¹	R ²	Ligand	Conversion % (62 , Yield %)
1	Ph	H	XPhos	90 (62a , 88)
2	Me	H	BINAP	78 (62b , 23) ¹⁴⁴
3	Me	CO ₂ Me	BINAP	95 (62c , 90)
4	nBu	H	BINAP	66 (62d , 53)
5	Me	H	XPhos	83
6	Me	CO ₂ Me	CyJohnPhos	100 (62c , 70)
7	Me	CO ₂ Me	DavePhos	84
8	Me	CO ₂ Me	SPhos	100 (62c , 88)

[a] Conversion of starting material **61** as measured by ¹H-NMR of the crude product. [b] Yield of isolated product **62** after chromatography.

In a further set of test experiments, heteroaryl moieties were introduced into the arylation substrates **66a-e** (Table 2). The unusual *C*-arylation of the 2-chinolinyl substrate **66d** was confirmed in benzylic position to product **68** (Table 2, entries 1-3). This chemoselective reaction was independent of the choice of Pd-ligand used and quite specific for the arylation of 2-chinolinyl substituted substrate **66d**. A corresponding *C*-arylated reaction product was observed only for arylations of 2-pyridinyl substituted amine **66a**, which again gave mixtures of *N*- and *C*-arylated products **67** and **68** (Table 2, entries 6 and 7). However, in this case, only small quantities of the *C*-arylated product were observed in the crude NMR and by HRMS analysis. There is limited precedence for Pd-catalyzed *C*-arylations in benzylic positions in the literature. The known examples are limited to electron poor benzylic positions with no competing reactive functionalization.¹⁵⁸⁻¹⁶¹

Table 2. Pd-catalyzed arylation of secondary amine **66**.

Entry	Ar	Ligand	Ratio ^[a]	Yield
			14:15	(adduct)
1	2-chinolyyl	CyJohnPhos	0:100	(15d) 41% ^[c]
2	2-chinolyyl	PCy ₃	0:100	(15d) 12% ^[c]
3	2-chinolyyl	SPhos	0:100	(15d) 26% ^[b]
4	4-chinolyyl	BINAP	100:0	(14e) 41% ^[c]
5	4-chinolyyl	CyJohnPhos	100:0	(14e) 57% ^[b]
6	2-pyridyl	BINAP	95:5	(14a) 58% ^[b]
7	2-pyridyl	PCy ₃	95:5	(14a) 26% ^[c]
8	3-pyridyl	BINAP	100:0	(14b) 57% ^[b]
9	3-pyridyl	PCy ₃	100:0	(14b) 54% ^[c]
10	3-pyridyl	PPh ₃	100:0	(14b) 36% ^[c]
11	4-pyridyl	dppf	100:0	(14c) 17% ^[c]
12	4-pyridyl	BINAP	100:0	(14c) 12% ^[b]

[a] Ratio of products, established by ¹H-NMR analysis of the crude reaction mixtures. [b] Isolated yield. [c] Yield established by ¹H-NMR analysis of the crude reaction mixtures.

Recently, Walsh has reported Pd-catalyzed benzylic C-arylations of azaarylmethylamines, bearing tertiary and therefore unreactive amines (Figure 34).¹⁶² They stated that neither addition nor removal of directing groups was necessary for facilitating the yields, except that sterically more hindered substrates failed to provide the desired product. However, under Buchwald Hartwig conditions, C-arylation in the presence of a competing N-arylation site (reactive secondary amine) has, to the best of our knowledge, not been reported so far.

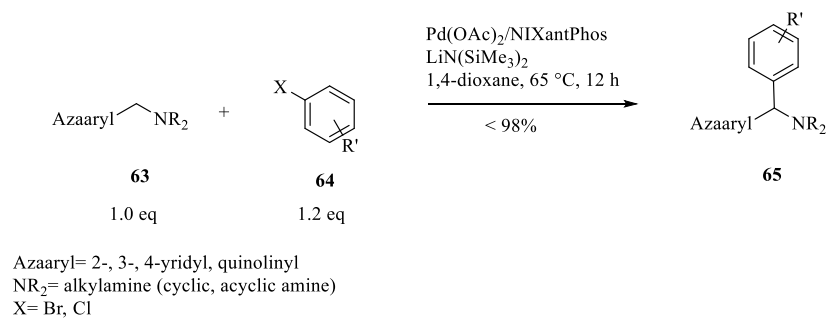


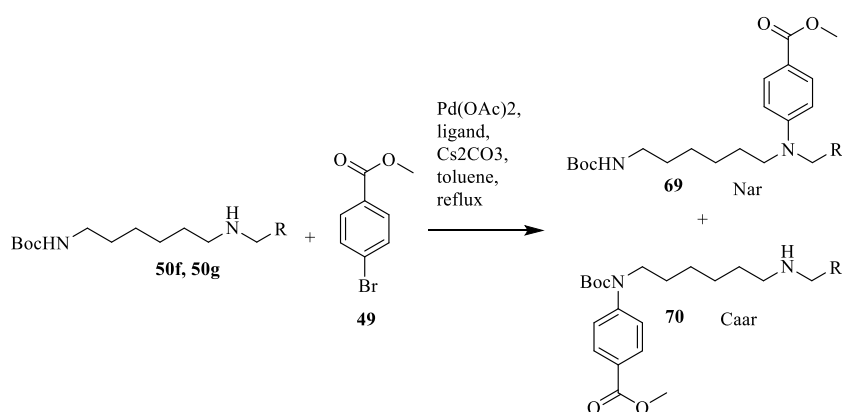
Figure 34: C-H-Functionalisation of (azaaryl)methylamines **63** by Walsh *et al.*¹⁶²

The unique reactivity of substrates like **66d** is most likely a consequence of the relatively high CH-acidity in the benzylic position combined with chelation assistance of the 2-azaarylmethylamine moiety. 4-chinolyl substituted substrate **66e**, in contrast, gave only the initially expected *N*-arylation to tertiary amine **67** (Table 2, entries 4 and 5). The same trend was observed with pyridyl substituted amines **66b** and **66c** (Table 2, entries 8-12). It is notable that conversions of heteroaryl-substituted starting materials **66a-e** were all lower than those for benzylamines **61** shown in Table 1. However, the obtained yields of 48-56% for products **14-15** are still in an acceptable range.

Next set of experiments included substrates that combined a Boc-protected aminoethyl residue with a benzyl or a cyclohexyl group in arylation precursors **50f**, **50g** (Table 3). The compounds were again submitted to Buchwald Hartwig arylation with different ligands (Table 3). After a short screening of solvents (toluene, THF, DMF, DME, MeCN) and bases (Cs₂CO₃, LiHMDS, K₃PO₄, K₂CO₃, KOtBu, NaOtBu), the reaction conditions depicted in Table 3 were the most efficient. Interestingly, the regiochemistry of arylation was dependent on the choice of Pd ligand. Arylations with classic chelating ligands like BINAP or dialkylbiarylphosphine ligands like SPhos gave excellent selectivity for arylation of the (more acidic) carbamate *NH* to give *N*-arylcarbamates **70**. This is in the alignment with observations of Buchwald on the selective Pd-dialkylbiarylphosphine-catalyzed arylation of more *NH*-acidic anilines compared to alkylamines.¹⁶³ However, in a related study, Buchwald has observed preferential Pd-catalyzed arylation of (non-hindered) anilines in the presence of competing carboxamides with dialkylbiarylphosphine ligands such as SPhos or XPhos.¹⁶⁴ These findings may be rationalized with a delicate influence of the binding ability of the nitrogen nucleophile to the Pd-catalyst (determined by its nucleophilicity) and deprotonation of the resulting amido-Pd-complex (determined by *NH* acidity). It is interesting to note, that monodentate ligands such as PCy₃ and PPh₃ led to a complete switch in chemoselectivity. With these ligands, substrates **50f**, **50g** were converted to arylamines **69** (Table 3, entries 1, 8 and 9). Compared to all model reactions before,

the introduction of the Boc-protected aminoethyl substituent in **50f** and **50g** led to less clean conversions which might be due to partial Boc-cleavage under alkaline conditions in refluxing toluene.¹⁶⁵

Table 3. Pd-catalyzed arylation of secondary amines **50f**, **50g**.



entry	R	ligand	Ratio ^[a]	Yield
			16:17	(adduct)
1	phenyl	PCy ₃	100:0	(69f) 11% ^[b]
2	phenyl	BINAP	0:100	(70f) 24% ^[b]
3	cyclohexyl	BINAP	0:100	(70f) 19% ^[c]
4	cyclohexyl	dppf	0:100	(70f) 0.6% ^[c]
5	cyclohexyl	JohnPhos	0:100	(70f) 22% ^[c]
6	cyclohexyl	SPhos	0:100	(70g) 24% ^[b]
7	cyclohexyl	XPhos	0:100	(70g) 36% ^[c]
8	cyclohexyl	PCy ₃	100:0	(69g) 17% ^[b]
9	cyclohexyl	PPh ₃	100:0	(69g) 54% ^[c]

[a] Ratio of products, established by ¹H-NMR analysis of the crude reaction mixtures. [b] Isolated yield. [c] Yield established by ¹H-NMR analysis of the crude reaction mixtures..

This selectivity trend might suggest that steric factors contribute to the selectivity of arylation next to the basicity of NH groups. Wolfe has noticed a preference of chelating ligands like dpePhos or BINAP for carbamate conversion over arylation of secondary amines in Pd-catalyzed domino cyclizations of alkenylamines or alkenylcarbamates, which is in agreement

with our findings.¹⁶⁶ Both arylation products can be easily distinguished by their ¹H-NMR spectra (Figure 35) due to a pronounced difference in chemical shifts for the benzylic protons (pink arrow) from 3.78 ppm (*N*-aryl carbamate **70f**), to 4.60 ppm for the tertiary amine **69f**. Moreover, the N-H signal of free secondary amine in **70f** appears at 2.94 ppm, whereas for **69f**, that signal doesn't appear in the spectrum. Additionally, the proton signal from *NH*-Boc in **70f** appears in form of a broad singlet at 4.49 ppm. Aromatic areas of these products also differ for the signal shifts of proton signals in *ortho* position of the phenyl ring (orange arrow).

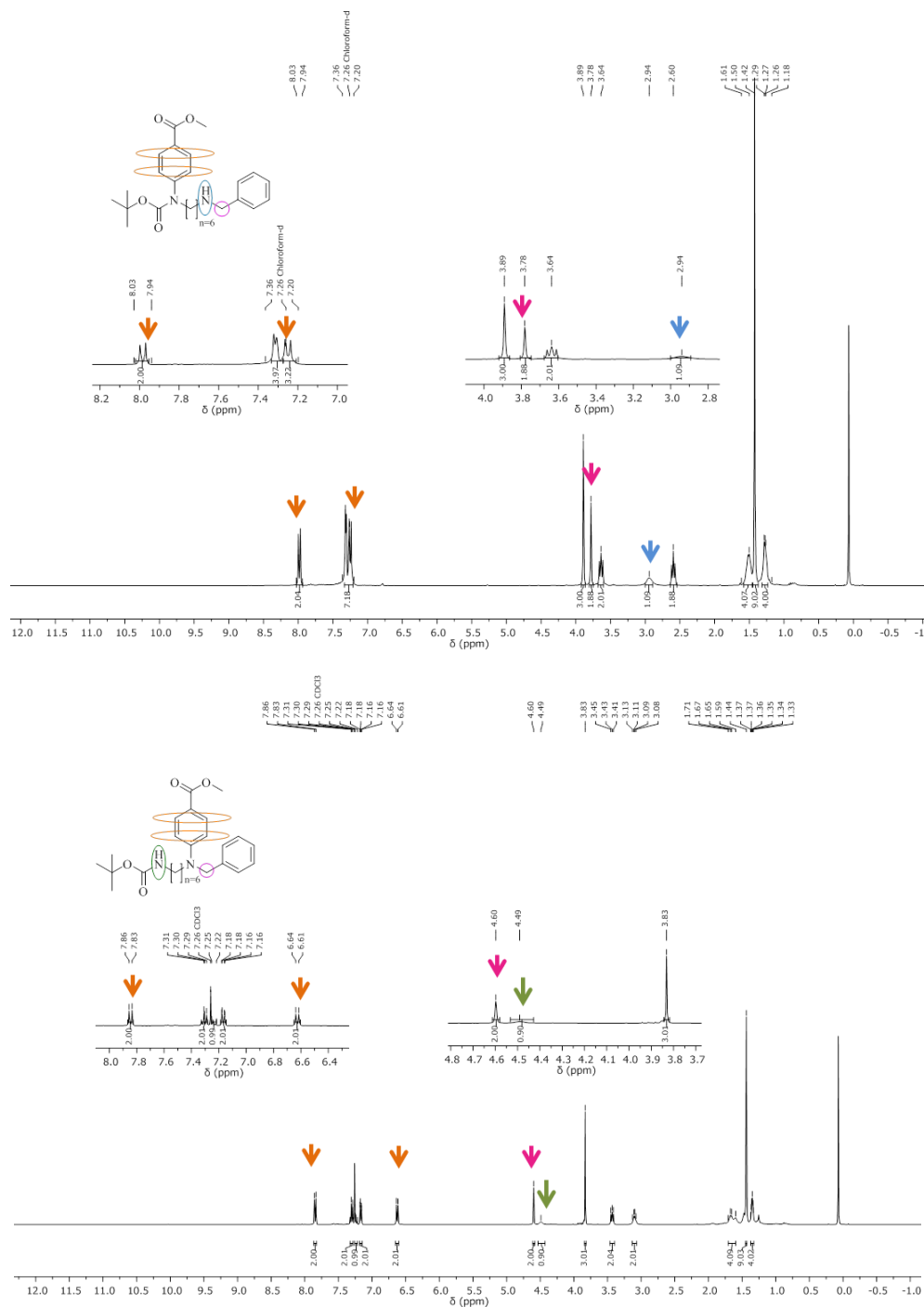
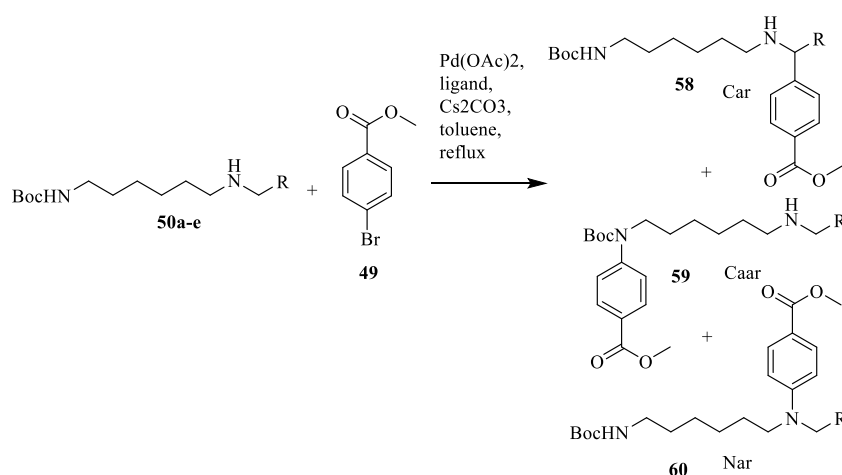


Figure 35: ¹H-NMR spectra of **68f** and **70f**.

After the screening studies of the folate mimics bearing benzyl and cyclohexyl group, the next step was to investigate the influence of the substrates bearing 2,3,4,6,8- chinolyl moieties (**50a-e**). The focus of this investigation was also finding the optimal conditions for synthesis of desired *N*-arylated folic mimics with chinolynyl moieties, suggested by docking studies in chapter 3.1. A number of heteroaryl- and Boc-aminohexyl-substituted secondary amines **50a-e** were converted with arylbromide **49** (Table 4). As mentioned previously (compare Figure 33), these substrates allow arylations in three different positions. All conversions of these more complex substrates were significantly less clean, then those of the model substrates investigated before and the products were isolated in only moderate yields after chromatography. With the 2-chinolyl substituted substrate **50a**, complete selectivity for the unusual *C*-arylated product **58** was observed, independent of the Pd-ligand used. Again, *C*-arylation was exclusively observed with 2-chinolyl. This finding suggests a strong influence of chelation assistance on these type of arylations. With all other substrates, only *N*-arylations of either carbamates or secondary amines were observed. Chemoselectivity was again strongly influenced by the choice of ligand. Monodentate ligands like PCy₃ were favoring the arylation of secondary amines to give tertiary amines **60** and dialkylbiarylphosphines like SPhos favoring carbamate arylation to give arylcarbamates **59**. These results are in good agreement with the reactivity trend observed with benzylamines **50f** (see Table 3).

Table 4. Pd-catalyzed arylation of secondary amine **50a-f**.



entry	R	ligand	Ratio ^[a] 58:59:60	Yield (adduct)
1	2-chinolyl	CyJohnPhos	100:0:0	(58a) 16% ^[b]
2	2-chinolyl	XPhos	100:0:0	(58a) 41% ^[c]
3	2-chinolyl	PCy ₃	100:0:0	(58a) 48% ^[b]
4	2-chinolyl	BINAP	5:55:40	(59a) 12% ^[b]

5	3-chinolyl	Xphos	0:70:30	(59b) 53% ^[c]
6	3-chinolyl	PCy ₃	0:0:100	(60b) 55% ^[b]
7	4-chinolyl	CyJohnPhos	0:56:44	(59c) 47% ^[c]
8	4-chinolyl	PCy ₃	0:0:100	(60c) 56% ^[b]
9	6-chinolyl	dppf	0:60:40	(59d) 48% ^[b]
10	6-chinolyl	PCy ₃	0:45:55	(60d) 15% ^[b]
11	8-chinolyl	dppf	0:100:0	(59e) 77% ^[c]
12	8-chinolyl	PCy ₃	0:8:92	(60e) 45% ^[c]
13	8-chinolyl	XPhos	0:100:0	(59e) 24% ^[b]
14	8-chinolyl	CyJohnPhos	0:100:0	(59e) 71% ^[c]
15	8-chinolyl	SPhos	0:73:27	(59e) 21% ^[c]

[a] Ratio of products, established by ¹H-NMR analysis of the crude reaction mixtures. [b] Isolated yield. [c] Yield established by ¹H-NMR analysis of the crude reaction mixtures.

Proton and two dimensional NMR investigation verified the C-arylation (Figure 36) as well as *N*-Boc arylation (Figure 37) with the substrate **50a**. The distinct proton signal at 5.07 ppm of the benzylic position (orange encircled) coupled with carbon at 67.6 ppm clearly shows in HSQC red signal of trisubstituted carbon for **58a**. In addition, *N*-Boc arylated product **59a** shows a proton signal at 4.06 ppm (dark red encircled) coupled with carbon at 54.1 ppm, as well as the blue signal in HSQC of disubstituted carbon, shown in Figure 37.

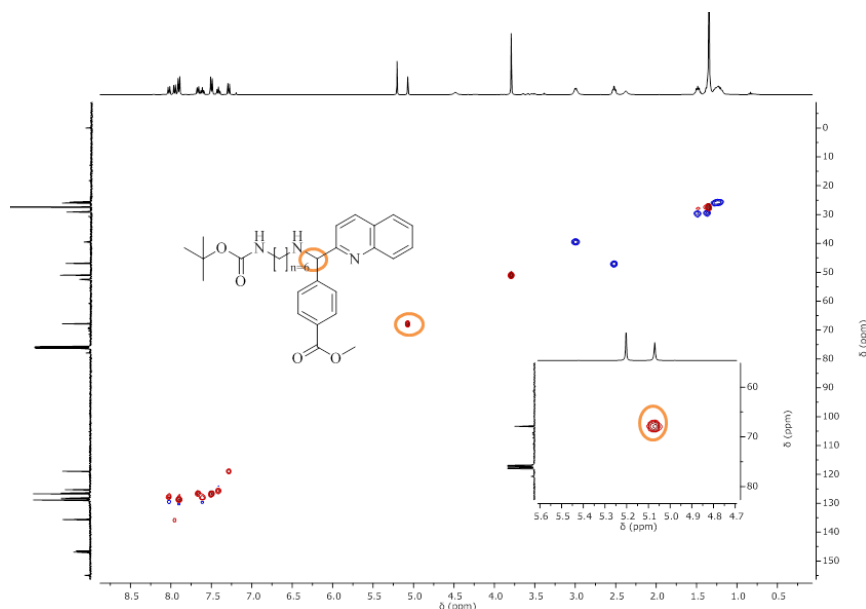


Figure 36: HSQC spectrum of C-arylated (**58a**) product.

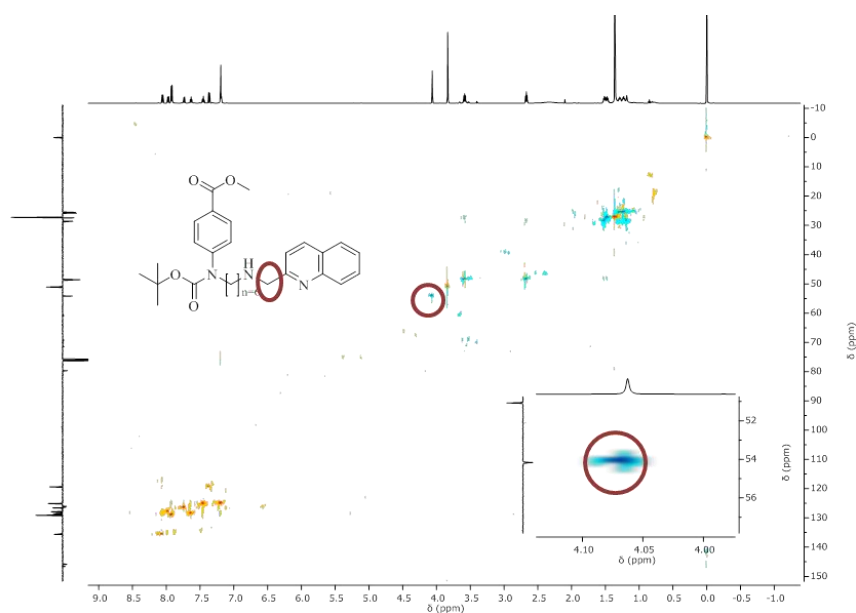


Figure 37: HSQC spectrum N-Boc arylated (**59a**) product.

An additional minor side product was detected for some of the arylation reactions depicted in Table 4. Particularly for arylations with dialkylbiarylphosphine ligands, biarylated compound **71** was observed in small quantities. If an additional equivalent of arylbromide **8** was added, *N*-biarylated product **74** would be the major reaction product (Figure 38).

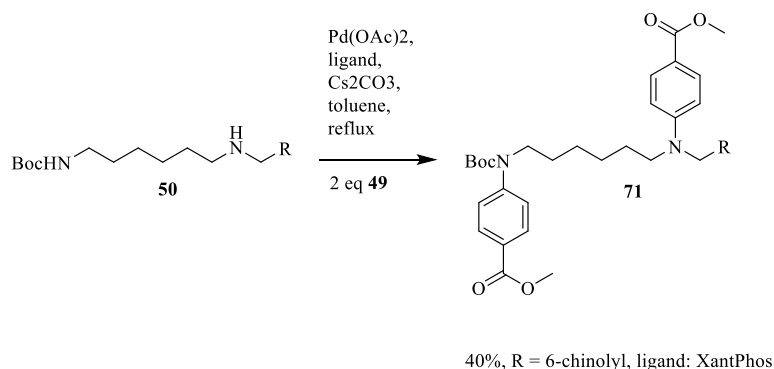


Figure 38: Pd-catalyzed biarylation of secondary amines **50**.

Secondary benzylamines are notoriously difficult substrates for Buchwald Hartwig type arylations. In particular, the functionalized derivatives bearing heterocyclic groups like pyridines and chinolines are very challenging. However, a careful choice of Pd-ligands allows the chemoselective arylation of competing groups such as carbamates, secondary amines, and strongly CH-acidic benzylic positions. As a general trend it was found that the use of monodentate Pd-ligands like PCy₃ leads to selective arylation of secondary amines. In contrast,

dialkylbiarylphosphine Pd-ligands led predominantly to carbamate arylations. Particularly challenging substrates for Pd-catalyzed arylations are heteroaryl-substituted amines like **66a-e** or **50a-e**. The CH-acidic benzylic position in these derivatives led to an increase in side reactions. With 2-chinoyl substituted amines **50a** and **66d**, a completely different arylation selectivity for the benzylic carbon was observed. These reactions gave *C*-arylated folate analogs **9** and **15**. Variants of chelation assisted Pd-catalyzed *C*-arylations of benzylamines have been reported only rarely in literature before. In these cases, no competing nucleophilic functionalities like amines or carbamates were present. The formation of *C*-arylated products like **58** and **68** was therefore unexpected. If ligands are chosen carefully, Pd-catalyzed arylations of secondary benzylamines allow the synthesis of novel *C*- and *N*-arylated structural analogs of folic acid, which are not easily accessible by other methods. These compounds are modular and allow the conjugation of modified folates to other functional molecules such as dyes or other contrast agents.

3.2.3. Synthesis of GPI

Several synthetic routes towards GPI **20** were already established by Feng, Barinka, and Coward.^{128,129,132} The first steps involved the synthesis of the two main building blocks of GPI: acryl ester **73** and phosphinic acid **75**. Following the synthesis protocols known from the literature, acryl ester **73** was obtained starting from the corresponding *tert*-butyl-acrylate **72**, *via* Baylis-Hillman reaction.^{167,168} The synthesis of the second building block **75** was performed by the protocol of Coward *et al.*¹²⁸ In the oxidative phosphorylation of the vinylglycine derivative **74** with ammoniumhypophosphite and triethylborane, the phosphinic acid **75** was obtained in a good yield. The following steps are the silylation of **75** with BSA and subsequent phosphorous Michael addition of already prepared acryl ester **73**. Lastly, the hydrolysis of all protecting groups with 6M HCl under reflux generated a diastereoisomeric mixture of GPI **20**.

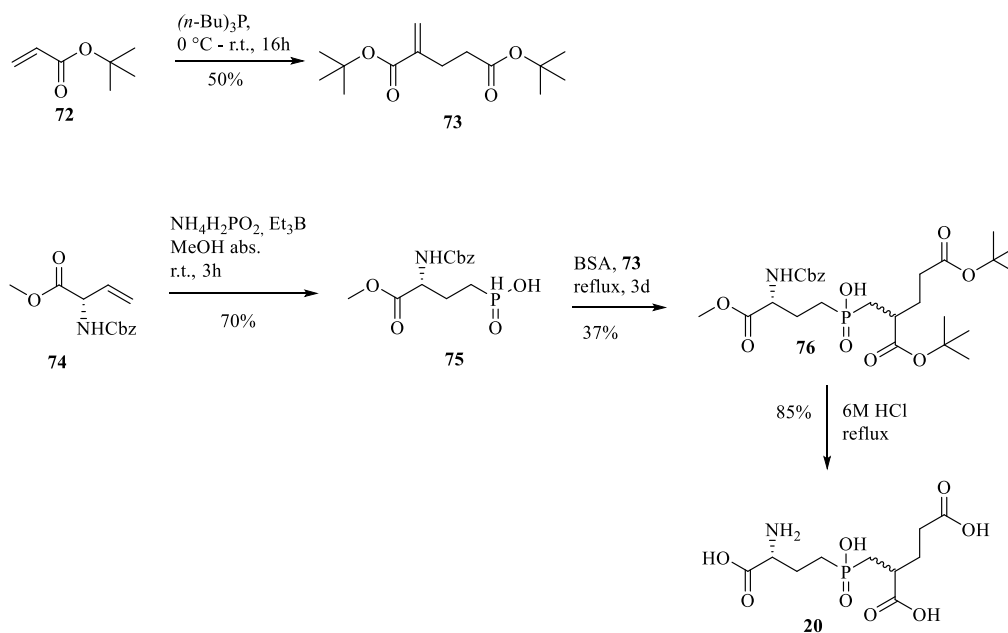


Figure 39: Synthesis of GPI 20.^{128,167}

3.2.4. Coupling of the tertiary amine with GPI

After establishing a robust protocol for the synthesis of tertiary amines by Pd-catalyzed Buchwald-Hartwig reactions, further steps involved deprotection of the methyl ester in order to generate a carboxylic acid for the subsequent coupling with GPI. Saponification was achieved for compounds **60b** and **60c**, using an excess of LiOH in water/THF. After full conversion of starting material, the solution was neutralized with hydrochloric acid and the compounds **77a** and **77f** were purified *via* reversed phase column chromatography.

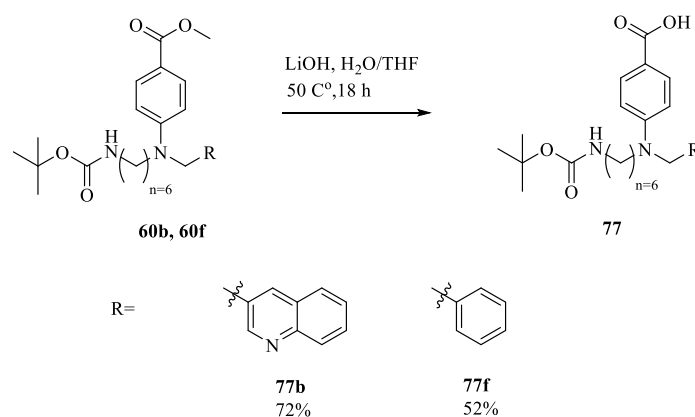


Figure 40: Synthesis of carboxylic acids **60b** and **60f**.

The following step considers the coupling with GPI **20** to the folate mimic **77**. As previously mentioned, this reaction is a crucial and at the same time very challenging step in the synthesis of folate-GPI hybrid structures. Carboxyl groups of glutamate rest are essential for the binding in PSMA active site. Therefore, the primary amine of GPI **20** is submitted to the coupling reaction with a free carboxylic acid of **77**. One strategy for the coupling reaction would be to use GPI with protected carboxyl groups. However, that would consider hydrolysis of all protecting groups in the final step. Since the hydrolysis of protected GPI goes under harsh conditions (6M HCl), this approach is incompatible with the highly functionalized folate-GPI conjugate. Hence, the coupling reaction has to proceed with the unprotected GPI, so that in the final step only Boc group needs to be hydrolyzed. Applying this strategy means that we need an active ester of **77** in order to successfully obtain coupled product. For activation of the carboxylic acid **77a**, a well-known additive in carbodiimide-mediated coupling, *N*-Hydroxysuccinimide, was applied.¹⁶⁹ Moreover, this method was already used for coupling of GPI with adamantane derivatives by Maison *et al.*^{95,130}

The first step is the formation of NHS-ester with the standard procedure by using EDC·HCl and HOSu. The conversion of starting material was monitored by LC-MS analysis and the crude NHS-ester was used without further purification. Since the NHS-ester is prone to hydrolysis in an aqueous medium, purification by reversed phase column chromatography couldn't be accomplished.

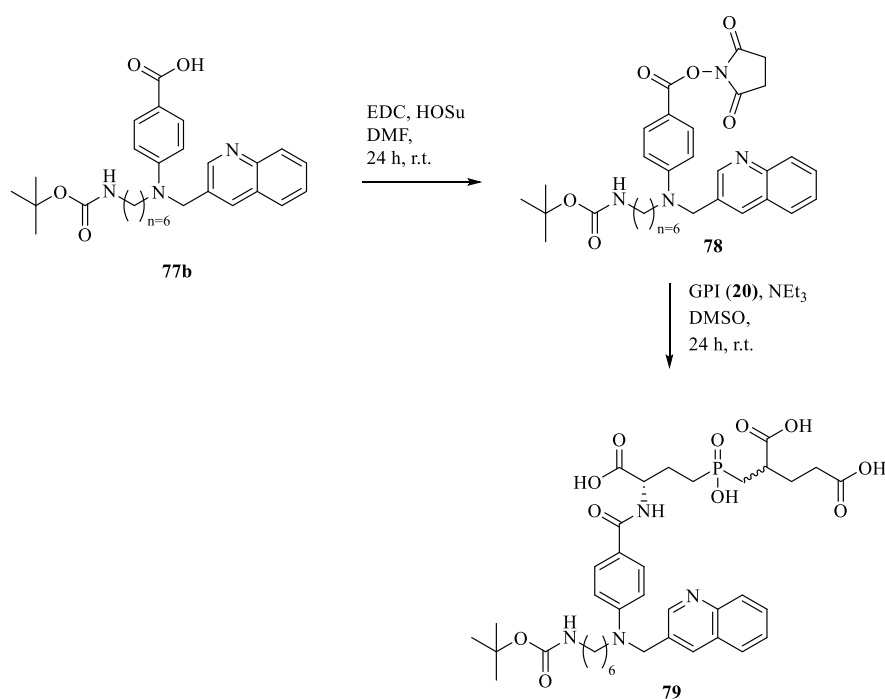


Figure 41: Coupling reaction of carboxylic acid **77b** with GPI via NHS-ester **78**.

The subsequent coupling of NHS-ester **78** with GPI was leading to a low conversion and complex mixtures. Additional LC-MS analysis clearly indicates the starting material remaining in the reaction solution and several side products could also be observed (Figure 42). Furthermore, the active NHS-ester **78** could still be detected in the reaction solution, indicating that NHS ester is not active enough for this system. Another point that has to be considered is that GPI is a very hygroscopic substance and that the presence of water might lead to the hydrolysis of NHS ester.

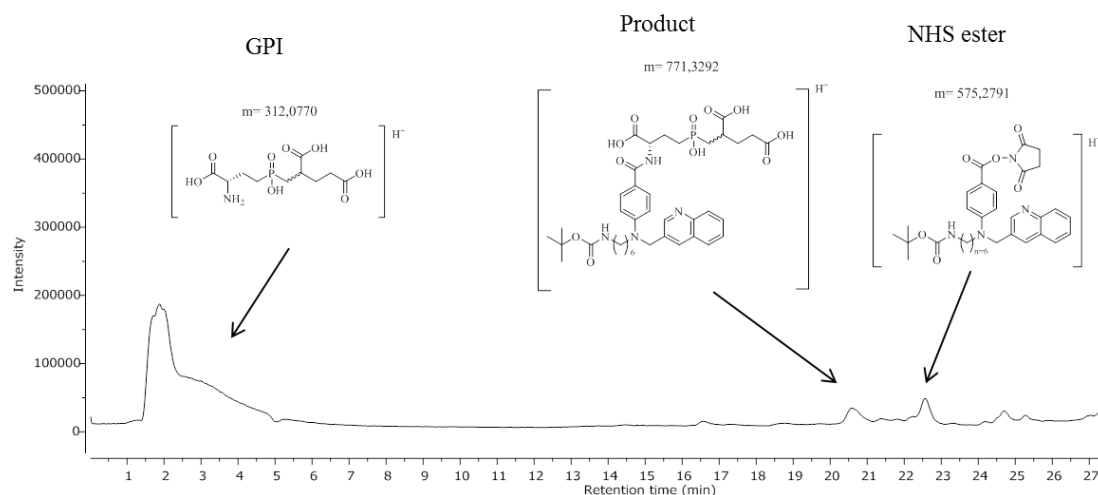


Figure 42: LC-MS chromatogram of the coupling reaction of **77b** and GPI. (20) Parameters: (a) VWR Hitachi LaChrom Elite, (b) Nucleodur RP- C18 Htec EC, (c) gradient H₂O/CH₃CN + 0.05% HCO₂H 98% to 2% in 30 min.

In the Ph.D. thesis of Florian Rüping, same challenges with the similar substrates were encountered. There were many attempts to optimize this reaction with increasing equivalents of the base, elevating reaction temperatures and longer reaction times. The investigation showed that the full conversion couldn't be accomplished and just the small amount of starting material was converted to the desired compound. In the conclusion, Rüping stated that NHS-ester wasn't reactive enough for conjugation with GPI **20** and very often led to side reactions. After encountering issues with the coupling reaction *via* NHS ester **78**, another strategy for GPI **20** coupling considered the protocol from Coward *et al.*¹²⁸ (Figure 43). Hereby, instead of NHS active ester, an azide is used as an active group. The carboxylic group of **77b** was transformed into the corresponding azide, which subsequently reacts with GPI. In the first step, a mixed anhydride was formed by adding isobutylchloroformiat, followed by NaN₃ addition which led to the desired carbonyl azide **80**. The full conversion to both mixed anhydride and azide was verified by LC-MS. In the following step, carbonyl azide **80** was submitted to the coupling

reaction with GPI, in abs. DMSO and tetramethylguanidine as a base. Coupling reaction of substrate bearing benzyl moiety **77f**, however, showed no conversion to the desired product. In the final step, deprotection of the primary amine with a mixture of TFA and CH₂Cl₂ gave **81**. The final compound **81** was obtained in a moderate yield after reversed phase column chromatography. During purification, folate-GPI conjugate **81** has shown an affinity to bind on the surface of silica, due to high number of free carboxylic groups. Consequently, this caused sticking and issues to obtain coupled compound in a higher yield.

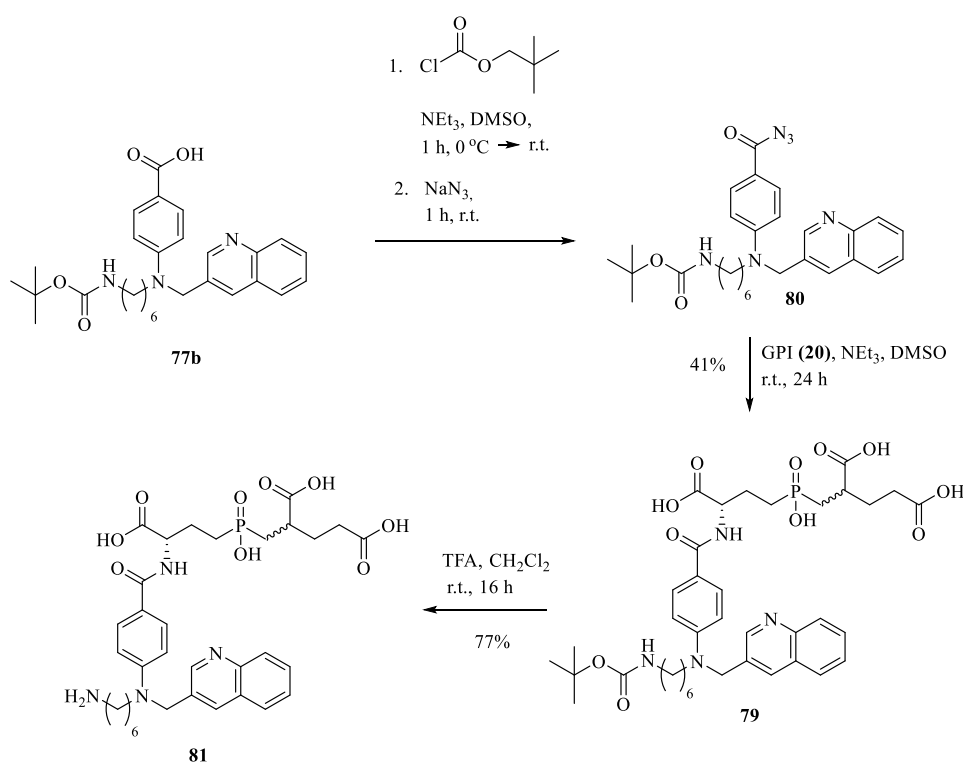


Figure 43: Conjugation of carboxylic acid **77** and GPI **20** using the method by Coward *et al.*¹²⁸

3.2.5. Coupling with DOTA

After establishing synthetic methods for the synthesis of the desired modular folate mimetic **81**, further steps included conjugation with an effector molecule. In cooperation with Malte Holzapfel, the folate mimetic **81** was conjugated with DOTA as an effector molecule following the protocol shown in Figure **44**. The DOTA conjugate **83** was assembled from a suitable NHS-ester **82** and **81**, under basic conditions in DMSO at r.t., for 16h. The Boc deprotection was accomplished with a TFA/DCM mixture at r.t. for 6 h. In the final step DOTA conjugate **83** is

obtained as metal complex in order to estimate binding affinity towards PSMA and it is usable for any metal-based diagnostic method. **conditions**

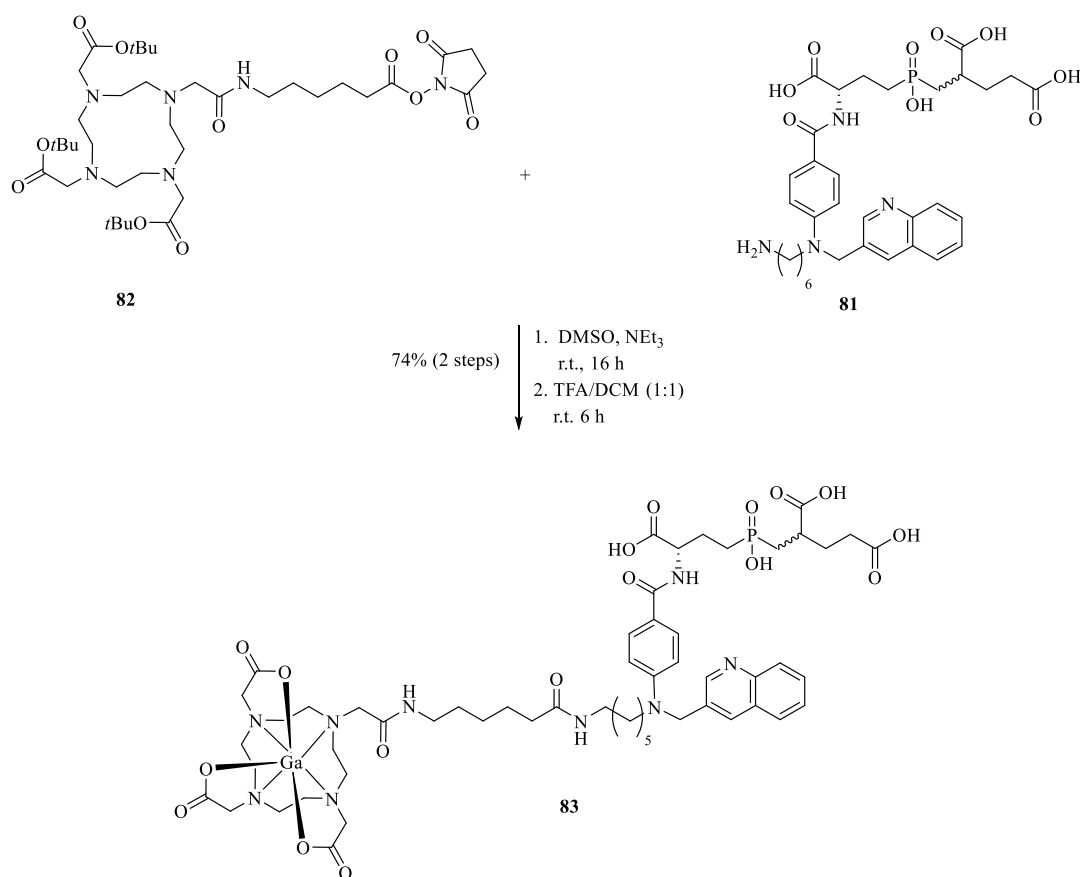


Figure 44: Coupling of folate mimic **81** with DOTA-NHS ester **82**.

3.3. Simplified folate-GPI conjugates with modified aryl linker

In the chapter 3.2. was shown that the synthesis of folate-GPI conjugates by *N*-arylation is possible, however highly demanding and dependent on heteroaromatic compounds. Therefore, it is difficult to build efficiently a library of folate-GPI conjugates with different heteroaromatics. Another way to optimize affinity is by modifying aryl linker. Literature suggests that altering length and nature of the linker group in modular PSMA ligands can lead to increased affinity and tumor uptake.^{134,170,171} In the study of Eder *et al.* the role of linker group was thoroughly investigated.¹³⁴ A series of urea-based DOTA-conjugated PSMA inhibitors were synthesized and evaluated *in vitro* and *in vivo*. To improve the binding affinity of the PSMA inhibitors, various linker moieties were investigated between the urea-based PSMA-ligand and DOTA (Figure 45).

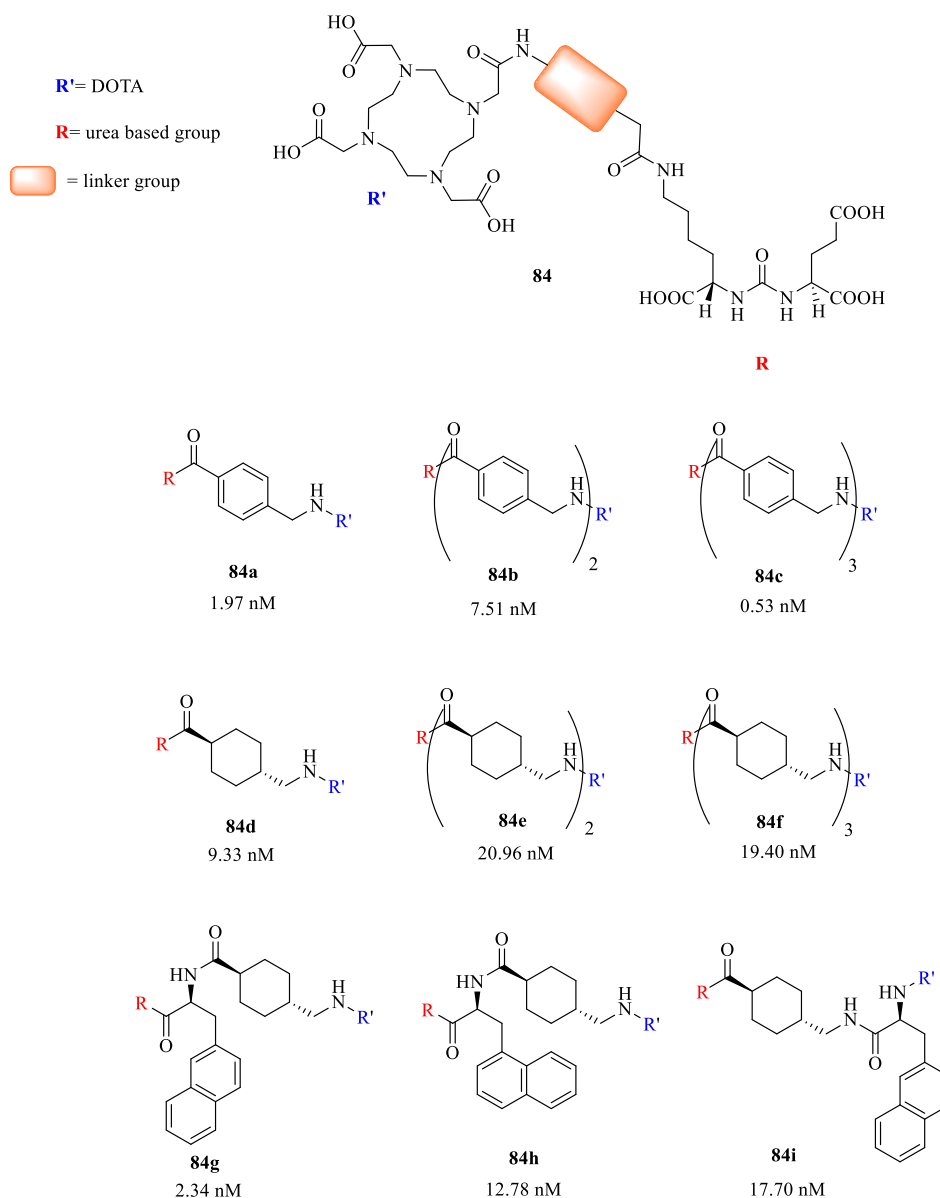


Figure 45: Urea-based DOTA-conjugated PSMA ligands by Eder *et al.* with estimated K_i values.¹³⁴

An analysis of various linker moieties and the corresponding binding affinities showed the following: the first set of compounds with benzylamine scaffold (**84a-c**) showed that the longer linker moiety (**84b**, **84c**) is correlated to a higher binding affinity in comparison to **84a** and that the optimal number of benzylamine units is three. Moreover, in the second set of ligands (**84d-f**), introducing a rigid system such as cyclohexyl group instead of an aromatic moiety led to lower affinity. Adding more cyclohexyl units decreased the binding affinity even more. The influence of substitution pattern was evaluated with the last set of ligands (**84g-i**). Ligand **84g** with the structural motif of PSMA-617, expressed overall the highest internalization ($16.17 \pm 3.66\%$) as well as good inhibitory potency ($K_i = 2.34$ nM). Based on the studies of Eder *et al.* that revealed a crucial effect of linker groups on PSMA binding affinity, a new set of

compounds was designed and synthesized in order to evaluate the role of linker groups in folate-GPI conjugates. The proposed structures are shown in Figure 46.

There are several notable points that are going to be investigated with this set of ligands: 1. Impact of spacing by altering aniline to benzylamine with ligands **84a-c**. 2. The geometry of the molecule with *meta*-substituted ligand **85b**. 3. The role of steric factors with the ligand **84c**, by substitution with chlorine in *meta*-position. 4. The importance of the aromaticity of the folate-GPI conjugates with ligand **84d** by introducing cyclohexyl ring instead of the aryl group. To keep the synthesis short and effective in order to build a library of folate-GPI conjugates, the secondary amines without heteroaromatics should first be prepared.

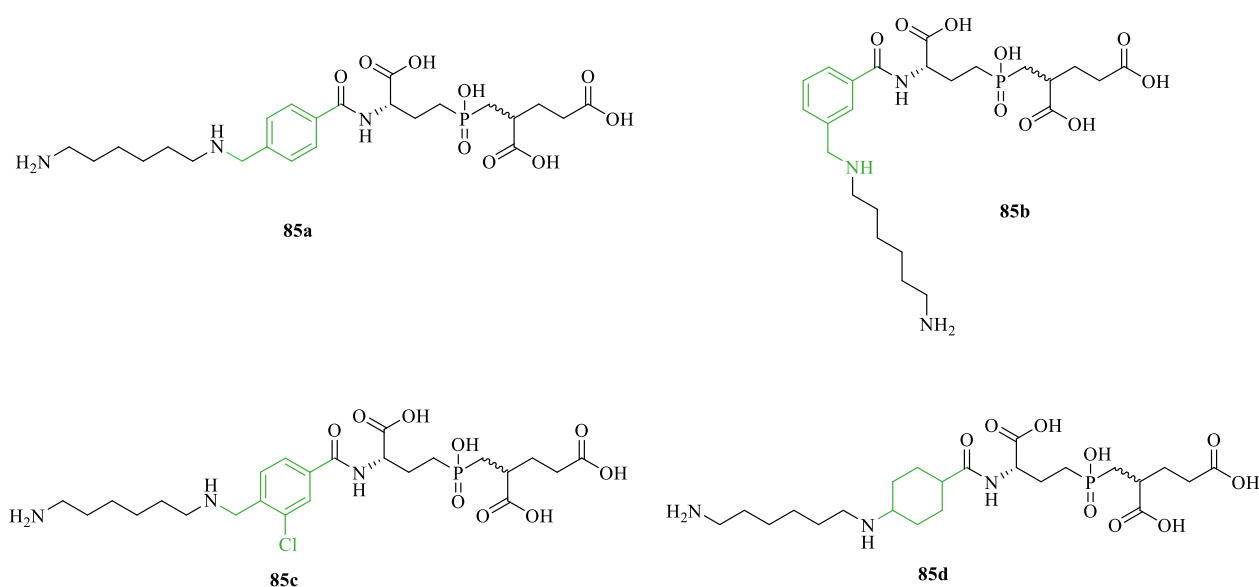


Figure 46: Proposed structures of folate-GPI conjugates with modified linker moieties. The main modifications are highlighted in green.

3.3.1. Docking studies of the simplified folate-GPI conjugates with modified aryl linker

Supporting docking studies of the proposed ligands **85a-d** were performed in order to evaluate the binding interactions in the active site of PSMA. Docking scores were calculated *via* Maestro 11.3 software using the crystal structure of PSMA (PDB reference: 4mcp).⁷⁴ As already described in chapter 1.2., the active site contains two zinc ions separated by 3.2 Å and it is connected to the extracellular domain through a ~20 Å deep tunnel.⁶³ First step was to model the binding of the natural substrate folic acid- γ -Glu (shown in orange, Figure 47) into the PSMA active site. Identified key interactions were: salt bridges of an α -carboxylate with Arg²¹⁰ (1.9 Å) and a γ -carboxylate with Lys⁶⁹⁹ (2.0 Å) in the hydrophilic pocket. The Glu- γ -Glu carboxamide is closely coordinated (2.3 Å) to a PSMA zinc atom *via* oxygen, (grey spheres,

Figure 10). The *p*-aminobenzoyl linking group is oriented for a possible π -stacking interaction (4.3 Å and 4.7 Å) with the Tyr⁷⁰⁰ aromatic system in the hydrophobic pocket of PSMA. Lastly, the aminopteridine heterocycle is oriented in a manner to participate in favorable π -stacking interaction (4.9 Å) with Trp⁵⁴¹. The total docking score for folic acid was -11.57, which indicates a good binding affinity to PSMA.

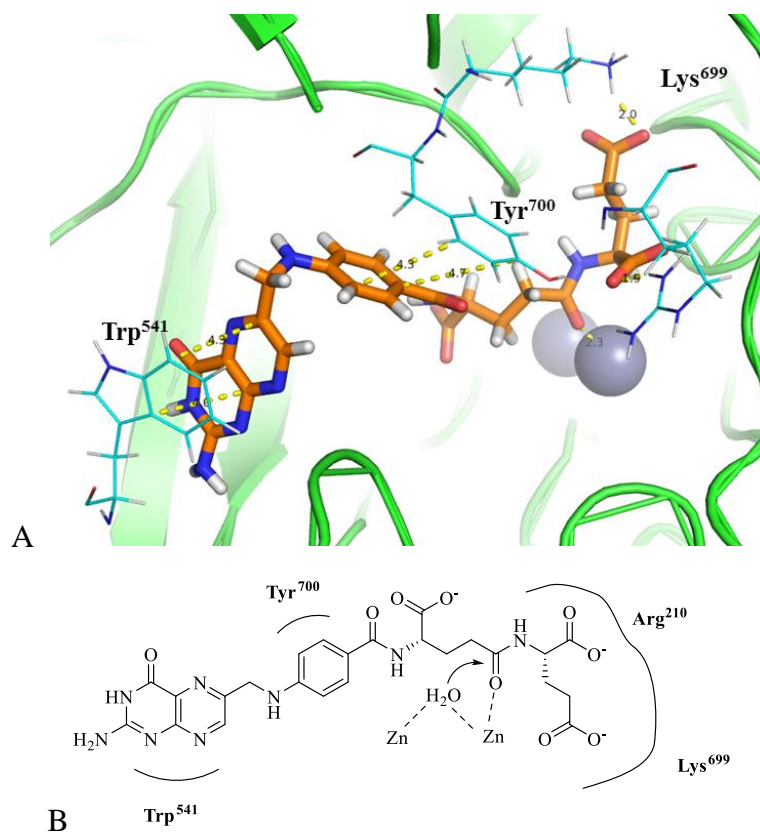


Figure 47: A Docking of folic acid to the PSMA binding site. Main interactions are shown as yellow dashed lines. Amino acids are colored in light blue. B Schematic representation showing key interactions of folate with the active site of PSMA.

For the docking studies of folate mimics with modified linker groups (**85a-d**), the main constraint included in this study was the interaction of a folate carboxylate with Lys⁶⁹⁹ in a hydrophilic region of the binding pocket of PSMA. Ligand **85a** (shown in light grey, Figure **48**) fits well with a docking score of -12.57. The phosphinic acid of GPI also binds to an active site Zn²⁺ ion (1.9 Å). Additional π -interactions of the benzene ring with Tyr⁷⁰⁰ (4.9 Å) can also be observed, as well as a salt bridge of the α -carboxyl group of GPI with Arg²¹⁰ (1.7 Å).

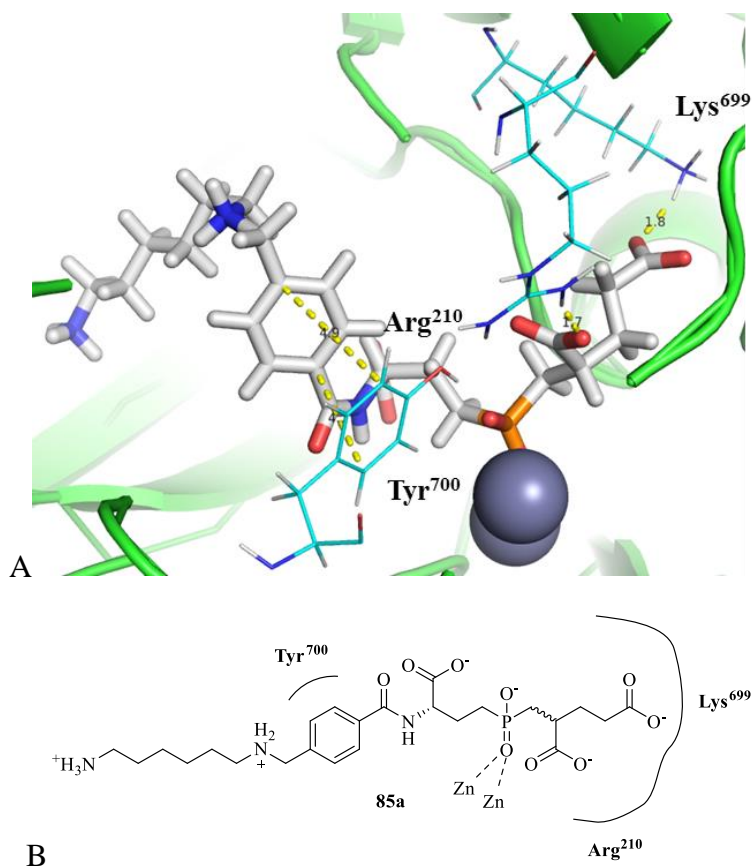


Figure 48: A: Docking of ligand **85a** (light grey) in the binding site of PSMA. Main interactions are shown as yellow dashed lines. Amino are colored in light blue. B Schematic representation showing key interactions of **85a** with the active site of PSMA.

Ligand **85b** (purple, Figure 49) showed the best fitting with the highest docking score -14.38 in this study. Compared to ligand **85a** the interaction between the benzene ring and tyrosine was sufficient to provide very close π stacking ($< 4 \text{ \AA}$). The groups of Barinka and Berckman have described the importance of these hydrophobic interactions for a good binding affinity to PSMA.^{135,172} The authors stated that ligands allowing full insertion of the phenyl ring into the accessory hydrophobic pocket had good binding affinities and were efficient inhibitors of PSMA. Additionally, ligand **85b** showed close interactions with Zn^{2+} ions (2.1 \AA). The salt bridge of the α -carboxyl group of GPI with Arg^{210} (1.8 \AA) was also crucial for a good binding affinity.

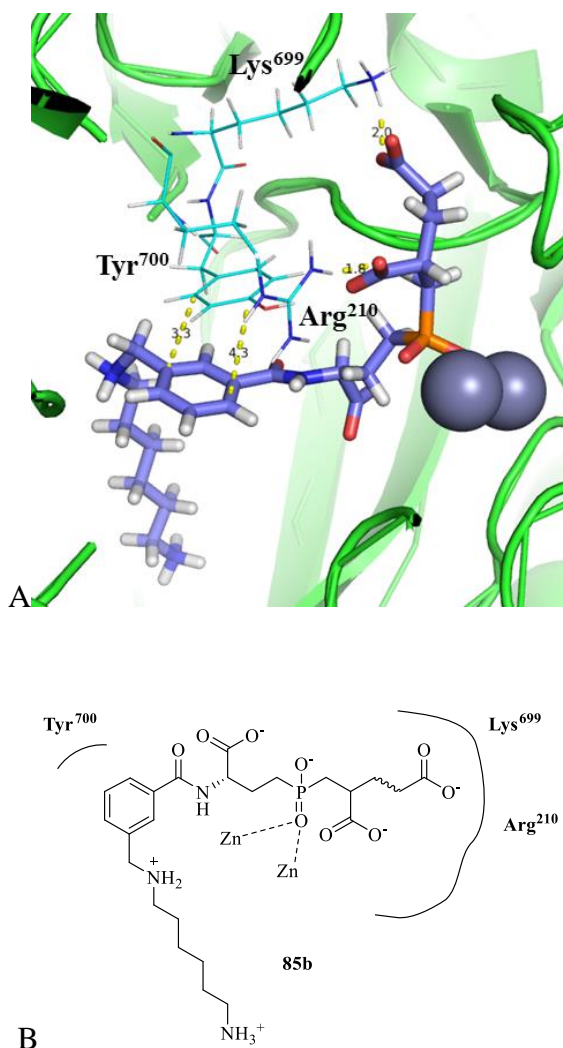


Figure 49: A: Docking of ligand **85b** (purple) in PSMA binding site. Main interactions are shown as yellow dashed lines. Amino acid are colored in light blue. B Schematic representation showing key interactions of **85b** with the PSMA active site.

Docking of ligand **85c** (shown in pink, Figure **50**) revealed also a better fitting in comparison to folic acid with a docking score of -12.30. In analogy to ligand **85a**, coordination of phosphinic acid of GPI to a Zn^{2+} ion (2.0 Å) was observed. Moreover, the salt bridges of γ - and α -carboxyl groups of GPI with corresponding amino acids (Lys⁶⁹⁹ - 2.0 Å and Arg²¹⁰ - 1.8 Å) were observed. Additional π -interactions of the benzene ring with Tyr⁷⁰⁰ (4.3 Å and 4.2 Å) also played an important role for a good fitting in the PSMA tunnel.

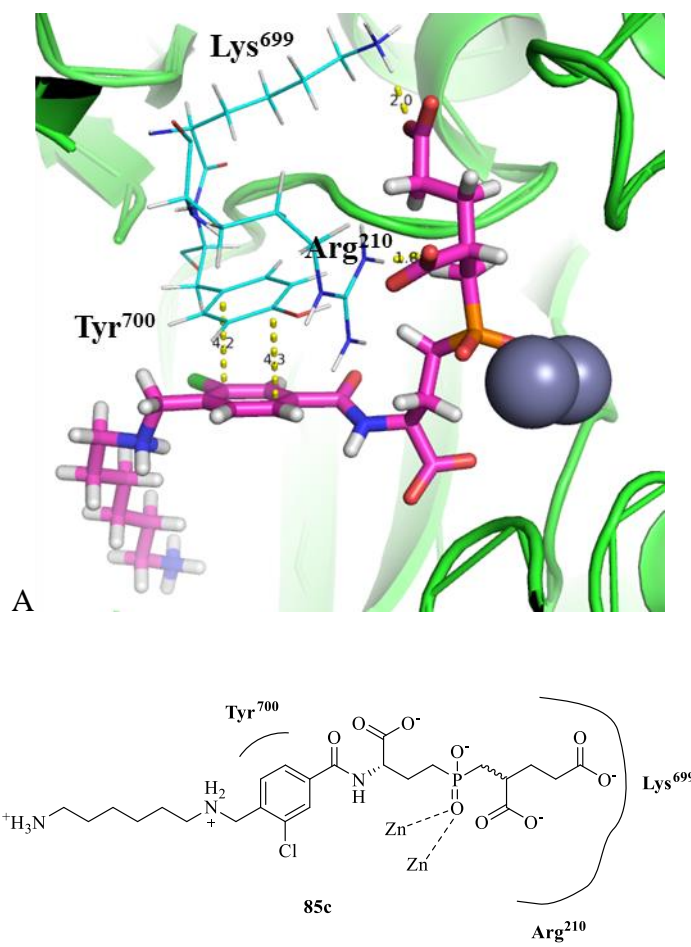


Figure 50: A: Docking studies of ligand **85c** (pink) in PSMA binding site. Main interactions are shown as yellow dashed lines. Amino acids are colored in light blue. B Schematic representation showing key interactions of **85c** with the active site of PSMA.

Docking of ligand **85d** (yellow, Figure 51) revealed good fitting and a higher docking score (-12.26) compared to folic acid (-11.57) as a reference. This ligand showed good key interactions in the active site of PSMA e.g. close interactions with a zinc ion (2.0 Å). The salt bridges of γ -carboxyl group with Lys⁶⁹⁹ (2.0 Å) as well as α -carboxyl group with Arg²¹⁰ (1.7 Å) in the hydrophilic pocket of PSMA. Additional π interactions with Tyr⁷⁰⁰, however, couldn't be provided compared to ligands **85a-c**, since this ligand doesn't have an aromatic system.

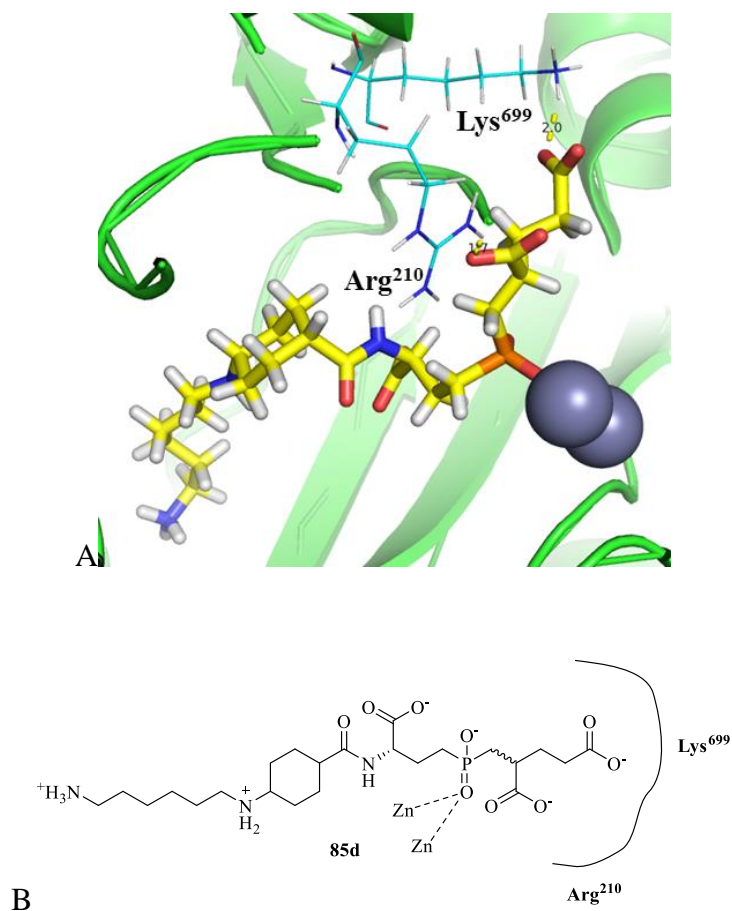


Figure 51: A: Docking studies of ligand **85c** (yellow) in PSMA binding site. Main interactions are shown as yellow dashed lines. Amino acids are colored in light blue. B Schematic representation showing key interactions of **85d** with the active site of PSMA.

The outcome of docking studies revealed following: aromatic group in the linker brings affinity for π -stacking, but may not be essential (see cyclohexyl derivative **85d**). Moreover, *meta*-substitution (ligand **85b**) gave the highest score indicating that the geometry of the molecule might play an important role in the binding affinity.

3.3.2. Synthesis plan

The synthetic concept to simplified folate-GPI derivatives is similar to the one mentioned earlier in Figure **25** on page **26**. However, it does not contain the problematic *N*-arylation and should thus more easily allow the synthesis of a small test library of compounds **85a-d**. The assembly of intermediate secondary amines **87** via reductive amination allows the variation of substituents and scaffolds starting from commercially available building blocks **51** and **88**.

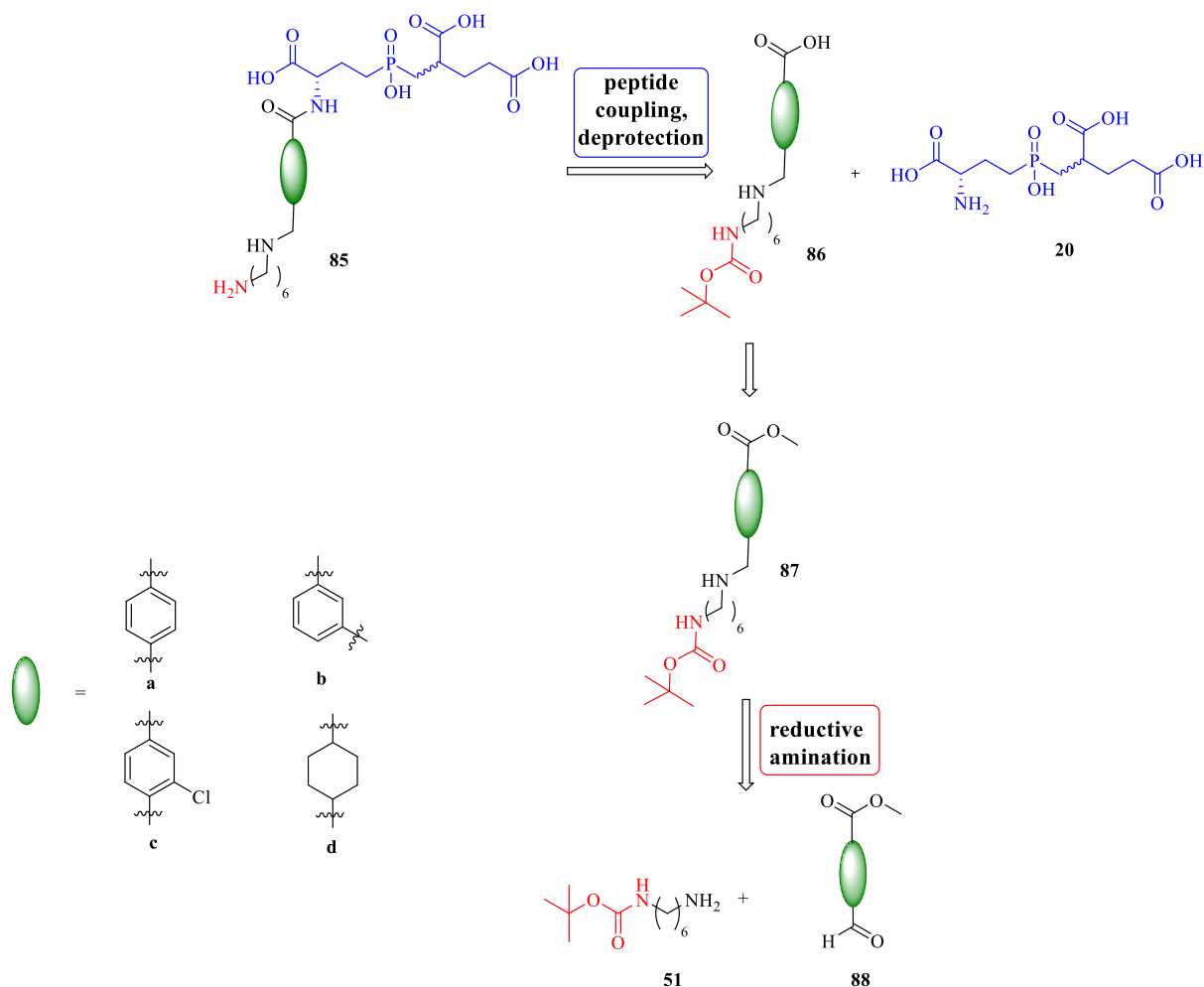


Figure 52: Retrosynthetic concept of simplified folate mimics.

3.3.3. Synthesis of the secondary amines

Secondary amines with modified linker groups were obtained *via* reductive amination of suitable aldehydes **88** and *N*-tert-butoxycarbonyl-1,6-hexanediamine **51** following the protocol of Nasr *et al.*¹³⁶ The commercially available primary amine **51** and aldehyde **88** were stirred under reflux for 24 h in methanol to ensure complete conversion to the imine. In first attempts, the imine was subsequently reduced with NaBH₄. This led to a significant amount of side products due to the reduction of the ester group. By changing to a milder hydride donor (Na(CH₃COO)₃BH), a selective imine reduction and formation of the desired secondary amine was achieved in good yields. Figure **53** shows the general reaction conditions and the obtained yields for each derivative.

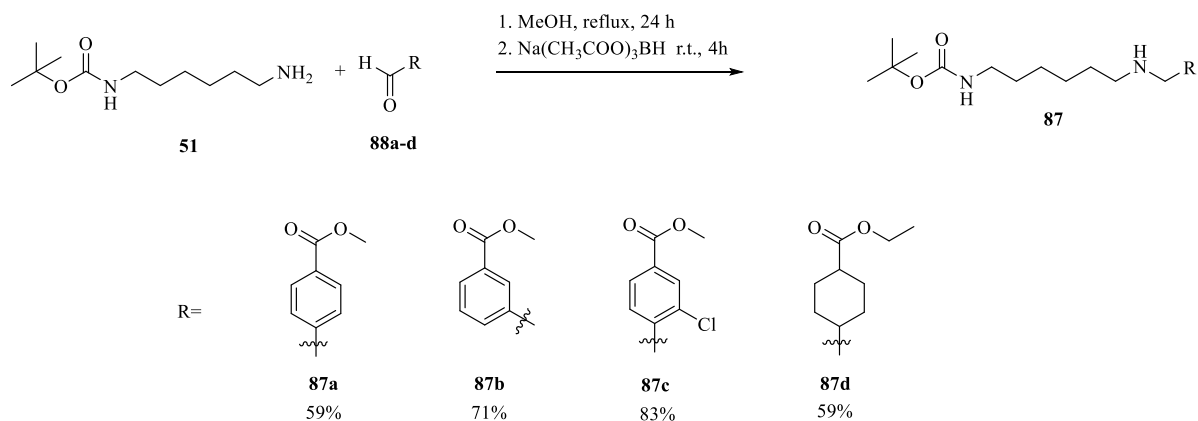


Figure 53: Synthesis of secondary amines **87a-d** via reductive amination.

3.3.4. Coupling with GPI

Saponification of ester **87** generated the free carboxylic acid **86** available for coupling to GPI. Four different derivatives **86a-d** were prepared in moderate to good yields using the same procedure from the chapter 3.2.4. (Figure 54).

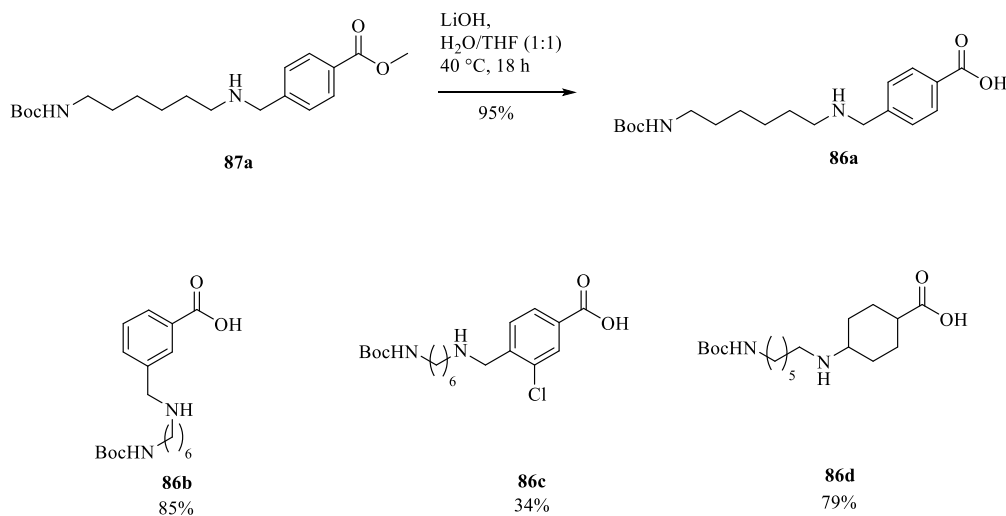


Figure 54: Synthesis of carboxylic acids **86a-d** under alkaline conditions.

As previously observed the coupling of GPI to similar derivatives was difficult and demanded several steps (see chapter 3.2.4.). GPI as a highly hygroscopic substance tends to slow and hinder the coupling reaction. Another issue was that the coupling reaction was not reproducible. In the case of simplified folate-GPI conjugates, it was best obtained by NHS active ester coupling, which is basically easier to perform. With the alteration of base equivalents, it was possible to obtain coupled compounds **85a-d** in moderate yields. However, the purification still

remained challenging. Long retention time and sticking of folate-GPI conjugates on the silica column was again observed, hence it was one of the main causes of lower overall yields.

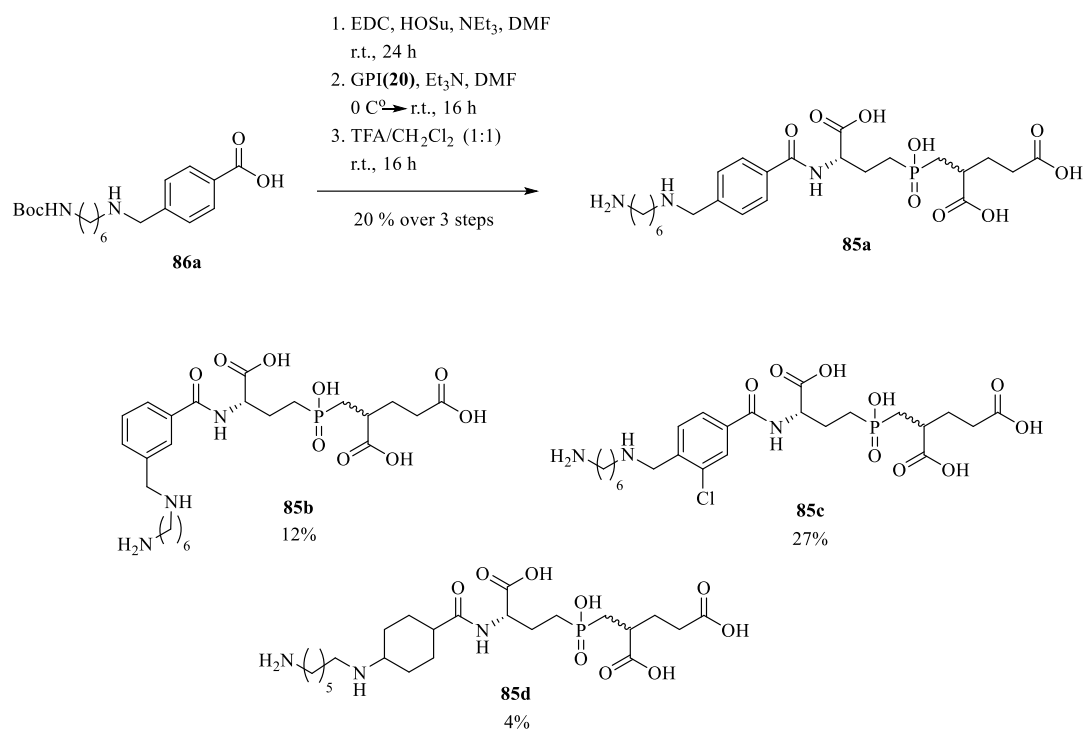


Figure 55: Coupling of folate mimics **86** with GPI **20** via active ester and overall yields for each compound.

3.3.5. Coupling of simplified folate-GPI conjugates with DOTA

Coupling of folate mimics **85a-d** with DOTA was successfully performed in cooperation with Malte Holzapfel. In analogy to the method described in chapter 3.2.5., the DOTA conjugate **89** was assembled from a suitable NHS-ester **82** and simplified folate-GPI conjugate **85**, under basic conditions in DMSO at r.t., for 16 h. Boc deprotection was accomplished in TFA/CH₂Cl₂ mixture at r.t. for 6 h. In the final step DOTA conjugate **89** was obtained as a metal complex in order to estimate the binding affinity towards PSMA and it can also be used further for any metal-based diagnostic method. Figure **56** shows general conditions as well as overall yields for each folate mimic.

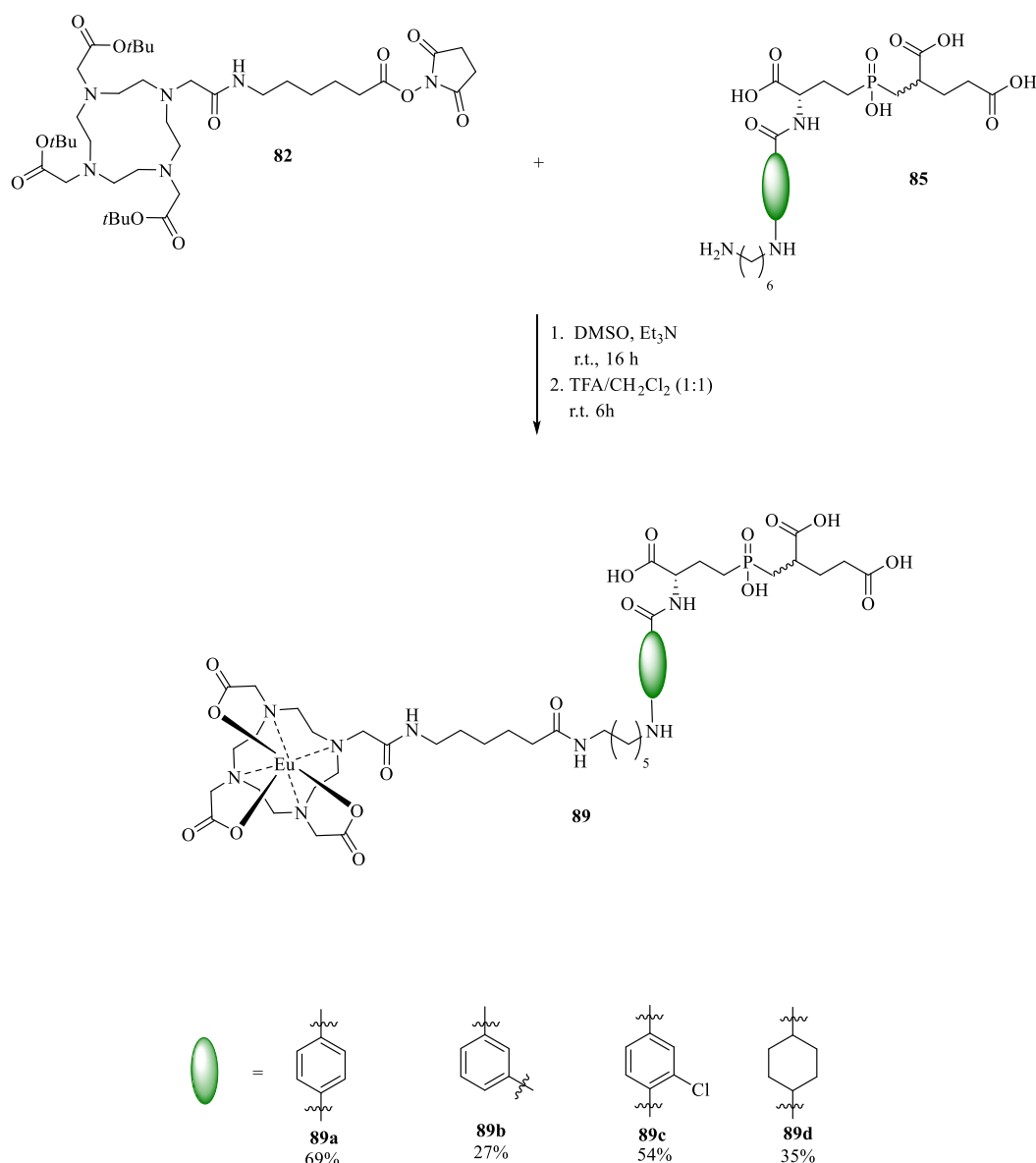


Figure 56: Coupling reaction of DOTA NHS-active ester **82** and folate mimics **85**, with overall yields for each compound. **conditions**

3.4. TRIS-GPI derivatives

As mentioned before, GPI binds selectively and with high affinity ($K_d=10.4$ nM) to PSMA as evaluated by in vitro assays in TRIS buffered solution.^{95,130} However, GPI shows low binding affinity in PBS buffer (phosphate buffered saline) and under in vivo conditions.^{95,130} On the contrary, it was observed that in TBS (TRIS buffered saline), GPI expresses high binding affinity. At this point, we have no clear explanation for this finding. However, one hypothesis is a competition of GPI and phosphate, which is also a reasonable zinc binder, for PSMA-binding. In order to enhance binding affinity, Maison *et al.* developed a tri-NHS-ester derivative of adamantane (**21**), which allows the conjugation of up to three targeting ligands (such as GPI) besides to a contrast agent or radiotracer. The results of the study revealed that the conjugation

of a GPI monomer to the adamantane scaffold (**90**) had a negligible effect on the affinity. Stepwise addition of GPI, improves significantly both affinity and competition with endogenous phosphate anions. In addition, GPI-trimer **21** was unaffected by serum and showed the highest binding affinity (Figure 57).

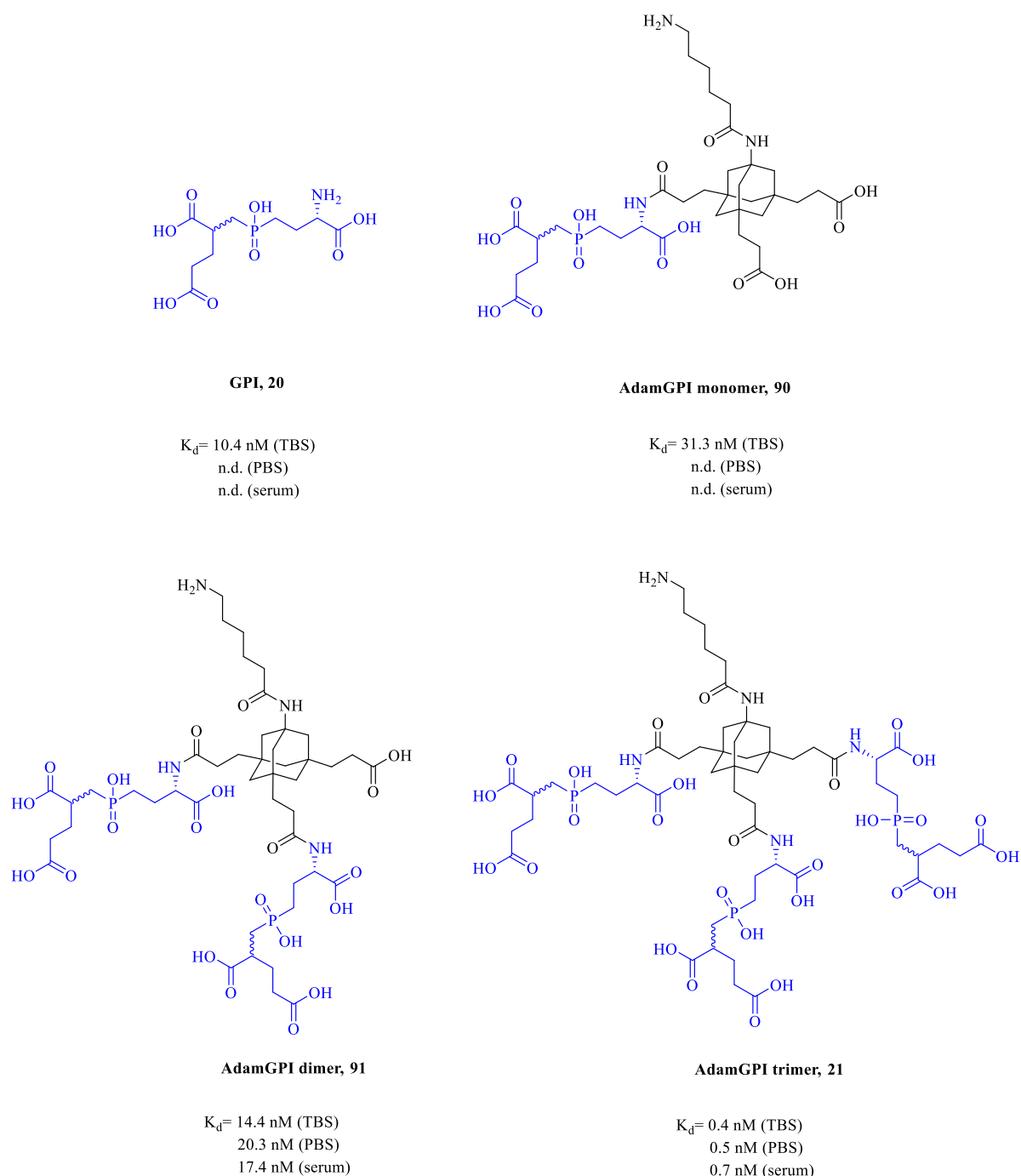


Figure 57: Binding affinities of GPI **20** and GPI-Adamantane conjugates (**90**, **91**, **21**) by Maison *et al.* ^{95,130}

We have currently two hypotheses which might explain the special binding properties of GPI-derivatives to PSMA: 1. phosphate anions compete with GPI in the active site of PSMA

resulting in higher binding affinity in TBS vs PBS or serum. 2. TRIS enhances the binding affinity of GPI with a hitherto unknown mechanism. To address the second hypothesis, we designed three different covalent GPI-TRIS conjugates **92-94**. These derivatives were docked to the binding site of PSMA by Dr. Thomas Lemcke. This study revealed the best binding properties for the GPI-TRIS conjugate **92**.

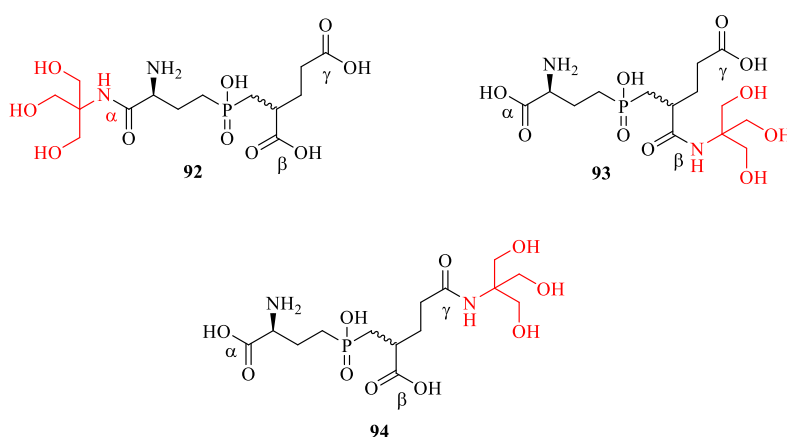


Figure 58: TRIS-GPI conjugates docked by Dr. Thomas Lemcke. TRIS is conjugated to GPI in three different positions highlighted in red.

An additional derivative **95b** combines TRIS, GPI and an aromatic moiety mimicking folate following our previously described design. Both derivatives **95a** and **95b** contain an aminohexanoyl spacer group which allows further coupling with an effector molecule.

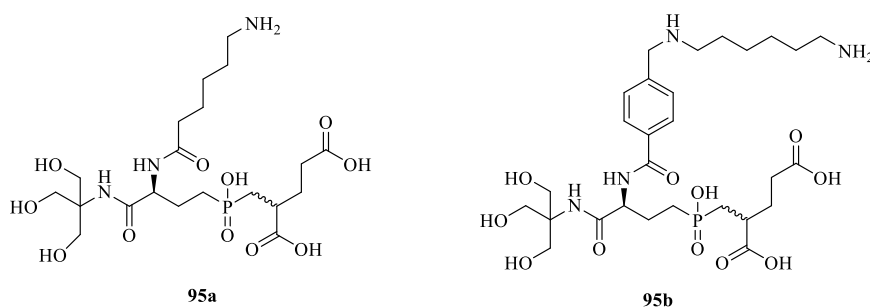


Figure 59: Proposed structures of new TRIS-GPI derivatives.

Supporting docking studies of the proposed ligands **95a** and **95b** were performed in order to evaluate their binding to PSMA. Docking scores were calculated *via* Maestro 11.3 software using the crystal structure of PSMA (PDB reference: 4mcp).⁷⁴ In analogy to the docking study in chapter 3.3.1., interaction with Lys⁶⁹⁹ (2.1 Å) in the hydrophilic pocket of PSMA was used as the main constraint in the docking calculations. Molecular modeling of ligand **95a** (shown

in light pink, Figure 60) showed close interactions (2.2 Å) of the phosphinic acid of GPI with the active site Zn^{2+} ions (shown as dark grey spheres, Figure 60), as well as the β -carboxyl group with Tyr⁷⁰⁰. The total docking score (-10.63) is lower compared to folic acid and ligands 1-4 in chapter 3.2.1. However, the TRIS hydroxyl groups showed additional interactions with Arg⁵³⁶ (3.2 Å) and Tyr⁵⁴⁹ (3.6 Å), which contributed to a good binding fit in the active site of PSMA.

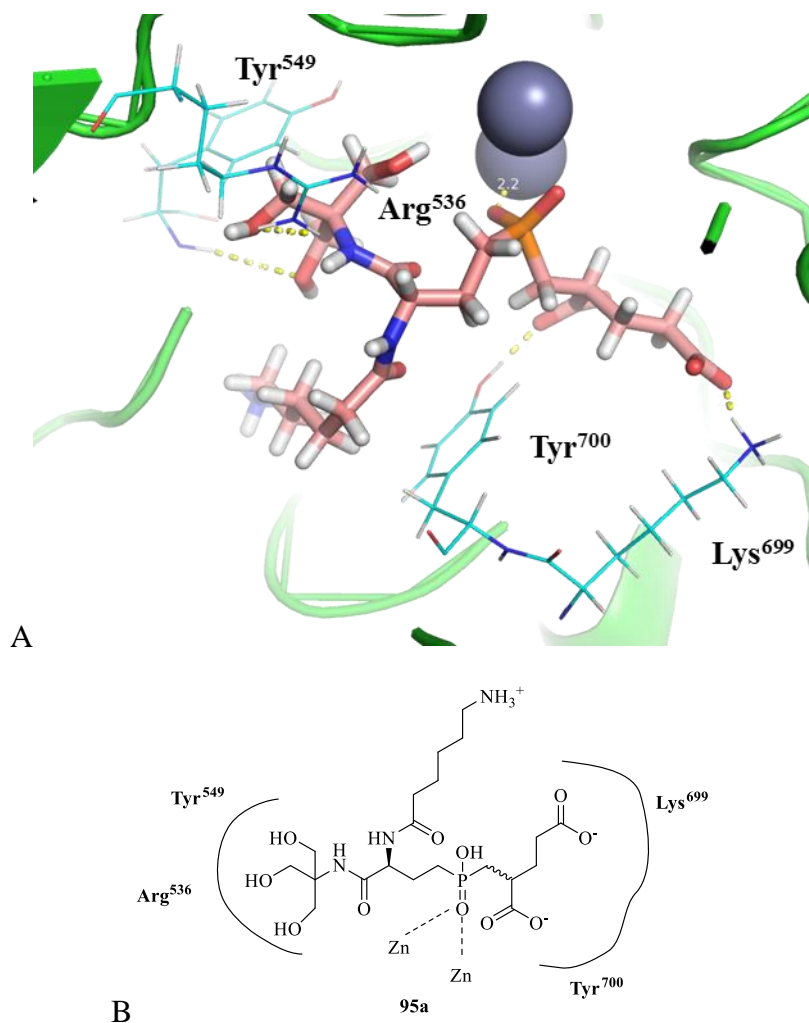


Figure 60: A. Docking of ligand 95a (light pink) to PSMA. Main interactions are shown as yellow dashed lines. Amino acids are colored in light blue. B Schematic representation showing key interactions of 95a with the active site of PSMA.

Ligand **95b** showed similar to the previous ligand 1 close interactions with Zn^{2+} (2.2 Å) ions and Lys⁶⁹⁹ (2.1 Å). Additional π interactions of the phenyl ring of **95b** were identified with Tyr⁷⁰⁰ (4.9 Å), which probably contributed to the slightly higher docking score (-10.91) compared to ligand 1. TRIS hydroxyl groups showed also close interactions with Arg⁵³⁶ (2.9 Å), Ser⁴⁵⁴ (2.1 Å) and Tyr⁵⁴⁹ (3.1 Å) in the hydrophilic pocket of PSMA.

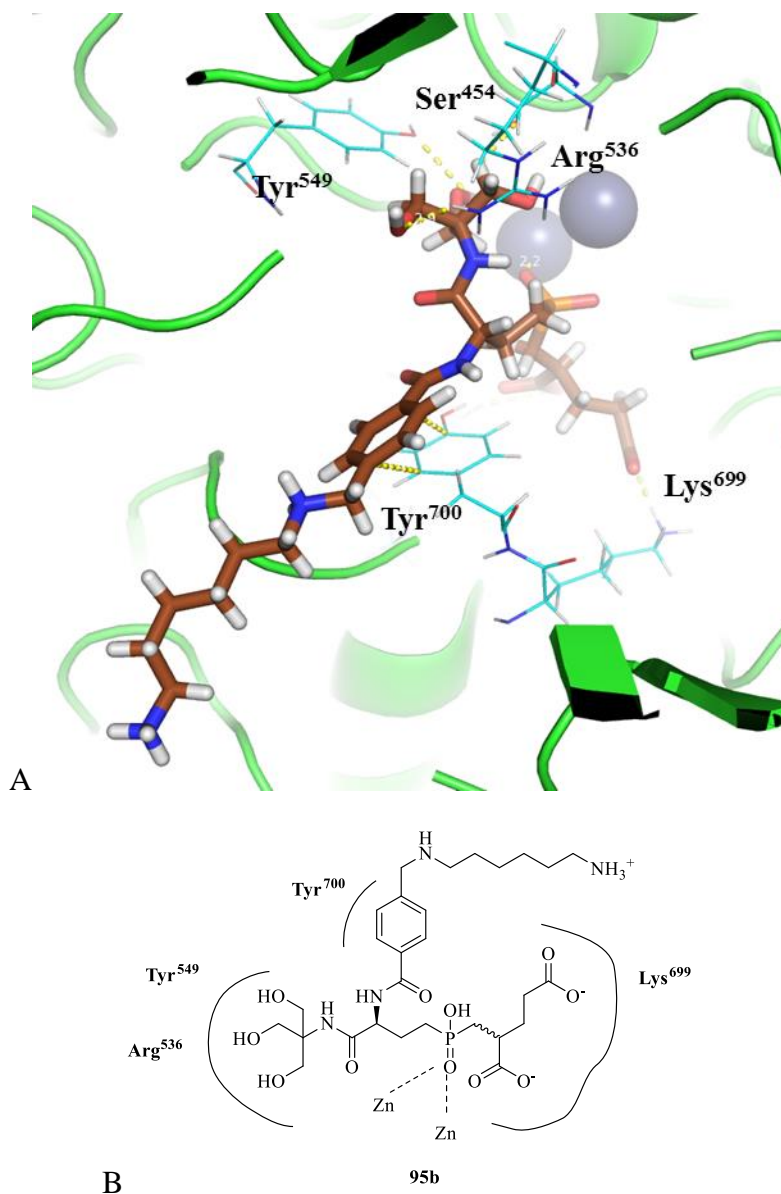


Figure 61: Docking of ligand **95b** (brown) to PSMA. Main interactions are shown as yellow dashed lines. Amino acids are colored in light blue. B Schematic representation showing key interactions of 95a with the active site of PSMA.

3.4.1. Synthesis of TRIS-GPI derivatives with different linker groups

The coupling reaction of protected GPI was performed by the protocol of Pucci *et al.*¹⁷³ The α carboxyl group of GPI was firstly hydrolyzed under basic conditions. In the following step, the product was dissolved together with TRIS (X, 1.50 eq) and EEDQ (1.50 eq) in the dry EtOH and stirred over 18h at 50 °C. The crude residue was purified over reversed phase column chromatography and the product **96** was obtained in moderate yield. Subsequent catalytic Cbz-deprotection of the amino group was accomplished in quantitative yield. *In situ* preparation of

an active Pd/C catalyst from Pd(OAc)₂ and charcoal in methanol under hydrogen atmosphere (1 atm) allows the efficient hydrogenolysis of *O*-benzyl ethers.¹⁷⁴

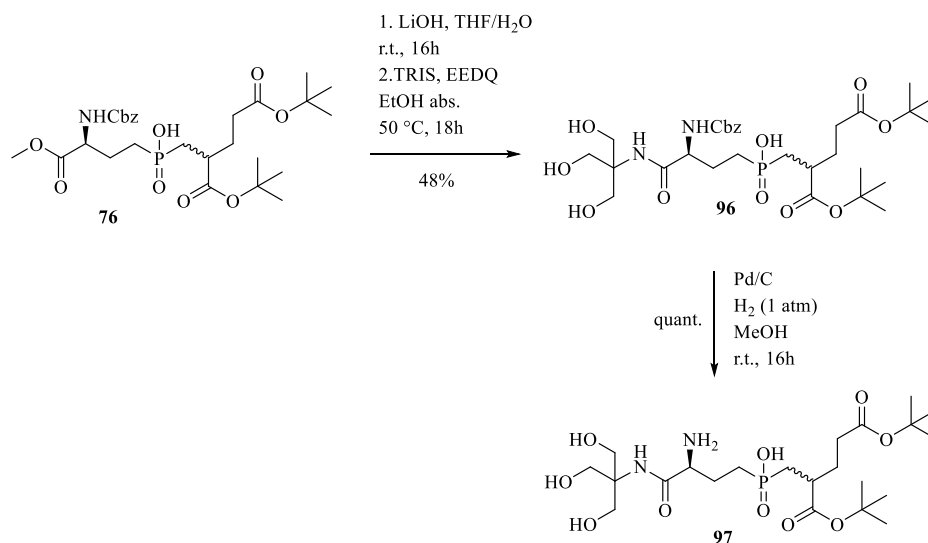


Figure 62: Coupling reaction of **76** and TRIS by the method of Pucci *et al.*¹⁷³ Catalytic Cbz- deprotection of **96**.

The final TRIS-GPI conjugates with linker moieties were assembled from a suitable NHS esters **98** and TRIS-GPI conjugate **97**, under basic conditions in DMF at r.t., for 18h. The following Boc deprotection was accomplished in the TFA/CH₂Cl₂ mixture at r.t. for 6h, which yielded the final products **95a** and **95b**.

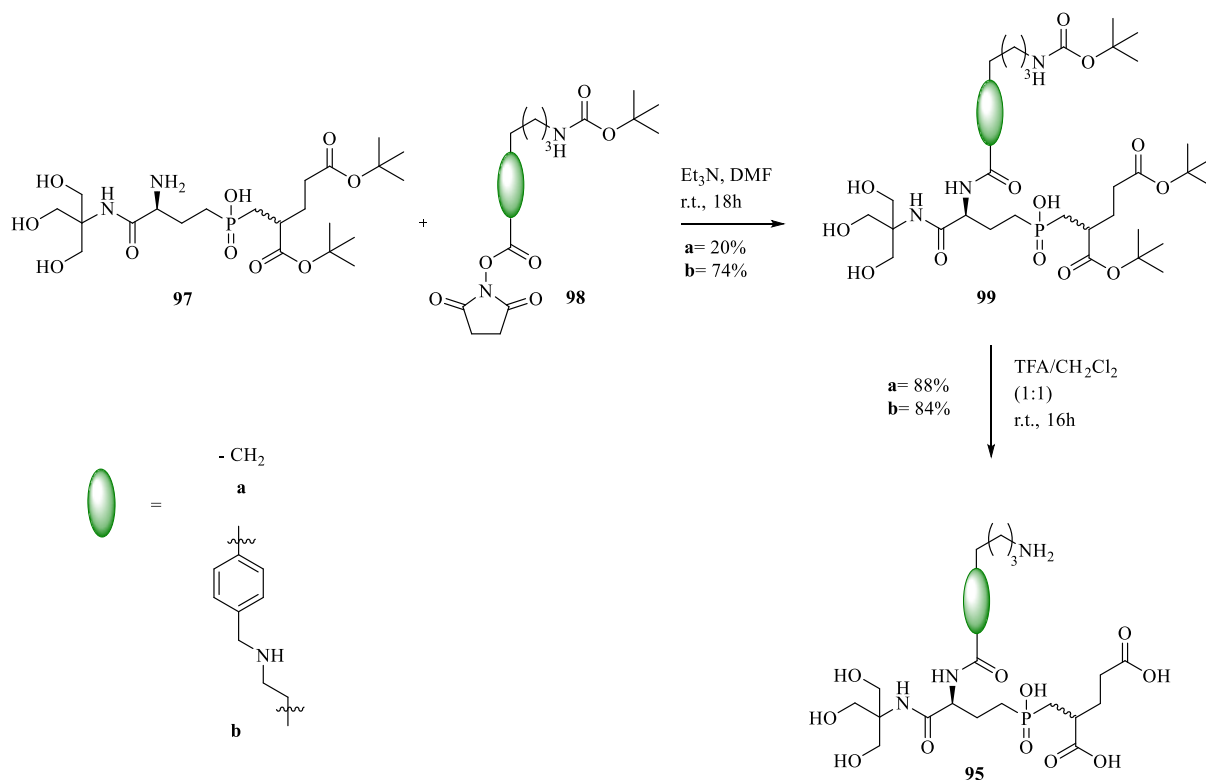


Figure 63: Coupling reaction of TRIS-GPI derivative **97** with NHS-ester **98a** and **98b** and subsequent full deprotection of **99** under acidic conditions yielded final compound **95**.

3.4.2. Coupling of TRIS-GPI derivatives with DOTA

Coupling of TRIS-GPI derivatives **95a** and **95b** with DOTA was accomplished in cooperation with Malte Holzapfel. In analogy to the method from chapter 3.2.5. the DOTA conjugate **100** was assembled from a suitable NHS ester **82** and TRIS-GPI derivative **95a** and **95b**, under alkaline conditions in DMSO at r.t., for 16h. Subsequent Boc deprotection was performed in a TFA/CH₂Cl₂ mixture at the room temperature, for 16h. Figure **64** shows the general conditions as well as overall yields for each derivative.

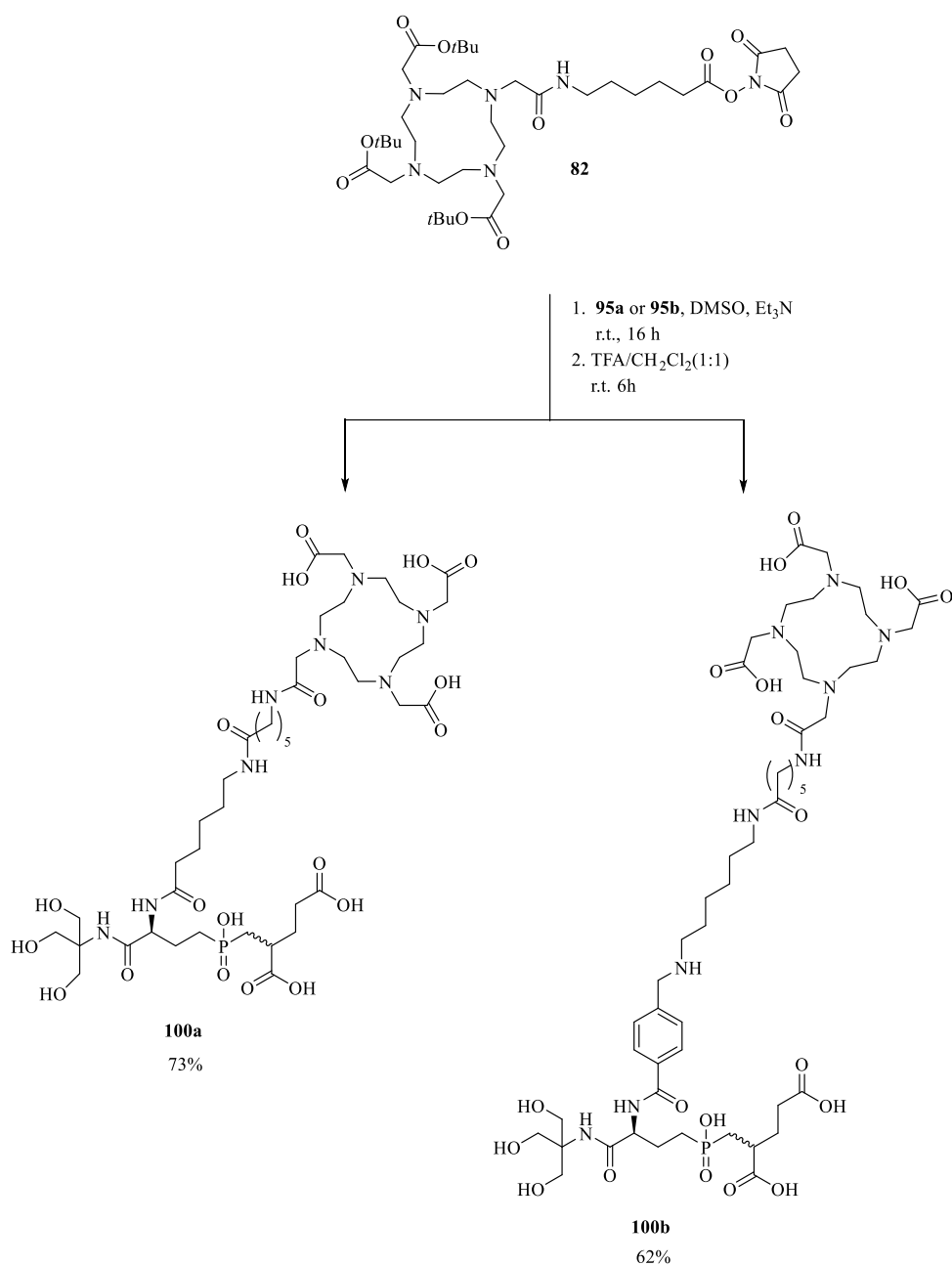


Figure 64: Coupling of TRIS-GPI derivatives **95a** and **95b** with DOTA-NHS ester **82**.

3.5. Biological evaluation

Preliminary biological tests were performed in cooperation with the research group of J. Lewis (Memorial Sloan Kettering Cancer Center, New York, USA). Kelly Henry established an internalization assay for folate mimetic **83** and reference substances GPI **101**. These ligands were radiolabeled (^{68}Ga) and incubated with LnCap-cells (PSMA positive) and PC3-cells (PSMA negative) in TBS buffer and serum (media) at 4 °C and 37 °C. The binding affinity was subsequently estimated by residual radioactive radiation from the internalized and surface-bound fraction after a washing process. The results of this preliminary study (shown in Figure **65**) indicated that the folate-GPI conjugate **83** showed a selective binding affinity for LnCap cells (blue column, Figure **65**) and a low affinity for PC3 (orange column, Figure **65**). However, the reference substance DOTA-GPI **101** shows a binding affinity for both LnCap and PC3 cells, which is not in agreement with the literature.¹³⁰ Therefore, further studies are essential in order to verify this outcome and obtain reliable, quantified results about the binding affinity.

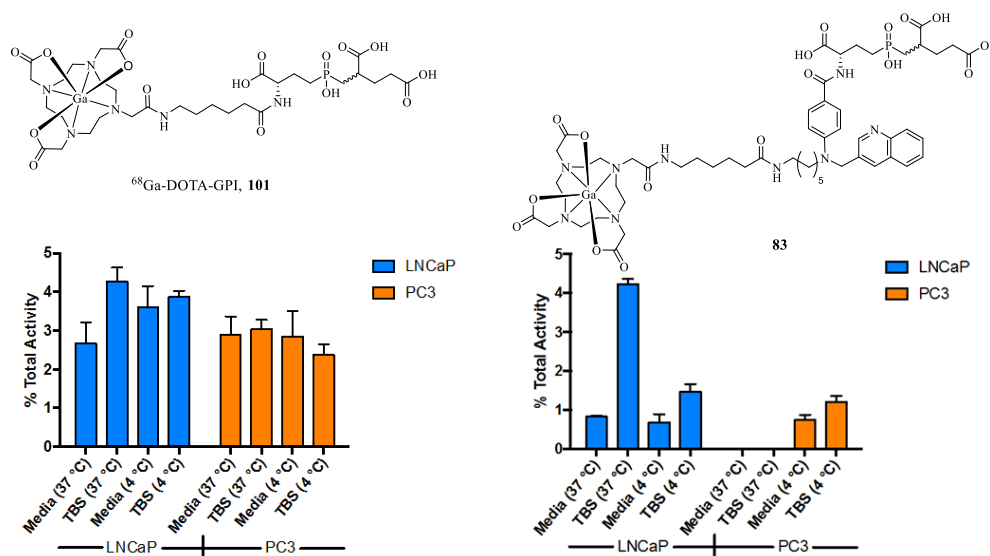


Figure 65: Results of the internalization assay of ^{68}Ga -DOTA-GPI **101** and **83** on LnCap and PCL3 cells in TBS Buffer and human serum.

In addition, a non-radioactive biological assay is investigated/tested by Malte Holzapfel in the research group Maison. In contrast to the preliminary tests of Lewis et al, the investigated ligands were labelled as DOTA- ^{151}Eu complex instead of the ^{68}Ga variant (see chapter 3.3.5.) and incubated with LnCap-cells and PC3-cells in PBS-buffer. After washing, the binding affinity was estimated by the residual ^{151}Eu -concentration which was measured by ICP-MS. A selective binding of folate derivative **89a** in 50nmol/L concentration to LnCap cells was

observed. It is remarkable, that this strong binding to LnCap-cells occurred in PBS-buffer, which has never been observed before for GPI derivatives. These findings support our initial design hypothesis and might allow the use of folate-GPI conjugates for targeting applications in physiological media. However, we have also noticed a constant and relatively high unspecific binding to PC3-cells (red column, Figure 66). We have currently no explanation for this finding and it is clear that further investigations are needed to confirm the promising binding characteristics of folate derivatives like **89a** to PSMA-positive cells. to verify this result.

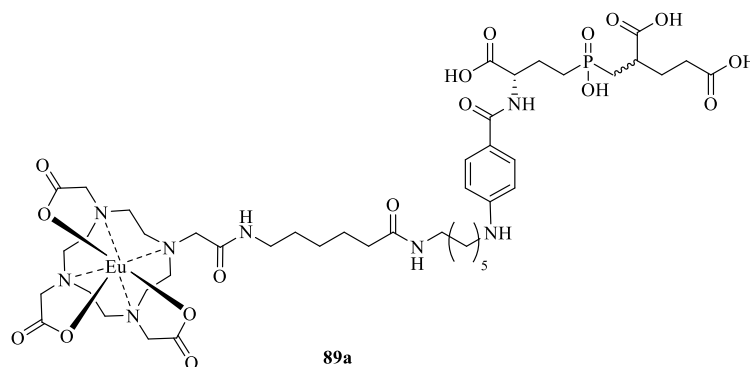
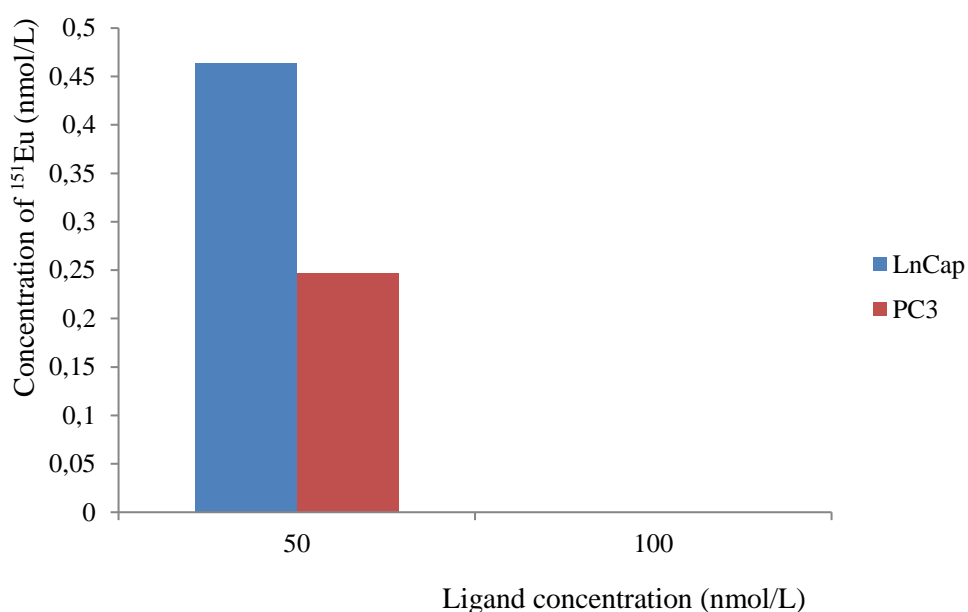


Figure 66: ICP-MS measurements of ^{151}Eu in LnCap and PC3 cells after incubation with ligand **89a**.

5 Conclusion

The aim of this work was to design and synthesize modular hybrid structures of GPI and folate for PSMA targeting. These structures were supposed to combine favorable binding characteristics of both structural elements and could thus overcome known limitations of GPI for in vivo applications. An important design criteria of these hybrid structures was modularity allowing the functionalization with effector molecules such as chemotherapeutics for targeted cancer therapy, fluorescent dyes or metal chelators for targeted cancer imaging. In order to address our hypothesis, docking studies were firstly pursued. These studies revealed that chinoline derivatives can be used as heteroaromatic moieties for the synthesis of folate mimics, due to their similarity to a pteridine. Moreover, the aniline nitrogen is a good anchor group for attachment of linkers to the effector molecule without compromising the binding affinity to PSMA. Since there are not so many literature known methods for obtaining this type of structures a new method was developed to generate these modular folates. Using Pd-catalyzed Buchwald-Hartwig arylations was shown that the synthesis of folate-GPI conjugates like **81** (Figure **68**) by *N*-arylation is possible, however highly demanding and dependent on heteroaromatic compounds. To our surprise during the synthesis, unexpected *C*- and *N*-arylations were observed for chinoline **58a**. Furthermore, variants of *C*-arylations of benzylamines have been reported only rarely in literature before.¹⁶² In these cases, no competing nucleophilic functionalities like carbamates were present. These results showed that careful alteration of ligands in Pd-catalyzed arylations of secondary heteroaryl benzylamines allows the regioselective arylation of densely functionalized precursors for modular folate analogs. Moreover, it allows the synthesis of novel *C*- and *N*-arylated structural analogs of folate, which are not easily accessible by other methods.

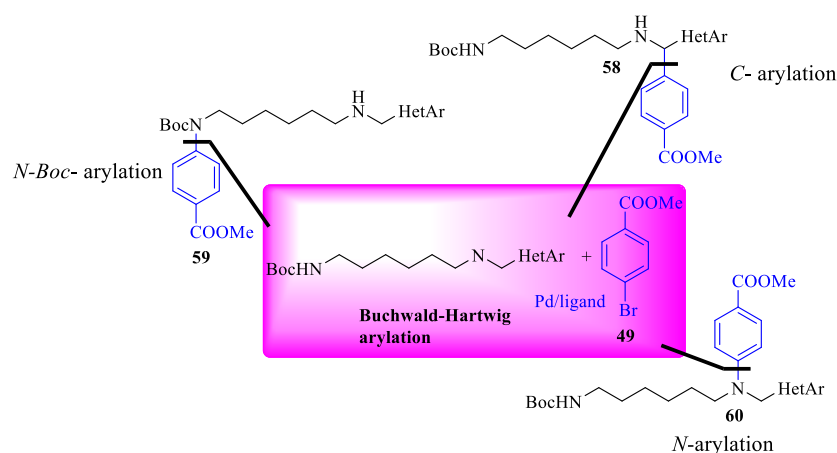


Figure 67: Regioselective arylations of secondary heteroaryl benzylamines.

Since it was highly challenging to establish efficiently a library of folate-GPI conjugates with different heteroaromatics, an alternative strategy was found to optimize affinity of PSMA binders. Following literature suggestions^{134,170,171} and focusing on altering length and nature of the aryl linker group, a novel set of simplified folate-GPI conjugates without heteroaromatics was designed (**86a-d**, Figure 68). In order to evaluate the role of linker groups in folate-GPI conjugates further docking studies were pursued and revealed following: aromatic moiety in the linker provides additional π -stacking in the PSMA binding pocket, and the geometry of molecule might play an important role for a good binding mode. For a detailed study of structure-activity relationships of hybrids **86**, a short and effective synthesis was developed, which allowed structural variation to build up a small library of test compounds.

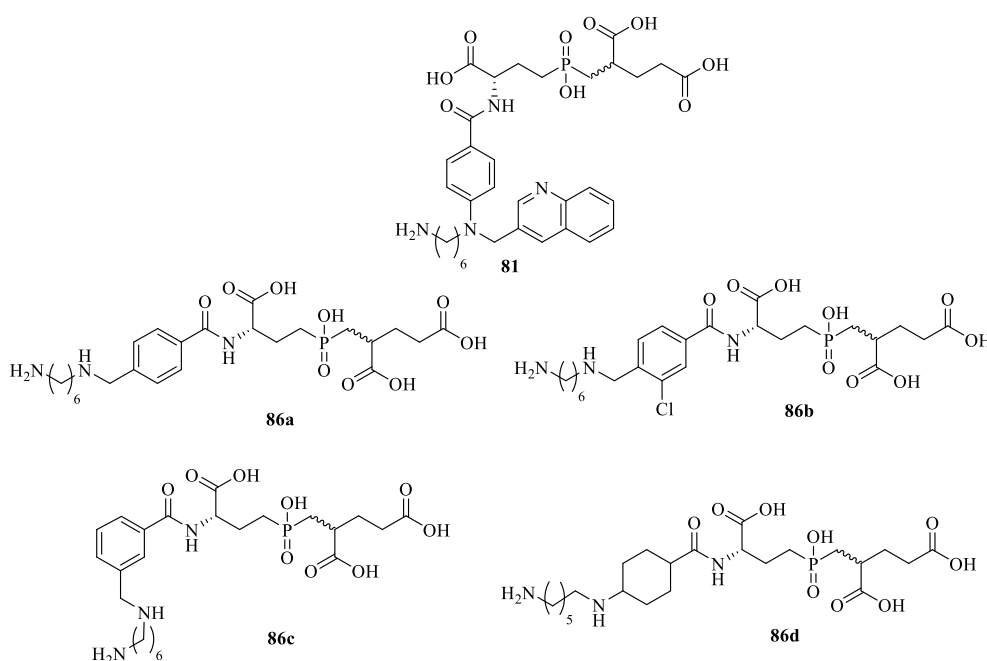


Figure 68: Library of new folate-GPI conjugates for PSMA targeting.

The previous binding studies by Maison et al of the GPI revealed low binding affinity in PBS buffer and under in vivo conditions.^{95,130} On the contrary, it was observed that in TBS GPI expresses high binding affinity. At this point, there is no clear explanation for this enhanced binding affinity in TRIS buffered medium. However, there are two hypothesis which might cause the special binding properties of GPI-derivatives to PSMA 1. phosphate anions compete with GPI in the active site of PSMA resulting in higher binding affinity in TBS vs PBS or serum. 2. TRIS enhances the binding affinity of GPI with a hitherto unknown mechanism. To address the second hypothesis, two different GPI-TRIS conjugates **95** were developed. Both derivatives **95a** and **95b** contain an aminohexanoyl spacer group, which allows further coupling

with an effector molecule. Additionally, GPI-TRIS derivative **95b** combines TRIS, GPI and an aromatic moiety mimicking folate following our previously described design.

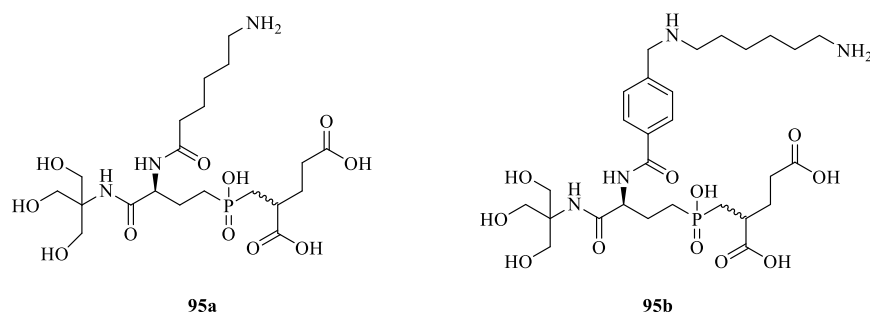


Figure 69: TRIS-GPI derivatives **95**.

The preliminary data about the binding properties of folate-GPI conjugates **83** and **89a** showed promising results and indicate selective binding to PSMA. Moreover, the strong binding of **89a** in 50 nmol/L conc. to LnCap-cells occurred in PBS-buffer, which has never been observed before for GPI derivatives. These results support the initial hypothesis of this thesis and might allow the use of folate-GPI conjugates for targeting applications in physiological media. Detailed studies are however necessary to evaluate the promising binding characteristics of novel folate analogs and also to improve further the rational design of these hybrid structures.

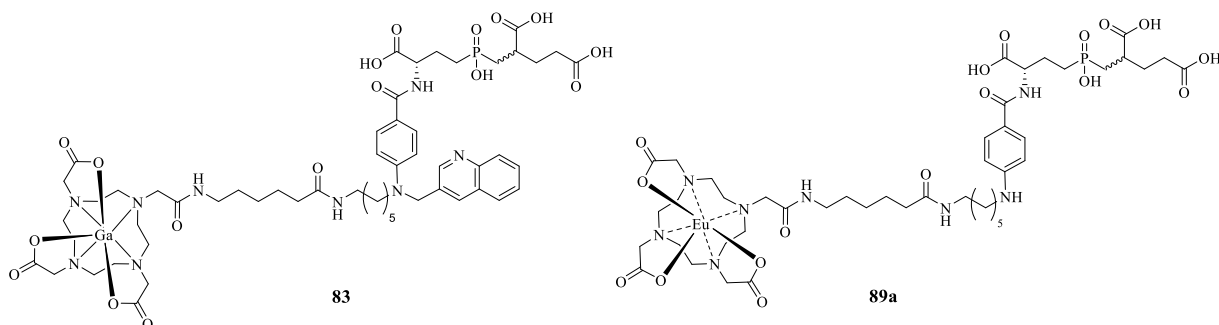


Figure 70: Investigated folate-GPI conjugates **83** and **89a** with respect to their binding affinities to PSMA.

To conclude, various folate-GPI conjugates with a broad range of structural variations were established for the purpose of PSMA targeting. These compounds are highly modular and allow the conjugation to other functional molecules such as chemotherapeutics for targeted cancer therapy, dyes or other contrast agents for targeted cancer imaging. They are thus valuable folate analogs for applications in targeted disease imaging.

6 Experimental part

6.1. General conditions

Oxygen and water sensitive reactions were carried out in flame dried glass apparatuses with dry solvents using Schlenk technique under a nitrogen or argon atmosphere. Solvents were dried by distillation under nitrogen atmosphere prior to application. Commercially available chemicals were used without further purification.

6.2. Chromatography

6.2.1. TLC

Reactions were monitored by thin layer chromatography silica-coated aluminum plates with a fluorescence indicator (Macherey-Nagel, DC Kieselgel Alugram[®] Xtra SIL G/UV₂₅₄, layer thickness 0.2 mm). UV-active compounds were detected by UV light ($\lambda = 254$ nm). Non-fluorescent compounds were stained with ninhydrin solution (0.2 g ninhydrin in 100 mL ethanol) or ceresulfate solution (5 g ammonium molybdate, 0.1 g cerium (IV)-sulfate, 90 mL H₂O, 10 mL sulfuric acid).

6.2.2. Flash chromatography

Synthesized compounds were purified by flash column chromatography on silica gel (40–60 μm) for the normal phase and for the reversed phase with RP-silica gel-columns CHROMABOND Flash RS 25 C₁₈ EC and CHROMABOND Flash RS 4 C_{18ec} with particle size 40–63 μm from *Macherey-Nagel*. Automated flash chromatography was performed with a Puriflash[®] 430 (by Interchim).

6.3. Analytics

6.3.1. Melting points

Melting points were determined in open capillary tubes on M550 instrument purchased from *A. Krüss Optronic* and the values are uncorrected.

6.3.2. NMR Spectroscopy

The NMR spectra were measured on following spectrometers: Fourier 300 MHz (F300 UHH), Avance 400 MHz (AV3400), Avance I 400 MHz (AV4001), DRX 500 MHz (AV500) and Avance III HD 600 MHz (AV3600) from *Bruker*. Chemical shifts were calibrated with signals

of residual non-deuterated solvents and are given in ppm. NMR numeration of synthesized compounds does not match with IUPAC nomenclature. All spectra were obtained at 298 K. Abbreviations used for signal patterns are: s, singlet; d, doublet; t, triplet; q, quartet; m, multiplet; dd, doublet of doublet; dt, doublet of triplet.

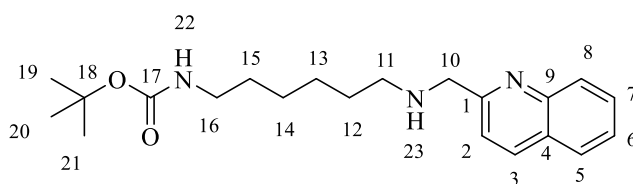
6.3.3. Infrared spectroscopy

IR spectra were measured on an ATR-FTIR spectrometer with an ATR PRO470-H unit (by *Jasco*) at room temperature.

6.3.4. Mass spectroscopy

ESI mass spectra were measured with *Agilent 6224* ESI-TOF (by *Agilent Technologies*) at 110-3200 m/z and *MicroTOF-Q* Spectrometer from *Bruker*. HRMS spectra were measured with sodiumformiat as standard. For the LC-MS measurements, a *VWR Hitachi* LaChrom Elite system was coupled with MS, and it contained L-2130 pump, L-2400 diode array detector and L-2200 autosampler. For the separation was used a column from *Macharey-Nagel*: Nucleodur C₁₈ Htec EC, 150 x 2 mm ID, particle size 5 μm .

Secondary amine 50a



N-*tert*-Butoxycarbonyl-1,6-hexanediamine (2.50 g, 11.6 mmol, 1.0 equiv.) and 2-quinolinecarboxaldehyde (2.00 g, 12.7 mmol, 1.1 equiv.) were dissolved in 17.0 mL MeOH and stirred under reflux for 48 h. NaBH₄ (4.37 g, 116 mmol, 10 equiv.) was added slowly and the reaction was stirred for another 4 h at 65 °C. The solvent was evaporated *in vacuo* and the residue was dissolved in CH₂Cl₂. The organic phase was washed three times with H₂O and dried over Na₂SO₄. The solvent was removed under reduced pressure and the crude residue was purified by flash column chromatography (silica, CH₂Cl₂/MeOH 60:1:0 → 20:1 + 0.05% NEt₃). The product **50a** was obtained as a yellow oil in a yield of 64% (1.60 g, 4.48 mmol).

TLC: *R*_f = 0.45 (CH₂Cl₂/MeOH 10:1, v/v, ninhydrin).

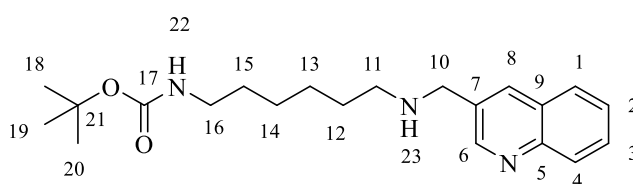
¹H NMR (400 MHz, CDCl₃, 25 °C): δ = 8.08 (d, ³*J* = 8.5 Hz, 1 H, 3-H), 8.02 (d, ³*J* = 8.5 Hz, 1 H, 8-H), 7.75 (d, ³*J* = 8.2, 1.4 Hz, 1 H, 5-H), 7.69-7.62 (m, 1 H, 7-H), 7.50-7.44 (m, 1 H, 6-H), 7.41 (d, ³*J* = 8.5 Hz, 1 H, 2-H), 4.62 (s, 1 H, 22-H), 4.10 (s, 2 H, 10-H), 3.80 (s, 1 H, 21-H), 3.09-3.00 (m, 2 H, 16-H), 2.72 (t, ³*J* = 7.3 Hz, 2 H, 11-H), 1.60-1.52 (m, 2 H, 15-H), 1.46-1.41 (m, 2 H, 12-H), 1.40 (s, 9 H, 19-H, 20-H, 21-H), 1.34-1.26 (m, 4 H, 13-H, 14-H) ppm.

¹³C-NMR (400 MHz, CDCl₃, 25 °C): δ = 159.2 (C-1), 156.1 (C-17), 147.7 (C-9), 136.6 (C-3), 129.6 (C-7), 129.0 (C-8), 127.6 (C-5), 127.4 (C-4), 126.2 (C-6), 120.5 (C-2), 78.9 (C-18), 55.3 (C-10), 49.5 (C-11), 40.5 (C-16), 30.0 (C-15), 29.6 (C-19, C-20, C-21), 28.5 (C-12), 26.9 (C-14), 26.7 (C-13) ppm.

IR (ATR): $\tilde{\nu}$ = 2929, 1719, 1634, 1178, 1101, 744 cm⁻¹.

HRMS (ESI) *m/z* calculated for C₂₁H₃₁N₃O₂ [M+H]⁺: 358.2489, found: 358.2494.

Secondary amine 50b



N-*tert*-Butoxycarbonyl-1,6-hexanediamine (1.00 g, 4.62 mmol, 1.0 equiv.) and 3-quinolinecarboxaldehyde (799 mg, 5.08 mmol, 1.1 equiv.) were dissolved in 8.00 mL MeOH and stirred under reflux for 48 h. After 48 h NaBH₄ (1.71 g, 46.2 mmol, 10 equiv.) was added slowly and the reaction was stirred for 4 h more under reflux. The solvent was evaporated *in vacuo* and the residue was dissolved in CH₂Cl₂. The organic phase was washed three times with H₂O and dried over Na₂SO₄. The solvent was removed under reduced pressure and the crude residue was purified by flash column chromatography (silica, CH₂Cl₂/MeOH 60:1 → 20:1+ 0.05% NEt₃). The product **50b** was obtained as a colorless solid in a yield of 94% (0.95 g, 2.66 mmol).

TLC: *R*_f = 0.45 (CH₂Cl₂/MeOH 10:1, v/v, ninhydrin).

¹H NMR (400 MHz, CDCl₃, 25 °C): δ = 8.94-8.81 (m, 1 H, 6-H), 8.15-8.04 (m, 2 H, 4-H, 8-H), 7.84-7.76 (m, 1 H, 1-H), 7.72-7.64 (m, 1 H, 3-H), 7.58-7.48 (m, 1 H), 4.52 (s, 1 H, 21-H), 3.99 (s, 2 H, 10-H), 3.15-3.00 (m, 2 H, 16-H), 2.73-2.59 (m, 2 H, 11-H), 1.59-1.28 (m, 17 H, 12-H, 13-H, 14-H, 15-H, 19-H, 20-H, 21-H) ppm.

¹³C NMR (101 MHz, CDCl₃, 25 °C): δ = 151.6 (C-6), 147.6 (C-17), 138.9 (C-5), 134.7 (C-8), 132.9 (C-10), 129.3 (C-1), 129.2 (C-2), 128.1 (C-9), 127.8 (C-3), 126.8 (C-4), 79.2 (C-21), 51.6 (C-10), 49.5 (C-11), 40.7 (C-16), 30.2 (C-15), 30.0 (C-14), 28.6 (C 18-20), 27.1 (C-13), 26.8 (C-12) ppm.

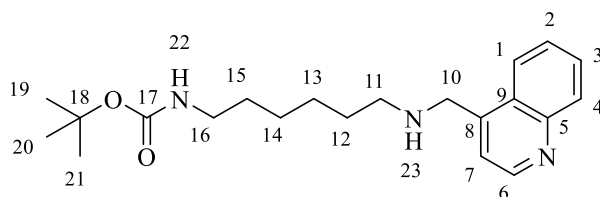
IR (ATR): $\tilde{\nu}$ = 2929, 1705, 1496, 1366, 1266, 1170, 743 cm⁻¹.

Mp: 44 °C.

CHN calcd. for C₂₁H₃₁N₃O₂: C, 70.55%; H, 8.74%; N, 11.75%, O, 8.95%. Found: C, 70.15%; H, 8.75%; N, 11.67%; O, 9.26%.

HRMS (ESI) *m/z* calculated for C₂₁H₃₁N₃O₂ [M+H]⁺: 358.2489, found: 358.2438.

Secondary amine 50c



N-*tert*-Butoxycarbonyl-1,6-hexanediamine (3.30 g, 15.6 mmol, 1.0 equiv.) and 6-quinolinecarboxaldehyde (2.64 g, 16.8 mmol, 1.1 equiv.) were dissolved in 15.0 mL MeOH

and stirred under reflux for 48 h. After 48 h NaBH₄ (5.77 g, 153 mmol, 10 equiv.) was added slowly and the reaction was stirred for 4 h more under reflux. The solvent was evaporated *in vacuo* and the residue was dissolved in CH₂Cl₂. The organic phase was washed three times with H₂O and dried over Na₂SO₄. The solvent was removed under reduced pressure and the crude residue was purified by flash column chromatography (silica, CH₂Cl₂/MeOH 60:1 → 20:1+ 0.05% NEt₃). The product **50c** was obtained as colorless oil in a yield of 95% (3.10 g, 8,68 mmol).

TLC: $R_f = 0.45$ (CH₂Cl₂/MeOH 10:1, v/v, ninhydrin).

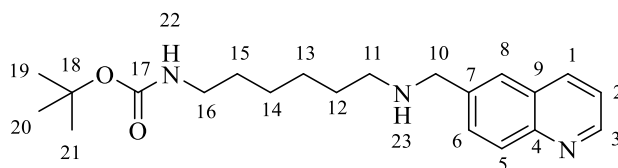
¹H NMR (600 MHz, CDCl₃, 25 °C): $\delta = 8.82$ (d, $^3J = 4.4$ Hz, 1 H, 6-H), 8.09 (dd, $^{3,4}J = 8.4$, 1.2 Hz, 1 H, 4-H), 8.03 (dd, $^{3,4}J = 8.4$, 1.2 Hz, 1 H, 1-H), 7.66 (ddd, $^{3,3,4}J = 8.4$, 6.7, 1.2 Hz, 1 H, 3-H), 7.53 (ddd, $^{3,3,4}J = 8.4$, 6.7, 1.2 Hz, 1 H, 2-H), 7.41 (d, $^3J = 4.4$ Hz, 1 H, 7-H), 4.66 (s, 1 H, 22-H), 4.21 (s, 2 H, 10-H), 3.06 (t, $^3J = 7.1$ Hz, 2 H, 16-H), 2.69 (t, $^3J = 7.1$ Hz, 2 H, 11-H), 2.23 (s, 2 H, 23-H), 1.56-1.49 (m, 2 H, 15-H), 1.46-1.42 (m, 2 H, 12-H), 1.40 (s, 9 H, 19-H, 20-H, 21-H), 1.34-1.27 (m, 4 H, 13-H, 14-H) ppm.

¹³C NMR (101 MHz, CDCl₃, 25 °C): $\delta = 156.1$ (C-17), 150.3 (C-6), 148.2 (C-5), 145.8 (C-8), 130.2 (C-9), 129.2 (C-3), 127.1 (C-2), 126.6 (C-4), 123.3 (C-1), 119.9 (C-7), 79.1 (C-18), 50.1 (C-10), 49.9 (C-11), 40.6 (C-16), 30.1 (C-15), 30.0 (C-12), 28.5 (C-19, C-20, C-21), 27.0 (C-14), 26.7 (C-13) ppm.

IR (ATR): $\tilde{\nu} = 2924, 1688, 1518, 11361, 1248, 1165, 752$ cm⁻¹.

HRMS (ESI) m/z calculated for C₂₁H₃₁N₃O₂ [M+H]⁺: 358.2489, found: 358.2500.

Secondary amine 50d



N-*tert*-Butoxycarbonyl-1,6-hexanediamine (1.60 g, 7.40 mmol, 1.0 equiv.) and 4-quinolinecarboxaldehyde (1.28 g, 8.14 mmol, 1.1 equiv.) were dissolved in 15.0 mL MeOH and stirred under reflux for 48 h. After 48 h NaBH₄ (2.80 g, 74.0 mmol, 10 equiv.) was added slowly and the reaction was stirred for 4 h more under reflux. The solvent was evaporated *in vacuo* and the residue was dissolved in CH₂Cl₂. The organic phase was washed three times with H₂O and dried over Na₂SO₄. The solvent was removed under reduced pressure and the crude residue was purified by flash column chromatography (silica, CH₂Cl₂/MeOH 60:1 → 20:1+

0.05% NEt₃). The product **50d** was obtained as colorless oil in a yield of 90% (1.50 g, 4.20 mmol).

TLC: $R_f = 0.45$ (CH₂Cl₂/MeOH 10:1, v/v, ninhydrin).

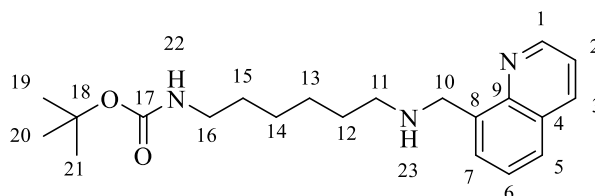
¹H NMR (300 MHz, CDCl₃, 25 °C): $\delta = 8.86\text{--}8.78$ (m, 1 H, 3-H), 8.12–8.05 (m, 1 H, 5-H), 8.03 (d, ³ $J = 8.5$ Hz, 1 H, 1-H), 7.75–7.70 (d, ⁴ $J = 1.9$ Hz, 1 H, 8-H), 7.69–7.63 (m, 1 H, 6-H), 7.34 (dd, ^{3,4} $J = 8.5, 4.2$ Hz, 1 H, 2-H), 4.66 (s, 1 H, 22-H), 3.94 (s, 2 H, 10-H), 3.03 (t, ³ $J = 7.1$ Hz, 2 H, 16-H), 2.81 (s, 1 H, 23-H), 2.63 (t, ³ $J = 7.1$ Hz, 2 H, 11-H), 1.56–1.47 (m, 2 H, 12-H), 1.44–1.34 (m, 11 H, 15-H, 19-H, 20-H, 21-H), 1.32–1.21 (m, 4 H, 13-H, 14-H) ppm.

¹³C NMR (101 MHz, CDCl₃, 25 °C): $\delta = 156.1$ (C-17), 150.2 (C-3), 147.7 (C-4), 138.1 (C-7), 135.9 (C-1), 130.3 (C-8), 129.6 (C-2), 128.2 (C-9), 126.5 (C-5), 121.3 (C-6), 79.1 (C-18), 53.6 (C-10), 49.2 (C-11), 40.5 (C-16), 30.1 (C-15), 29.7 (C-14), 28.5 (C-19, C-20, C-21), 27.0 (C-13), 29.7 (C-12) ppm.

IR (ATR): $\tilde{\nu} = 3360, 2915, 1684, 1513, 1357, 1262, 1157, 839$ cm⁻¹.

HRMS (ESI) m/z calculated for C₂₁H₃₁N₃O₂ [M+H]⁺: 358.2489, found: 358.2468.

Secondary amine 50e



N-*tert*-Butoxycarbonyl-1,6-hexanediamine (1.40 g, 6.47 mmol, 1.0 equiv.) and 8-quinolinecarboxaldehyde (1.12 mg, 7.12 mmol, 1.1 equiv.) were dissolved in 15.0 mL MeOH and stirred under reflux for 48 h. After 48 h NaBH₄ (2.45 g, 64.7 mmol, 10 equiv.) was added slowly and the reaction was stirred for 4 h more under reflux. The solvent was evaporated *in vacuo* and the residue was dissolved in CH₂Cl₂. The organic phase was washed three times with H₂O and dried over Na₂SO₄. The solvent was removed under reduced pressure and the crude residue was purified by flash column chromatography (silica, CH₂Cl₂/MeOH 60:1 → 20:1 + 0.05% NEt₃). The product **50e** was obtained as a colorless oil in a yield of 80% (1.30 g, 3.64 mmol).

TLC: $R_f = 0.40$ (CH₂Cl₂/MeOH 20:1, ninhydrin stain).

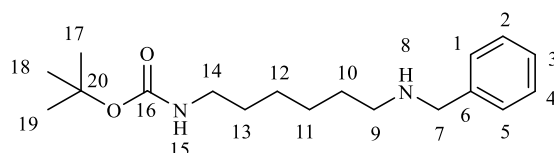
¹H NMR (600 MHz, CDCl₃, 25 °C): δ = 8.79 (dd, ^{3,4}J = 6.3, 1.9 Hz, 1 H, 1-H), 8.05 (dd, ^{3,4}J = 6.3, 1.9 Hz, 1 H, 3-H), 7.64 (d, ³J = 8.2, 1.6 Hz, 1 H, 5-H), 7.62-7.59 (m, 1 H, 7-H), 7.41-7.36 (m, 1 H, 6-H), 7.30 (dd, ^{3,4}J = 6.3, 1.9 Hz, 1 H, 2-H), 4.41 (s, 1 H, 22-H), 4.32 (s, 1 H, H-10), 3.00-2.91 (m, 2 H, 16-H), 2.59 (t, ³J = 7.4 Hz, 2 H, 11-H), 1.48 (t, ³J = 7.4 Hz, 2 H, 12-H), 1.33 (s, 11 H, 13-H, 19-H, 20-H, 21-H), 1.20-1.15 (m, 4 H, 14-H, 15-H) ppm.

¹³C NMR (151 MHz, CDCl₃, 25 °C): δ = 156.1 (C-17), 149.6 (C-1), 146.8 (C-9), 136.6 (C-3), 136.1 (C-8), 129.7 (C-7), 128.4 (C-6), 127.7 (C-5), 126.4 (C-4), 121.3 (C-2), 78.9 (C-18), 50.6 (C-10), 48.8 (C-11), 40.5 (C-16), 30.0 (C-15), 29.2 (C-14), 28.5 (C-19, C-20, C-21), 26.9 (C-13), 26.6 (C-12) ppm.

IR (ATR): $\tilde{\nu}$ = 2967, 1675, 1505, 1375, 1165, 782 cm⁻¹.

HRMS (ESI) *m/z* calculated for [C₂₁H₃₁N₃O₂+H⁺]: 358.2489, found 358.2503.

Secondary amine 50f



N-*tert*-Butoxycarbonyl-1,6-hexanediamine (3.30 g, 15.3 mmol, 1.0 equiv.) and benzylcarboxaldehyde (1.78 g, 16.8 mmol, 1.1 equiv.) were dissolved in 20.0 mL MeOH and stirred for 24 h stirred under reflux. NaBH₄ (5.77 g, 152 mmol, 10 equiv.) was added slowly and the reaction was stirred for 4 h at 65 °C. The solvent was evaporated *in vacuo* and the residue was dissolved in CH₂Cl₂. The organic phase was washed three times with H₂O and dried over Na₂SO₄. The solvent was removed under reduced pressure and the crude residue was purified by flash column chromatography (silica, CH₂Cl₂/MeOH 60:1 → 20:1+ 0.05% NEt₃). The product **50f** as colorless hygroscopic solid was obtained in a yield of 74% (2.10 g, 6.86 mmol).

TLC: *R*_f = 0.40 (CH₂Cl₂/MeOH 20:1, v/v, ninhydrin).

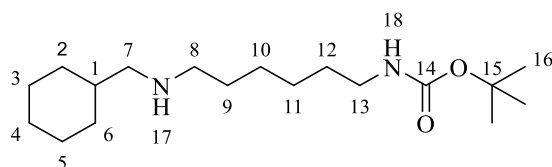
¹H NMR (300 MHz, CDCl₃, 25 °C): δ = 7.30-7.14 (m, 5 H, 1-H, 2-H, 3-H, 4-H, H-5), 4.51 (s, 1 H, 15-H), 3.73 (s, 2 H, 7-H), 3.11-2.95 (m, 2 H, 14-H), 2.57 (t, ³J = 7.6 Hz, 2 H, 9-H), 1.87 (s, 1 H, 8-H), 1.53-1.14 (m, 17 H, 10-H, 11-H, 12-H, 13-H, 17-H, 18-H, 19-H) ppm.

$^{13}\text{C-NMR}$ (300 MHz CDCl_3 , 25 °C): δ = 156.1 (C-16), 140.2 (C-6), 128.5 (C-2, C-4), 128.3 (C-1, C-5), 127.1 (C-3), 79.1 (C-20), 54.1 (C-7), 49.3 (C-9), 40.6 (C-14), 30.1 (C-13), 29.9 (C-10), 28.5 (C-17, C-18, C-19), 27.1 (C-12), 26.8 (C-13) ppm.

IR (ATR): $\tilde{\nu}$ = 2927, 1701, 1522, 1453, 1364, 1247, 7323 cm^{-1} .

HRMS (ESI) m/z calculated for $\text{C}_{18}\text{H}_{30}\text{N}_2\text{O}_2$ $[\text{M}+\text{H}]^+$: 307.2380, found: 307.2379.

Secondary amine 50g



N-tert-Butoxycarbonyl-1,6-hexanediamine (2.00 g, 9.23 mmol, 1.0 equiv.) and cyclohexancarbaldehyd (1.14 g, 10.2 mmol, 1.1 equiv.) were dissolved in 20.0 mL MeOH and stirred under reflux for 22 h. After 24 h NaBH_4 (3.85 g, 101 mmol, 10 equiv.) was added slowly and the reaction was stirred for 4 h more under reflux. The crude residue was purified by flash column chromatography (silica, $\text{CH}_2\text{Cl}_2/\text{MeOH}$ 60:1:0 \rightarrow 20:1+0.05% NEt_3). The product **50g** was obtained as colorless oil in a yield of 78% (2.32 g, 7.24 mmol).

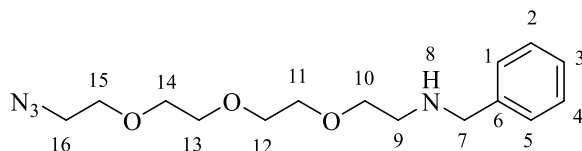
$^1\text{H-NMR}$ (400 MHz, CDCl_3 , 25 °C): δ = 4.52 (s, 1 H, 20-H), 3.13-3.04 (m, 2 H, 13-H), 2.57 (t, $^3J = 7.3$ Hz, 2 H, 8-H), 2.43 (d, $^3J = 6.7$ Hz, 2 H, 7-H), 1.78-1.65 (m, 6 H, 3-H, 4-H, 5-H), 1.52-1.46 (m, 4 H, 2-H, 9-H), 1.43 (s, 9 H, 16-H, 14-H, 18-H), 1.35-1.29 (m, 4 H, 10-H, 11-H), 1.26-1.12 (m, 3 H, 1-H, 12-H), 0.94-0.84 (m, 2 H, 6-H) ppm.

$^{13}\text{C-NMR}$ (101 MHz, CDCl_3 , 25 °C): δ = 156.4 (C-14), 79.3 (C-15), 56.9 (C-7), 50.2 (C-8), 40.7 (C-12, C-13), 38.0 (C-1), 31.6 (C-2), 30.2 (C-6), 30.0 (C-9) 28.6 (C-16), 27.2 (C-10, C-11), 26.8 (C-4), 26.2 (C-3,C-5) ppm.

IR (ATR): $\tilde{\nu}$ = 2925, 2850, 1702, 1519, 1453, 1370, 1262, 1153, 1001, 740 cm^{-1} .

MS (ESI) m/z (%): 313.3 (100) $[\text{M}+\text{H}]^+$.

Secondary amine 50h



11-Azido-3,6,9-trioxaundecan-1-amine (493 mg, 1.60 mmol, 1.0 equiv.) and benzyl-carboxaldehyde (187 mg, 1.76 mmol, 1.1 equiv.) were dissolved in 10.0 mL MeOH and stirred for 24 h stirred under reflux. NaBH₄ (605 mg, 16.0 mmol, 10 equiv.) was added slowly and the reaction was stirred for 5 h at 65 °C. The solvent was evaporated *in vacuo* and the residue was dissolved in CH₂Cl₂. The organic phase was washed three times with H₂O and dried over Na₂SO₄. The solvent was removed under reduced pressure and the crude residue was purified by flash column chromatography (silica, CH₂Cl₂/MeOH 60:1 → 20:1+ 0.05% NEt₃). The product **50h** as colorless oil was obtained in a yield of 81% (397 mg, 1.29 mmol).

TLC: $R_f = 0.30$ (CH₂Cl₂/MeOH 10:1, ninhydrin stain).

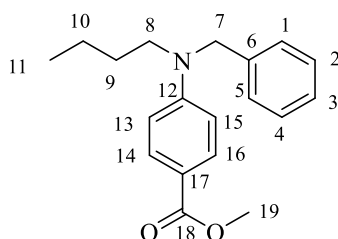
¹H NMR (300 MHz, CDCl₃): $\delta = 7.32$ -7.14 (m, 5 H, 1-H, 2-H, 3-H, 4-H, 5-H), 3.76 (s, 2 H, 7-H), 3.63-3.52 (m, 12 H, 10-H, 11-H, 12-H, 13-H, 14-H), 3.30 (t, ³ $J = 5.2$ Hz, 2 H, 16-H), 2.77 (t, ³ $J = 5.2$ Hz, 2 H, 9-H), 2.62 (s, 1 H, 8-H) ppm.

¹³C NMR (151 MHz, CDCl₃): $\delta = 139.6$ (C-6), 128.4 (C-2, C-4), 128.3 (C-1, C-5), 127.1 (C-3), 70.6 (C-10), 70.3 (C-11, C-12), 70.2 (C-13, C-14), 69.9 (C-15), 53.7 (C-7), 50.7 (C-16), 48.5 (C-9) ppm.

IR (ATR): $\tilde{\nu}$ [cm⁻¹] = 3263, 2881, 2105, 1745, 1648, 1262, 1109, 931.

HRMS (ESI) m/z calculated for [C₁₅H₂₄N₄O₃+H⁺]: 309.1921 found: 309.1925.

Methyl 4-(benzyl(butyl)amino)benzoate **62d**



N-benzylbutan-1-amine (197 mg, 0.890 mmol, 1.0 equiv.), 4-bromobenzoic acid methyl ester (192 mg, 0.890 mmol, 1.0 equiv.), Pd(OAc)₂ (2.00 mg, 8.92 μ mol, 10 mol%), BINAP (11.1 mg, 17.8 μ mol, 20 mol%) and Cs₂CO₃ (580 mg, 1.78 mmol, 2.0 equiv.) were dissolved in 8.00 mL pre-dried, degassed toluene and stirred at 110 °C for 18 h. The reaction solution was cooled to room temperature and diluted with EtOAc. The solution was filtered over a small silica plug which was rinsed with EtOAc. The filtrate was concentrated under reduced pressure and the crude residue was purified by column chromatography (silica, *n*-pentane/EtOAc 4:1).

The desired product **62d** was obtained in a yield of 53% (69.4 mg, 0.233 mmol,) as a yellow oil.

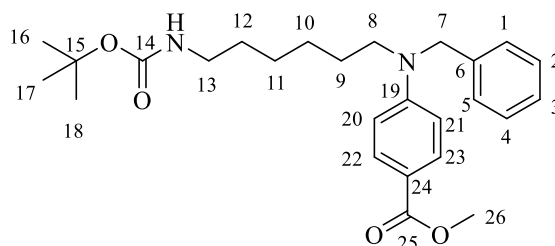
TLC: $R_f = 0.25$ ($\text{CH}_2\text{Cl}_2/\text{MeOH}$ 60:1, v/v, ninhydrin).

$^1\text{H NMR}$ (400 MHz, CDCl_3 , 25 °C): $\delta = 7.80$ (d, $^3J = 9.1$ Hz, 2 H, 13-H, 15-H), 7.29-7.24 (m, 2 H, 1-H, 5-H), 7.20 (d, $^3J = 6.7$ Hz, 1 H, 3-H), 7.14-7.10 (m, 2 H, 2-H, 4-H), 6.58 (d, $^3J = 9.1$ Hz, 2 H, 14-H, 16-H), 4.56 (s, 1 H, 7-H), 3.78 (s, 2 H, 19-H), 3.42-3.36 (m, 2 H, 8-H), 1.65-1.58 (m, 2 H, 9-H), 1.33 (q, $^3J = 7.5$ Hz, 2 H, 10-H), 0.91 (t, $^3J = 7.5$ Hz, 3 H, 11-H) ppm.

$^{13}\text{C NMR}$ (151 MHz, CDCl_3 , 25 °C): $\delta = 167.7$ (C-18), 152.2 (C-12), 138.1 (C-6), 131.8 (C-14, C-16), 129.0 (C-2, C-4), 127.4 (C-3), 126.3 (C-1, C-5), 117.3 (C-17), 111.1 (C-13, C-15), 54.5 (C-7), 51.8 (C-19), 51.4 (C-8), 29.6 (C-9), 20.6 (C-10), 14.3 (C-11) ppm.

IR (ATR): $\tilde{\nu} = 2956, 1702, 1277, 1277, 1182, 1106, 768$ cm^{-1} . **HRMS** (ESI) m/z calculated for $\text{C}_{19}\text{H}_{23}\text{NO}_2$ $[\text{M}+\text{H}]^+$: 298.1802, found: 298.1808.

Methyl-4-(benzyl(6-((*tert*-butoxycarbonyl)amino)hexyl)amino)benzoate **69f**



Secondary amine **50f** (327 mg, 1.07 mmol, 1.2 equiv.), 4-bromobenzoic acid methyl ester (192 mg, 0.891 mmol, 1.0 equiv.), $\text{Pd}(\text{OAc})_2$ (2.00 mg, 8.89 μmol , 10 mol%), PCy_3 (5.00 mg, 17.8 μmol , 20 mol%) and Cs_2CO_3 (580 mg, 1.78 mmol, 2.0 equiv.) were dissolved in 10.0 mL pre-dried, degassed toluene and stirred at 110 °C for 18 h. The reaction solution was cooled to room temperature and diluted with EtOAc. The solution was filtered over a small silica plug which was rinsed with EtOAc. The filtrate was concentrated under reduced pressure. The crude residue was purified by flash column chromatography (silica, *n*-pentane/EtOAc 90:10 \rightarrow 50:50 + 0.05% NEt_3). and the product **69f** was obtained in a yield of 11% (51.7 mg, 0.117 mmol,) as a yellow oil.

TLC: $R_f = 0.40$ (*n*-pentane/EtOAc 1:1, v/v, ninhydrin).

$^1\text{H NMR}$ (400 MHz, CDCl_3 , 25 °C): $\delta = 7.84$ (d, $^3J = 9.1$ Hz, 2 H, 20-H, 21-H), 7.34-7.28 (m, 2 H, 1-H, 5-H), 7.25-7.22 (m, 1 H, 3-H), 7.19-7.15 (m, 2 H, 2-H, 4-H), 6.63 (d, $^3J = 9.1$ Hz,

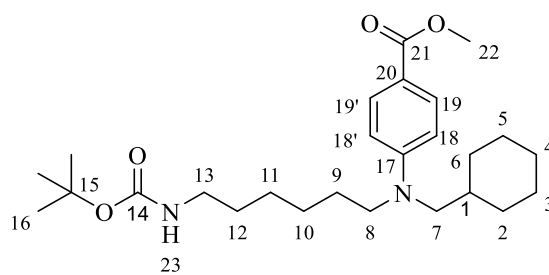
2 H, 22-H, 23-H), 4.60 (s, 2 H, 7-H), 3.83 (s, 3 H, 26-H), 3.47-3.40 (m, 2 H, 13-H), 3.14-3.06 (m, 2 H, 8-H), 1.71-1.59 (m, 4 H, 9-H, 12-H), 1.44 (s, 9 H, 16-H, 17-H, 18-H), 1.37-1.32 (m, 4 H, 9-H,10-H) ppm.

^{13}C NMR (151 MHz, CDCl_3 , 25 °C): δ = 167.5 (C-25), 156.1 (C-14), 152.0 (C-19), 137.9 (C-6), 131.6 (C-22, C-23), 128.8 (C-2, C-4), 127.2 (C-3), 126.4 (C-1, C-5), 117.2 (C-24), 110.9 (C-21, C-22), 79.3 (C-15), 54.3 (C-7), 51.6 (C-26), 51.4 (C-8), 40.6 (C-13), 30.2 (C-12), 28.6 (C 16, C-17, C-18), 27.2 (C-11), 26.9 (C-10), 26.8 (C-9) ppm.

IR (ATR): $\tilde{\nu}$ = 2929, 1701, 1603, 1521, 1278, 1181, 769 cm^{-1} .

HRMS (ESI) m/z calculated for $\text{C}_{26}\text{H}_{36}\text{N}_2\text{O}_4$ $[\text{M}+\text{H}]^+$: 441.2748, found: 441.2754.

Methyl 4-((6-((*tert*-butoxycarbonyl)amino)hexyl)(cyclohexylmethyl)amino)benzoate **69g**



Secondary amine **50g** (603 mg, 1.92 mmol, 1.0 equiv.), 4-bromobenzoic acid methyl ester (413 mg, 1.92 mmol, 1.0 equiv.), $\text{Pd}(\text{OAc})_2$ (43.1 mg, 192 μmol , 10 mol%), PCy_3 (107 mg, 382 μmol , 20 mol%) and Cs_2CO_3 (230 mg, 0.706 mmol, 3.0 equiv.) were dissolved in 9.00 mL pre-dried, degassed toluene and then heated to 110 °C for 20 h. The crude product was purified by column chromatography (silica, *n*-pentane/EtOAc 10:1 \rightarrow 2:1+0.05% NEt_3). The product **69g** was obtained in a yield of 17 % (147 mg, 0.329 mmol) as colorless oil.

TLC: R_f = 0.28. (*n*-pentane/EtOAc 10:1, v/v, ninhydrin).

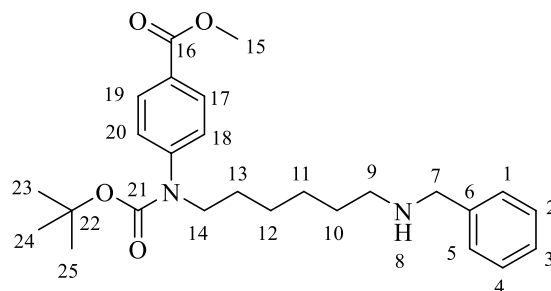
^1H -NMR (400 MHz, CDCl_3 , 25 °C): δ = 7.85 (d, 3J = 9.2 Hz, 2 H, 22-H, 23-H), 6.56 (d, 3J = 9.2 Hz, 2 H, 20-H, 21-H), 4.51 (s, 1 H, 27-H), 3.83 (s, 3 H, 26-H), 3.32 (m, 2 H, 8-H), 3.14 (d, 3J = 6.9 Hz, 2 H, 7-H), 3.12-3.07 (m, 2 H, 13-H), 1.62 - 1.06 (m, 28 H, 1-H, 2-H, 3-H, 4-H, 5-H, 6-H, 9-H, 10-H, 11-H, 12-H,16-H, 17-H, 18-H) ppm.

^{13}C -NMR (101 MHz, CDCl_3 , 25 °C): δ = 167.6 (C-25), 156.1 (C-14), 151.7 (C-19), 131.5 (C-22, C-23), 116.1 (C-24), 110.7 (C-20, C-21), 77.4 (C-15), 57.8 (C-7), 52.0 (C-26), 51.5 (C-8), 40.6 (C-13), 36.7 (C-1), 31.3 (C-2, C-6), 30.2 (C-12), 28.6 (C-16, C-17, C-18), 26.9 (C-9), 26.8 (C-3, C-5), 26.6 (C-10, C-11), 26.6 (C-4) ppm.

IR (ATR): $\tilde{\nu}$ = 3369, 2929, 1697, 1610, 1519, 1441, 1366, 1275, 1174, 1114, 1013, 826, 766 cm^{-1} .

MS (ESI) m/z (%): 447.3 (100).

Methyl 4-((6-(benzylamino)hexyl)(tert-butoxycarbonyl)amino)benzoate 70f



Secondary amine **50f** (600 mg, 1.96 mmol, 1.2 equiv.), 4-bromobenzoic acid methyl ester (350 mg, 1.63 mmol, 1.0 equiv.), Pd(OAc)₂ (36.6 mg, 16.3 μmol , 10 mol%), BINAP (203 mg, 32.6 μmol , 10 mol%) and Cs₂CO₃ (1.06 g, 3.26 mmol, 2.0 equiv.) were dissolved in 10.0 mL predried, degassed toluene and stirred at 110 °C for 18 h. The crude residue was purified by flash column chromatography (silica, CH₂Cl₂/MeOH 40:1+ 0.05% NEt₃). The product was obtained in a yield of 24% (210 mg, 0.477 mmol) as dark yellow oil.

TLC: R_f = 0.20 (CH₂Cl₂/MeOH 40:1, v/v, ninhydrin).

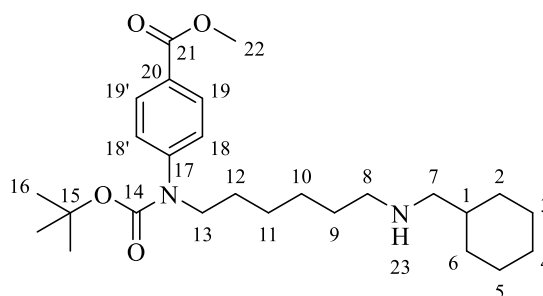
¹H-NMR (400 MHz, CDCl₃, 25 °C): δ = 7.98 (d, 3J = 8.6 Hz, 2 H, 17-H, 19-H), 7.36-7.20 (m, 7 H, 1-H, 2-H, 3-H, 4-H, 5-H, 18-H, 20-H), 3.89 (s, 3 H, 15-H), 3.78 (s, 2 H, 7-H), 3.67-3.60 (m, 2 H, 14-H), 2.94 (s, 1 H, 8-H), 2.65-2.64 (m, 2 H, 9-H), 1.58-1.46 (m, 4 H, 10-H, 11-H), 1.42 (s, 9 H, 23-H, 24-H, H-25), 1.32-1.23 (m, 4 H, 12-H, 13-H) ppm.

¹³C-NMR (101 MHz, CDCl₃): δ = 166.7 (C-16), 154.2 (C-21), 147.0 (C-26), 139.6 (C-6), 130.2 (C-17, 19), 128.5 (C-2, C-4), 128.4 (C-1, C-5), 127.2 (C-3), 126.2 (C-18, C-20), 80.8 (C-22), 53.8 (C-7), 52.2 (C-15), 49.7 (C-14), 49.1 (C-9), 29.7 (C-10), 28.4 (C-11), 28.6 (C-23, C-24, C-25), 27.0 (C-12), 26.7 (C-13) ppm.

IR (ATR): $\tilde{\nu}$ = 2927, 1698, 1605, 1366, 1154, 1111, 699 cm^{-1} .

HRMS (ESI) m/z calculated for C₂₆H₃₆N₂O₄ [M+H]⁺: 441.2748, found: 441.2753.

Methyl 4-((tert-butoxycarbonyl)(6-((cyclohexylmethyl)amino)hexyl)amino)benzoate 70g



Secondary amine **50g** (302 mg, 966 μmol , 1.0 equiv.), 4-bromobenzoic acid methyl ester (209 mg, 972 μmol , 1.0 equiv.), Pd(OAc)₂ (302 mg, 966 μmol , 10 mol%), SPhos (78.8 mg, 192 μmol , 20 mol%) and Cs₂CO₃ (626 mg, 1.92 mmol, 2.0 equiv.) were dissolved in 5 mL pre-dried, degassed toluene and then stirred at 110 °C for 20 h. The crude residue was purified by column chromatography (silica, *n*-pentane/EtOAc 10:1 → 2:1+0.05% NEt₃). The product was obtained in a yield of 24 % (101 mg, 0.226 mmol) as colorless oil.

TLC: $R_f = 0.28$ (CH₂Cl₂/MeOH 30:1, v/v, ninhydrin).

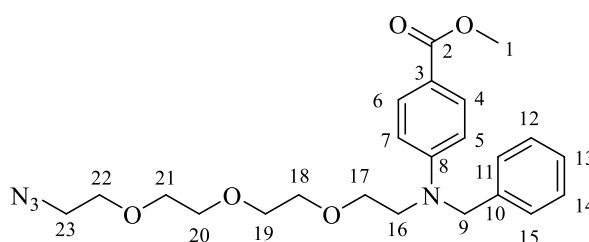
¹H NMR (400 MHz, CDCl₃, 25 °C): $\delta = 7.98$ (d, $^3J = 8.5$ Hz, 2 H, 22-H, 23-H), 7.25 (d, $^3J = 8.5$ Hz, 2 H, 20-H, 21-H), 3.89 (s, 3 H, 26-H), 3.67-3.62 (m, 2 H, 13-H), 2.52 (t, $^3J = 7.3$ Hz, 2 H, 8-H), 2.40 (d, $^3J = 6.7$ Hz, 2 H, 7-H), 1.76-1.45 (m, 11 H, 1-H, 2-H, 3-H, 4-H, 5-H, 6-H), 1.42 (s, 9 H, 16-H, 17-H, 18-H), 1.32-1.09 (m, 8 H, 9-H, 10-H, 11-H, 12-H) ppm.

¹³C NMR (101 MHz, CDCl₃, 25 °C): $\delta = 166.7$ (C-25), 154.2 (C-14), 147.0 (C-19), 130.3 (C-22, C-23), 127.2 (C-24), 126.2 (C-20, C-21), 80.8 (C-15), 56.9 (C-7), 52.2 (C-26), 50.2 (C-8), 49.8 (C-13), 38.0 (C-1), 31.6 (C-2, C-6), 30.1 (C-9), 28.6 (C-12), 28.4 (C-16, C-17, C-18), 27.1 (C-3, C-5), 26.8 (C-10, C-11), 26.2 (C-4) ppm.

IR (ATR): $\tilde{\nu} = 2921, 2846, 1702, 1610, 1444, 1370, 1275, 1153, 1101, 761, 696$ cm⁻¹.

HRMS (ESI) m/z calculated for C₂₆H₄₂N₂O₄ [M+H]⁺: 447.3217, found: 447.3256.

Methyl 4-((2-(2-(2-(2-azidoethoxy)ethoxy)ethoxy)ethyl)(benzyl)amino)benzoate **60h**



Secondary amine **50h** (70.0 mg, 0.227 mmol, 1.0 equiv.), 4-bromobenzoic acid methyl ester (73.2 mg, 0.340 mmol, 1.5 equiv.), Pd(OAc)₂ (509 μg , 2.27 μmol , 10 mol%), CyJohnPhos (159 μg , 4.54 μmol , 20 mol%) and Cs₂CO₃ (148 mg, 0.454 mmol, 2.0 equiv.) were dissolved

in 5.00 mL pre-dried, degassed toluene and stirred at 110 °C for 24 h. The reaction solution was cooled to room temperature and diluted with EtOAc. The solution was filtered over a small silica plug which was rinsed with EtOAc. The filtrate was concentrated under reduced pressure and the crude residue was purified by flash column chromatography (silica, CH₂Cl₂/MeOH 50:1 + 0.05% NEt₃). The product was obtained in a yield of 38% (38.2 mg, 86.4 μmol) as a yellow oil.

TLC: R_f = 0.35 (CH₂Cl₂/MeOH 40:1, ninhydrin stain).

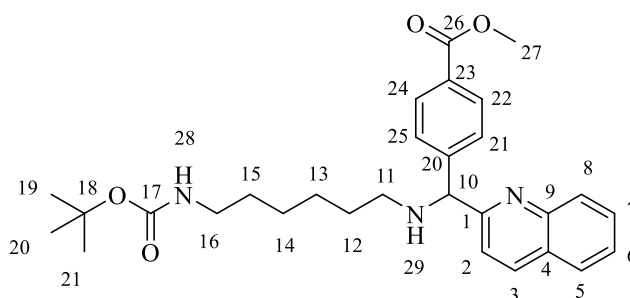
¹H NMR (600 MHz, CDCl₃): δ = 7.85 (d, ³*J* = 9.0 Hz, 2 H, 4-H, 6-H), 7.32-7.28 (m, 2 H, 11-H, 15-H), 7.26-7.23 (m, 1 H, 13-H), 7.19-7.14 (m, 2 H, 12-H, 14-H), 6.69 (d, ³*J* = 9.0 Hz, 2 H, 5-H, 7-H), 4.69 (s, 2 H, 9-H), 3.83 (s, 3 H, 1-H), 3.73-3.69 (m, 4 H, 22-H, 23-H), 3.66-3.59 (m, 10 H, 17-H, 18-H, 19-H, 20-H, 21-H), 3.36 (t, ³*J* = 5.0 Hz, 2 H, 16-H) ppm.

¹³C NMR (151 MHz, CDCl₃): δ = 167.4 (C-2) 152.0 (C-8), 137.8 (C-10), 131.5 (C-4, C-6) 128.8 (C-11, C-15), 127.2 (C-13), 126.4 (C-12, C-14), 117.5 (C-3), 111.2 (C-5, C-7), 70.9 (C-17, C-18), 70.2 (C-19, C-20), 68.8 (C-21, C-22), 54.8 (C-9), 51.6 (C-1), 50.9 (C-16), 50.8 (C-23) ppm.

IR (ATR): $\tilde{\nu}$ [cm⁻¹] = 3372, 2889, 2105, 1684, 1588, 1270, 1109, 760.

HRMS (ESI) m/z calculated for [C₂₃H₃₀N₄O₅+H⁺]: 443.2216, found: 443.2232.

4-[2-Quinoliny][6-[[[(1,1-dimethylethoxy)carbonyl]-amino]-hexylamino]methyl]-methylbenzoat **58a**



Secondary amine **50a** (35.0 mg, 97.9 μmol, 1.0 equiv.), 4-bromobenzoic acid methyl ester (21.0 mg, 97.9 μmol, 1.0 equiv.), Pd(OAc)₂ (1.10 mg, 4.90 μmol, 5 mol%), PCy₃ (3.43 mg, 97.9 μmol, 10 mol%) and Cs₂CO₃ (64 mg, 0.20 mmol, 2.0 equiv.) were dissolved in 8.00 mL predried, degassed toluene and stirred at 110 °C for 20 h. The reaction solution was cooled to room temperature and diluted with EtOAc. The solution was filtered over a small silica plug which was rinsed with EtOAc. The filtrate was concentrated under reduced pressure and the crude residue was purified by flash column chromatography (silica, CH₂Cl₂/MeOH 60:1 →

20:1 + 0.05% NEt₃). The product **58a** was obtained in a yield of 48% (20.7 mg, 42.1 μmol) as a dark yellow oil.

TLC: *R*_f = 0.30 (CH₂Cl₂/MeOH 40:1, v/v, ninhydrin).

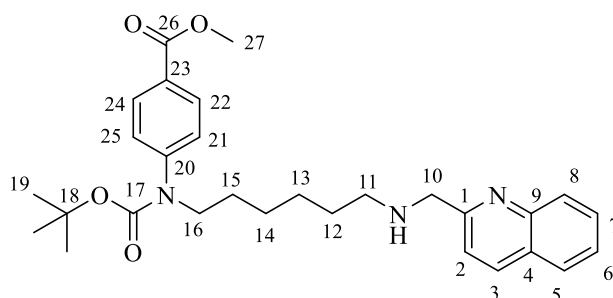
¹H NMR (300 MHz, CDCl₃, 25 °C): δ = 8.09 (dd, ^{3,4}*J* = 8.5, 6.9 Hz, 1 H, 3-H), 8.02 (dd, ^{3,4}*J* = 8.5, 6.9 Hz, 1 H, 8-H), 7.97 (d, ³*J* = 8.4 Hz, 2 H, 22-H, 24-H), 7.74 (dd, ^{3,4}*J* = 8.5, 6.9 Hz, 1 H, 5-H), 7.68 (ddd, ^{3,3,4}*J* = 8.5, 6.9, 1.5 Hz 1 H, 7-H), 7.57 (d, ³*J* = 8.4 Hz, 2 H, 21-H, 25-H), 7.48 (ddd, ^{3,3,4}*J* = 8.5, 6.9, 1.5 Hz, 1 H, 6-H), 7.36 (d, ³*J* = 8.5 Hz, 1 H, 2-H), 5.14 (s, 1 H, 10-H), 4.55 (s, 1 H, 28-H), 3.86 (s, 3 H, 27-H), 3.14-2.98 (m, 2 H, 16-H), 2.64-2.54 (m, 2 H, 11-H), 2.45 (s, 1 H, 29-H), 1.61-1.49 (m, 2 H, 12-H), 1.41 (s, 9 H, 19-H, 20-H, 21-H), 1.39-1.18 (m, 6 H, 13-H, 14-H, 15-H) ppm.

¹³C NMR (75 MHz, CDCl₃, 25 °C): δ = 166.9 (C-26), 161.9 (C-1), 156.0 (C-17), 148.0 (C-20), 147.6 (C-9), 136.7 (C-3), 129.9 (C-22, C-24), 129.5 (C-23), 129.3 (C-7), 129.2 (C-6), 127.8 (C-21, C-25), 127.5 (C-8), 127.4 (C-5), 126.4 (C-4), 120.0 (C-2), 79.0 (C-18), 68.9 (C-10), 53.5 (C-27), 52.1 (C-11), 48.6 (C-16), 30.2 (C-15), 30.1 (C-12), 28.5 (C-19, C-20, C-21), 27.0 (C-13), 26.7 (C-14) ppm.

IR (ATR): $\tilde{\nu}$ = 2929, 1719, 1634, 1178, 1101, 744 cm⁻¹.

HRMS (ESI) *m/z* calculated for C₂₉H₃₇N₃O₄ [M+H]⁺: 492.2857, found: 492.2864.

Methyl-4-((*tert*-butoxycarbonyl)(6-((quinolin-2-ylmethyl)amino)hexyl)amino)benzoate **59a**



Secondary amine **50a** (370 mg, 1.04 mmol, 1.2 equiv.), 4-bromobenzoic acid methyl ester (186 mg, 0.865 mmol, 1.0 equiv.), Pd(OAc)₂ (19.0 mg, 84.6 μmol, 10 mol%), BINAP (107 mg, 0.172 mmol, 20 mol%) and Cs₂CO₃ (840 mg, 2.58 mmol, 3.0 equiv.) were dissolved in 5.00 mL pre-dried, degassed toluene and stirred at 110 °C for 20 h. The reaction solution was cooled to room temperature and diluted with EtOAc. The solution was filtered over a silica plug which was rinsed with EtOAc. The filtrate was concentrated under reduced pressure and the crude residue was purified by flash column chromatography (silica, CH₂Cl₂/MeOH 40:1+

0.05% NEt₃). The product **59a** was obtained in a yield of 12% (60.0 mg, 0.122 mmol) as a dark yellow oil.

TLC: $R_f = 0.30$ (CH₂Cl₂/MeOH 20:1, v/v, ninhydrin).

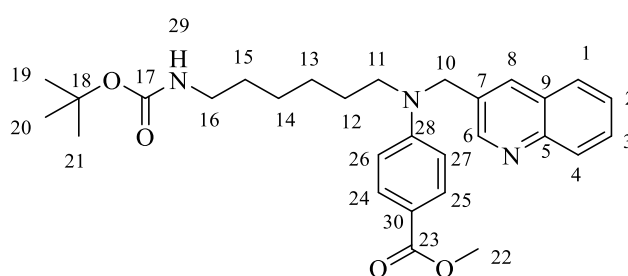
¹H-NMR (600 MHz, CDCl₃): $\delta = 8.12$ (d, $^3J = 8.3$ Hz, 1 H, 3-H), 8.04 (d, $^3J = 8.3$ Hz, 1 H, 8-H), 7.99 (d, $^3J = 8.6$ Hz, 2 H, 22-H, 24-H), 7.80 (dd, $^3,4J = 8.3, 1.3$ Hz, 1 H, 5-H), 7.70 (ddd, $^3,3,4J = 8.3, 6.9, 1.5$ Hz, 1 H, 7-H), 7.52 (ddd, $^3,3,4J = 8.3, 6.9, 1.5$ Hz, 1 H, 6-H), 7.43 (d, $^3J = 8.3$ Hz, 1 H, 2-H), 7.27-7.24 (m, 2 H, H-21, H-25), 4.13 (s, 2 H, 10-H), 3.90 (s, 3 H, 27-H), 3.68-3.62 (m, 2 H, 16-H), 2.74 (t, $^3J = 7.3$ Hz, 2 H, 11-H), 1.61-1.51 (m, 4 H, 12-H, 15-H), 1.43 (s, 9 H, 19-H, 20-H, 21-H), 1.37-1.33 (m, 2 H, 13-H), 1.32-1.28 (m, 2 H, 14-H) ppm.

¹³C NMR (151 MHz, CDCl₃, 25 °C): $\delta = 166.8$ (C-26), 159.2 (C-1), 154.3 (C-17), 147.7 (C-20), 147.0 (C-9), 136.8 (C-3), 130.3 (C-22, C-24), 129.7 (C-7), 129.1 (C-8), 127.7 (C-6), 127.5 (C-23), 127.2 (C-4), 126.4 (C-5), 126.3 (C-21, C-25), 120.6 (C-2), 80.8 (C-18), 55.3 (C-10), 52.2 (C-27), 49.7 (C-11), 49.7 (C-16), 29.8 (C-15), 28.6 (C-12), 28.4 (C-19), 27.0 (C-13), 26.7 (C-14) ppm.

IR (ATR): $\tilde{\nu} = 2929, 1719, 1634, 1433, 1275, 1178, 1101, 767$ cm⁻¹.

HRMS (ESI) m/z calculated for C₂₉H₃₇N₃O₄ [M+H]⁺: 492.2857, found: 492.2883.

Methyl-4-((6-((*tert*-butoxycarbonyl)amino)hexyl)(quinolin-3-ylmethyl)amino)benzoate **60b**



Secondary amine **50ab** (30.0 mg, 83.9 μ mol, 1.0 equiv.), 4-bromobenzoic acid methyl ester (18.0 mg, 83.9 μ mol, 1.0 equiv.), Pd(OAc)₂ (1.88 mg, 8.39 μ mol, 10 mol%), PCy₃ (4.71 mg, 16.8 μ mol, 20 mol%) and Cs₂CO₃ (54.7 mg, 0.168 mmol, 2.0 equiv.) were dissolved in 3.00 mL pre-dried, degassed toluene and stirred at 110 °C for 18 h. The reaction solution was cooled to room temperature and diluted with EtOAc. The solution was filtered over a small silica plug which was rinsed with EtOAc. The filtrate was concentrated under reduced pressure and the crude residue was purified by flash column chromatography (silica, *n*-pentane/EtOAc

90:10 → 50:50 +0.05% NEt₃). The desired product **60b** was obtained in a yield of 55% (23.0 mg, 0.468 mmol) as a yellow oil.

TLC: $R_f = 0.30$ (*n*-pentane/EtOAc 1:1, v/v, ninhydrin).

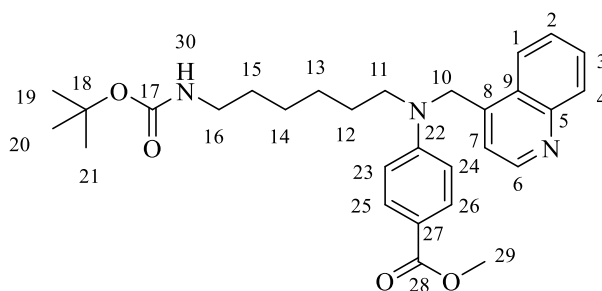
¹H NMR (400 MHz, CDCl₃, 25 °C): $\delta = 8.83$ (d, $^4J = 2.2$ Hz 1 H, H-6), 8.13 (d, $^3J = 8.3$ Hz, 1 H, H-4), 7.92-7.82 (m, 3 H, H- 26,27,8), 7.77-7.67 (m, 2 H, 1-H, 3-H), 7.54 (ddd, $^{3,3,4}J = 8.3, 6.8, 1.2$ Hz, 1 H, 2-H), 6.67 (d, $^3J = 9.1$ Hz, 2 H, 24-H, 25-H), 4.80 (s, 2 H, 10-H), 4.50 (s, 1 H, 29-H), 3.84 (s, 3 H, 22-H), 3.56-3.48 (m, 2 H, 16-H), 3.15-3.01 (m, 2 H, 11-H), 1.82-1.69 (m, 2 H, 12-H), 1.51-1.21 (m, 15 H, 13-H, 14-H, 15-H 1, 19-H, 20-H, 21-H) ppm.

¹³C NMR (101 MHz, CDCl₃, 25 °C): $\delta = 167.3$ (C-23), 164.4 (C-17), 151.5 (C-5), 149.3 (C-6), 137.5 (C-28), 131.8 (C-24, C-25), 130.9 (C-7), 129.9 (C-8), 128.7 (C-1), 128.1 (C-9), 127.8 (C-2), 127.5 (C-3), 127.3 (C-4), 118.1 (C-30), 111.2 (C-26, C-27), 80.8 (C-18), 52.5 (C-10), 51.7 (C-22), 51.6 (C-11), 40.5 (C-16), 30.2 (C-15), 28.6 (C-18, C-19, C-20), 27.3 (C-14), 26.9 (C-13), 26.7 (C-12) ppm.

IR (ATR): $\tilde{\nu} = 2929, 1702, 1603, 1278, 1182, 1108, 769$ cm⁻¹.

HRMS (ESI) m/z calculated for C₂₉H₃₇N₃O₄ [M+H]⁺: 492.2857, found: 492.2862.

Methyl-4-((6-((*tert*-butoxycarbonyl)amino)hexyl)(quinolin-4-ylmethyl)amino)benzoate
60c



Secondary amine **50c** (30.0 mg, 83.9 μ mol, 1.0 equiv.) 4-bromobenzoic acid methyl ester (18.0 mg, 83.9 μ mol, 1.0 equiv.), Pd(OAc)₂ (1.88 mg, 8.39 μ mol, 10 mol%), PCy₃ (4.71 mg, 16.8 μ mol, 20 mol%) and Cs₂CO₃ (54.7 mg, 0.168 mmol, 2.0 equiv.) were dissolved in 3.00 mL pre-dried, degassed toluene and stirred at 110 °C for 18 h. The reaction solution was cooled to room temperature and diluted with EtOAc. The solution was filtered over a silica plug which was rinsed with EtOAc. The filtrate was concentrated under reduced pressure and the crude residue was purified by flash column chromatography (silica, *n*-pentane/EtOAc 90:10 →

50:50 +0.05% NEt₃). The desired product **60c** was obtained in a yield of 56% (23.0 mg, 0.468 mmol) as a yellow oil.

TLC: $R_f = 0.30$ (*n*-pentane/EtOAc 1:1, v/v, ninhydrin).

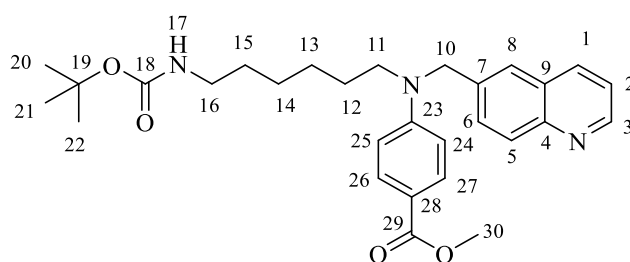
¹H NMR (600 MHz, 400 MHz, CDCl₃, 25 °C): $\delta = 8.83$ (d, $^4J = 2.2$ Hz 1 H, 6-H), 8.13 (d, $^3J = 8.3$ Hz, 1 H, 4-H), 7.92-7.82 (m, 3 H, 26-H, 27-H, 7-H), 7.77-7.67 (m, 2 H, 1-H, 3-H), 7.54 (ddd, $^3,^3,^4J = 8.3, 6.8, 1.2$ Hz, 1 H, 2-H), 6.67 (d, $^3J = 9.1$ Hz, 2 H, 24-H, 25-H), 4.80 (s, 2 H, 10-H), 4.50 (s, 1 H, 29-H), 3.84 (s, 3 H, 22-H), 3.56-3.48 (m, 2 H, 16-H), 3.15-3.01 (m, 2 H, 11-H), 1.82-1.69 (m, 2 H, 12-H), 1.51-1.21 (m, 15 H, 13-H, 14-H, 15-H, 19-H, 20-H, 21-H) ppm.

¹³C NMR (151 MHz, CDCl₃, 25 °C): $\delta = 167.5$ (C-28), 156.3 (C-17), 151.6 (C-5), 150.1 (C-6), 146.7 (C-22), 143.8 (C-8), 131.9 (C 23, C-24), 130.4 (C-3), 130.1 (C-2), 127.4 (C-4), 126.6 (C-9), 122.5 (C-1), 118.4 (C-7), 118.3 (C-27), 111.2 (C-25, C-26), 79.5 (C-18), 52.0 (C-10), 51.9 (C-29), 51.9 (C-11), 40.7 (C-16), 30.4 (C-15), 28.8 (C-19, C-20, C-21), 27.6 (C-12), 27.1 (C-13), 26.9 (C-14) ppm.

IR (ATR): $\tilde{\nu} = 2933, 1705, 1610, 1523, 1288, 1183, 722$ cm⁻¹.

HRMS (ESI) m/z calculated for C₂₉H₃₇N₃O₄ [M+H]⁺: 492.2857, found: 492.2877.

Methyl-4-((6-((*tert*-butoxycarbonyl)amino)hexyl)(quinolin-6-ylmethyl)amino)benzoate **60d**



Secondary amine **50d** (30.0 mg, 83.9 μ mol, 1.0 equiv.) 4-bromobenzoic acid methyl ester (18.0 mg, 83.9 μ mol, 1.0 equiv.), Pd(OAc)₂ (1.88 mg, 8.39 μ mol, 10 mol%), PCy₃ (4.71 mg, 16.8 μ mol, 20 mol%) and Cs₂CO₃ (54.7 mg, 0.168 mmol, 2.0 equiv.) were dissolved in 3 mL pre-dried, degassed toluene and stirred at 110 °C for 18 h. The reaction solution was cooled to room temperature and diluted with EtOAc. The solution was filtered over a small silica plug which was rinsed with EtOAc. The filtrate was concentrated under reduced pressure and the crude residue was purified by flash column chromatography (silica, *n*-pentane/EtOAc 90:10 \rightarrow 50:50

+0.05% NEt₃). The desired product was obtained in a yield of 15% (6.16 mg, 0.468 mmol) as a yellow oil.

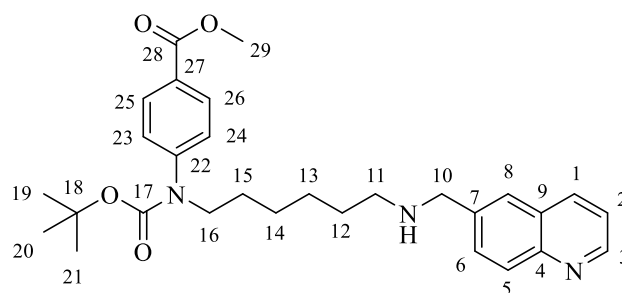
¹H NMR (400 MHz, CDCl₃, 25 °C): δ = 8.91 (m, 2 H, 3-H), 8.12-8.06 (m, 2 H, 5-H) 7.86 (d, ³J = 8.8 Hz, 2 H, 26-H, 27-H), 7.60-7.52 (m, 2 H, 8-H, 6-H), 7.39 (dd, ^{3,4}J = 8.3, 4.2 Hz, 1 H, 2-H), 6.66 (d, ³J = 8.8 Hz, 2 H, 24-H, 25-H), 4.78 (s, 2 H, 10-H), 4.49 (s, 1 H, 17-H), 3.83 (s, 3 H, 30-H), 3.54-3.46 (m, 2 H, 16-H) 3.15 (m, 2 H, 11-H), 1.79-1.60 (m, 4 H, 12-H, 15-H), 1.52-1.46 (m, 2 H, 13-H), 1.43 (s, 9 H, 20-H, 21-H, 22-H), 1.40-1.34 (m, 2 H, 14-H) ppm.

¹³C NMR (151 MHz, CDCl₃, 25 °C): δ = 167.3 (C-29), 160.1 (C-18), 156.3 (C-23), 150.0 (C-9), 145.7 (C-3), 138.3 (C-7), 134.4 (C-1), 133.0 (C-6), 132.0 (C-23, C-24), 129.6 (C-4), 125.2 (C-8), 123.4 (C-2), 121.8 (C-5), 120.7 (C-28), 111.7 (C-26, C-27), 77.2 (C-19), 54.8 (C-16), 52.4 (C-10), 52.3 (C-30), 40.7 (C-11), 30.5 (C-15), 28.8 (C-19, C-20, C-21), 27.5 (C-14), 27.0 (C-13), 26.9 (C-12) ppm.

IR (ATR): $\tilde{\nu}$ = 2830, 1710, 1624, 1550, 1293, 1337, 720 cm⁻¹.

HRMS (ESI) *m/z* calculated for C₂₉H₃₇N₃O₄ [M+H]⁺: 492.2857, found 492.2880.

Methyl-4-((*tert*-butoxycarbonyl)(6-((quinolin-6-ylmethyl)amino)hexyl)amino) benzoate **59d**



Secondary amine **50d** (600 mg, 1.70 mmol, 1.0 equiv.), 4-bromobenzoic acid methyl ester (360 mg, 1.70 mmol, 1.0 equiv.), Pd(OAc)₂ (30.0 mg, 0.170 mmol, 10 mol%), dppf (180 mg, 0.340 mmol, 20 mol%) and Cs₂CO₃ (1.00 g, 6.70 mmol, 2.0 equiv.) were dissolved in 5.00 mL pre-dried, degassed toluene and stirred at 110 °C for 20 h. The reaction solution was cooled to room temperature and diluted with EtOAc. The solution was filtered over a small silica plug which was rinsed with EtOAc. The filtrate was concentrated under reduced pressure and the crude residue was purified by flash column chromatography (silica, *n*-pentane/EtOAc 95:5 → 50:50 + 0.05% NEt₃). The product **59d** was obtained in a yield of 48% (400 mg, 0.815 mmol,) as a dark yellow oil.

TLC: *R_f* = 0.30 (CH₂Cl₂/MeOH 20:1, v/v, ninhydrin).

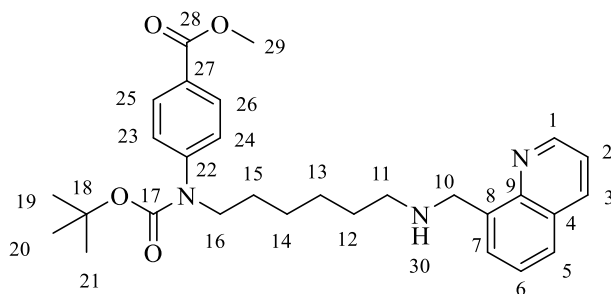
¹H NMR (600 MHz, CDCl₃, 25 °C): δ = 8.84 (dd, ^{3,4}J = 8.3, 1.7 Hz, 1 H, 3-H), 8.08 (dd, ^{3,4}J = 8.3, 1.7 Hz, 1 H, 1-H), 8.02 (d, ³J = 8.7 Hz, 1 H, 5-H), 7.96 (d, ³J = 8.6 Hz, 2 H, 23-H, 24-H), 7.70 (d, ³J = 2.0 Hz, 1 H, 8-H), 7.65 (dd, ^{3,4}J = 8.7, 1.9 Hz, 1 H, 6-H), 7.34 (dd, ^{3,4}J = 8.3, 1.7 Hz, 1 H, 2-H), 7.23 (d, ³J = 8.6 Hz, 2 H, 25-H, 26-H), 3.92 (s, 2 H, 10-H), 3.86 (s, 3 H, 29-H), 3.65-3.59 (m, 2 H, 16-H), 2.61 (t, ³J = 7.2 Hz, 2 H, 11-H), 1.54-1.45 (m, 4 H, 12-H, 15-H), 1.40 (s, 9 H, 19-H, 20-H, 21-H), 1.33-1.24 (m, 4 H, H-13, H-14) ppm.

¹³C NMR (101 MHz, CDCl₃, 25 °C): δ = 166.8 (C-28), 154.3 (C-17), 152.3 (C-22), 150.2 (C-3), 147.9 (C-4), 147.1 (C-9), 139.0 (C-7), 136.0 (C-1), 131.1 (C-6), 130.4 (C-23, C-24), 129.7 (C-8), 128.4 (C-2), 127.3 (C-5), 126.4 (C-25, C-26), 121.4 (C-27), 80.9 (C-18), 53.9 (C-10), 52.3 (C-29), 49.8 (C-11), 49.6 (C-16), 30.2 (C-15), 28.7 (C-12), 28.5 (C-19, C-20, C-21), 27.2 (C-14), 26.8 (C-13) ppm.

IR (ATR): $\tilde{\nu}$ = 2920, 1688, 1592, 1370, 1257, 1153, 708 cm⁻¹.

HRMS (ESI) *m/z* calculated for C₂₉H₃₇N₃O₄ [M+H]⁺: 492.2857, found 492.2863.

Methyl-4-((*tert*-butoxycarbonyl)(6-((quinolin-8-ylmethyl)amino)hexyl)amino)benzoate
59e



Secondary amine **50e** (30.0 mg, 83.9 μmol, 1.0 equiv.), 4- bromobenzoic acid methyl ester (18.0 mg, 83.9 μmol, 1.0 equiv.), Pd(OAc)₂ (1.88 mg, 8.39 μmol, 10 mol%), XPhos (8.01 mg, 16.8 μmol, 20 mol%) and Cs₂CO₃ (54.7 mg, 0.168 mmol, 2.00 equiv.) were dissolved in 3.00 mL pre-dried, degassed toluene and stirred at 110 °C for 18 h. The reaction solution was cooled to room temperature and diluted with EtOAc. The solution was filtered over a small silica plug which was rinsed with EtOAc. The filtrate was concentrated under reduced pressure and the crude residue was purified by column chromatography (silica, *n*-pentane/EtOAc 95:5 → 50:50 + 0.05% NEt₃). The product **59e** was obtained as bright yellow oil in a yield of 24% (10.0 mg, 20.4 μmol).

TLC: *R*_f = 0.51 (CH₂Cl₂/MeOH 20:1, v/v, ninhydrin).

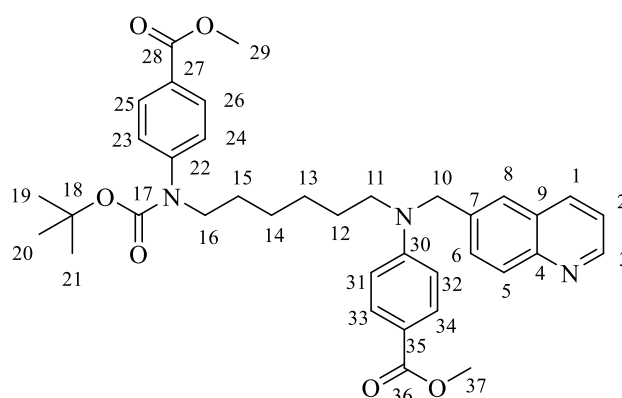
¹H NMR (400 MHz, CDCl₃, 25 °C): δ = 8.85 (dd, ^{3,4}J = 8.3, 1.7 Hz, 1 H, 1-H), 8.27 (dd, ^{3,4}J = 8.3, 1.7 Hz, 1 H, 3-H), 7.98 (d, ³J = 8.6 Hz, 2 H, 25-H, 26-H), 7.89 (dd, ^{3,4}J = 8.3, 1.3 Hz, 1 H, 5-H), 7.76 (dd, ^{3,4}J = 8.3, 1.3 Hz, 1 H, 7-H), 7.57 (dd, ^{3,4}J = 8.3, 1.3 Hz, 1 H, 6-H), 7.53 (dd, ^{3,4}J = 8.3, 1.7 Hz, 1 H, 2-H), 7.22 (d, ³J = 8.6 Hz, 2 H, 24-H, 26-H), 4.66 (s, 2 H, 10-H), 3.90 (s, 3 H, 29-H), 3.63-3.56 (m, 2 H, 16-H), 2.95 (s, 1 H, 30-H), 2.90-2.87 (m, 2 H, 11-H), 1.82-1.74 (m, 2 H, 15-H), 1.47 (t, ³J = 7.4 Hz, 2 H, 12-H), 1.40 (s, 9 H, 19-H, 20-H, 21-H), 1.31-1.26 (m, 2 H, 13-H), 1.25-1.20 (m, 2 H, 14-H) ppm.

¹³C NMR (101 MHz, CDCl₃, 25 °C): δ = 166.7 (C-28), 154.2 (C-17), 149.9 (C-1), 146.9 (C-22), 146.5 (C-9), 137.7 (C-8), 131.8 (C-3), 130.3 (C-25, C-26), 129.6 (C-7), 128.7 (C-6), 128.3 (C-2), 127.3 (C-5), 127.0 (C-4), 126.3 (C-24, C-23), 122.2 (C-27), 80.9 (C-18), 52.2 (C-29), 50.2 (C-10), 49.5 (C-11), 46.8 (C-16), 28.4 (C-19, C-20, C-21), 28.4 (C-15), 26.7 (C-14), 26.4 (C-13), 26.2 (C-12) ppm.

IR (ATR): $\tilde{\nu}$ = 2933, 1693, 1592, 1274, 1139, 1009, 778, 70 cm⁻¹.

HRMS (ESI) *m/z* calculated for C₂₉H₃₇N₃O₄ [M+H]⁺: 492.2857, found: 492.2868.

Biarylated amine 71



Secondary amine **50d** (600 mg, 1.70 mmol, 1.0 equiv.), 4-bromobenzoic acid methyl ester (720 mg, 3.40 mmol, 2.0 equiv.), Pd(OAc)₂ (30.0 mg, 170 μmol, 10 mol%), XantPhos (194 mg, 336 μmol, 20 mol%) and Cs₂CO₃ (1.00 g, 6.70 mmol, 2.0 equiv.) were dissolved in 5.00 mL pre-dried, degassed toluene and stirred at 110 °C for 20 h. The reaction solution was cooled to room temperature and diluted with EtOAc. The solution was filtered over a small silica plug which was rinsed with EtOAc. The filtrate was concentrated under reduced pressure and the crude residue was purified by flash column chromatography (silica, *n*-pentane/EtOAc 95:5 → 50:50 + 0.05% NEt₃). The product was obtained in a yield of 40% (420 mg, 0.672 mmol,) as a yellow oil.

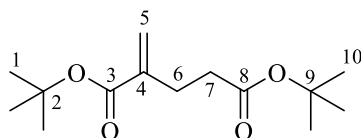
¹H NMR (400 MHz, CDCl₃, 25 °C): δ = 8.88 (d, ³J = 4.0 Hz, 1 H, 3-H), 8.11-8.04 (m, 2 H, 33-H, 34-H), 8.01-7.96 (m, 2 H, 25-H, 26-H), 7.87-7.83 (m, 2 H, 1-H, 5-H), 7.58-7.51 (m, 2 H, 6-H, 8-H), 7.38 (dd, ^{3,4}J = 8.4, 4.2 Hz, 1 H, 2-H), 7.27-7.22 (m, 2 H, 31-H, 32-H), 6.65 (d, ³J = 8.2 Hz, 2 H, 23-H, 24-H), 4.75 (s, 2 H, 10-H), 3.90 (s, 3 H, H-37), 3.83 (s, 3 H, 29-H), 3.66 (t, ³J = 7.6 Hz, 2 H, 16-H), 3.48 (t, ³J = 7.6 Hz, 2 H, 11-H), 1.69 (t, ³J = 7.6 Hz, 2 H, 12-H), 1.55 (t, ³J = 7.6 Hz, 2 H, 15-H), 1.42 (s, 9 H, 19-H, 20-H, 21-H) 1.38-1.30 (m, 4 H, H-13, H-14) ppm.

¹³C NMR (151 MHz, CDCl₃, 25 °C): δ = 167.4 (C-36), 166.7 (C-28), 154.2 (C-17), 151.8 (C-22), 150.3 (C-3), 147.8 (C-30), 147.0 (C-4), 136.3 (C-7), 136.0 (C-1), 131.6 (C-31, C-32), 130.3 (C-23, C-24), 130.2 (C-6), 128.4 (C-8), 128.4 (C-2), 127.3 (C-9), 126.3 (C-5), 124.6 (C-25, C-26), 121.5 (C-27), 117.6 (C-35), 111.02 (C-33, C-34), 80.9 (C-18), 54.3 (C-10), 52.3 (C-29), 51.6 (C-37), 51.5 (C-11), 49.6 (C-16), 28.6 (C-15), 28.4 (C-12), 27.2 (C-19, C-20, C-21), 26.8 (C-14), 26.7 (C-13) ppm.

IR (ATR): $\tilde{\nu}$ = 2930, 1699, 1600, 1458, 1264, 1177, 710 cm⁻¹.

MS (ESI) *m/z* (%): 625.3 (100) [M+H]⁺.

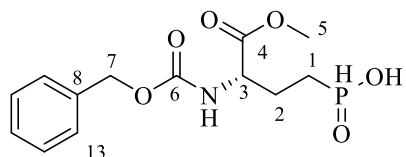
Di-*tert*-butyl 2-methylenepentanedioate **73** ^{167,168}



Tert-butyl acrylate (4.54 mL, 31.2 mmol, 1.0 equiv.) was cooled to 0 °C and tributylphosphine (0.934 mL, 3.74 mmol, 0.12 equiv.) was added in a dropwise manner. The reaction solution was stirred at the room temperature over 18 h. After removing solvent under reduced pressure, the crude residue was purified by flash column chromatography (silica, *n*-pentane/EtOAc 10:1 → 100% EtOAc). The product **73** was obtained as a light yellow liquid in a yield of 20% (1.58 g, 6.16 mmol).

¹H-NMR (300 MHz, CDCl₃): δ = 6.13 (s, 1 H, 5a-H), 5.49 (s 1 H, 5b-H), 2.61-2.52 (m, 2 H, 6-H), 2.44-2.37 (m, 2 H, 7-H), 1.51 (s, 9 H, 10-H), 1.44 (s, 9 H, 1-H) ppm.

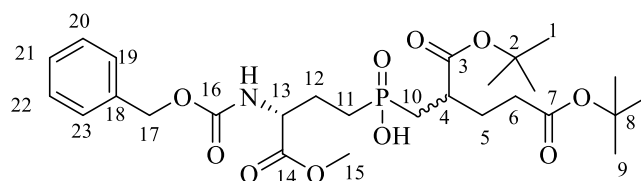
Phosphinic acid **75** ^{167,168}



Methyl-2-(((benzyloxy)carbonyl)amino)but-3-enoate (500 mg, 2.00 mmol, 1.0 equiv.) and ammonium hypophosphit (410 mg, 5.00 mmol, 2.50 equiv.) were predried for 4 h *in vacuo*. Vinylglycine derivative **74** was solved in 4.00 mL dry methanol. Subsequently, the ammonium hypophosphit was added under nitrogen atmosphere followed by dropwise adding of 2 mL of triethylborane (1 M in THF). The reaction mixture was then stirred under air at room temperature over 16 h. MeOH was removed under reduced pressure and the residue was dissolved in saturated NaHCO₃-solution (20.0 mL) and extracted with EtOAc (3x20.0 mL). The aqueous phase was adjusted with 2M hydrochloric acid to pH 2 and extracted with EtOAc (3x20 mL). The combined organic phases were dried over Na₂SO₄, filtered and the solvent was removed under reduced pressure. The product was obtained in yield 87% (548 mg, 1.74 mmol) and it was used without further purification.

¹H-NMR (300 MHz, CDCl₃): δ = 7.39-7.29 (m, 5 H, 9-H, 10-H, 11-H, 12-H, 13-H), 6.14 (s, 1 H, NH), 5.09 (s, 2 H, 7-H), 4.47-4.38 (m, 1 H, 3-H), 3.75 (s, 3 H, 5-H), 1.60-2.31 (m, 4 H, 1-H, 2-H) ppm.

Protected GPI **76**^{167,168}

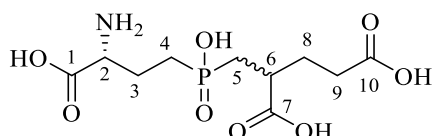


Phosphinic acid **75** has been previously dried under vacuum for 3 h and dissolved in 10.0 mL dry CH₂Cl₂. *N*, *O*-Bis(trimethylsilyl)acetamide (2.80 mL, 11.4 mmol, 6.0 equiv.) was added and the reaction solution was heated to reflux. After 4 h **73** (487 mg, 1.90 mmol, 1.0 equiv.) was added. The reaction solution was stirred for 60 h under reflux. Afterwards, 8.00 mL 1M hydrochloric acid was added and stirred for 2 h, followed by extraction with EtOAc (3x20 mL). The organic phases were collected, dried over Na₂SO₄ and the solvent was removed under reduced pressure. The crude residue was purified by reversed phase column chromatography

(RP-C₁₈, H₂O/CH₃CN 100:0 → 0:100). The product **76** was obtained in a yield of 37 % (280 mg, 0.490 mmol) as colorless oil.

¹H-NMR (300 MHz, MeOD-*d*₄): δ = 7.36-7.31 (m, 5 H, 19-H, 20-H, 21-H, 22-H, 23-H), 5.09 (s, 2 H, 17-H), 4.29-4.25 (m, 1 H, 13-H), 3.73 (s, 3 H, 15-H), 2.72-2.67 (m, 1 H, 4-H), 2.32-2.26 (m, 2 H, 10-H), 2.21-2.04 (m, 2 H, 11-H), 2.00-1.67 (m, 6 H, 5-H, 6-H, 12-H), 1.47 (d, ³J = 3.9 Hz, 18 H, 1-H, 9-H) ppm.

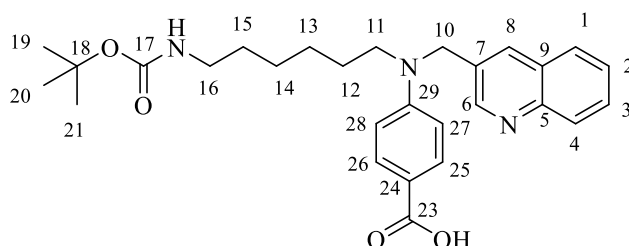
GPI **20**^{167,168}



Protected GPI **76** 500 mg (1.01 mmol, 1.0 equiv.) was dissolved in 6M hydrochloric acid (10 mL) and stirred under reflux for 18 h. Solvent was removed under reduced pressure and the residue was purified by reversed phase column chromatography (RP-C₁₈, H₂O/CH₃CN 100:0 → 0:100). After lyophilization, the isolated product **20** was obtained in a yield of 85 % (230 mg, 0.739 mmol) as a colorless powder.

¹H NMR (400 MHz, D₂O): δ = 4.09-4.06 (m, 1 H, 2-H), 2.78 (s, 1 H, 6-H), 2.50-2.43 (m, 2 H, 8-H), 2.24-2.12 (m, 3 H, 3-H, 5a-H), 2.02-1.92 (m, 2 H, 9-H), 1.90-1.75 (m, 3 H, 5b-H, 4-H) ppm.

Carboxylic acid **77b**



Tertiary amine **60b** (10.0 mg, 20.4 μmol, 1.0 equiv.) and LiOH (12.1 mg, 509 μmol, 25 equiv.) were dissolved in 3.00 mL mixture of THF/H₂O (1:1) and stirred at 40 °C for 48 h. After full conversion of starting material (ESI MS control), the solution was neutralized with 1M hydrochloric acid and extracted three times with EtOAc. The solvent was removed under

reduced pressure and the deprotected acid **77b** was obtained in a yield of 72% (7.01 mg, 14.6 μmol) as colorless solid and it was used without further purification.

^1H NMR (600 MHz, $\text{DMSO-}d_6$): δ = 8.82 (s, 1 H, H-6), 8.05-7.97 (m, 2 H, H-4, H-8), 7.91 (dd, $^3J = 8.1, 1.4$ Hz, 1 H, 1-H), 7.70 (d, $^3J = 9.1$ Hz, 2 H, 26-H, 27-H), 7.59-7.54 (m, 1 H, 2-H), 6.75 (d, $^3J = 9.1$ Hz, 2 H, 24-H-24, H-25), 4.87 (s, 2 H, 10-H), 3.58-3.52 (m, 2 H, 16-H), 2.92-2.85 (m, 2 H, 11-H), 1.66-1.59 (m, 2 H, 12-H), 1.40-1.23 (m, 15 H, 13-H, 14-H, 15-H, 19-H, 20-H, 21-H) ppm.

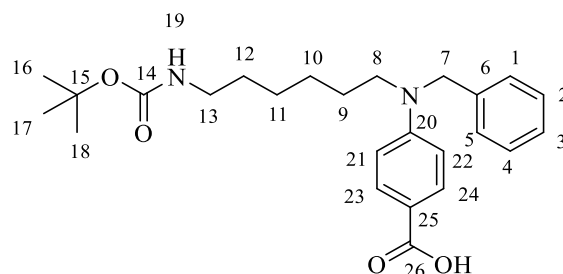
^{13}C NMR (151 MHz, $\text{DMSO-}d_6$): δ = 167.4 (C-23), 155.6 (C-17), 151.0 (C-5), 150.3 (C-6), 146.8 (C-29), 132.5 (C-7), 131.5 (C-8), 131.1 (C-25, 26), 129.0 (C-1), 128.7 (C-2), 127.8 (C-3), 127.5 (C-4), 126.8 (C-9), 118.9 (C-24), 110.9 (C-28, 27), 77.3 (C-18), 51.4 (C-10), 50.7 (C-11), 29.4 (C-14, 15), 28.2 (C 19-21), 26.6 (C-12), 26.1 (C-13), 26.0 (C-16) ppm.

IR (ATR): $\tilde{\nu}$ [cm^{-1}] = 2931, 1702, 1603, 1365, 1278, 828.

Mp.: 166.1 $^{\circ}\text{C}$.

HRMS (ESI) m/z calculated for $[\text{C}_{28}\text{H}_{35}\text{N}_3\text{O}_4+\text{H}^+]$: 478.2700, found: 478.2691.

Carboxylic acid **77f**



Methyl-4-(benzyl(6-((*tert*-butoxycarbonyl)amino)hexyl)amino)benzoate (160 mg, 0.364 mmol, 1.0 equiv.) and LiOH (217 mg, 9.08 mmol, 25 equiv.) were dissolved in 8.00 mL mixture of THF/ H_2O (1:1) and stirred at 40 $^{\circ}\text{C}$ for 48 h. After full conversion of starting material (ESI MS control), the solution was neutralized with 1M hydrochloric acid and extracted three times with EtOAc. The solvent was removed under reduced pressure and the deprotected acid **77f** was obtained in a yield of 52% (80.0 mg, 0.188 mmol,) as a yellow oil and it was used without further purification.

^1H NMR (500 MHz, CDCl_3): δ = 7.89 (d, $^3J = 9.1$ Hz, 2 H, 21-H, 22-H), 7.33-7.28 (m, 2 H, 1-H, 5-H), 7.25 -7.22 (m, 1 H, 3-H), 7.17 (d, $^3J = 7.3$ Hz, 2 H, 2-H, 4-H), 6.64 (d, $^3J = 9.1$ Hz,

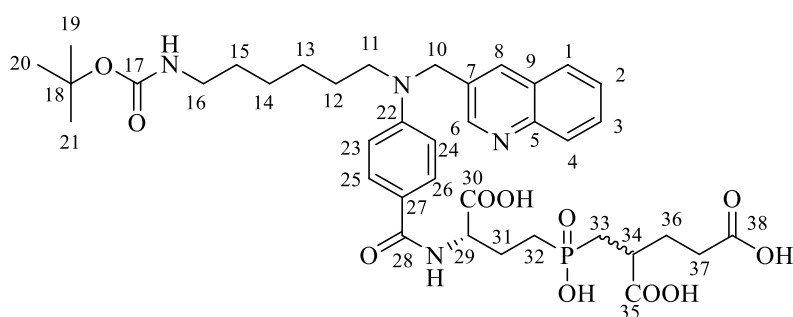
2 H, 23-H, 24-H), 4.61 (s, 2 H, 7-H), 4.49 (s, 1 H, 19-H), 3.49-3.41 (m, 2 H, 13-H), 3.17–3.04 (m, 2 H, 8-H), 1.54-1.13 (m, 17 H, 12-H, 13-H, 14-H, 15-H, 16-H, 17-H, 18-H) ppm.

^{13}C NMR (126 MHz, CDCl_3): δ = 166.5 (C-26), 154.7 (C-14), 152.5 (C-20), 137.8 (C-6), 132.3 (C-23, C-24), 128.9 (C-2, C-4), 127.3 (C-3), 126.5 (C-1, C-5), 116.0 (C-25), 111.0 (C-21, C-22), 84.7 (C-15), 54.4 (C-7), 51.4 (C-8), 40.4 (C-13), 30.2 (C-12), 28.6 (C-16, C-17, C-18), 27.2 (C-11), 26.9 (C-10), 26.8 (C-9) ppm.

IR (ATR): $\tilde{\nu}$ [cm^{-1}] = 2932, 1686, 1603, 1592, 1405, 1098, 608.

HRMS (ESI) m/z calculated for $[\text{C}_{25}\text{H}_{34}\text{N}_2\text{O}_4+\text{H}^+]$: 427.2591, found: 427.2595.

Boc-protected folate-GPI conjugate **79**



Carboxylic acid **77f** (20.0 mg, 41.9 μmol , 1.0 equiv.) was added to a dry Schlenk tube under nitrogen atmosphere and dissolved in 250 μl anhydrous DMSO. The solution was cooled to 20 $^\circ\text{C}$, followed by the addition of Et_3N (29.2 μL , 0.209 mmol, 5.0 equiv.) and stirred for 5 min. Afterwards, isobutyl chloroformate (6.86 mg, 50.2 μmol , 1.2 equiv.) was added to the solution and stirred for 1 h followed by the addition of NaN_3 (3.27 mg, 50.2 μmol , 1.2 equiv.). The solution was allowed to stir for another 1 h at the room temperature. Reaction completion was monitored by LC-MS. After removing DMSO *in vacuo*, the crude product was dissolved in 5 mL 1M hydrochloric acid and extracted with CH_2Cl_2 (3x5 mL). The combined organic layers were dried over Na_2SO_4 , filtered and concentrated under reduced pressure. The formed azide **80** was dissolved in 1.00 mL dry DMSO in a Schlenk tube under nitrogen atmosphere. Following, tetramethylguanidine (16.9 μl , 0.135 mmol, 3.0 equiv.) and GPI (7.00 mg, 22.5 μmol , 0.5 equiv.) were added into solution and stirred at room temperature over 18 h. After concentration under reduced pressure, the crude product was purified via reversed phase column chromatography (RP- C_{18} , $\text{H}_2\text{O}/\text{CH}_3\text{CN}$ 100:0 \rightarrow 0:100 + 0.05% HCO_2H). The Boc protected folate-GPI conjugate **81** was obtained as a colorless powder in yield of 41% (13.0 mg, 16.9 μmol). ^{13}C spectrum shows the mixture of two diastereomers.

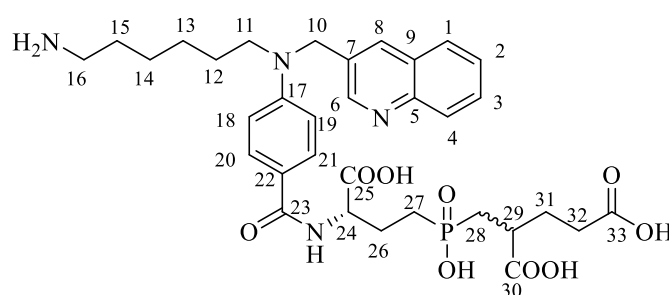
¹H NMR (600 MHz, DMSO-*d*₆): δ = 8.83 (d, ⁴*J* = 2.2 Hz, 1 H, 6-H), 8.04-8.02 (m, 1 H, 4-H), 8.00 (dd, ^{3,4}*J* = 8.3, 1.4 Hz, 1 H, 1-H), 7.91 (dd, ^{3,4}*J* = 8.3, 1.4 Hz, 1 H, 3-H), 7.74-7.70 (m, 3 H, 8-H, 24-H, 25-H), 7.57 (ddd, ^{3,4}*J* = 8.3, 1.4, 1.2 Hz, 1 H, 2-H), 6.75 (d, ³*J* = 9.1 Hz, 2 H, 26-H, 27-H), 4.87 (s, 2 H, 10-H), 4.37-4.32 (m, 1 H, 29-H), 3.55 (t, ³*J* = 7.6 Hz, 2 H, 16-H), 2.92-2.84 (m, 2 H, 11-H), 2.59-2.52 (m, 1 H, 34-H), 2.24-2.20 (m, 2 H, 33-H), 2.05-1.97 (m, 2 H, 37-H), 1.97-1.69 (m, 6 H, 31-H, 32-H, 36-H), 1.69-1.58 (m, 4 H, 14-H, 15-H) 1.41-1.21 (m, 13 H, 12-H, 13-H, 19-H, 20-H, 21-H) ppm.

¹³C NMR (151 MHz, DMSO-*d*₆): δ = 175.3 (C-35), 173.6 (C-30), 173.3 (C-38), 166.0 (C-23), 155.3 (C-22), 150.1 (C-6), 149.7 (C-17), 146.5 (C-5), 132.3 (C-8), 131.5 (C-7), 128.8 (C-25, C-26), 128.7 (C-1), 128.4 (C-2), 127.5 (C-3), 127.2 (C-9), 126.5 (C-4), 120.5 (C-27), 110.5 (C-23, C-24), 77.0 (C-18), 52.8 (³*J*_{31P-13C} = 11.8 Hz, C-29), 51.1 (C-10), 50.4 (C-11), 39.8 (C-16), 38.0 + 37.9 (diastereomers, ²*J*_{31P-13C} = 7.5 Hz, C-34), 30.9 (C-37), 30.6 (C-36), 30.0 (C-32), 29.2 (C-31), 28.0 (C-19, C-20, C-21), 27.9 (diastereomers, ¹*J*_{31P-13C} = 10.0 Hz, C-33), 26.5+26.3 (diastereomers, C-15), 25.8 (C-13), 25.8 (C-12), 23.3 (C-14) ppm.

IR (ATR): $\tilde{\nu}$ [cm⁻¹] = 2923, 1686, 1602, 1510, 1164, 754, 694.

HRMS (ESI) *m/z* calculated for [C₃₈H₅₁N₄O₁₁P+H⁺]: 771.3365, found: 771.3327.

Deprotected folate-GPI conjugate **81**



The folate-GPI conjugate **79** (3.00 mg, 3.89 μmol, 1.0 equiv.) was dissolved in a 2.00 mL mixture of CH₂Cl₂/TFA (1:1) and stirred over 16 h at room temperature. The solvent was removed under a stream of N₂. After lyophilization, the product was obtained in yield of 77% (2.00 mg, 2.98 μmol) as a colorless powder. Due to the low amount of the substance, ¹³C spectrum could not be obtained. ³¹P spectrum shows the mixture of two diastereomers.

¹H NMR (600 MHz, D₂O): δ = 9.00 (d, *J* = 2.0 Hz, 1 H, 6-H), 8.90 (s, 1 H, 4-H), 8.22 (dd, ^{3,4}*J* = 8.6, 1.0 Hz, 1 H, 1-H), 8.19 (d, ³*J* = 8.6, 1.0 Hz, 1 H, 3-H), 8.15-8.11 (m, 1 H, 2-H), 7.97-7.92 (m, 1 H, 8-H), 7.75 (d, ³*J* = 8.4 Hz, 2 H, 20-H, 21-H), 6.87 (d, ³*J* = 8.4 Hz, 2 H, 18-H, 19-H), 5.06 (s, 2 H, 10-H), 4.55 (s, 1 H, 24-H), 3.73-3.67 (m, 2 H, 16-H), 3.03-2.97 (m, 2 H, 11-

H), 2.68 (s, 1 H, 29-H), 2.34-2.25 (m, 2 H, 28-H), 2.25-2.12 (m, 2 H, 32-H), 2.12-2.00 (m, 2 H, 31-H), 1.94-1.83 (m, 2 H, 26-H), 1.81-1.71 (m, 4 H, 15-H, 27-H), 1.71-1.66 (m, 2 H, 14-H), 1.50-1.40 (m, 4 H, 12-H, 13-H) ppm.

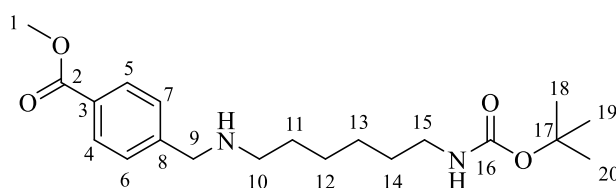
^{31}P NMR (243 MHz, DMSO- d_6): δ = 58.45, 57.81 ppm.

IR (ATR): $\tilde{\nu}$ [cm^{-1}] = 2926, 1686, 1608, 1504, 1488, 1200, 1130, 832, 712.

HRMS (ESI) m/z calculated for $[\text{C}_{33}\text{H}_{43}\text{N}_4\text{O}_9\text{P}+\text{H}^+]$: 671.2840, found: 671.2841.

HPLC Nucleodur C18 Htec EC, 150 x 2 mm ID, particle size 5 μm : gradient $\text{H}_2\text{O}/\text{MeCN}$ + 0.05% FA, 98% to 2% in 25 min, t_{R} = 14min.

Secondary amine 87a



N-*tert*-Butoxycarbonyl-1,6-hexanediamine (1.00 g, 4.62 mmol, 1.0 equiv.) and methyl 4-formylbenzoate (835 mg, 5.10 mmol, 1.1 equiv.) were dissolved in 10.0 mL MeOH and stirred under reflux for 24 h. $\text{Na}(\text{CH}_3\text{COO})_3\text{BH}$ (1.75 g, 46.2 mmol, 10 equiv.) was added slowly and the reaction was stirred for 4 h at room temperature. The solvent was evaporated *in vacuo* and the residue was dissolved in CH_2Cl_2 . The organic phase was washed three times with H_2O and dried over Na_2SO_4 . The solvent was removed under reduced pressure and the crude residue was purified by flash column chromatography (silica, $\text{CH}_2\text{Cl}_2/\text{MeOH}$ 60:1 \rightarrow 20:1 + 0.05% NEt_3). The product **87a** was obtained as a yellow oil in a yield of 59% (1.00 g, 2.75 mmol).

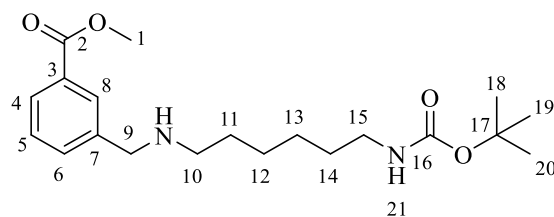
^1H NMR (400 MHz, MeOD- d_4): δ = 8.00 (d, 3J = 8.3 Hz, 2 H, 4-H, 5-H), 7.47 (d, 3J = 8.3 Hz, 2 H, 6-H, 7-H), 3.91 (s, 3 H, 1-H), 3.82 (s, 2 H, 9-H), 3.04 (t, 3J = 7.0 Hz, 2 H, 15-H), 2.62-2.53 (m, 2 H, 10-H), 1.62-1.47 (m, 4 H, 11-H, 12-H), 1.45 (s, 9 H, 18-H, 19-H, 20-H), 1.38-1.30 (m, 4 H, 13-H, 14-H) ppm.

^{13}C NMR (101 MHz, MeOD- d_4): δ = 168.3 (C-2), 158.5 (C-16), 146.4 (C-8), 130.6 (C-4, C-5), 130.1 (C-3), 129.5 (C-6, C-7), 79.7 (C-17), 54.0 (C-9), 52.6 (C-1), 49.9 (C-10), 41.2 (C-15), 30.9 (C-12), 30.4 (C-13), 28.8 (C-18, C-19, C-20), 28.1 (C-14), 27.7 (C-15) ppm.

IR (ATR): $\tilde{\nu}$ [cm^{-1}] = 2929, 2857, 1721, 1521, 1439, 1272, 1164, 1102, 857, 754.

MS (ESI) m/z (%): 351.2 (100) $[\text{M}+\text{H}]^+$.

Secondary amine 87b



N-*tert*-Butoxycarbonyl-1,6-hexanediamine 814 mg, (3.70 mmol, 1.0 equiv.) and methyl 3-formylbenzoate (680 mg, 4.15 mmol, 1.1 equiv.) were dissolved in 10.0 mL MeOH and stirred under reflux for 24 h. Na(CH₃COO)₃BH (1.20 g, 5.66 mmol, 1.5 equiv.) was added slowly and the reaction was stirred for 4 h at room temperature. The solvent was evaporated *in vacuo* and the residue was dissolved in CH₂Cl₂. The organic phase was washed three times with H₂O and dried over Na₂SO₄. The solvent was removed under reduced pressure and the crude residue was purified by flash column chromatography (silica, CH₂Cl₂/MeOH 60:1 → 20:1 + 0.05% NEt₃). The product **87b** was obtained as a yellow oil in a yield of 71 % (930 mg, 2.55 mmol).

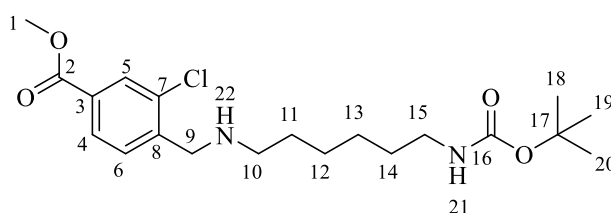
¹H NMR (400 MHz, CDCl₃): δ = 7.86 (d, ⁴J = 1.7 Hz, 1 H, 8-H), 7.79 (dd, ^{3,4}J = 7.7, 1.7 Hz, 1 H, 4-H), 7.40 (d, ³J = 7.7 Hz, 1 H, 6-H), 7.30-7.23 (m, 1 H, 5-H), 4.71 (s, 1 H, 21-H), 3.78 (s, 3 H, 1-H), 3.69 (s, 2 H, 9-H), 2.95 (t, ³J = 7.1 Hz, 2 H, 15-H), 2.48 (t, ³J = 7.1 Hz, 2 H, 10-H), 1.42-1.34 (m, 4 H, 11-H, 12-H), 1.31 (s, 9 H, 18-H, 19-H, 20-H), 1.24-1.15 (m, 4 H, 14-H, 13-H) ppm.

¹³C NMR (126 MHz, CDCl₃): δ = 167.0 (C-2), 155.9 (C-16), 140.8 (C-3), 132.6 (C-8), 130.1 (C-7), 129.1 (C-4), 128.3 (C-5), 128.1 (C-6), 78.7 (C-17), 53.5 (C-9), 51.9 (C-1), 49.2 (C-10), 40.4 (C-15), 29.9 (C-11), 29.8 (C-12), 28.3 (C 18-20), 26.9 (C-13), 26.6 (C-14) ppm.

IR (ATR): $\tilde{\nu}$ [cm⁻¹] = 2925, 2857, 1707, 1521, 1364, 1279, 1160, 1102, 981, 745.

HRMS (ESI) *m/z* calculated for [C₂₀H₃₂N₂O₄+H⁺]: 365.2435, found: 365.2430.

Secondary amine **87c**



N-*tert*-Butoxycarbonyl-1,6-hexanediamine (300 mg, 1.38 mmol, 1.0 equiv.) and methyl 3-chloro-4-formylbenzoate (300 mg, 1.52 mmol, 1.1 equiv.) were dissolved in 5.00 mL MeOH

and stirred under reflux for 24 h. Na(CH₃COO)₃BH (445 mg, 2.07 mmol, 1.5 equiv.) was added slowly and the reaction was stirred for 4 h at room temperature. The solvent was evaporated *in vacuo* and the residue was dissolved in CH₂Cl₂. The organic phase was washed three times with H₂O and dried over Na₂SO₄. The solvent was removed under reduced pressure and the crude residue was purified by flash column chromatography (silica, CH₂Cl₂/MeOH 60:1 → 20:1+ 0.05% NEt₃). The product **87c** was obtained as a yellow oil in a yield of 83% (457 mg, 1.15 mmol).

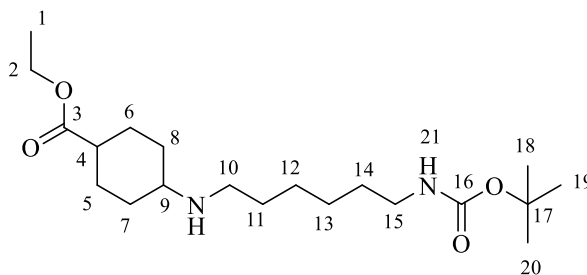
¹H NMR (500 MHz, CDCl₃): δ = 7.97 (d, ⁴J = 1.7 Hz, 1 H, 5-H), 7.85 (dd, ^{3,4}J = 8.0, 1.7 Hz, 1 H, 4-H), 7.46 (d, ³J = 8.0 Hz, 1 H, 6-H), 4.61 (s, 1 H, 21-H), 3.89 (s, 3 H, 1-H), 3.85 (s, 2 H, 9-H), 3.08-3.04 (m, 2 H, 15-H), 2.58 (t, ³J = 7.2 Hz, 2 H, 10-H), 2.18 (s, 1 H, 22-H), 1.52-1.41 (m, 4 H, 11-H, 12-H), 1.39 (s, 9 H, 18-H, 19-H, 20-H), 1.34-1.24 (m, 4 H, 13-H, 14-H) ppm.

¹³C NMR (126 MHz, CDCl₃): δ = 166.2 (C-2), 156.3 (C-16), 143.1 (C-3), 134.3 (C-8), 130.8 (C-5), 130.5 (C-7), 130.0 (C-4), 128.2 (C-6), 79.3 (C-17), 52.6 (C-1), 51.4 (C-9), 49.5 (C-10), 40.8 (C-15), 30.3 (C-11), 30.2 (C-12), 28.7 (C-18, C-19, C-20), 27.2 (C-13), 27.0 (C-14) ppm.

IR (ATR): $\tilde{\nu}$ [cm⁻¹] = 2935, 2833, 1707, 1521, 1357, 1279, 1164, 1108, 1047, 970, 758.

HRMS (ESI) *m/z* calculated for [C₂₀H₃₁ClN₂O₄+H⁺]: 399.2045, found: 399.2038.

Secondary amine **87d**



N-tert-Butoxycarbonyl-1,6-hexanediamine (100 mg, 0.460 mmol, 1.0 equiv.) and methyl ethyl 4-oxocyclohexane-1-carboxylate (86.6 mg, 0.509 mmol, 1.1 equiv.) were dissolved in 5.00 mL THF and stirred under reflux for 24 h. Na(CH₃COO)₃BH (150 mg, 0.690 mmol, 1.5 equiv.) was added slowly and the reaction was stirred for 4 h at room temperature. The solvent was evaporated *in vacuo* and the residue was dissolved in CH₂Cl₂. The organic phase was washed three times with H₂O and dried over Na₂SO₄. The solvent was removed under reduced pressure and the crude residue was purified by flash column chromatography (silica, CH₂Cl₂/MeOH 60:1 → 20:1+ 0.05% NEt₃). The product **87d** was obtained as a yellow oil in a yield of 59% (100 mg, 0.270 mmol).

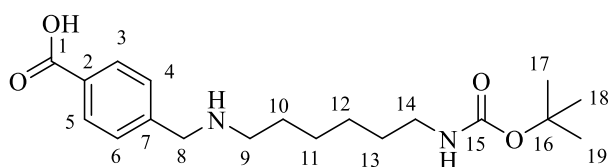
¹H NMR (500 MHz, CDCl₃): δ = 4.83 (s, 1 H, 21-H), 4.15-4.06 (m, 2 H, 2-H), 3.04 (d, ³*J* = 6.6 Hz, 2 H, 15-H), 2.93-2.85 (m, 1 H, 4-H), 2.84-2.75 (m, 2 H, 10-H), 2.55 (t, ³*J* = 4.2 Hz, 1 H, 9-H), 2.25-2.12 (m, 2 H, 5-H), 1.97-1.83 (m, 2 H, 6-H), 1.78-1.57 (m, 4 H, 7-H, 8-H), 1.55-1.47 (m, 2 H, 11-H), 1.46-1.42 (m, 2 H, 12-H), 1.39 (s, 9 H, 18-H, 19-H, 20-H), 1.33-1.25 (m, 4 H, 13-H, 14-H), 1.23-1.18 (m, 3 H, 1-H) ppm.

¹³C NMR (126 MHz, CDCl₃): δ = 174.0 (C-3), 156.2 (C-16), 79.0 (C-17), 61.0 (C-2), 55.9 (C-4), 44.3 (C-10), 42.0 (C-9), 40.4 (C-15), 29.8 (C-11), 28.5 (C-18, C-19, C-20), 28.1 (C-12), 27.2 (C-13), 26.6 (C-14), 26.6 (C-6), 26.3 (C-5), 26.2 (C-7), 25.4 (C-8), 14.3 (C-1) ppm.

IR (ATR): $\tilde{\nu}$ [cm⁻¹] = 2935, 2824, 1711, 1570, 1458, 1348, 1167, 1047, 758.

HRMS (ESI) *m/z* calculated for [C₂₀H₃₈N₂O₄+H⁺]: 371.2904, found: 371.2957.

Carboxylic acid **86a**



Secondary amine **87a** (110 mg, 0.302 mmol, 1.0 equiv.) and LiOH (51.0 mg, 2.12 mmol, 7.0 equiv.) were dissolved in 6.00 mL mixture of THF/H₂O (1:1) and stirred at 40 °C for 18 h. After full conversion of starting material (ESI MS reaction control), the solution was neutralized with 1M hydrochloric acid and extracted three times with EtOAc. The solvent was removed under reduced pressure and the crude residue was purified by reversed phase column chromatography (RP-C₁₈, H₂O/CH₃CN 100:0 → 0:100 + 0.05% HCO₂H). The desired product **86a** was obtained in a yield of 95% (100 mg, 0.286 mmol) as colorless solid.

¹H NMR (600 MHz, MeOD₄): δ = 8.13 (d, ³*J* = 8.3 Hz, 2 H, 3-H, 5-H), 7.65 (d, ³*J* = 8.3 Hz, 2 H, 4-H, 6-H), 4.31 (s, 2 H, 8-H), 3.14-3.02 (m, 4 H, 9-H, 14-H), 1.76 (t, ³*J* = 7.8 Hz, 2 H, 11-H), 1.55-1.31 (m, 15 H, 12-H, 13-H, 14-H, 17-H, 18-H, 19-H) ppm.

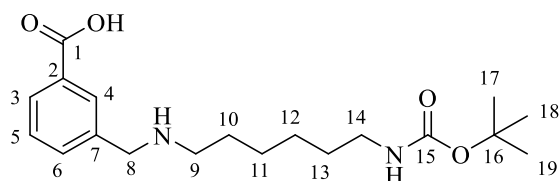
¹³C NMR (151 MHz, MeOD₄): δ = 169.2 (C-1), 158.9 (C-15), 137.7 (C-2), 133.5 (C-7), 131.7 (C-3, C-5), 131.3 (C-4, C-6), 80.1 (C-16), 52.1 (C-8), 41.3 (C-9), 40.8 (C-14), 31.0 (C-10), 29.1 (C-17, C-18, C-19), 28.6 (C-11), 27.5 (C-12), 27.2 (C-13) ppm.

IR (ATR): $\tilde{\nu}$ [cm⁻¹] = 3361, 2935, 2859, 1688, 1531, 1364, 1242, 1171, 1040, 994, 860, 761, 620.

Mp.: 226.5 °C.

HRMS (ESI) m/z calculated for $[C_{19}H_{30}N_2O_4+H^+]$: 351.2278, found: 351.2201.

Carboxylic acid **86b**



Secondary amine **87b** (100 mg, 0.273 mmol, 1.0 equiv.) and LiOH (132 mg, 5.47 mmol, 20.0 equiv.) were dissolved in 10.0 mL mixture of CH_3CN/H_2O (1:1) and stirred at 40 °C for 18 h. After full conversion of starting material (ESI MS control), the solution was neutralized with 1M hydrochloric acid and extracted three times with EtOAc. The solvent was removed under reduced pressure and the crude residue was purified by reversed phase column chromatography (RP- C_{18} , H_2O/CH_3CN 100:0 \rightarrow 0:100 + 0.05% HCO_2H). The desired product **86b** was obtained in a yield of 85% (82.5 mg, 0.235 mmol) as colorless solid.

1H NMR (400 MHz, $MeOD-d_4$): δ = 7.99 (d, 4J = 1.8 Hz, 1 H, 4-H), 7.94-7.88 (m, 1 H, 3-H), 7.52-7.46 (m, 1 H, 6-H), 7.41-7.34 (s, 1 H, 5-H), 4.15 (s, 2 H, 8-H), 3.02-2.89 (m, 4 H, 9-H, 14-H), 1.67 (t, 3J = 7.8 Hz, 2 H, 10-H), 1.44-1.25 (m, 15 H, 11-H, 12-H, 13H, 17-H, 18-H, 19-H) ppm.

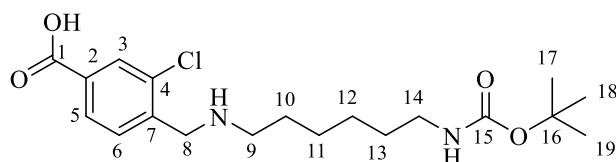
^{13}C NMR (101 MHz, $MeOD-d_4$): δ = 173.4 (C-1), 158.6 (C-15), 138.9 (C-2), 133.2 (C-4), 132.5 (C-7), 131.8 (C-3), 131.3 (C-6), 129.8 (C-5), 79.8 (C-16), 52.1 (C-8), 49.4 (C-9), 41.1 (C-14), 30.7 (C-10), 28.8 (C-17, C-18, C-19), 27.3 (C-11, C-12), 27.1 (C-13) ppm.

IR (ATR): $\tilde{\nu}$ [cm^{-1}] = 2974, 2938, 1747, 1704, 1534, 1452, 1367, 1240, 1171, 1000, 771, 693.

Mp.: 130.3 °C.

HRMS (ESI) m/z calculated for $[C_{19}H_{30}N_2O_4+H^+]$: 351.2278, found: 351.2268.

Carboxylic acid **86c**



Secondary amine **87c** (300 mg, 7.52 mmol, 1.0 equiv.) and LiOH (360 mg, 15.0 mmol, 20 equiv.) were dissolved in 10.0 mL mixture of CH_3CN/H_2O (1:1) and stirred at 40 °C for 18 h. After full conversion of starting material (ESI MS control), the solution was neutralized

with 1M hydrochloric acid and extracted three times with EtOAc. The solvent was removed under reduced pressure and the crude residue was purified by reversed phase column chromatography (RP-C₁₈, H₂O/CH₃CN 100:0 → 0:100 + 0.05% HCO₂H). The desired product **86c** was obtained in a yield of 34% (100 mg, 0.260 mmol) as colorless hygroscopic solid.

¹H NMR (600 MHz, MeOD-*d*₄): δ = 7.97 (d, ⁴*J* = 1.6 Hz, 1 H, 3-H), 7.86 (d, ³*J* = 7.9 Hz, 1 H, 5-H), 7.44 (d, ³*J* = 7.9 Hz, 1 H, 6-H), 3.90 (s, 2 H, 8-H), 3.03 (t, ³*J* = 7.0 Hz, 2 H, 14-H), 2.63-2.57 (m, 2 H, 9-H), 1.61-1.53 (m, 2 H, 10-H), 1.48 (t, ³*J* = 7.0 Hz, 2 H, 11-H), 1.44 (s, 9 H, 17-H, 18-H, 19-H), 1.38-1.33 (m, 4 H, 12-H, 13-H) ppm.

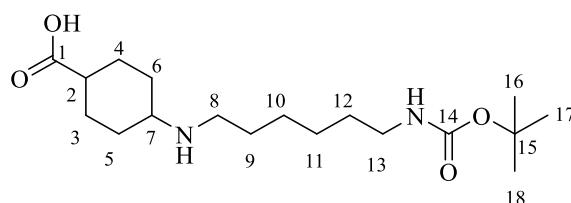
¹³C NMR (151 MHz, MeOD-*d*₄): δ = 173.4 (C-1), 158.6 (C-15), 140.2 (C-2), 139.8 (C-7), 134.3 (C-4), 131.3 (C-3), 130.8 (C-5), 128.9 (C-6), 79.8 (C-16), 51.5 (C-8), 49.8 (C-9), 41.3 (C-14), 30.9 (C-10), 30.4 (C-11), 28.8 (C-17, C-18, C-19), 28.1 (C-12), 27.7 (C-13) ppm.

IR (ATR): $\tilde{\nu}$ [cm⁻¹] = 2929, 2859, 1685, 1576, 1544, 1383, 1246, 1164, 1003, 771.

Mp.: 295.1 °C.

HRMS (ESI) *m/z* calculated for [C₁₉H₂₉ClN₂O₄+H⁺]: 385.1889, found: 385.1897.

Carboxylic acid **86d**



Secondary amine **87d** (100 mg, 0.270 mmol, 1.00 equiv.) and LiOH (110 mg, 4.57 mmol, 20.0 equiv.) were dissolved in 10.0 mL mixture of THF/H₂O (1:1) and stirred at 40 °C for 18 h. After full conversion of starting material (ESI MS control), the solution was neutralized with 1M hydrochloric acid and extracted three times with EtOAc. The solvent was removed under reduced pressure and the crude residue was purified by reversed phase column chromatography (RP-C₁₈, H₂O/CH₃CN 100:0 → 0:100 + 0.05% HCO₂H). The desired product **86d** was obtained in a yield of 79% (73.3 mg, 0.214 mmol) as colorless hygroscopic solid.

¹H NMR (400 MHz, D₂O): δ = 3.21 (s, 1 H, 2-H), 3.09-3.03 (m, 4 H, 8-H, 13-H), 2.60 (t, ³*J* = 4.4 Hz, 1 H, 7-H), 2.21-1.90 (m, 4 H, 3-H, 4-H), 1.74-1.58 (m, 4 H, 5-H, 6-H), 1.54-1.34 (m, 17 H, 9-H, 10-H, 11-H, 12-H, 16-H, 17-H, 18-H) ppm.

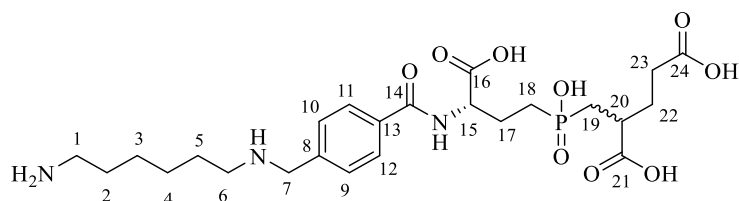
^{13}C NMR (101 MHz, D_2O): δ = 181.5 (C-1), 158.3 (C-14), 80.8 (C-15), 56.0 (C-2), 44.6 (C-8), 44.1 (C-13), 39.8 (C-7), 28.6 (C-9), 28.0 (C-10), 27.7 (C-16, C-17, C-18), 27.3 (C-11), 25.7 (C-12), 25.5 (C4), 25.4 (C-3), 25.3 (C-6), 24.9 (C-5) ppm.

IR (ATR): $\tilde{\nu}$ [cm^{-1}] = 2935, 2824, 1711, 1570, 1458, 1348, 1167, 1047, 758.

Mp.: 199.9 °C.

HRMS (ESI) m/z calculated for $[\text{C}_{18}\text{H}_{34}\text{N}_2\text{O}_4+\text{H}^+]$: 343.2591, found: 343.2588.

Simplified folate-GPI conjugate **85a**



To a solution of carboxylic acid **86a** (50.0 mg, 0.143 mmol, 1.0 equiv.) in 3.00 mL of DMF were added EDC·HCl (31.6 mg, 0.165 mmol, 1.2 equiv.) and HOSu (18.9 mg, 0.165 mmol, 1.2 equiv.) and stirred at the room temperature over 24 h under nitrogen atmosphere. The solvent was removed under reduced pressure and the crude residue was dissolved in CH_2Cl_2 , washed with sat. NaCl solution (3x5 mL) and dried over Na_2SO_4 . The solvent was removed under reduced pressure and the residue was dissolved in 1.00 mL DMF.

To a solution of GPI **20** (33.0 mg, 0.106 mmol, 1.0 equiv.) in 1.00 mL of DMF and NEt_3 (0.739 mL, 5.30 mmol, 50 equiv.) the NHS ester in DMF was added in a dropwise manner at 0 °C. The reaction mixture was stirred at the room temperature over 16 h. The solvent was removed under reduced pressure and the crude residue was purified by reversed phase column chromatography (RP- C_{18} , $\text{H}_2\text{O}/\text{CH}_3\text{CN}$ 100:0 \rightarrow 0:100 + 0.05% HCO_2H).

After lyophilization, the isolated Boc-protected product was obtained as a colorless powder and dissolved in CH_2Cl_2 (1.00 mL) and TFA (1.00 mL). The reaction solution stirred at the room temperature over 16 h. Solvents were removed under a stream of N_2 and after lyophilization the final product **85a** was obtained as a colorless powder in a yield of 81% (11.0 mg, 20.2 μmol).

^{13}C spectrum shows the mixture of two diastereomers.

^1H NMR (600 MHz, $\text{DMSO}-d_6$): δ = 7.99 (d, $^3J = 7.7$ Hz, 2 H, 11-H, 12-H), 7.58 (d, $^3J = 7.7$ Hz, 2 H, 9-H, 10-H), 4.41 (s, 1 H, 15-H), 4.20 (s, 2 H, 7-H), 2.88-2.86 (m, 2 H, 6-H), 2.77-2.74 (m, 2 H, 1-H), 2.60-2.54 (m, 1 H, 20-H), 2.27-2.20 (m, 2 H, 19-H), 2.05-1.96 (m, 2 H, 17-H), 1.87-

1.72 (m, 4 H, 18-H, 22-H), 1.70-1.54 (m, 6 H, 4-H, 5-H, 23-H), 1.32-1.25 (m, 4 H, 2-H, 3-H) ppm.

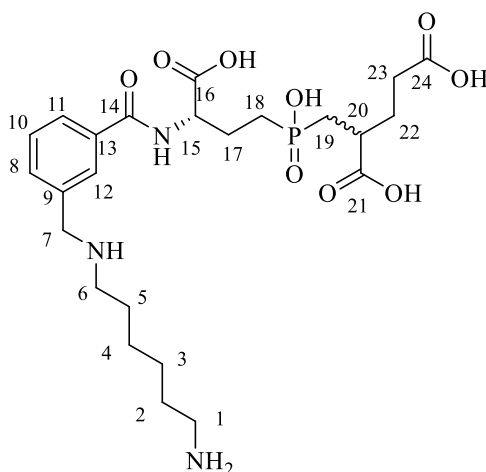
^{13}C NMR (151 MHz, DMSO- d_6): δ = 175.9 + 175.8 (diastereomers, C-21), 174.4 (C-16), 173.5 (C-24), 166.0 (C-14), 135.4 (C-13), 134.6 (C-8), 129.9 + 122.17 (diastereomers, C-11, C-12), 128.1 + 120.43 (diastereomers, C-9, C-10), 53.7 ($^3J_{31\text{P}-13\text{C}}$ = 6.74 Hz, C-15), 49.8 + 46.6 (diastereomers, C-7), 39.9 (C-6), 38.9 + 38.7 (diastereomers, $^2J_{31\text{P}-13\text{C}}$ = 15.67 Hz, C-20), 31.6 (C-2), 31.4 + 31.20 (diastereomers, C-22), 31.0 + 30.8 (diastereomers, C-23), 28.6 (diastereomers, $^1J_{31\text{P}-13\text{C}}$ = 17.42 Hz, C-19), 27.0 (C-3), 26.8+26.3 (diastereomers, $^1J_{31\text{P}-13\text{C}}$ = 13.65 Hz, C-18), 25.7 (C-5), 25.5 (C-4), 25.4 (C-1), 23.9 (C-17) ppm.

^{31}P NMR (243 MHz, DMSO- d_6): δ = 61.34 ppm.

IR (ATR): $\tilde{\nu}$ [cm^{-1}] = 2906, 1652, 1540, 1249, 1181, 1128, 1000, 794, 716.

HRMS (ESI) m/z calculated for $[\text{C}_{24}\text{H}_{38}\text{N}_3\text{O}_9\text{P}+\text{Na}^+]$: 566.2238, found: 566.2214.

Simplified folate-GPI conjugate **85b**



To a solution of carboxylic acid **86b** (90.0 mg, 0.257 mmol, 1.0 equiv.) in 5.00 mL of DMF, EDC·HCl (59.1 mg, 0.308 mmol, 1.0 equiv.) and HOSu (35.5 mg, 0.308 mmol, 1.2 equiv.) were added and stirred at the room temperature over 24 h. Solvents were removed and the crude residue was dissolved in CH_2Cl_2 , washed with sat. NaCl solution (3x5 mL) and dried over Na_2SO_4 . The solvent was removed under reduced pressure and the residue was dissolved in 3.00 mL DMF.

To a solution of GPI **20** (56.0 mg, 0.180 mmol, 1.0 equiv.) in 1.00 mL of DMF and NEt_3 (1.25 mL, 9.00 mmol, 50 equiv.) the NHS ester solution in DMF was added in a dropwise manner at 0 °C. The reaction mixture was stirred at the room temperature over 16 h. The solvent was removed under reduced pressure and the crude residue was purified by RP column

chromatography (H₂O/CH₃CN 100:0 → 0:100 + 0.05% HCO₂H). After lyophilization, the isolated Boc-protected was obtained as a colorless powder and dissolved in CH₂Cl₂ (1.50 mL) and TFA (1.50 mL). The reaction solution stirred at the room temperature over 16 h. Solvents were removed under a stream of N₂ and after lyophilization the final product **85b** was obtained as a colorless powder in a yield of 88% (12.0 mg, 22.1 μmol).

¹³C spectrum shows the mixture of two diastereomers.

¹H NMR (600 MHz, MeOD-*d*₄): δ = 8.05-8.03 (m, 1 H, 10-H), 7.94 (d, ³J = 7.8 Hz, 1 H, 9-H), 7.7 (d, ³J = 7.8 Hz, 1 H, 10-H), 7.6 (d, ³J = 7.8 Hz, 1 H, 11-H), 4.59-4.57 (m, 1 H, 15-H), 4.27 (s, 2 H, 7-H), 3.06 (t, ³J = 7.9 Hz, 2 H, 6-H), 2.91 (t, ³J = 7.7 Hz, 2 H, 1-H), 2.82-2.74 (m, 1 H, 20-H), 2.38-2.31 (m, 2 H, 19-H), 2.18-2.10 (m, 2 H, 17-H), 1.98-1.91 (m, 2 H, 18-H), 1.86-1.71 (m, 6 H, 5-H, 22-H, 23-H), 1.69-1.63 (m, 2 H, 4-H), 1.46-1.39 (m, 4 H, 2-H, 3-H) ppm.

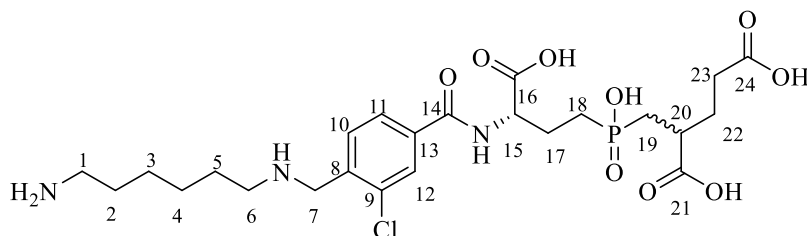
¹³C NMR (151 MHz, MeOD-*d*₄): δ = 178.5 (C-21), 176.9 (C-16), 175.0 (C-24), 169.9 (C-14), 136.5 (C-13), 134.6 (C-12), 133.4 (C-8), 130.8 (C-9), 130.5 (C-11), 130.0 (C-10), 55.3 (diastereomers, ³J_{31P-13C} = 10.7 Hz, C-15), 52.2 (C-7), 40.8 (C-6), 40.7 (C-20), 33.26 (diastereomers, ³J_{31P-13C} = 4.33 Hz, C-22), 33.1 (C-2), 32.6 (C-3), 32.4 (C-23), 30.3 (diastereomers, J = 10.9 Hz, C-19), 28.6+28.5 (diastereomers, C-4), 27.9 (C-18), 27.4 + 27.3 (diastereomers, C-5), 27.2+27.1 (diastereomers, C-1), 25.1 (C-17) ppm.

³¹P NMR (162 MHz, DMSO-*d*₆): δ = 38.37 ppm.

IR (ATR): $\tilde{\nu}$ [cm⁻¹] = 2935, 1655, 1540, 1420, 1246, 1177, 1128, 1026, 791, 716.

HRMS (ESI) *m/z* calculated for [C₂₄H₃₈N₃O₉P+H⁺]: 544.2418, found: 544.2398.

Simplified folate-GPI conjugate **85c**



To a solution of carboxylic acid **86c** (50.0 mg, 0.130 mmol, 1.0 equiv.) in 3.00 mL of DMF, EDC·HCl (30.0 mg, 0.156 mmol, 1.20 equiv.) and HOSu (18.0 mg, 0.156 mmol, 1.2 equiv.) were added and stirred at the room temperature over 24 h. Solvents were removed and the crude residue was dissolved in CH₂Cl₂, washed with sat. NaCl solution (3x5 mL) and dried over

Na₂SO₄. The solvent was removed under reduced pressure and the residue was dissolved in 1.00 mL DMF.

To a solution of GPI **20** (20.0 mg, 64.3 μmol, 2.0 equiv.) in 1.00 mL of DMF and NEt₃ (434 μl, 3.11 mmol, 100 equiv.) the NHS ester solution in DMF was added in a dropwise manner at 0 °C. The reaction mixture was stirred at the room temperature over 16h. The solvent was removed under reduced pressure and the crude residue was purified by reversed phase column chromatography (RP-C₁₈, H₂O/CH₃CN 100:0 → 0:100 + 0.05% HCO₂H).

After lyophilization, the isolated Boc-protected was obtained as a colorless powder and dissolved in CH₂Cl₂ (1.00 mL) and TFA (1.00 mL). The reaction solution stirred at the room temperature over 16 h. The solvent was removed under a stream of N₂ and after lyophilization, the final product **85c** was obtained as a colorless powder in a yield of 84% (10.0 mg, 17.3 μmol). ¹³C spectrum shows the mixture of two diastereomers.

¹H NMR (600 MHz, MeOD-*d*₄): δ = 8.04 (d, ⁴*J* = 1.8 Hz, 1 H, 12-H), 7.95 (dd, ^{3,4}*J* = 8.1, 1.8 Hz, 1 H, 11-H), 7.72 (d, ³*J* = 8.1 Hz, 1 H, 10-H), 4.58 (s, 1 H, 15-H), 4.44 (s, 2 H, 7-H), 3.18-3.13 (m, 2 H, 6-H), 2.96-2.92 (m, 2 H, 1-H), 2.83-2.74 (m, 1 H, 20-H), 2.42-2.33 (m, 2 H, 19-H), 2.32-2.19 (m, 1 H, 18a-H), 2.14-2.04 (m, 2 H, 17-H), 2.01-1.90 (m, 3 H, 18b-H, 19H), 1.85-1.75 (m, 4 H, 22-H, 23-H), 1.73-1.64 (m, 2 H, 4-H, 5-H), 1.50-1.42 (m, 4 H, 2-H, 3-H) ppm.

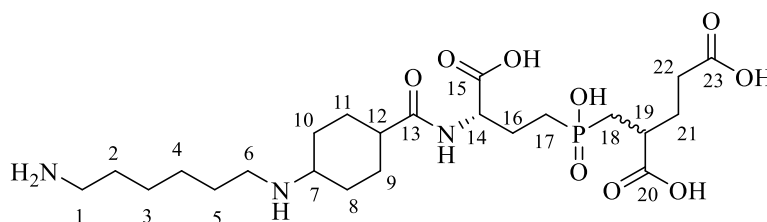
¹³C NMR (151 MHz, MeOD-*d*₄): δ = 178.7 (C-21), 177.0 (C-16), 175.2 + 174.6 (diastereomer, C-24), 168.2 (C-14), 138.5 + 138.4 (diastereomers, C-13), 136.3 + 136.2 (diastereomers, C-9), 134.2 + 134.1 (diastereomers, C-8), 133.3 (C-12), 130.6 + 130.5 (diastereomers, C-11), 128.2 + 128.1 (diastereomers, C-10), 55.6 (³*J*_{31P-13C} = 12.6 Hz, C-15), 46.1 (C-7), 40.8 (C-6), 40.7 + 40.6 (²*J*_{31P-13C} = 6.8 Hz, C-20), 33.4 (C-22), 32.7 (*J* = 3.6, C-2), 30.3 (diastereomers, ¹*J*_{31P-13C} = 9.6 Hz, C-19), 28.6 (C-3), 28.3 + 27.7 (diastereomers, C-23), 27.4 + 27.3 (diastereomers, C-4), 27.2 + 27.2 (diastereomers, C-5), 27.1 + 27.1 (diastereomers, C-1), 26.4 (C-18), 25.5 (C-17) ppm.

³¹P NMR (243 MHz, D₂O) δ = 41.86, 41.77 ppm.

IR (ATR): $\tilde{\nu}$ [cm⁻¹] = 1662, 1521, 1242, 1132, 1024, 794, 726.

HRMS (ESI) *m/z* calculated for [C₂₄H₃₇ClN₃O₉P+H⁺]: 578.2029, found: 578.2046.

Simplified folate-GPI conjugate **85d**



To a solution of carboxylic acid **86d** (70.0 mg, 0.204 mmol, 1.0 equiv.) in 4.00 mL of DMF, EDC·HCl (47.0 mg, 0.245 mmol, 1.00 equiv.) and HOSu (28.2 mg, 0.245 mmol, 1.2 equiv.) were added and stirred at the room temperature over 24 h. Solvents were removed and the crude residue was dissolved in CH₂Cl₂, washed with sat. NaCl solution (3x5 mL) and dried over Na₂SO₄. The solvent was removed under reduced pressure and the residue was dissolved in 1.00 mL DMF.

To a solution of GPI **20** (71.0 mg, 0.228 mmol, 1.0 equiv.) in 2.00 mL of DMF and NEt₃ (1.58 mL, 11.4 mmol, 50 equiv.) the NHS ester in DMF was added in a dropwise manner at 0 °C. The reaction mixture was stirred at the room temperature over 16 h. The solvent was removed under reduced pressure and the crude residue was purified by reversed phase column chromatography (RP-C₁₈, H₂O/CH₃CN 100:0 → 0:100 + 0.05% HCO₂H). After lyophilization, the isolated Boc-protected was obtained as a colorless powder and dissolved in CH₂Cl₂ (1.00 mL) and TFA (1.00 mL). Reaction solution stirred at the room temperature over 16 h. Solvents were removed under a stream of N₂ and after lyophilization the final product **85d** was obtained as a colorless powder in a yield of 96% (5.00 mg, 9.30 μmol).

¹³C spectrum shows the mixture of two diastereomers.

¹H NMR (600 MHz, MeOD-*d*₄): δ = 4.41 (s, 1 H, 14-H), 3.13-3.06 (m, 1 H, 12-H), 3.03 (t, ³J = 8.0 Hz, 2 H, 6-H), 2.94 (t, ³J = 7.7 Hz, 2 H, 1-H), 2.79 (s, 1 H, 20-H), 2.48 (s, 1 H, 7-H), 2.48-2.44 (m, 4 H, 10-H, 19-H), 2.29-2.10 (m, 4 H, 11-H, 17-H), 2.08-2.00 (m, 2 H, 8-H), 1.98-1.89 (m, 4 H, 9-H, 18-H), 1.84-1.74 (m, 2 H, 5-H), 1.73-1.65 (m, 4 H, 22-H, 23-H) 1.62-1.54 (m, 2 H, 4-H), 1.50-1.42 (m, 4 H, 2-H, 3-H) ppm.

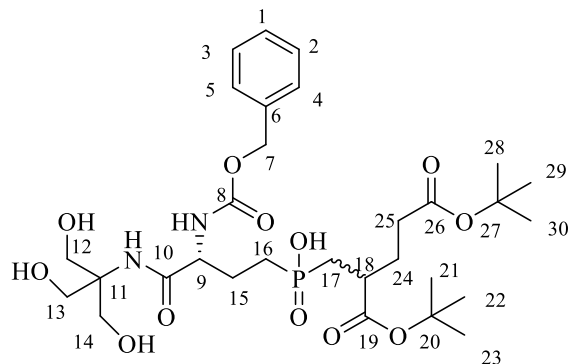
¹³C NMR (151 MHz, MeOD-*d*₄): δ = 176.0 (C-20), 175.0 (C-15), 173.8 (C-23), 163.5 (C-13), 57.9 (C-12), 54.3 (³J_{31P-13C} = 2.2 Hz, C-14), 46.1 (C-1), 44.7 (C-7), 40.8 (C-6), 40.4 (diastereomers, ²J_{31P-13C} = 3.30 Hz, C-19), 32.6 (C-8, C-10), 32.1 (C-22), 30.3 (diastereomers, ¹J_{31P-13C} = 11.5 Hz, C-18), 29.7 (C-9, C-11), 28.9 (C-2), 28.7 + 28.6 (diastereomers, C-17), 28.7 (C-3), 27.6 (C-4), 27.4 (C-5), 27.3+27.2 (diastereomers, C-1), 25.6 (²J_{31P-13C} = 5.6 Hz, C-16) ppm.

³¹P NMR (243 MHz, CDCl₃): δ = 48.60, 30.03 ppm.

IR (ATR): $\tilde{\nu}$ [cm^{-1}] = 2932, 2866, 1669, 1537, 1420, 1181, 1128, 834, 794, 722.

HRMS (ESI) m/z calculated for $[\text{C}_{23}\text{H}_{42}\text{N}_3\text{O}_9\text{P}+\text{H}^+]$: 536.2731, found: 536.2719.

TRIS-GPI conjugate **96**



The protected GPI **76** (100 mg, 1.75 mmol, 1.0 equiv.) was dissolved in 6.00 mL THF/H₂O (1:1). LiOH (8.00 mg, 0.333 mmol, 2.0 equiv.) was added to the solution and stirred at the room temperature for 16 h. After full conversion of starting material (ESI MS control), the solution was neutralized with 1M hydrochloric acid and extracted three times with EtOAc. The solvent was removed under reduced pressure and the crude residue was purified by reversed phase column chromatography (RP-C₁₈, H₂O/CH₃CN v/v 98:2 → 0:100 + 0.05% HCO₂H). Methyl deprotected GPI derivative (55.0 mg, 0.099 mmol, 1.0 equiv.), TRIS (23.3 mg, 0.148 mmol, 1.5 equiv.) and EEDQ (36.2 mg, 0.148 mmol, 1.5 equiv.) were dissolved in 2.50 mL dry EtOH and stirred over 18 h at 50 °C. The solvent was removed under reduced pressure and the crude residue was purified over reversed phase column chromatography (RP-C₁₈, H₂O/ CH₃CN 100:0 → 0:100 + 0.05% HCO₂H). The desired product **96** was obtained as a colorless powder in a yield of 48% (31.5 mg, 477 μmol). ¹³C spectrum shows the mixture of two diastereomers.

¹H NMR (600 MHz, MeOD-*d*₄): δ = 7.42-7.23 (m, 5 H, 1-H, 2-H, 3-H, 4-H, 5-H), 5.09 (s, 2 H, 7-H), 4.18-4.16 (m, 1 H, 9-H), 3.76-3.62 (m, 6 H, 12-H, 13-H, 14-H), 2.71-2.63 (m, 1 H, 18-H), 2.28-2.24 (m, 2 H, 17-H), 2.15-2.02 (m, 2 H, 16-H), 1.95-1.87 (m, 2 H, 15-H), 1.85-1.62 (m, 4 H, 24-H, 25-H), 1.48-1.41 (m, 18 H, 21-H, 22-H, 23-H, 28-H, 29-H, 30-H) ppm.

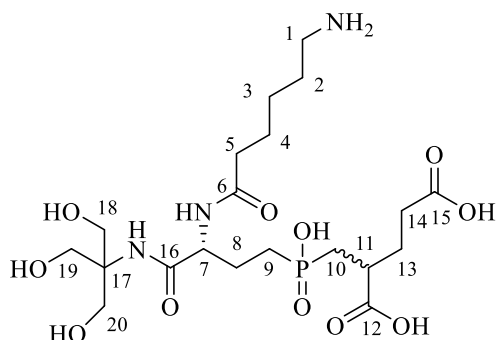
¹³C NMR (151 MHz, MeOD-*d*₄): δ = 175.7 + 175.6 (diastereomers, C-19), 174.9 (C-10), 174.1 (C-26), 158.8 (C-8), 138.3 (C-6) 129.8 (C-4, C-5), 129.3 (C-1), 129.2 (C-2, C-3), 82.7 (C-20), 82.0 (C-27), 68.1 (C-7), 64.3+63.9 (diastereomers, C-11), 62.6 (C-12, C-13, C-14), 57.4 (³*J*_{31P-¹³C} = 13.7 Hz C-9), 41.2 (C-18), 34.0+33.9 (diastereomers, C-25), 32.6 + 32.0 (diastereomers, C-24), 30.8 (diastereomers, ¹*J*_{31P-¹³C} = 11.3 Hz C-17), 28.7 (C-21, C-22, C-23, C-28, C-29, C-30), 27.5+27.5 (diastereomers, C-16), 26.2+26.2 (diastereomers, C-15) ppm.

^{31}P NMR (243 MHz, CD_3CN) $\delta = 43.03, 39.54$ ppm.

IR (ATR): $\tilde{\nu}$ [cm^{-1}] = 2955, 1669, 1521, 1449, 1360, 1240, 1132, 1040, 948, 827, 683.

HRMS (ESI) m/z calculated for $[\text{C}_{30}\text{H}_{49}\text{N}_2\text{O}_{12}\text{P}+\text{H}^+]$: 661.3096, found: 661.3109.

TRIS-GPI-AHX conjugate **95a**



TRIS-GPI conjugate **96** (30.0 mg, 45.4 μmol , 1.0 equiv.) was dissolved in 2.00 mL MeOH and 100 μl of H_2O under H_2 atmosphere (1atm). 3.00 mg (10% m/m , 5 mol%) of Pd/C was added and stirred over 16 h at the room temperature. The solvent was removed under reduced pressure. The crude residue was subsequently dissolved in 4.00 mL $\text{H}_2\text{O}/\text{CH}_3\text{CN}$ (1:1) mixture and filtered over a silica pad. The filtrate was concentrated under reduced pressure and lyophilized. The product **97** was obtained as a colorless powder and used in following reaction without further purification.

TRIS-GPI derivative **97** (23.0 mg, 0.437 mmol 1.0 equiv.) was dissolved in 1.30 mL mixture of DMF/ NEt_3 (3:1). In a separated flask, AHX-NHS ester **98a** (29.0 mg, 88.3 μmol , 2.0 equiv.) was dissolved in 1.00 mL dry DMF. Both solutions were cooled to 0 $^\circ\text{C}$ for 30 min. The solution of **98a** was added dropwise into the solution of **97** and stirred at the room temperature over 18 h. The solvent was removed under reduced pressure and the crude residue was purified subsequently over reversed phase column chromatography (RP- C_{18} , $\text{H}_2\text{O}/\text{CH}_3\text{CN}$ 100:0 \rightarrow 0:100 + 0.05% HCO_2H). The product **99a** was obtained as a colorless powder.

99a (24.0 mg, 32.4 μmol) was dissolved in a 4.00 mL mixture of $\text{CH}_2\text{Cl}_2/\text{TFA}$ (1:1). The reaction solution was stirred at the room temperature over 16 h. Solvents were removed under a stream of N_2 and after lyophilization the final product **95a** was obtained as a colorless powder in a yield of 84% (15.0 mg, 28.4 μmol). ^{13}C spectrum shows the mixture of two diastereomers.

^1H NMR (600 MHz, MeOD- d_4): δ = 4.44 (s, 1 H, 7-H), 3.72-3.59 (m, 6 H, 18-H, 19-H, 20-H), 2.92-2.81 (m, 4 H, 1-H, 5-H), 2.72 (s, 1 H, 11-H), 2.29-2.25 (m, 2 H, 10-H), 1.96-1.84 (m, 4 H, 8-H, 9-H), 1.65-1.56 (m, 6 H, 2-H, 3-H, 4-H), 1.42-1.35 (m, 4 H, 13-H, 14-H) ppm.

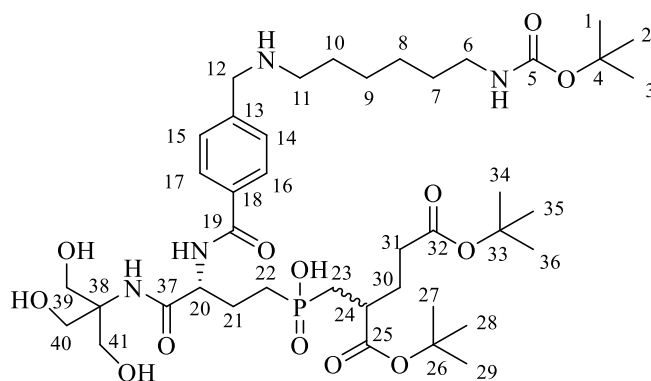
^{13}C NMR (151 MHz, MeOD- d_4): δ = 177.4 (C-12), 176.9 (C-16), 174.6 (C-15), 172.7 (C-6), 62.5 + 61.1 (diastereomers, C-17), 62.4+61.1 (diastereomers, C-18, C-19, C-20), 56.0 + 54.6 (diastereomers, C-7), 40.7 (C-5), 40.4 ($^2J_{31\text{P}-13\text{C}}$ = 26.3 Hz, C-11), 36.4 + 36.3 (diastereomers, $^3J_{31\text{P}-13\text{C}}$ = 14.8 Hz, C-13), 36.3 (C-14), 34.6 (C-9), 32.5 ($^2J_{31\text{P}-13\text{C}}$ = 5.9 Hz C-8), 30.2 (C-10), 28.4+28.3 (diastereomers, C-1), 27.0 + 26.9 (diastereomers, C-4), 26.2 (C-3), 25.5 (C-2) ppm.

^{31}P NMR (162 MHz, MeOD $_4$): δ = 43.51, 41.17 ppm.

IR (ATR): $\tilde{\nu}$ [cm^{-1}] = 2932, 1658, 1528, 1420, 1186, 1118, 1010, 836, 794, 716.

HRMS (ESI) m/z calculated for $[\text{C}_{20}\text{H}_{38}\text{N}_3\text{O}_{11}\text{P}+\text{H}^+]$: 528,2317, found: 528.2307.

Folate-TRIS-GPI conjugate **99b**



TRIS-GPI derivative **97** (18.0 mg, 34.2 μmol , 1.0 equiv.) and NEt_3 (0.238 mL, 1.71 mmol, 50 equiv.) were dissolved in 1.00 mL of dry DMF. In a separated flask, NHS-folate ester **98b** (15.3 mg, 34.2 μmol , 1.0 equiv.) was dissolved in 1.00 mL dry DMF. Both solutions were cooled to 0 $^\circ\text{C}$ for 30 min. The solution of **98b** was added dropwise into the solution of **97** and stirred further at the room temperature over 18 h. Solvents were removed under reduced pressure and the mixture was purified by reversed phase column chromatography (RP-C $_{18}$, $\text{H}_2\text{O}/\text{CH}_3\text{CN}$ 100:0 \rightarrow 0:100 + 0.05% HCO_2H). The product **99b** was obtained as a colorless powder in a yield of 20% (6.00 mg, 6.99 μmol). ^{13}C spectrum shows the mixture of two diastereomers.

^1H NMR (600 MHz, MeOD- d_4): δ = 8.07-8.00 (m, 2 H, 16-H, 17-H H), 7.59 (d, 3J = 7.9 Hz, 2 H, 14-H, 15-H), 4.53-4.47 (m, 1 H, 20-H), 4.25 (s, 2 H, 12-H), 3.79-3.70 (m, 6 H, 39-H, 40-

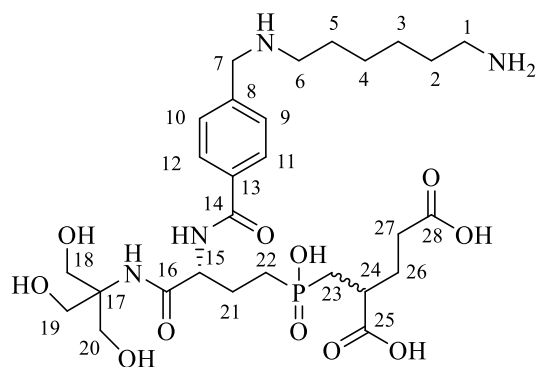
H, 41-H), 3.08-3.00 (m, 4 H, 6-H, 11-H), 2.69 (s, 1 H, 24-H), 2.29-2.22 (m, 2 H, 23-H), 2.18-2.08 (m, 2 H, 31-H), 2.02-1.95 (m, 2 H, 30-H), 1.90-1.78 (m, 2 H, 22-H), 1.76-1.71 (m, 2 H, 21-H), 1.68-1.61 (m, 2 H, 10-H), 1.59-1.49 (m, 4 H, 8-H, 9-H), 1.47-1.43 (m, 27 H, 1-H, 2-H, 3-H, 27-H, 28-H, 29-H, 34-H, 35-H, 36-H) ppm.

^{13}C NMR (151 MHz, MeOD- d_4): δ = 176.8 (C-25), 174.3 (C-37), 171.7 (C-32), 170.0 (C-5), 152.3 (C-19), 136.9 (C-13), 136.4 (C-18), 131.3 + 131.2 (diastereomers, C-16, C-17), 130.1 + 129.9 (diastereomers, C-14, C-15), 82.0 (C-26), 81.8 (C-33), 78.0 (C-4), 64.0 (C-18), 62.7 (C-39, C-40, C-41), 57.5+57.4 (diastereomers, $^3J_{31\text{P}-13\text{C}}$ = 8.9 Hz C-20), 52.2 (C-6), 48.1 (C-12), 42. (C-24), 41.3 (C-11), 34.3 ($^3J_{31\text{P}-13\text{C}}$ = 4.6 Hz C-30), 34.1 (C-31), 32.7 (C-22), 32.4 (C-21), 31.0 (diastereomers, $^1J_{31\text{P}-13\text{C}}$ = 26.2 Hz C-23), 29.1 (C-1, C-2, C-3), 28.7 (C-27, C-28, C-29, C-34, C-35, C-36), 27.6 (C-7, C-8), 26.3 (C-9), 26.1 (C-10) ppm.

IR (ATR): $\tilde{\nu}$ [cm^{-1}] = 2932, 2866, 1691, 1619, 1531, 1452, 1387, 1367, 1272, 1249, 1164, 1036, 752.

HRMS (ESI) m/z calculated for $[\text{C}_{41}\text{H}_{71}\text{N}_4\text{O}_{13}\text{P}+\text{H}^+]$: 859.4828 found: 859.4828.

Folate-TRIS-GPI conjugate **95b**



Folate-TRIS-GPI conjugate **99b** (6.00 mg, 6.99 μmol , 1.0 equiv.) was dissolved in 2.00 mL mixture of TFA/ CH_2Cl_2 (1:1). The reaction solution was stirred at the room temperature over 16 h. Solvents were removed under a stream of N_2 and after the lyophilization the final product **95b** was obtained in yield of 88% (4.00 mg, 6.19 μmol .) as a colorless powder. ^{13}C spectrum shows the mixture of two diastereomers.

^1H NMR (600 MHz, MeOD- d_4): δ = 8.01 (d, 3J = 8.0 Hz, 2 H, 11-H, 12-H), 7.62 (d, 3J = 8.0 Hz, 2 H, 9-H, 10-H), 4.67 (s, 1 H, 15-H), 4.28 (s, 2 H, 7-H), 3.78-3.65 (m, 6 H, 18-H, 19-H, 20-H), 3.11-3.03 (m, 2 H, 6-H), 2.97-2.89 (m, 2 H, 1-H), 2.80 (s, 1 H, 24-H), 2.46-2.30 (m, 2 H, 23-H), 2.22-2.05 (m, 4 H, 26-H, 27-H), 2.00-1.94 (m, 2 H, 22-H), 1.82-1.72 (m, 4 H, 4-H, 5-H), 1.71-1.65 (m, 2 H, 21-H), 1.48-1.43 (m, 4 H, 2-H, 3-H) ppm.

^{13}C NMR (151 MHz, MeOD- d_4): δ = 176.7 (C-25), 174.4 (C-16), 172.5 (C-28), 169.9 (C-14), 136.4 (C-8), 135.9 (C-13), 131.1 (C-11, C-12), 129.5 (C-9, C-10), 64.0 + 62.3 (diastereomers, C-17), 61.4 + 61.0 (diastereomers, C-18, C-19, C-20), 55.4 ($^3J_{31\text{P}-13\text{C}}$ = 10.8 Hz, C-15), 51.8 (C-1), 47.9 + 47.9 (diastereomers, C-7), 40.5 (C-6), 40.5 + 40.4 (diastereomers, $^2J_{31\text{P}-13\text{C}}$ = 7.4 Hz, C-24), 32.4 (C-27), 31.4 (C-26), 30.0 (diastereomers, $^1J_{31\text{P}-13\text{C}}$ = 11.6 Hz, C-23), 28.3 (C-22), 27.7 (C-21), 27.1 (C-5), 26.9 (C-4), 24.7 (C-2, C-3) ppm.

^{31}P NMR (243 MHz, MeOD- d_4) δ = 43.24 ppm.

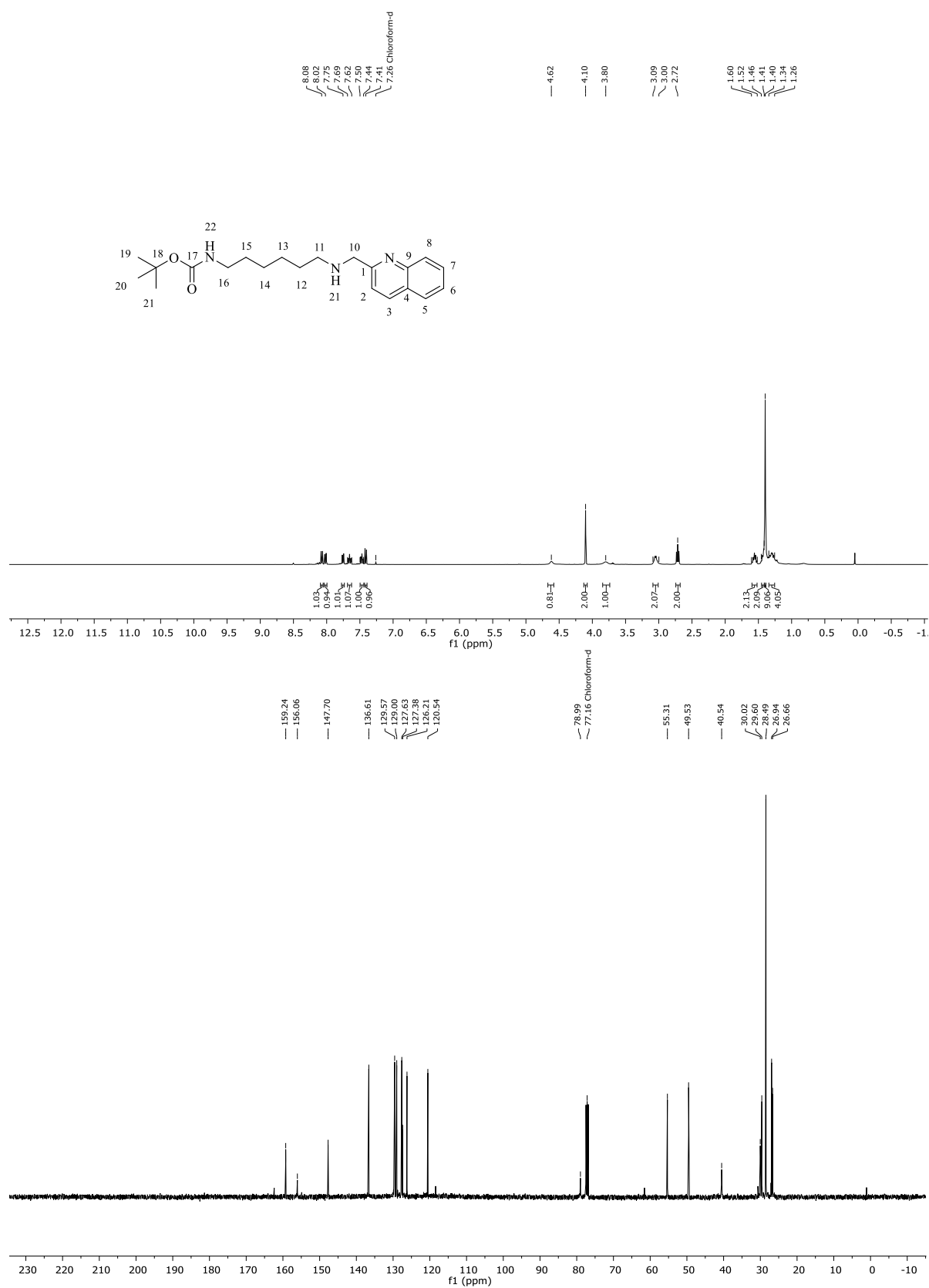
IR (ATR): $\tilde{\nu}$ [cm^{-1}] = 2929, 2854, 1655, 1534, 1429, 1181, 1125, 834, 791, 705.

HRMS (ESI) m/z calculated for [$\text{C}_{28}\text{H}_{47}\text{N}_4\text{O}_{11}\text{P}+\text{H}^+$]: 647.3052, found: 647.3024.

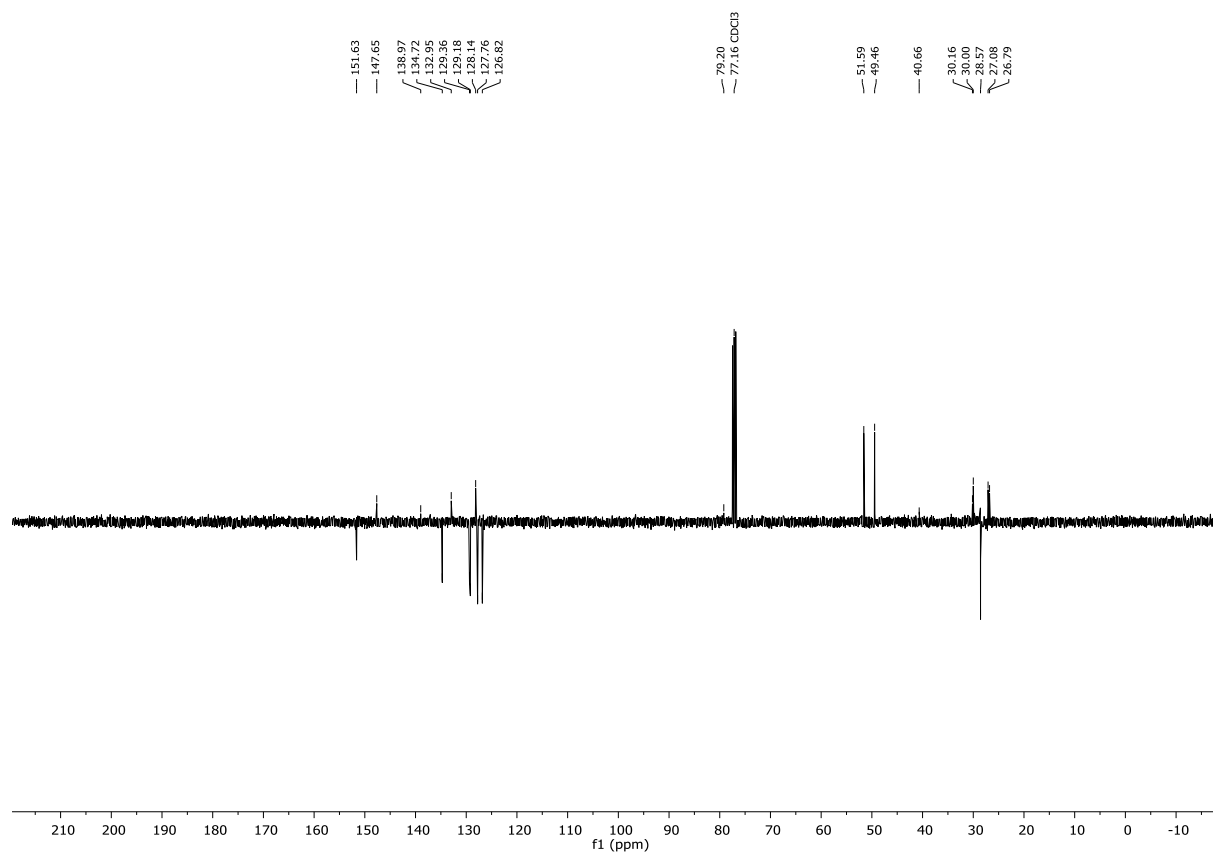
8 Appendix

NMR

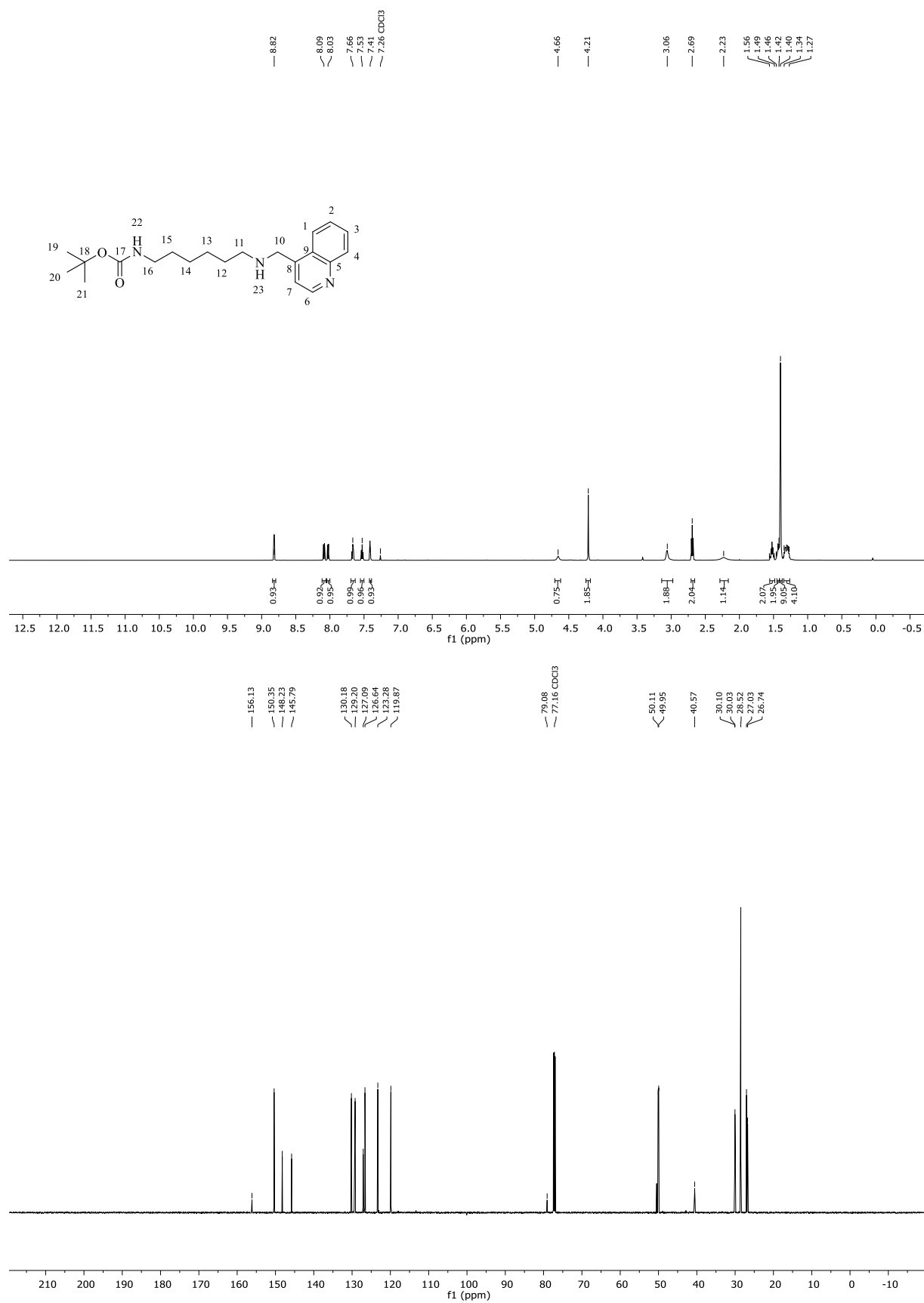
Secondary amine 50a



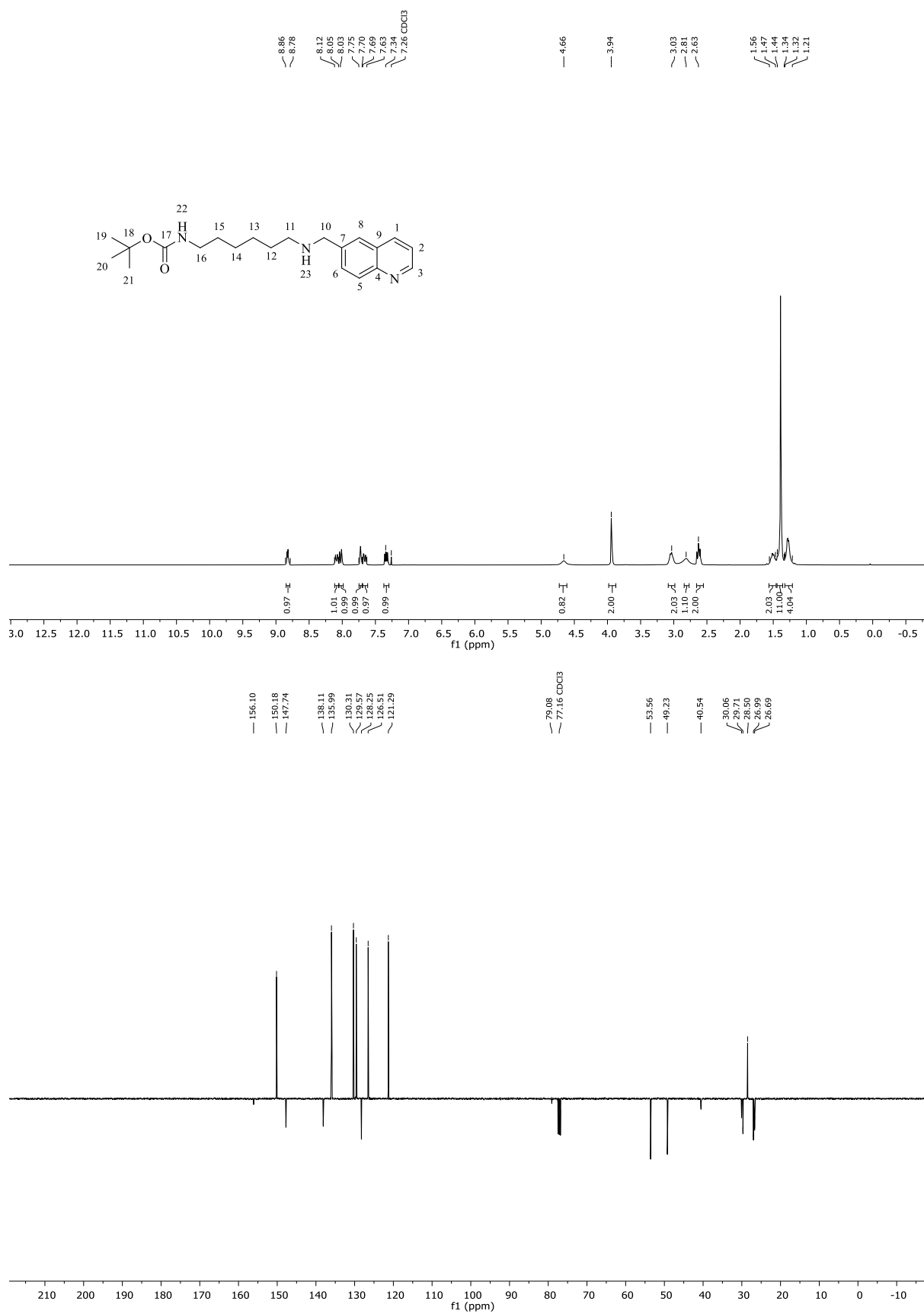
Secondary amine 50b



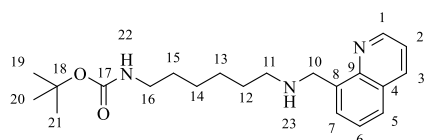
Secondary amine 50c

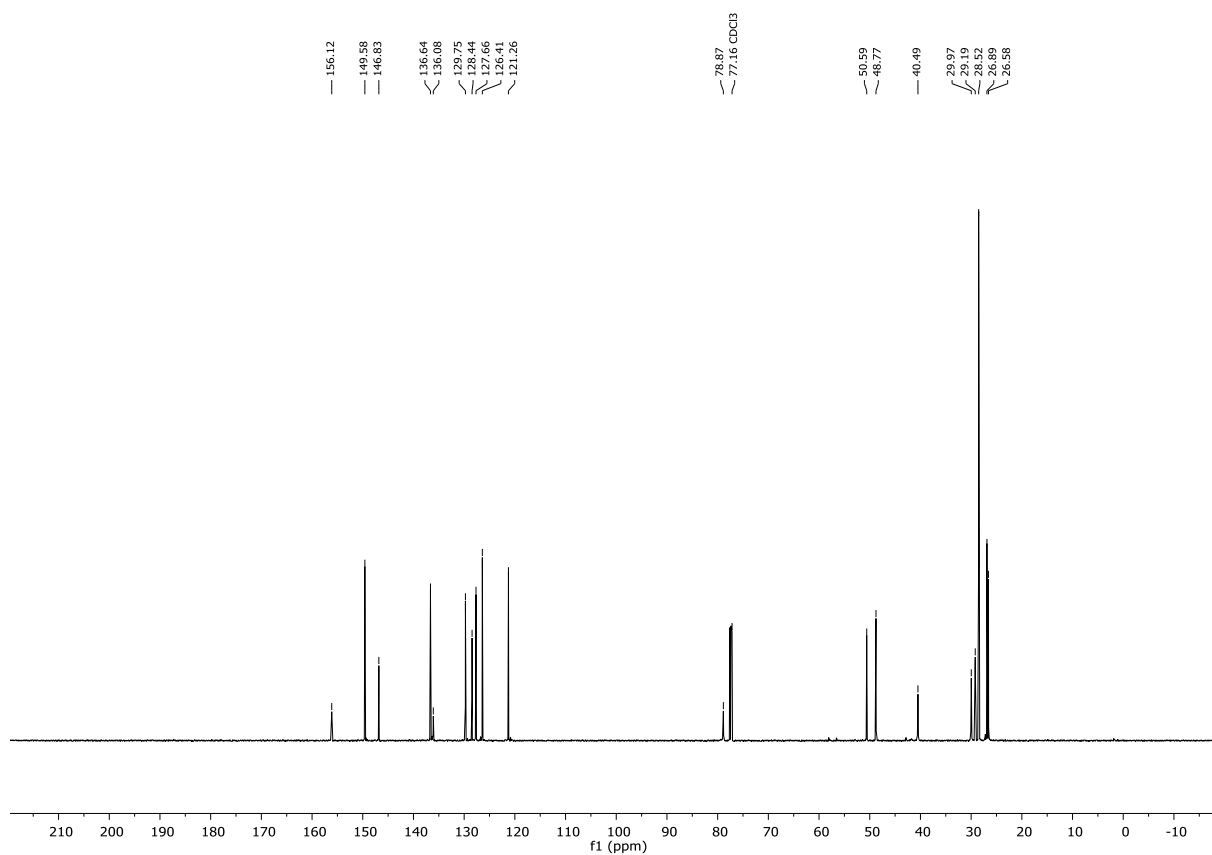
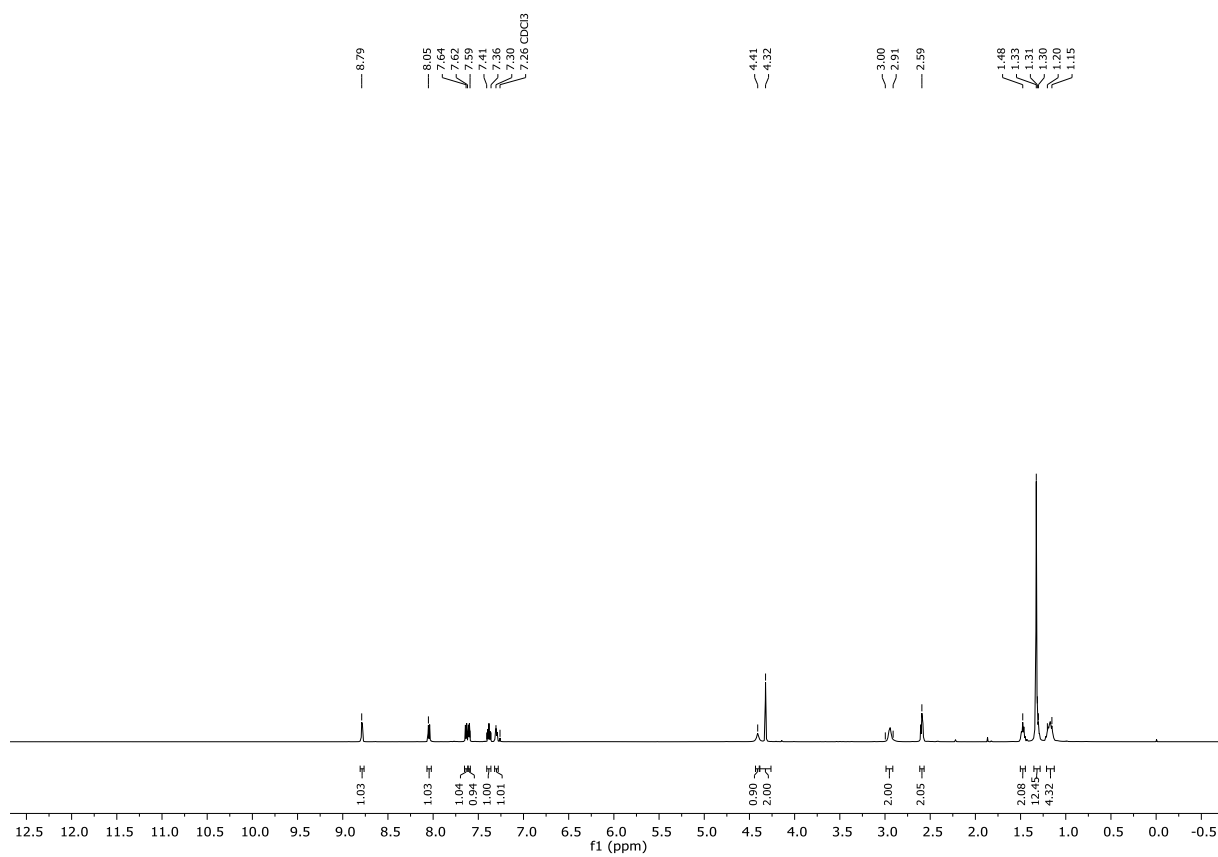


Secondary amine 50d

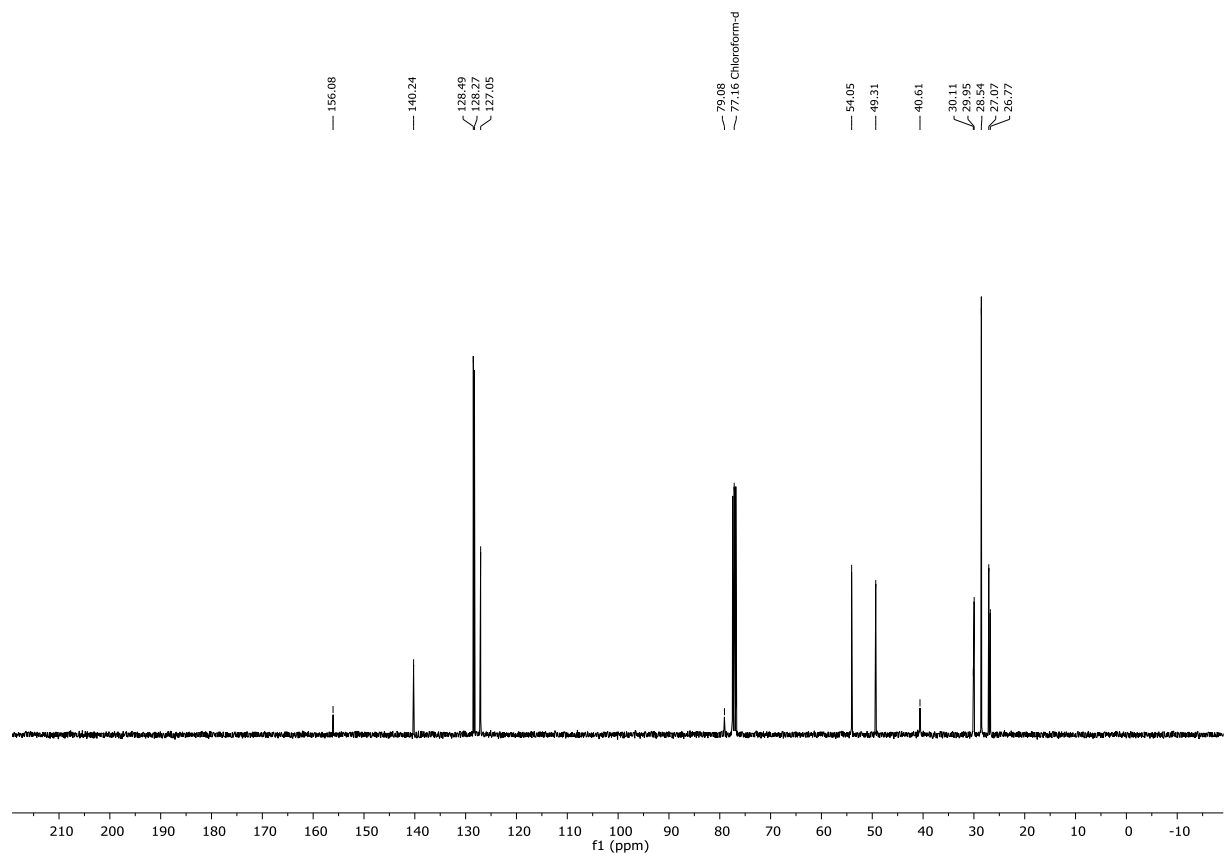
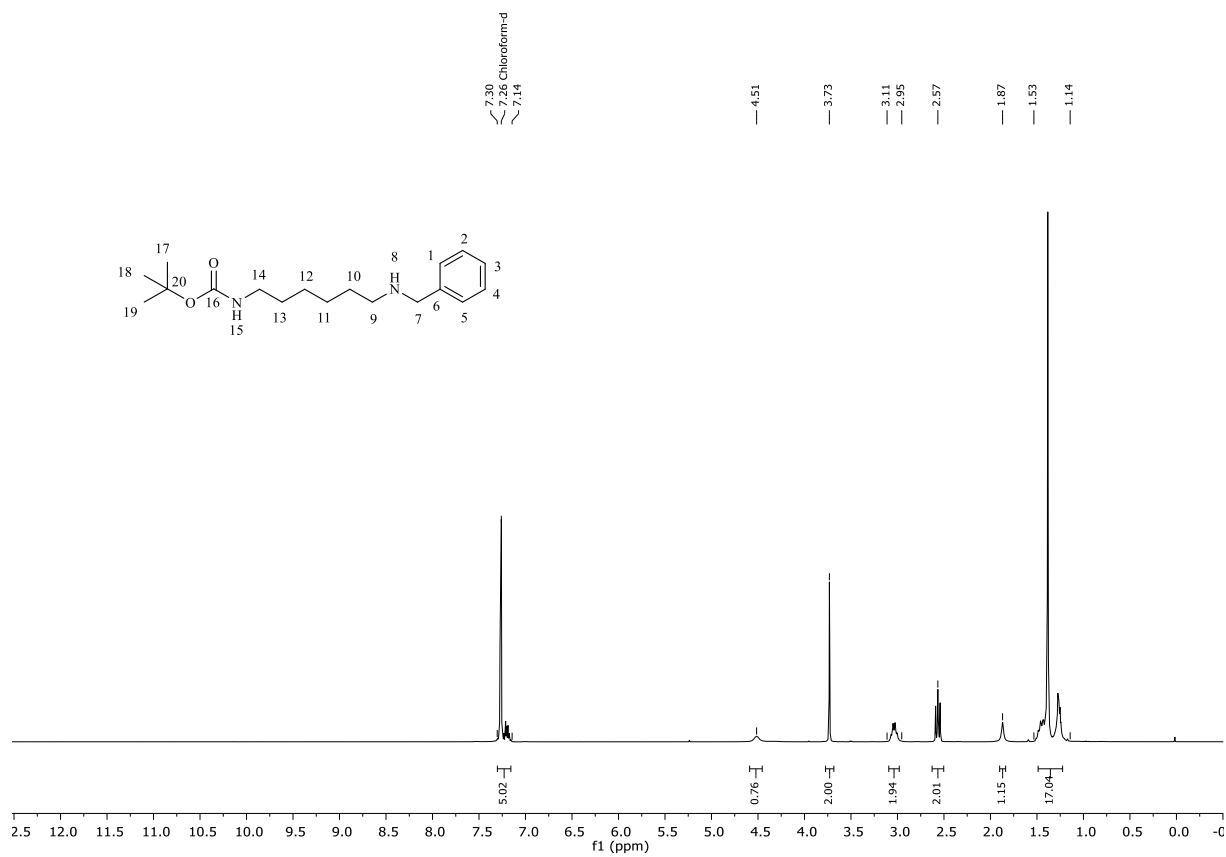


Secondary amine 50e



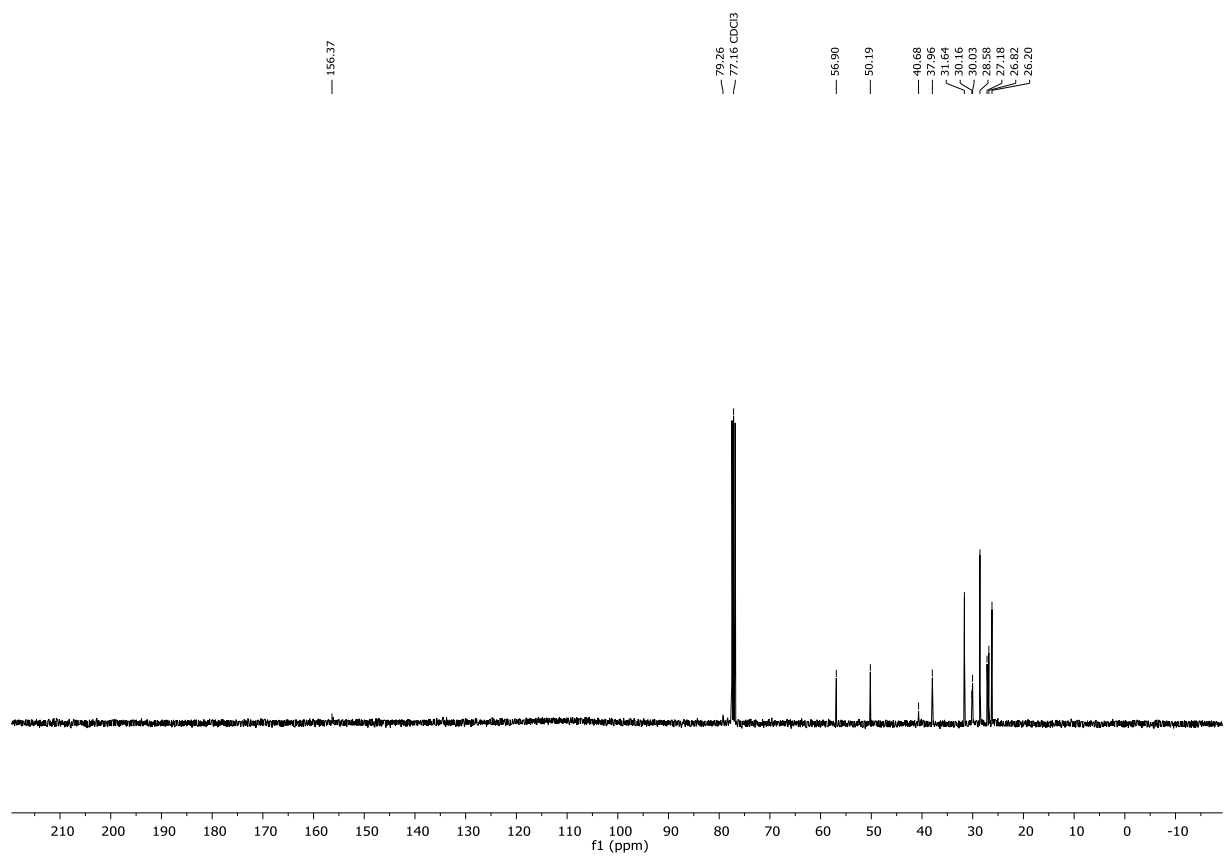
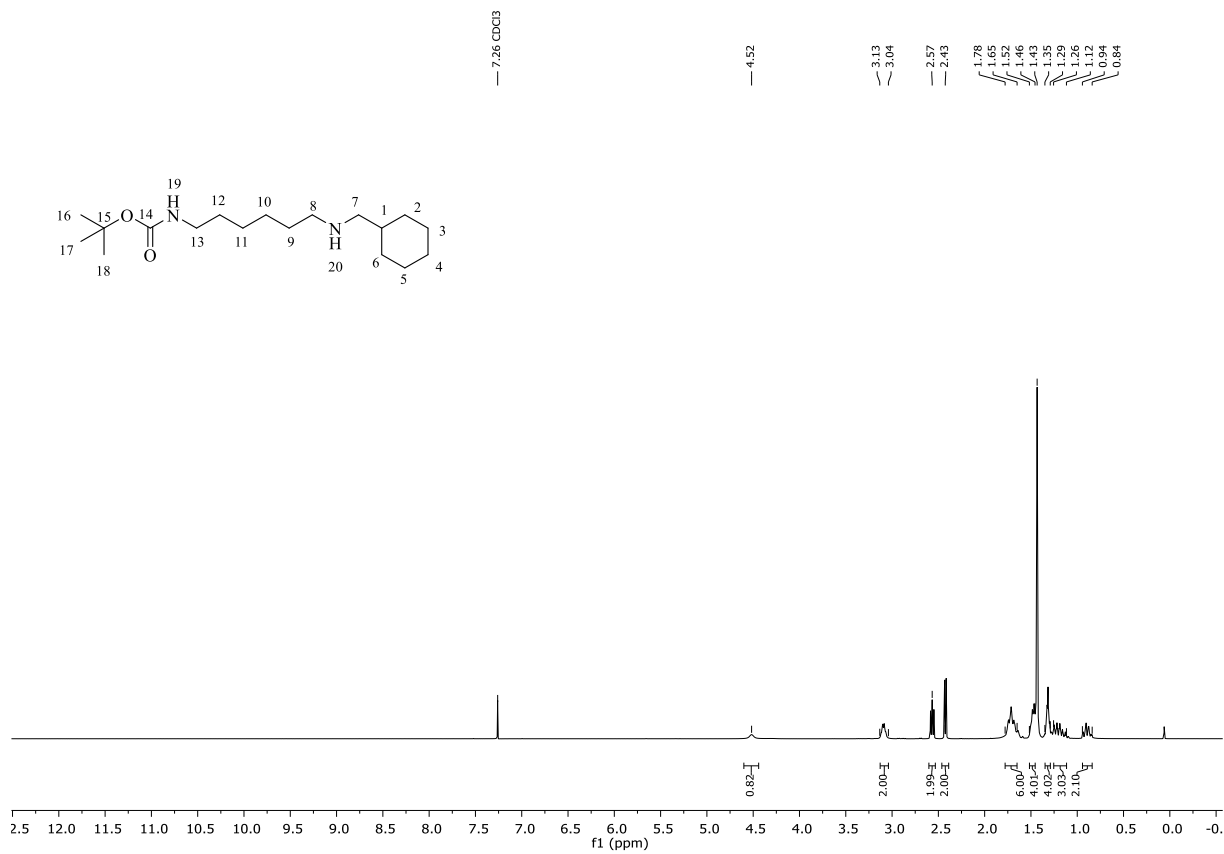


Secondary amine 50f

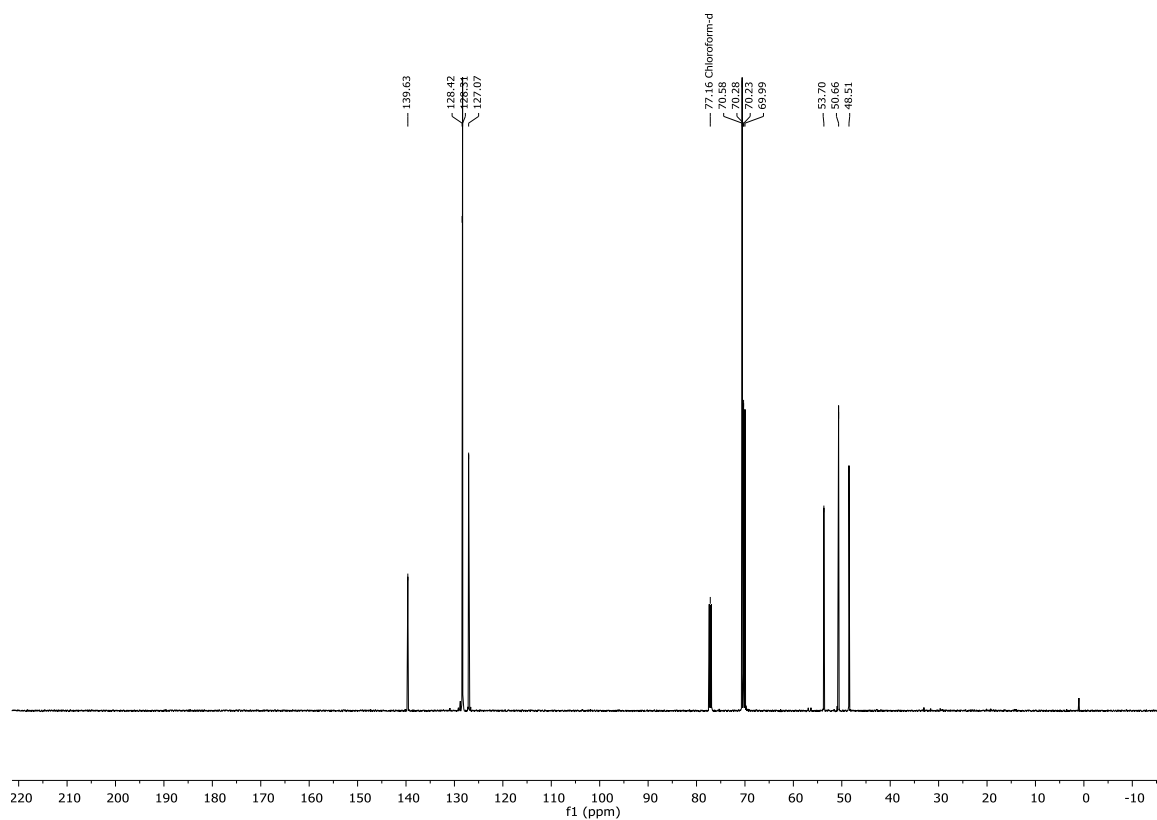
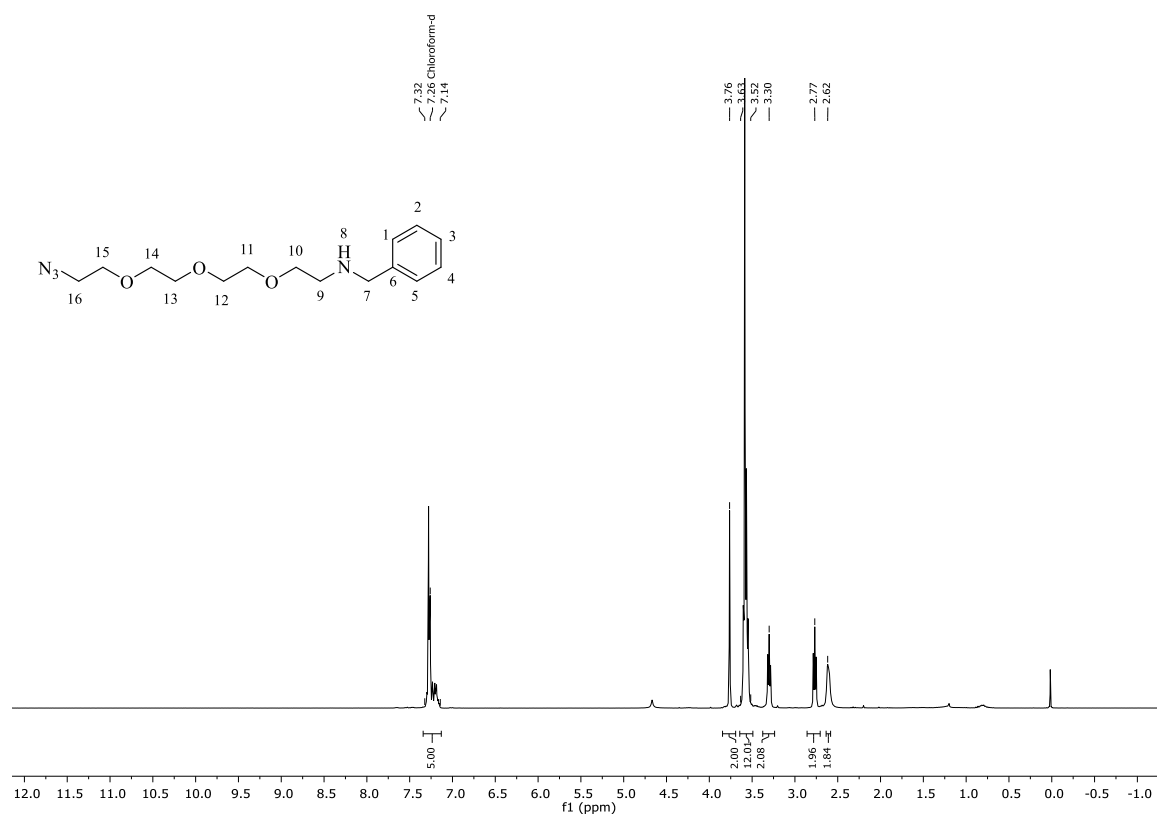


Secondary amine 50g

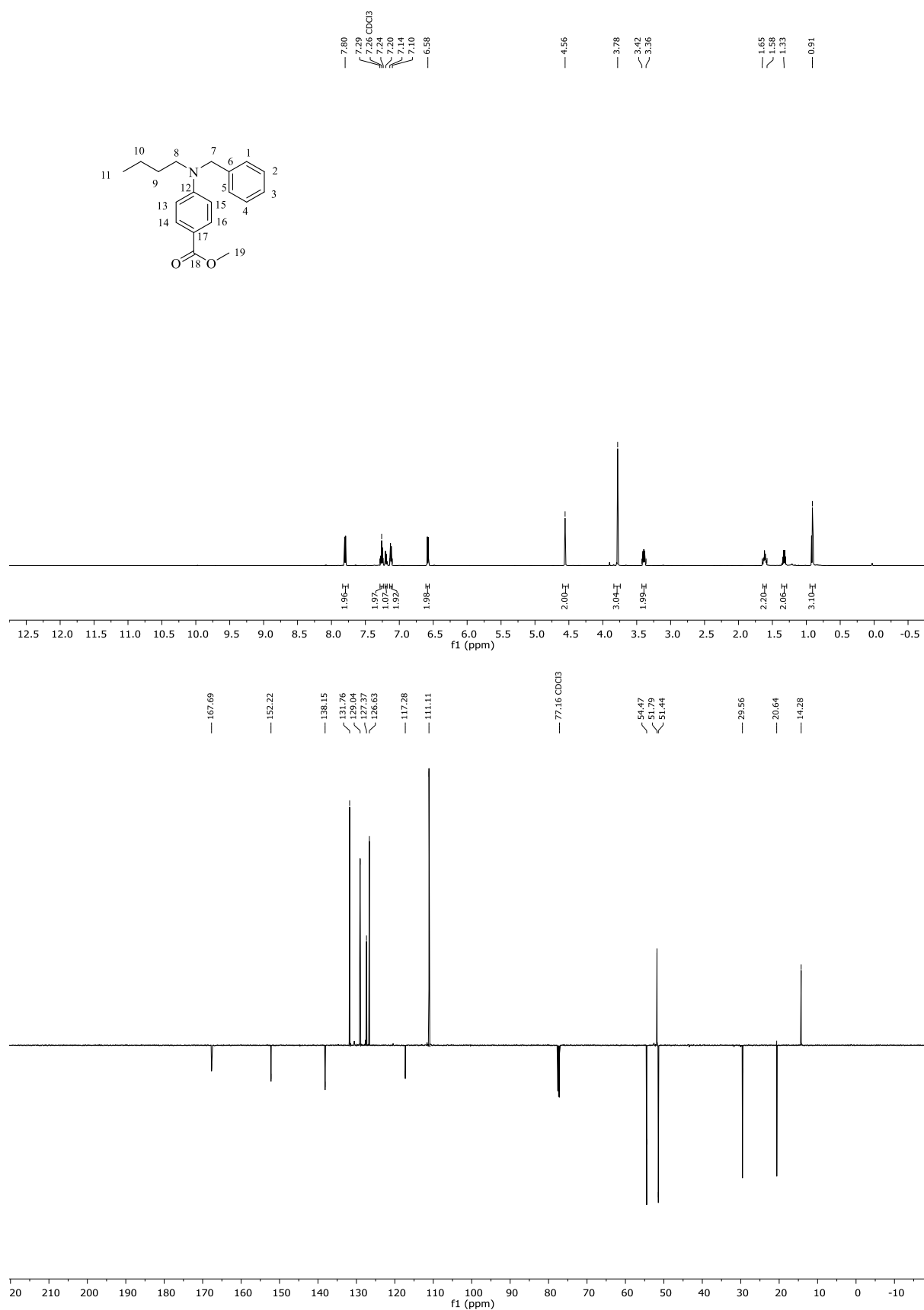
Appendix

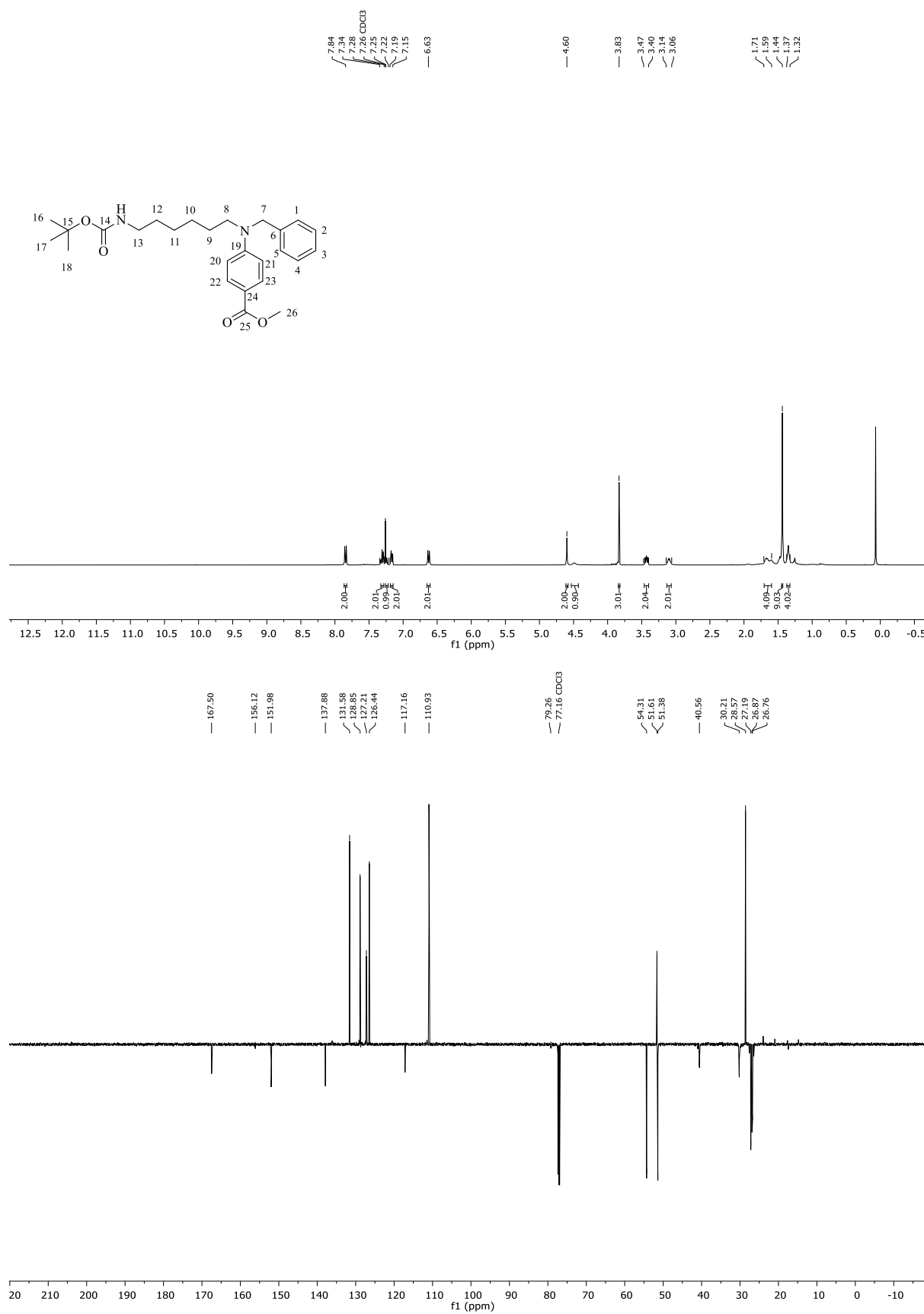


Secondary amine 50h

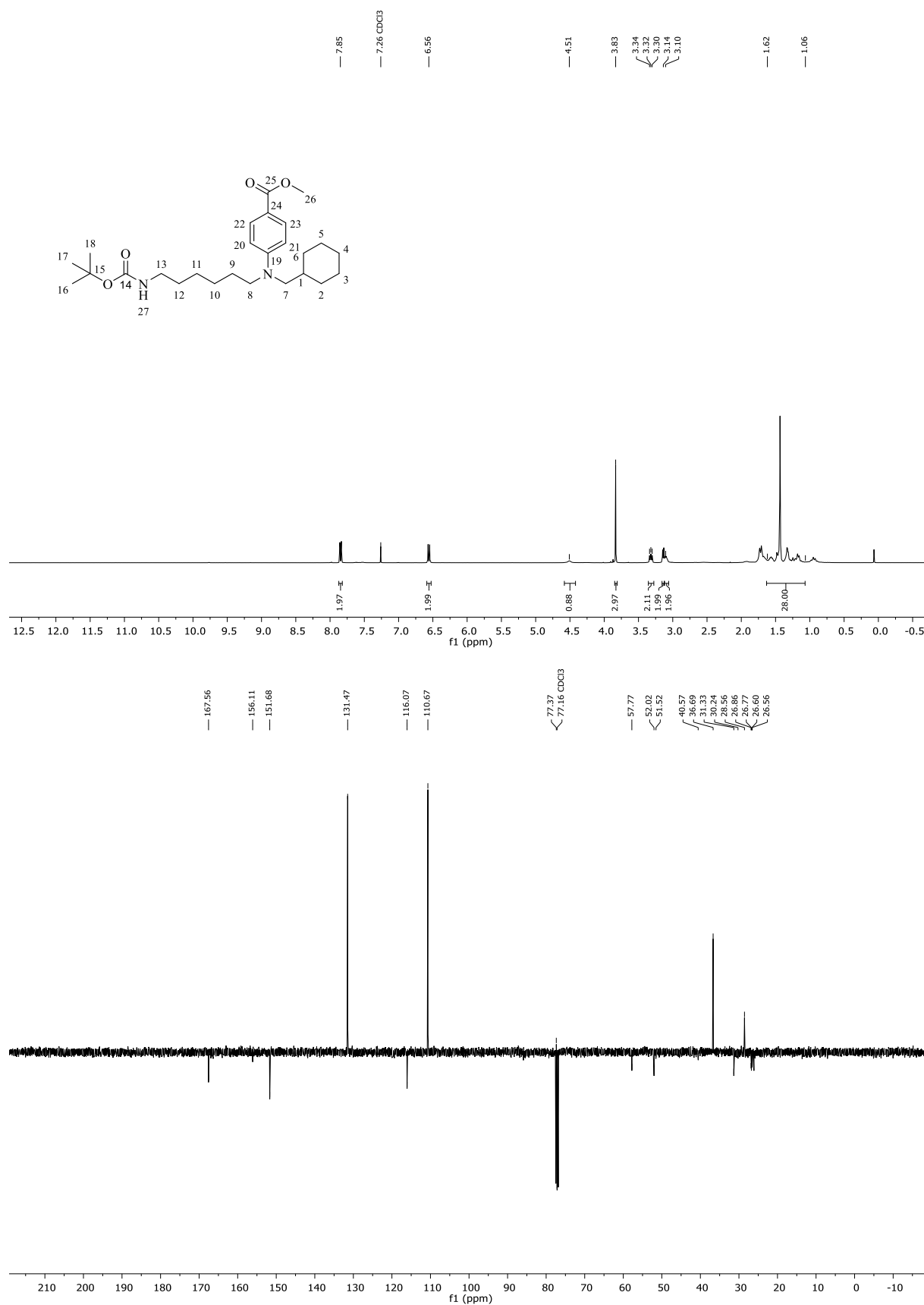


Methyl 4-(benzyl(butyl)amino)benzoate 62d

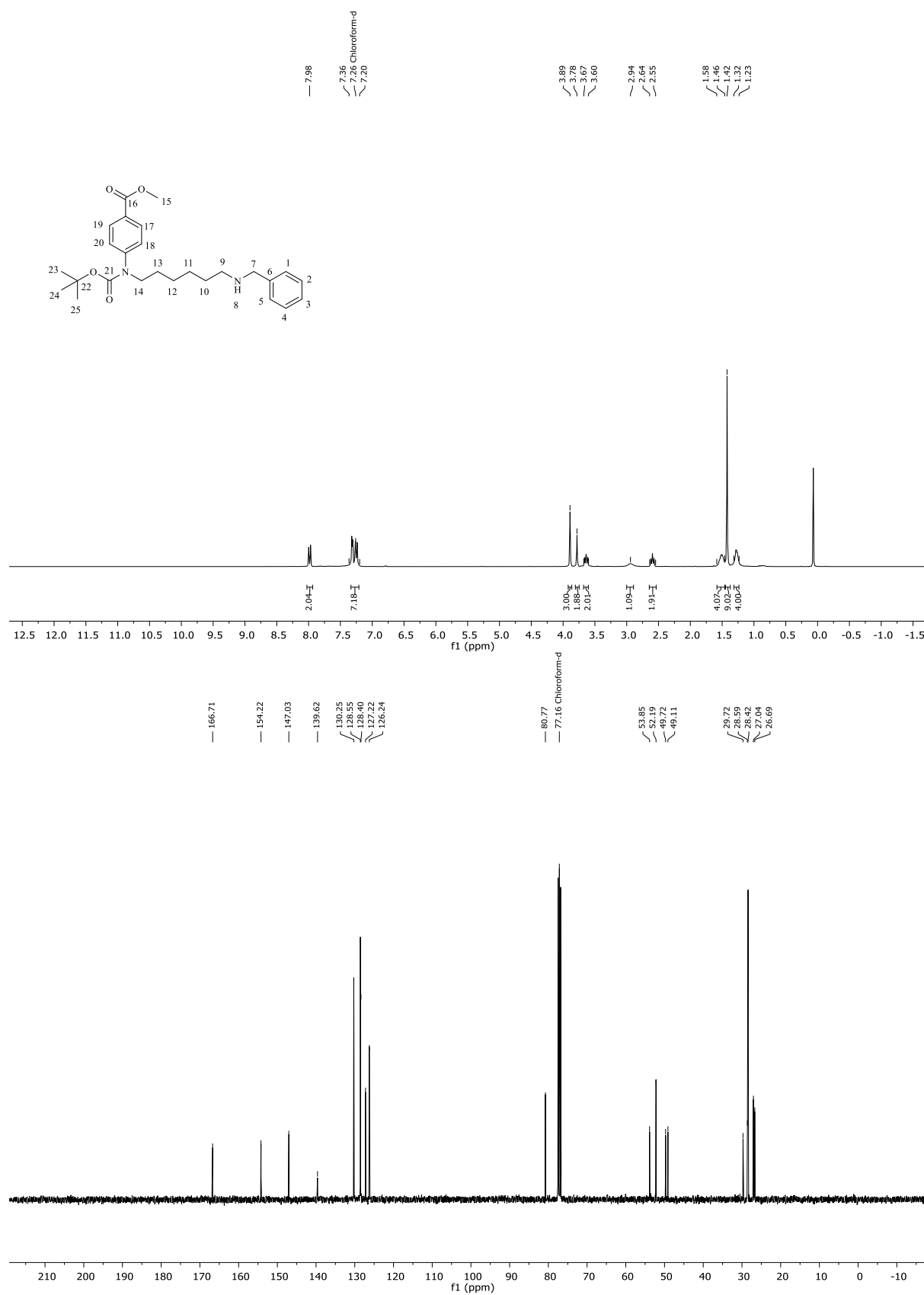
Methyl-4-(benzyl(6-((*tert*-butoxycarbonyl)amino)hexyl)amino)benzoate 69f



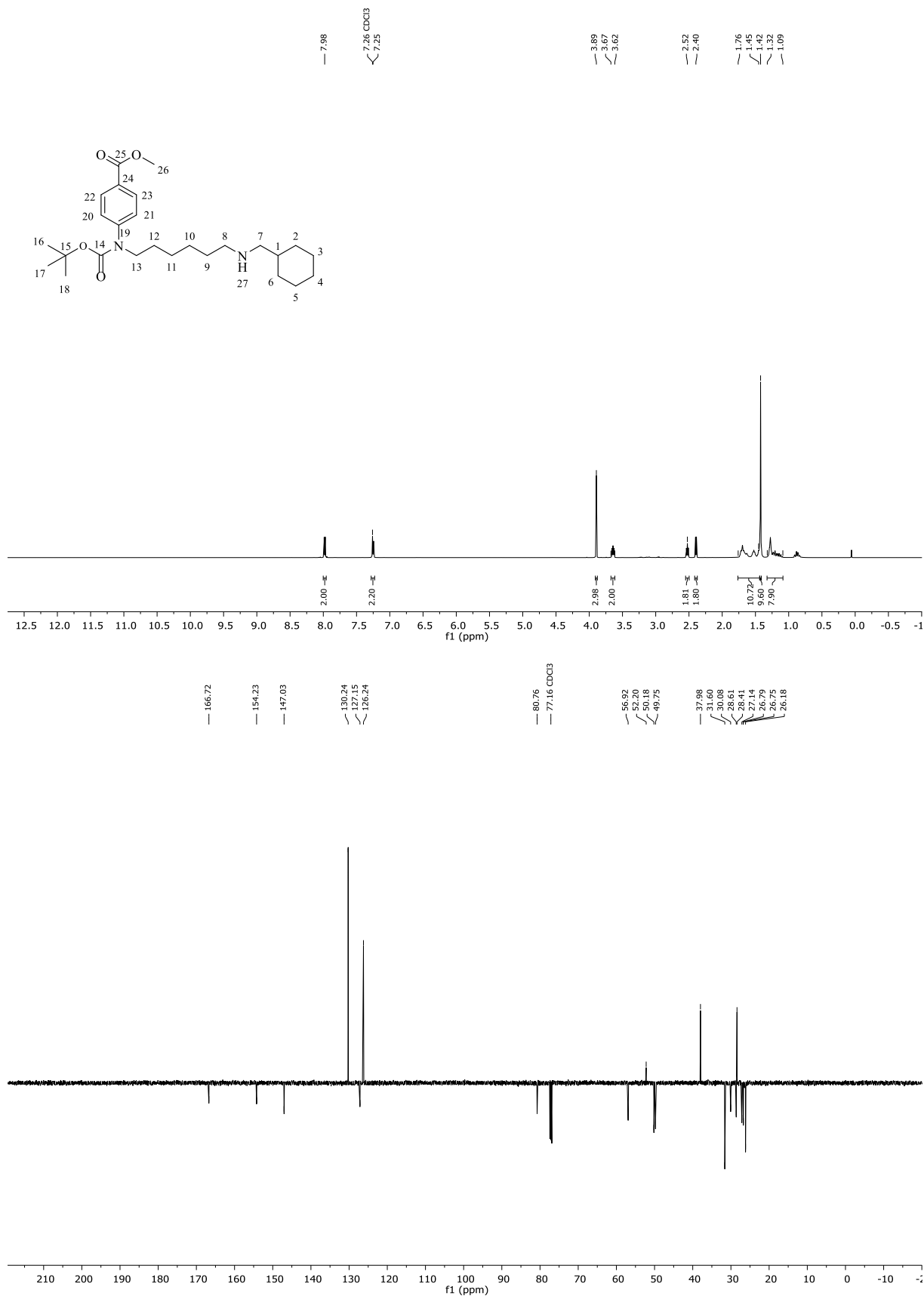
Methyl 4-((6-((tert-butoxycarbonyl)amino)hexyl)(cyclohexylmethyl)amino)benzoate 69g



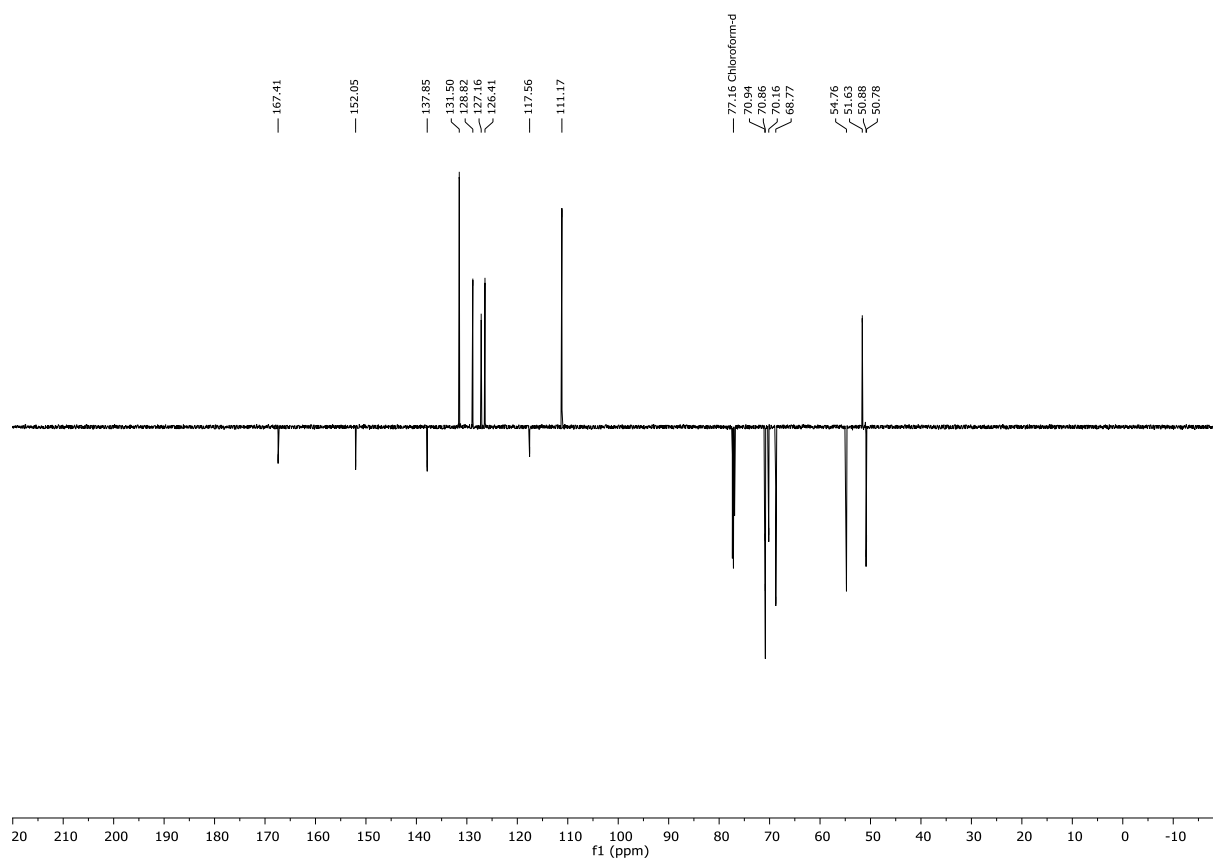
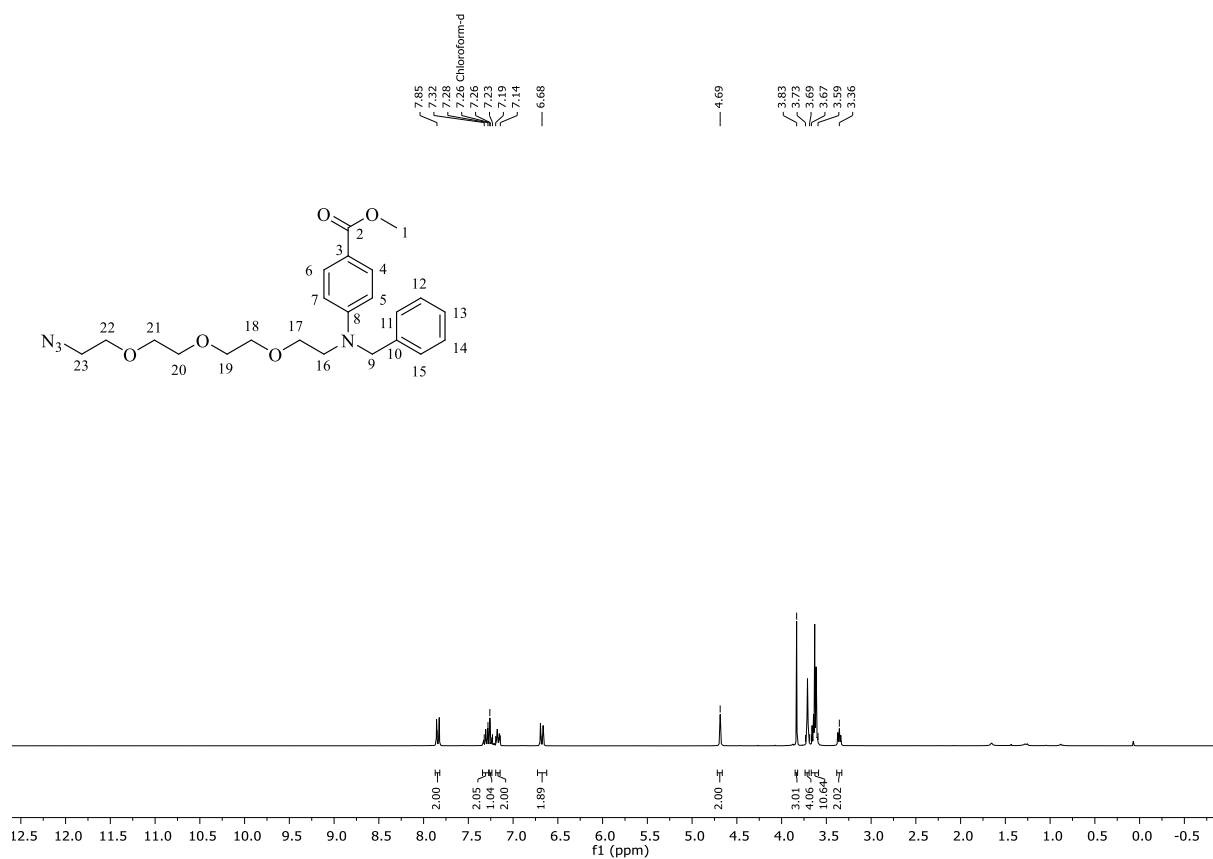
Methyl 4-((6-(benzylamino)hexyl)(tert-butoxycarbonyl)amino)benzoate 70f



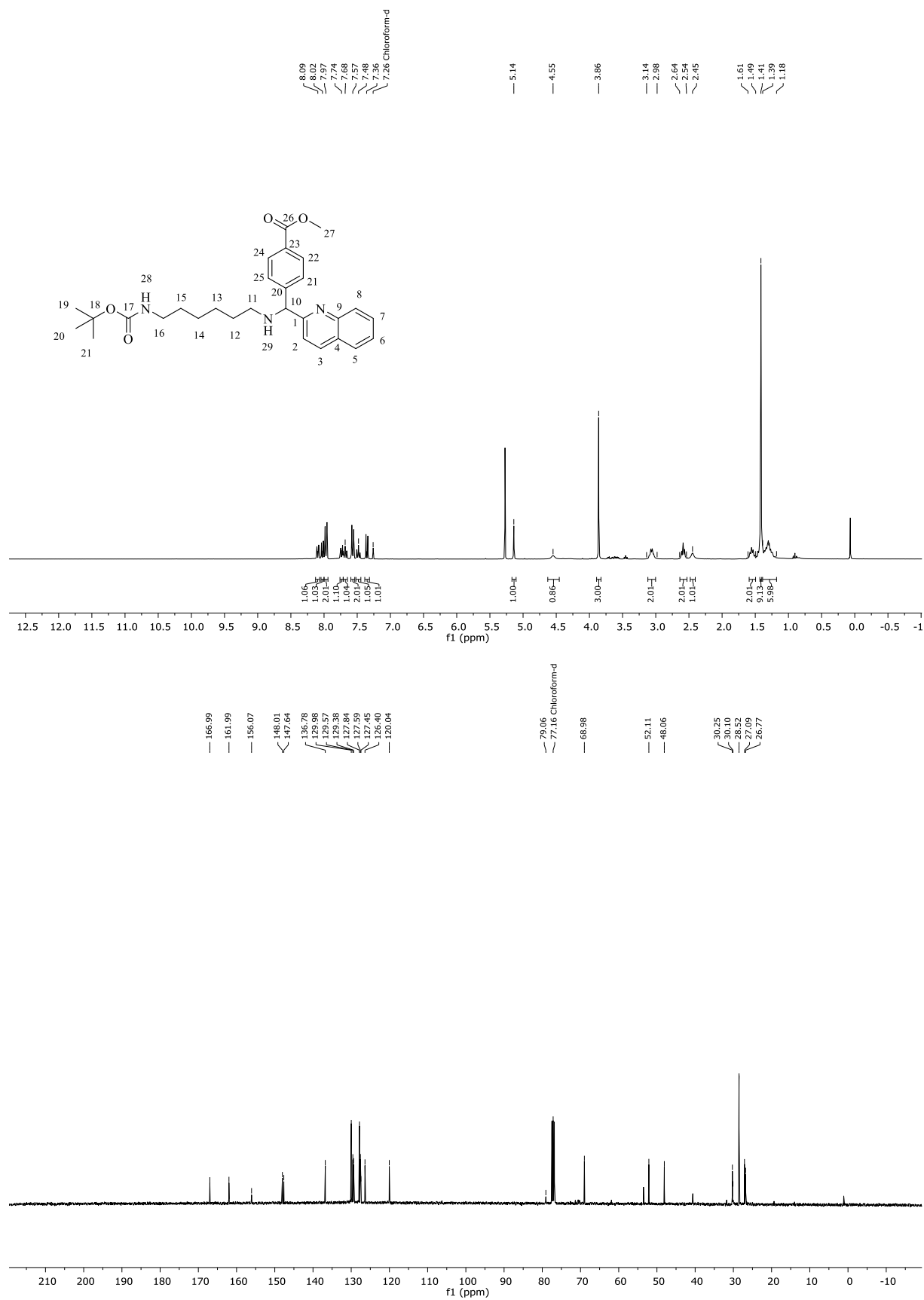
Methyl 4-((tert-butoxycarbonyl)(6-((cyclohexylmethyl)amino)hexyl)amino)benzoate 70g

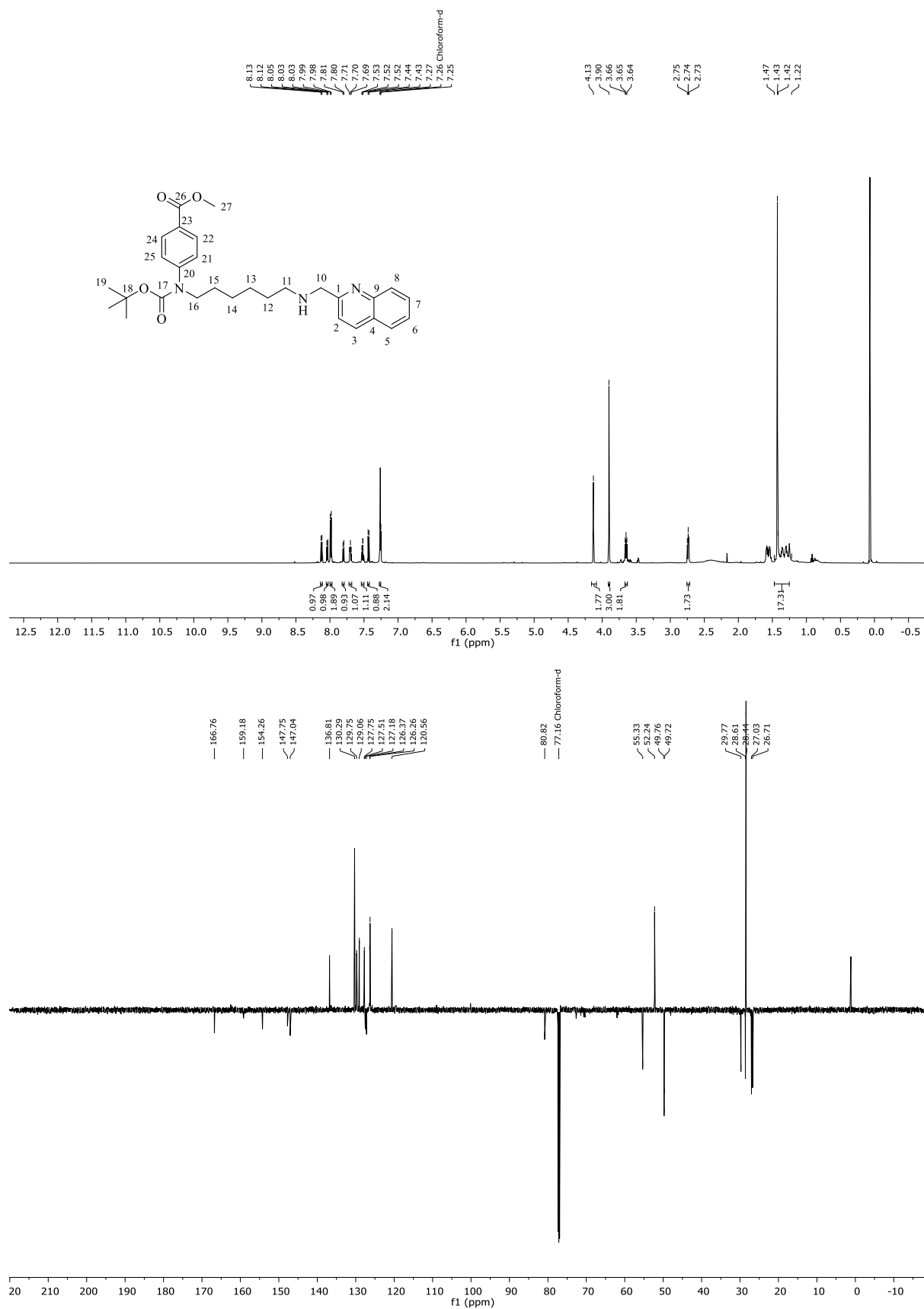


Methyl 4-((2-(2-(2-(2-azidoethoxy)ethoxy)ethoxy)ethyl)(benzyl)amino)benzoate 60h

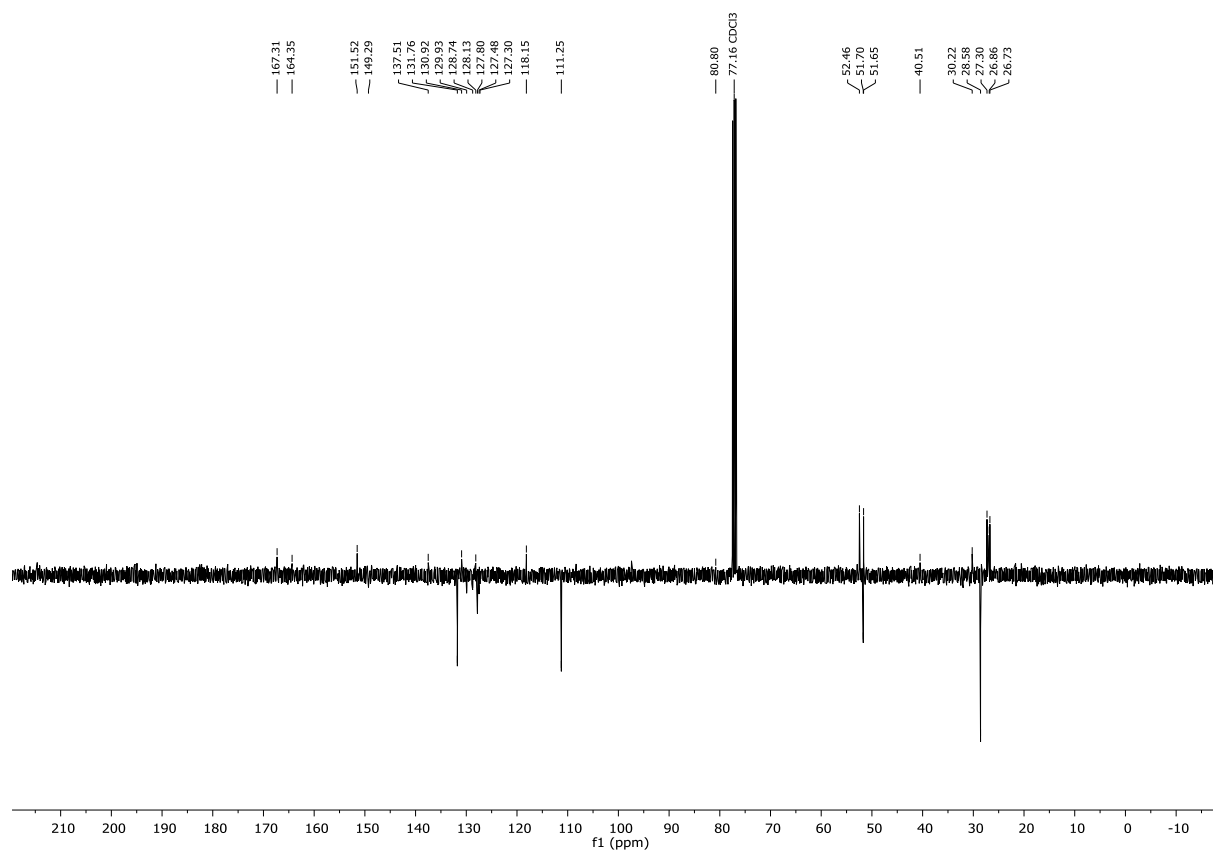
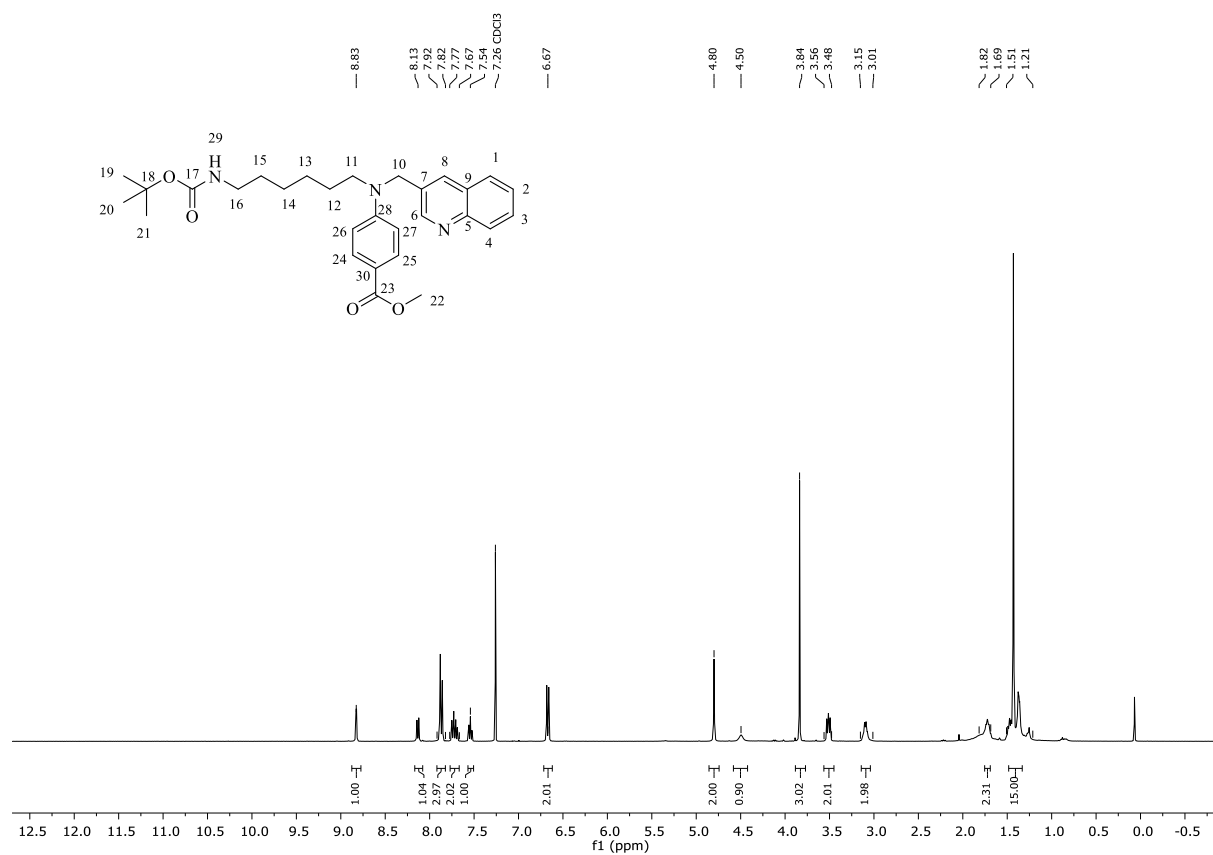


4-[2-Quinolinyl[6-[[[(1,1-dimethylethoxy)carbonyl]-amino]-hexylamino]methyl]-methyl]benzoat 58a

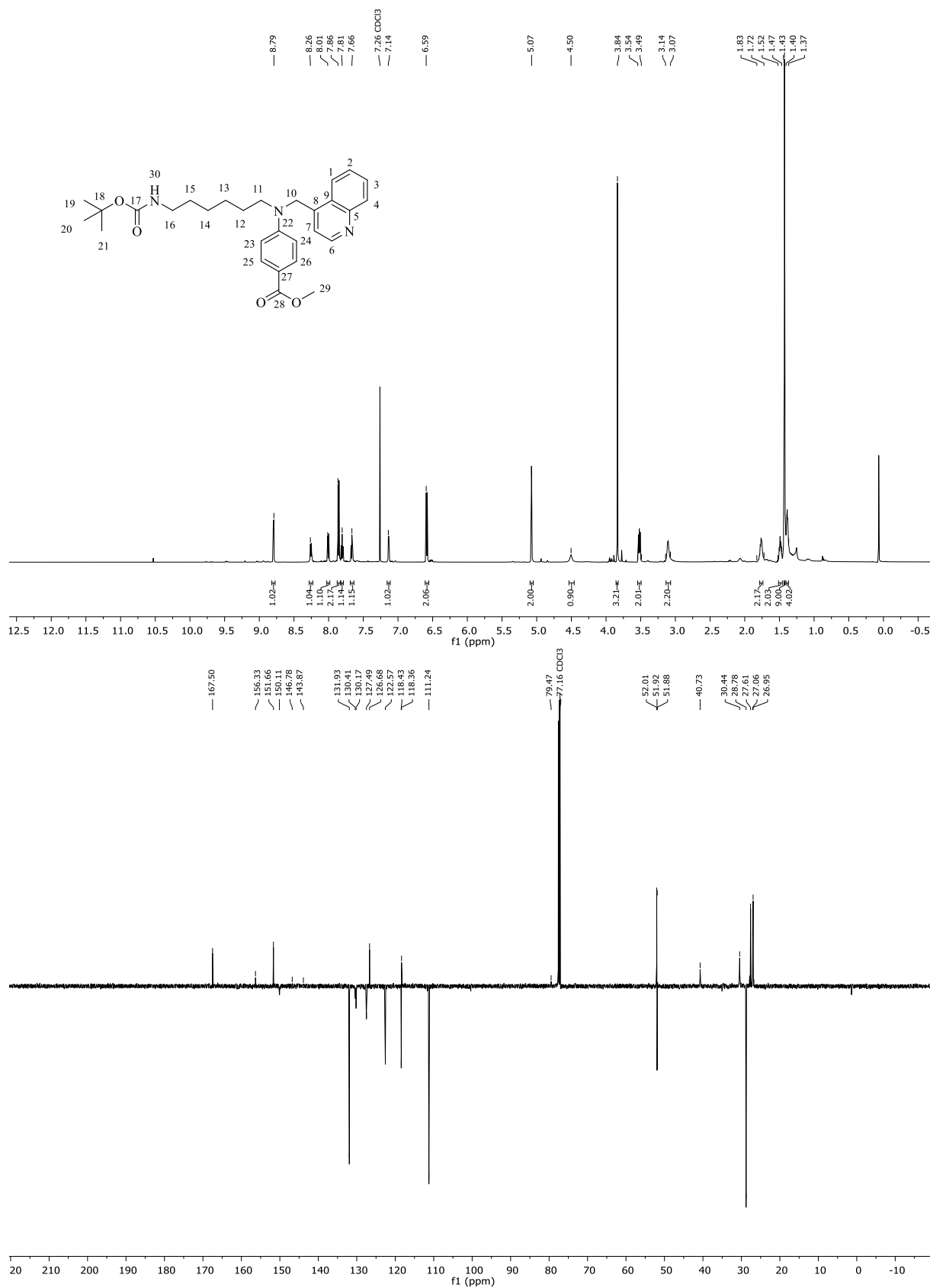


Methyl-4-((*tert*-butoxycarbonyl)(6-((quinolin-2-ylmethyl)amino)hexyl)amino)benzoate**59a**

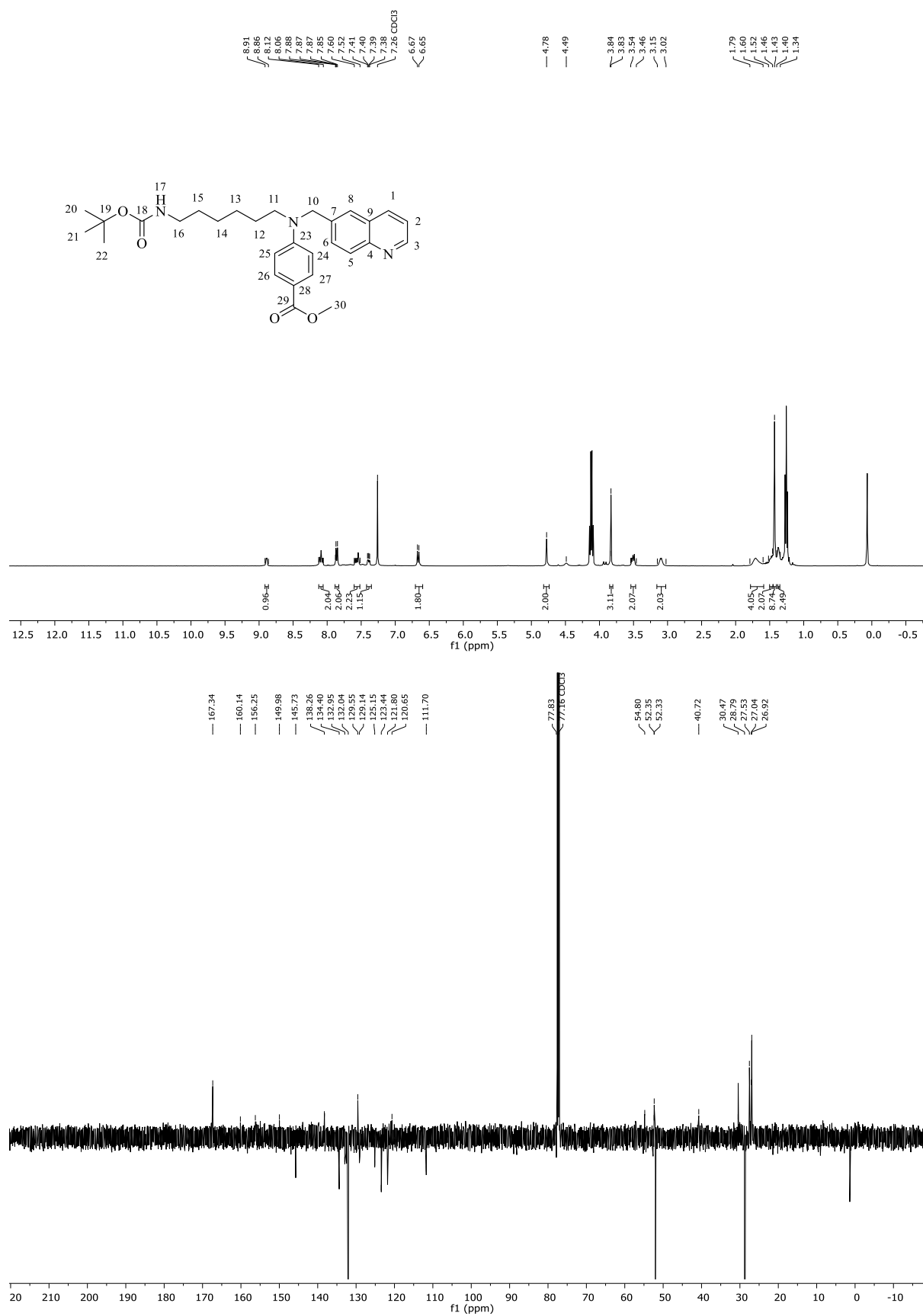
**Methyl-4-((6-((*tert*-butoxycarbonyl)amino)hexyl)(quinolin-3-ylmethyl)amino)benzoate
60b**



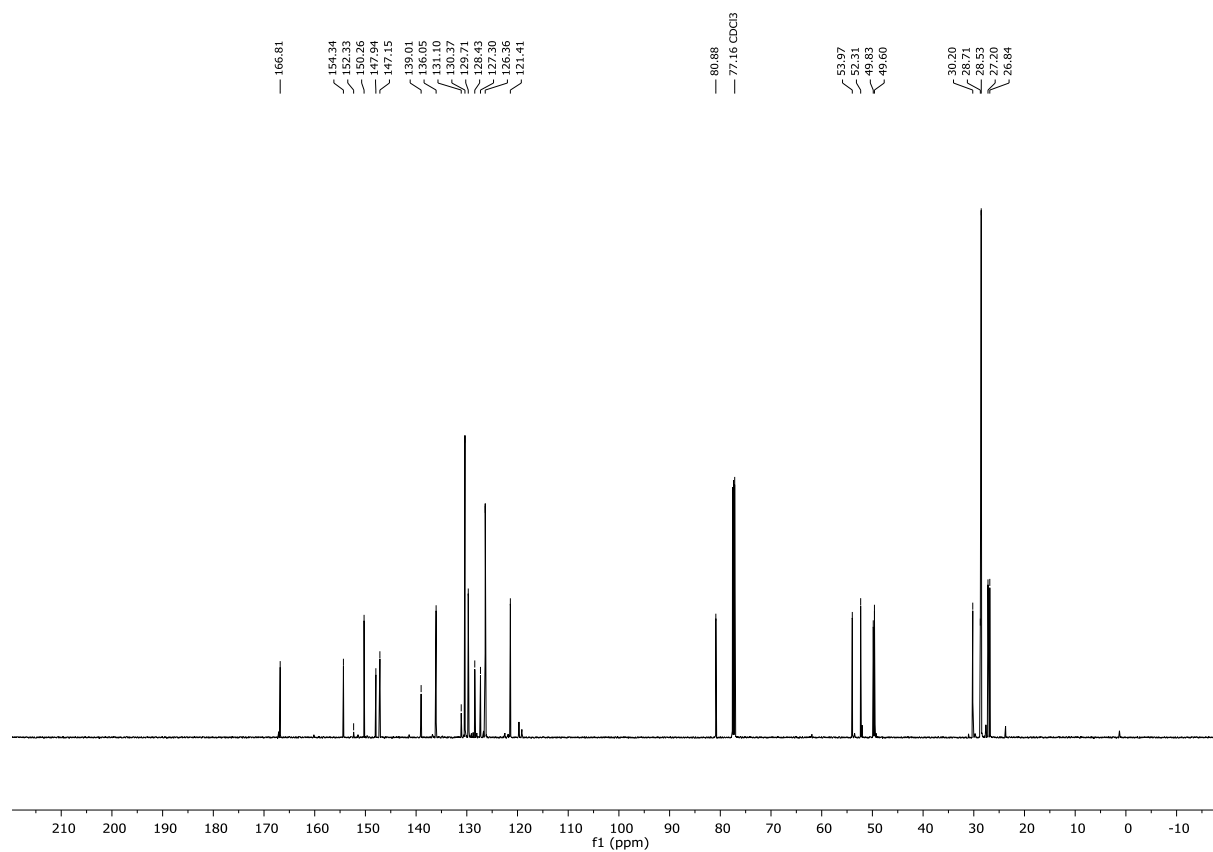
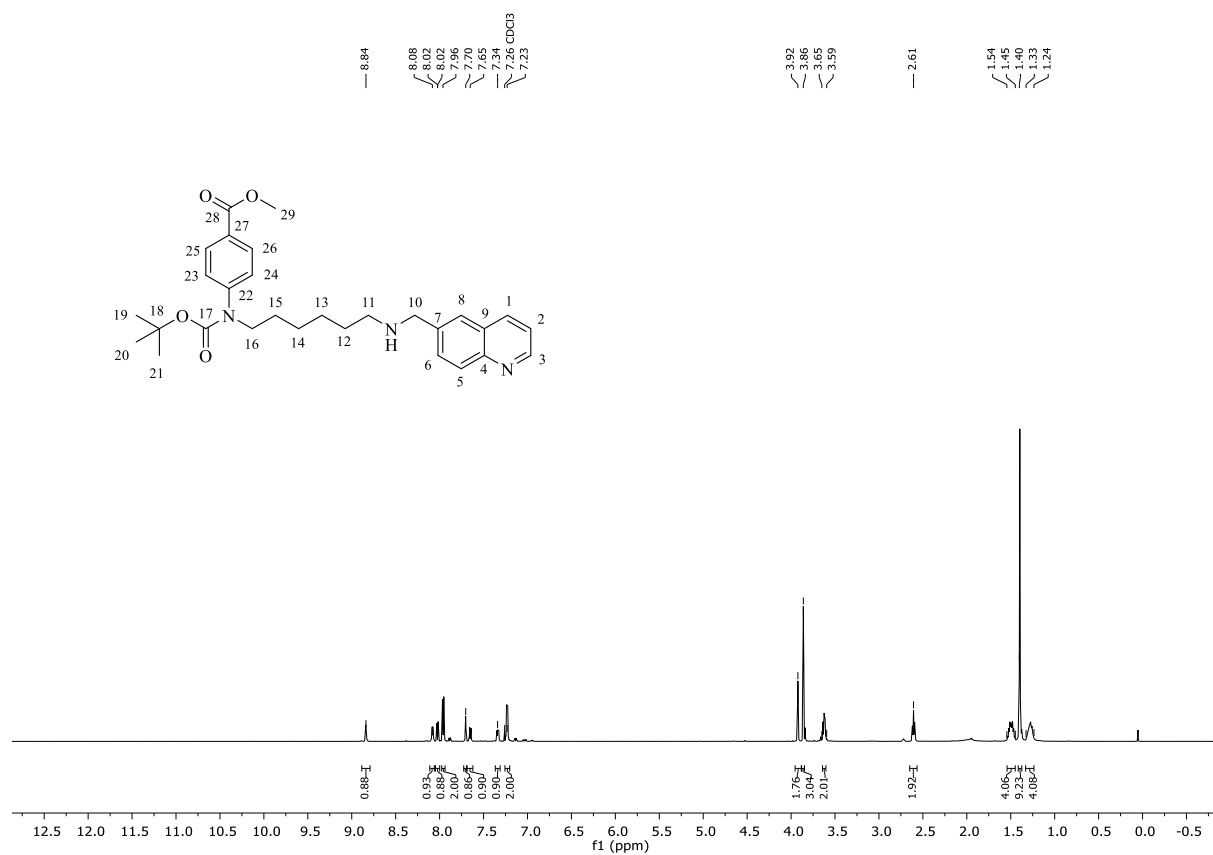
Methyl-4-((6-((*tert*-butoxycarbonyl)amino)hexyl)(quinolin-4-ylmethyl)amino)benzoate
60c



**Methyl-4-((6-((tert-butoxycarbonyl)amino)hexyl)(quinolin-6-ylmethyl)amino)benzoate
60d**

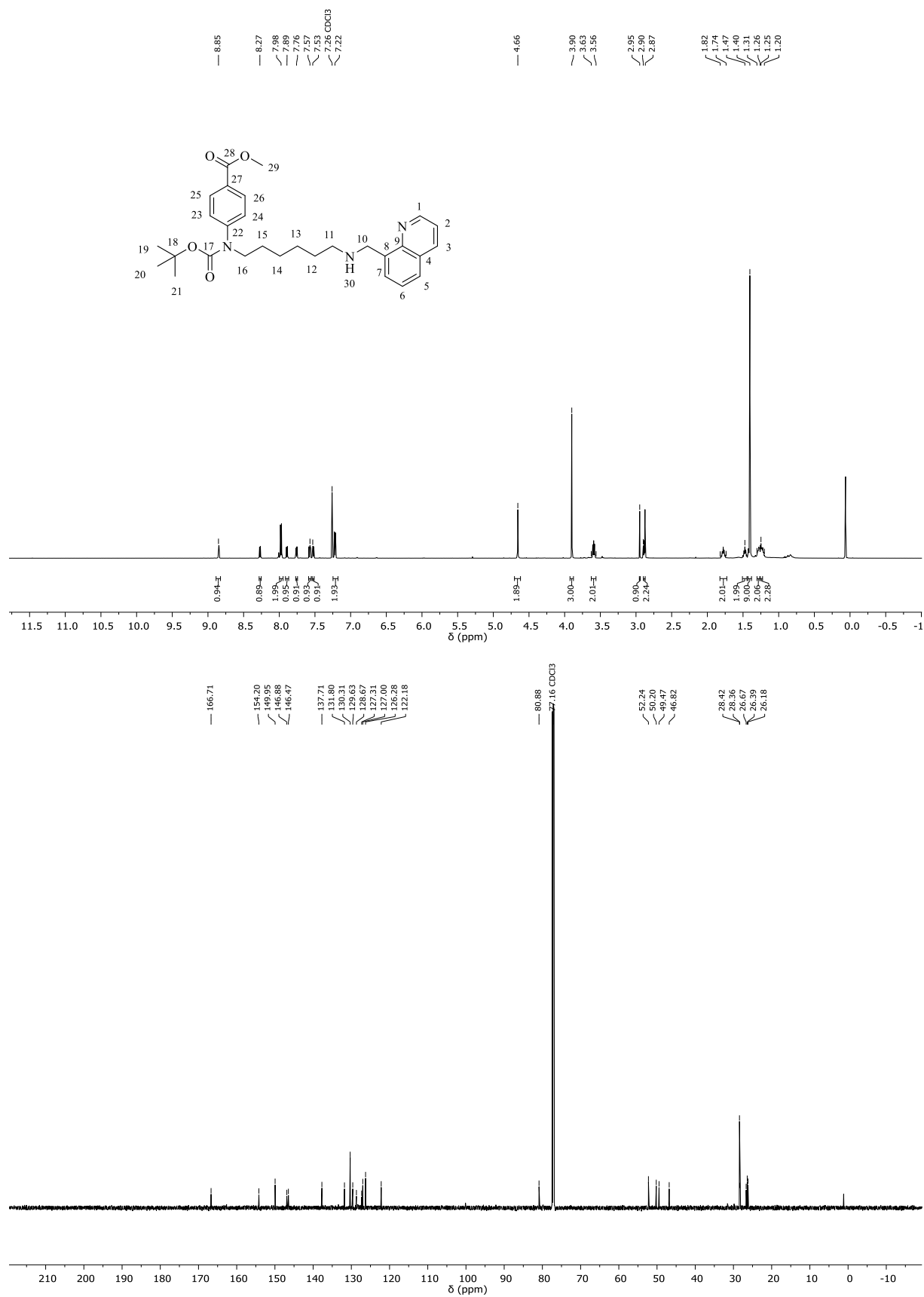


Methyl-4-((*tert*-butoxycarbonyl)(6-((quinolin-6-ylmethyl)amino)hexyl)amino) benzoate 59d

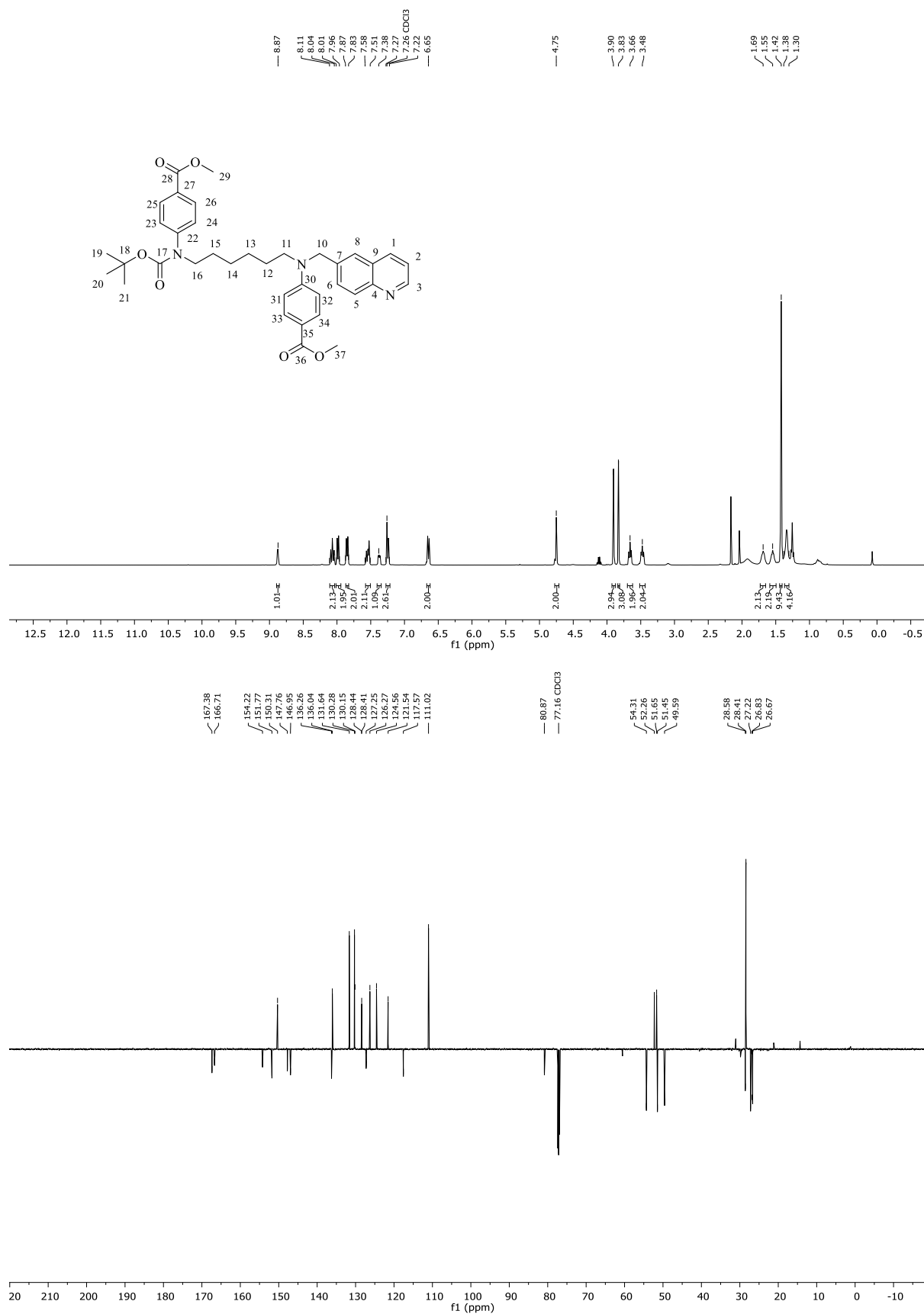


Methyl-4-((*tert*-butoxycarbonyl)(6-((quinolin-8-ylmethyl)amino)hexyl)amino)benzoate

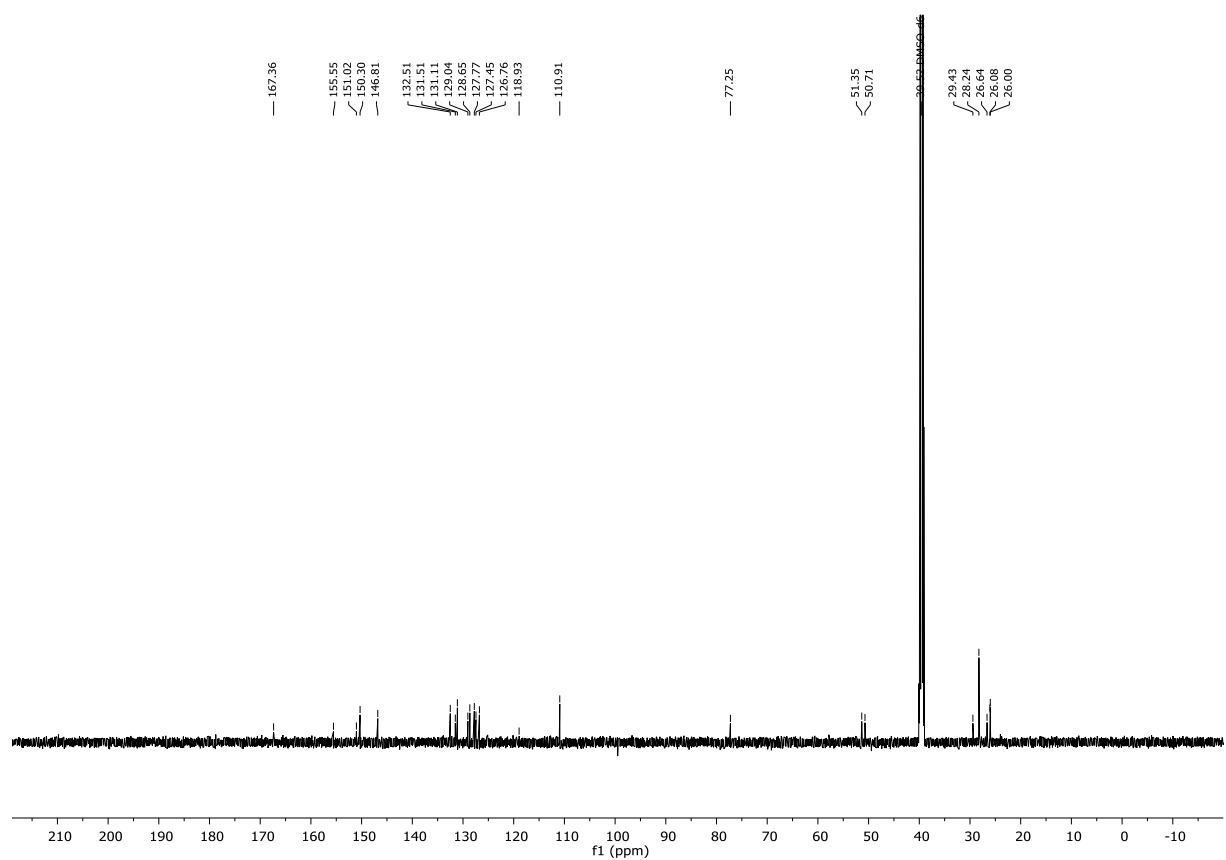
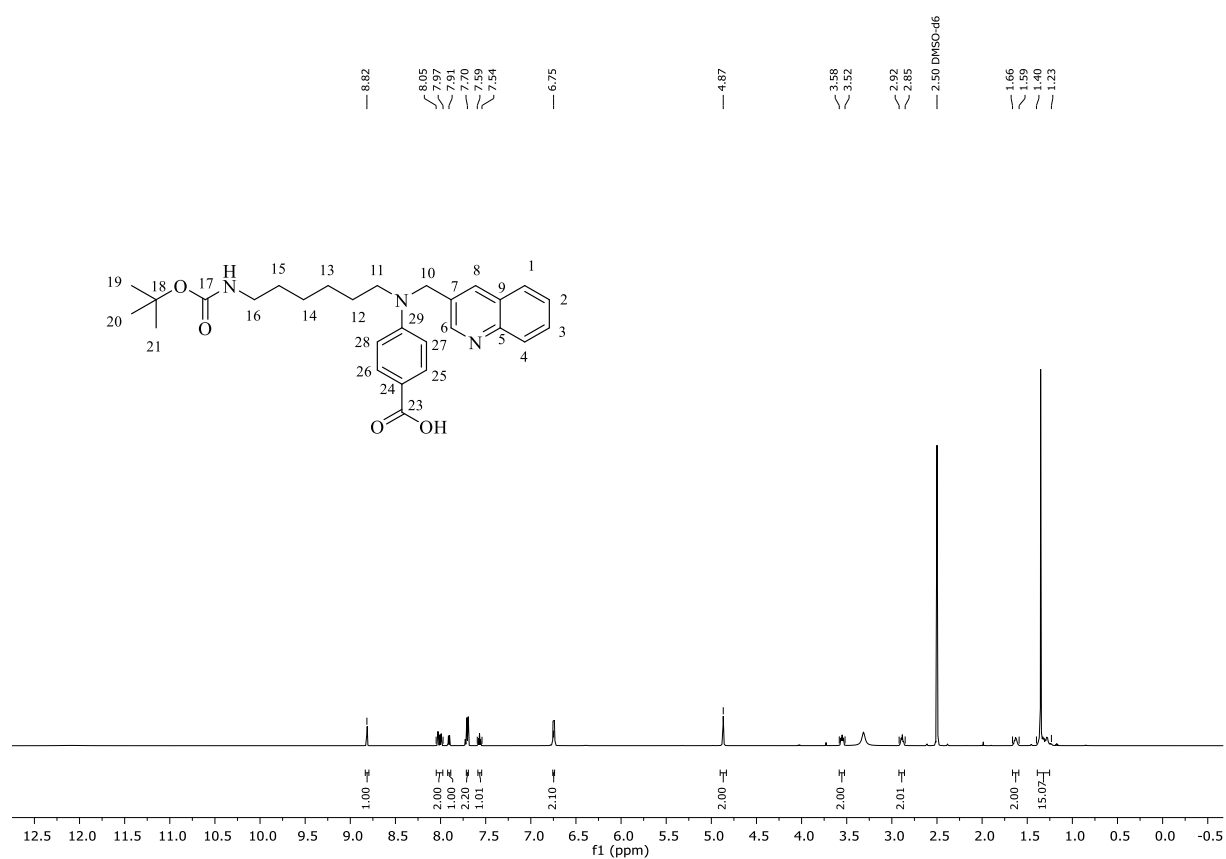
59e



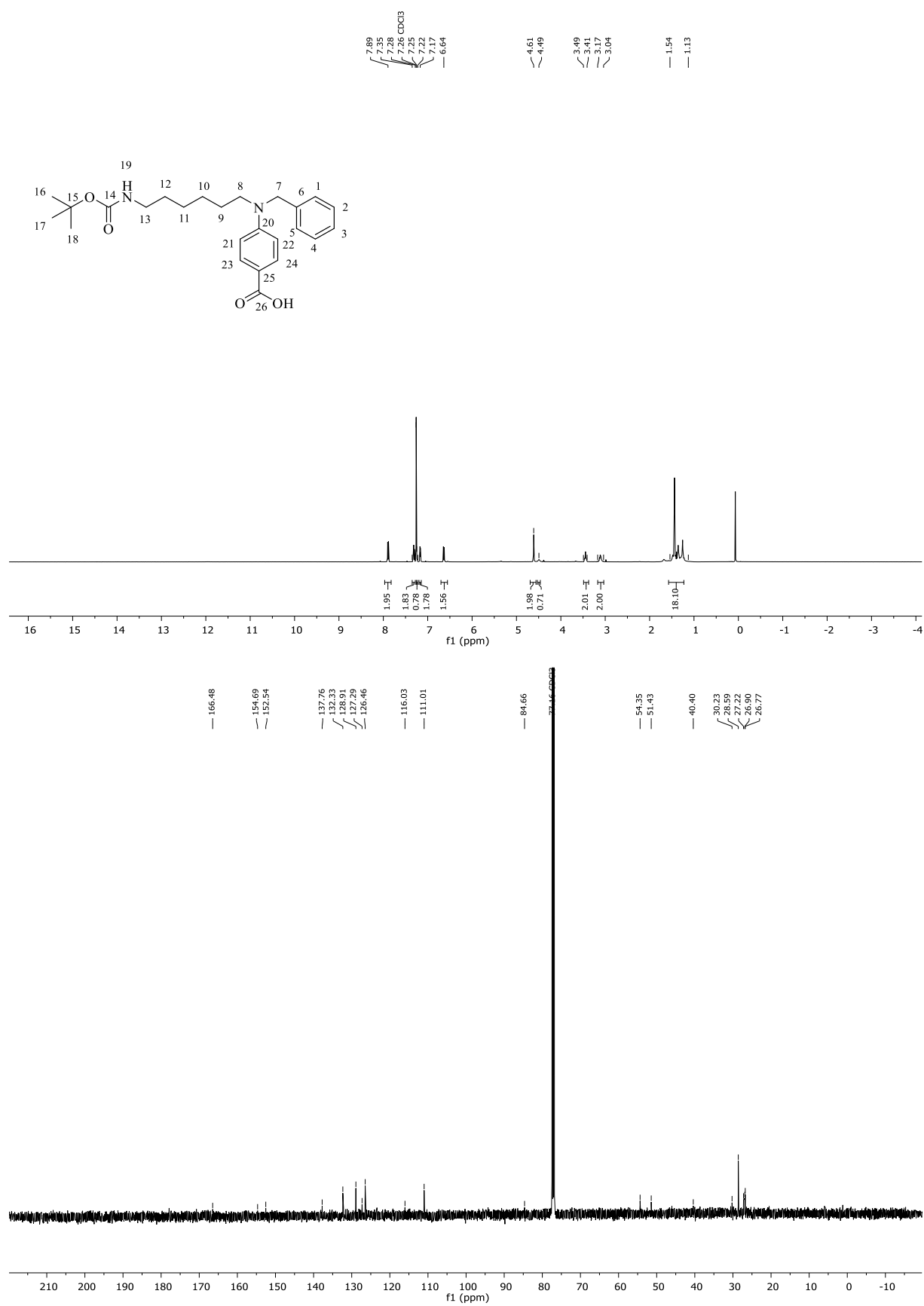
Biarylated amine 71



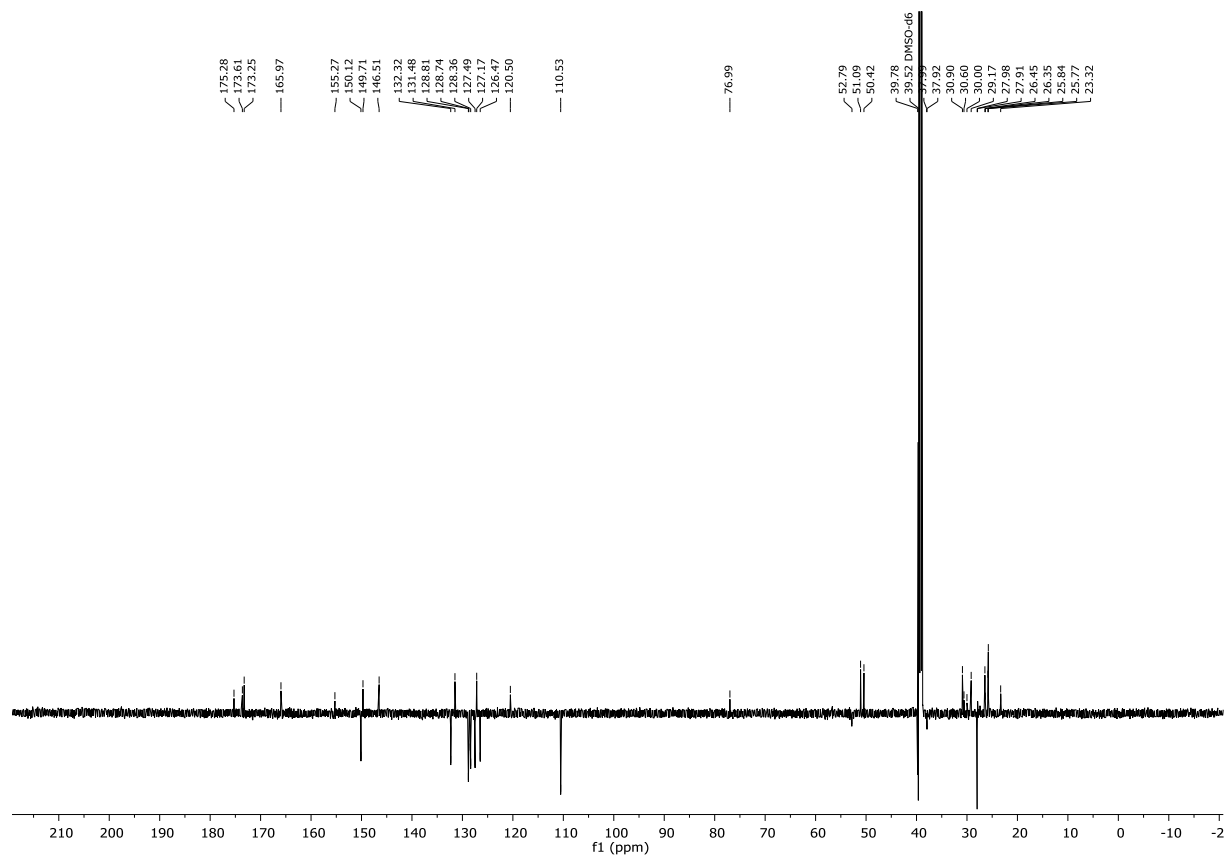
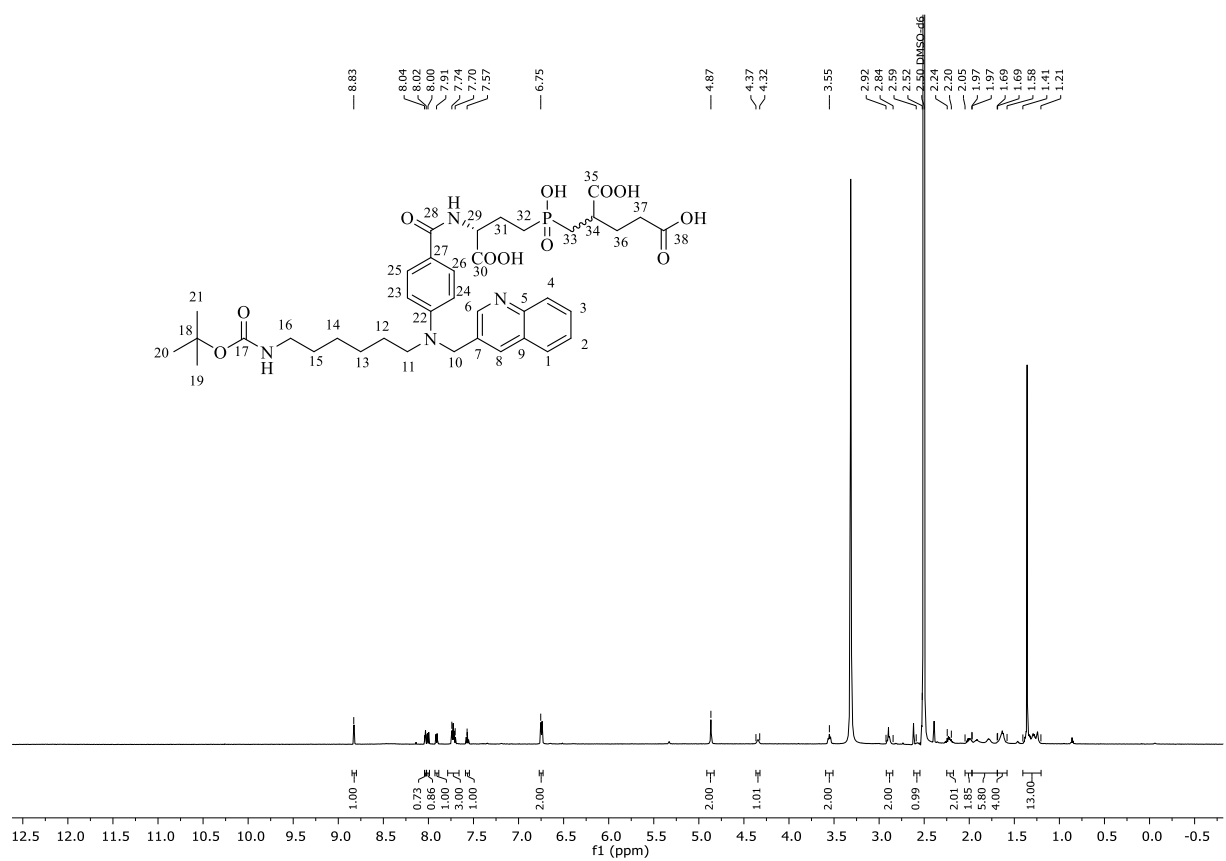
Carboxylic acid 77b



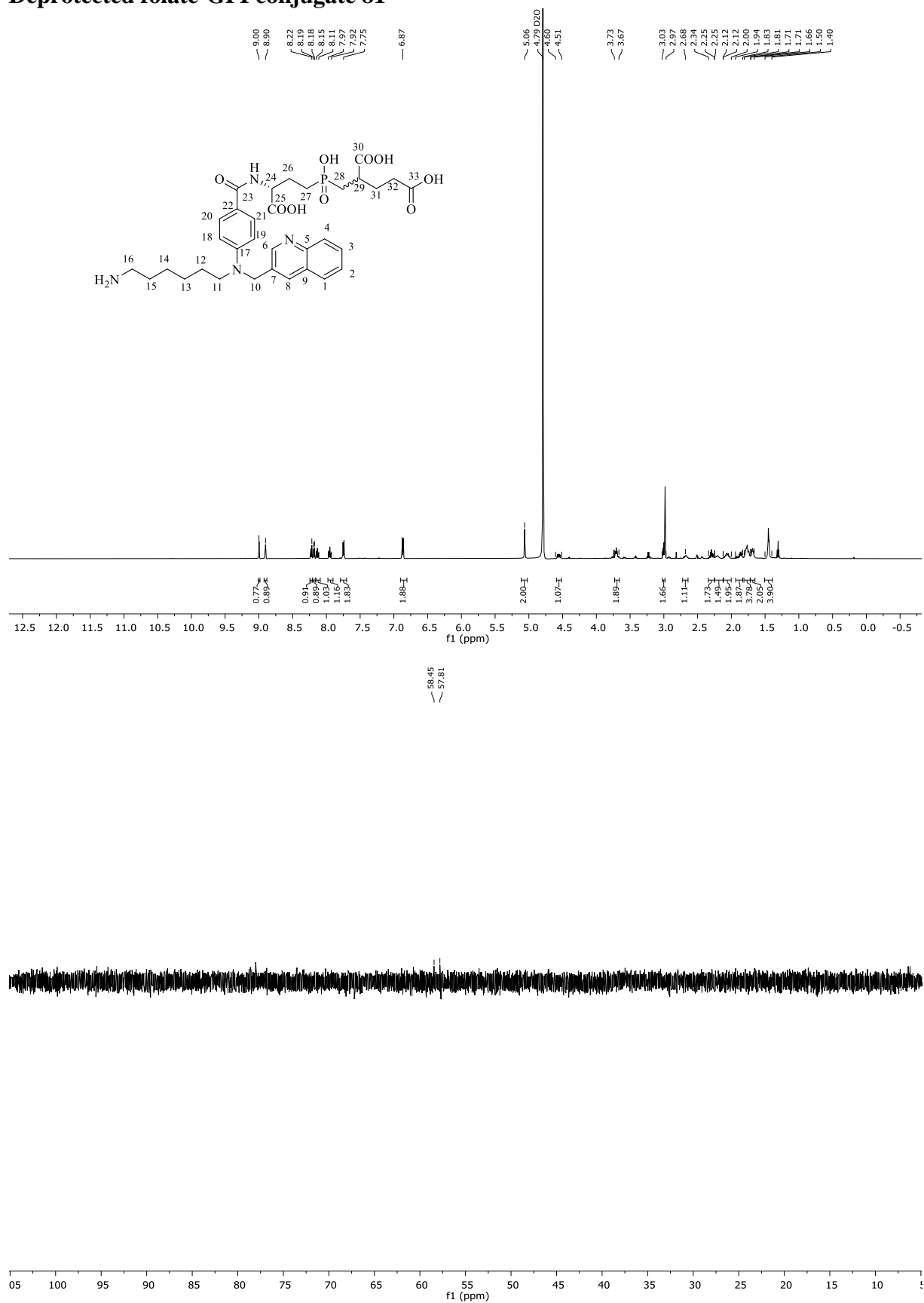
Carboxylic acid 77f



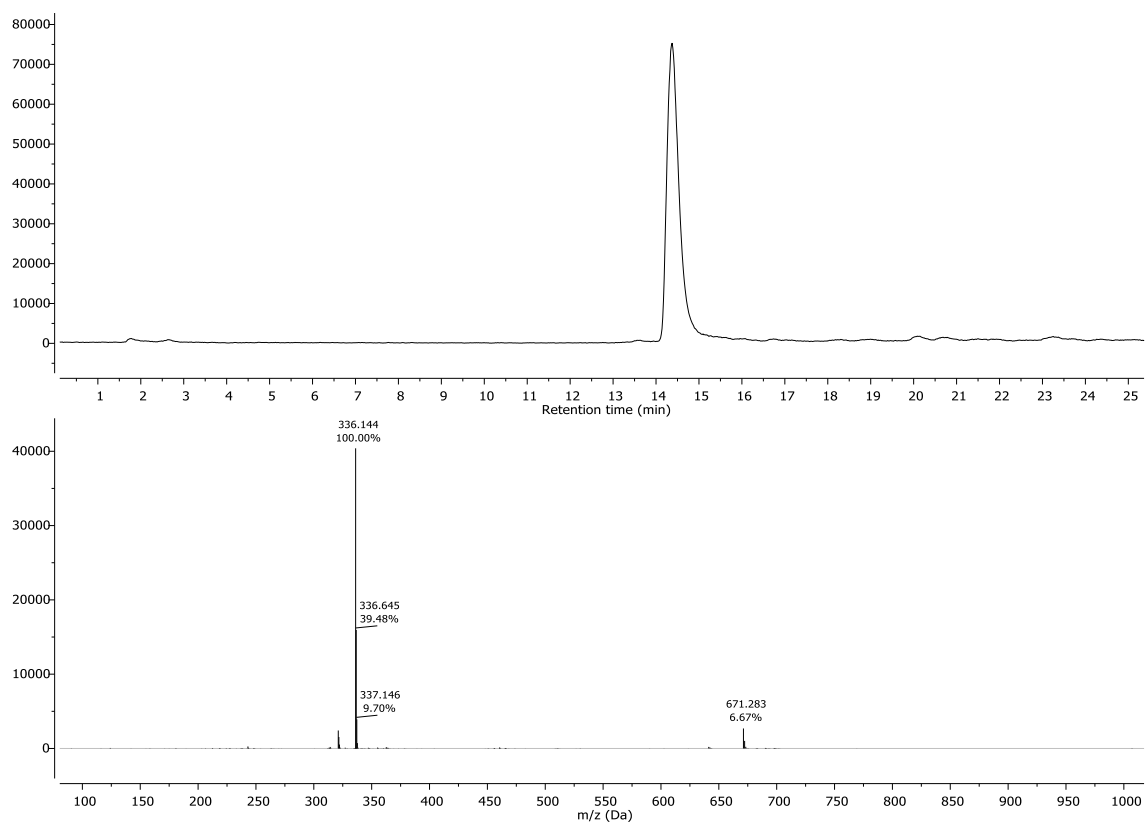
Boc-protected folate-GPI conjugate 79



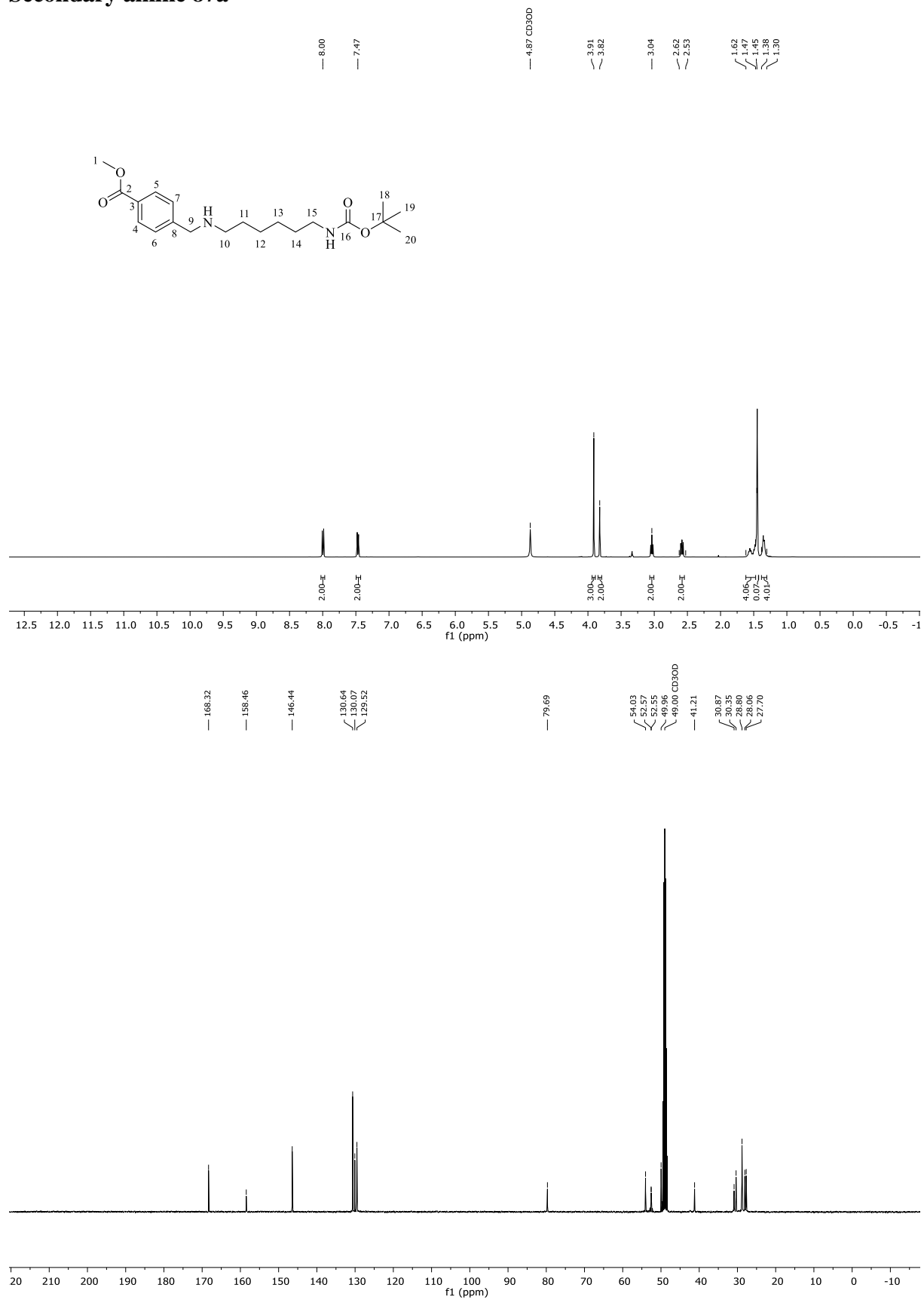
Deprotected folate-GPI conjugate 81



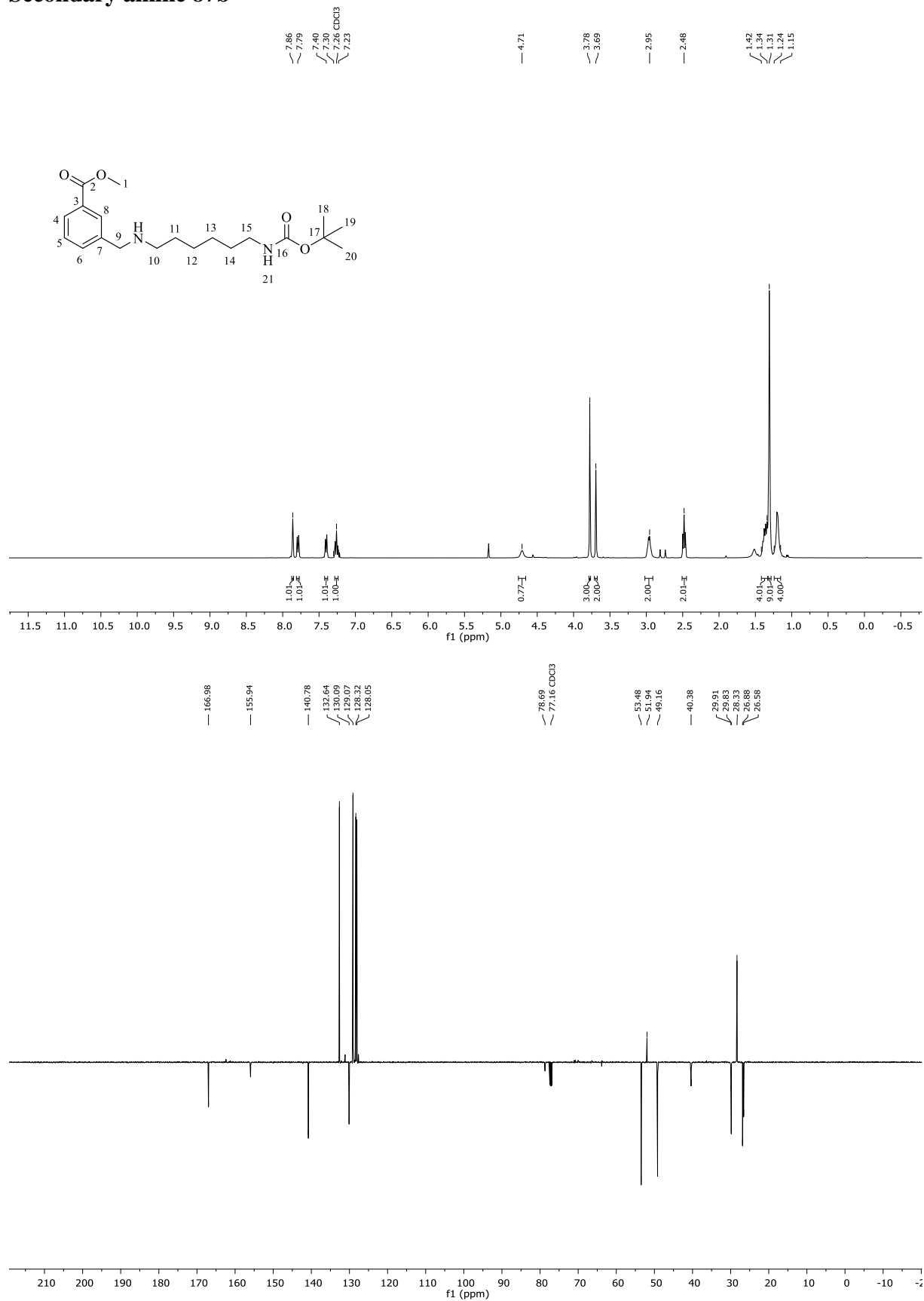
LC-MS



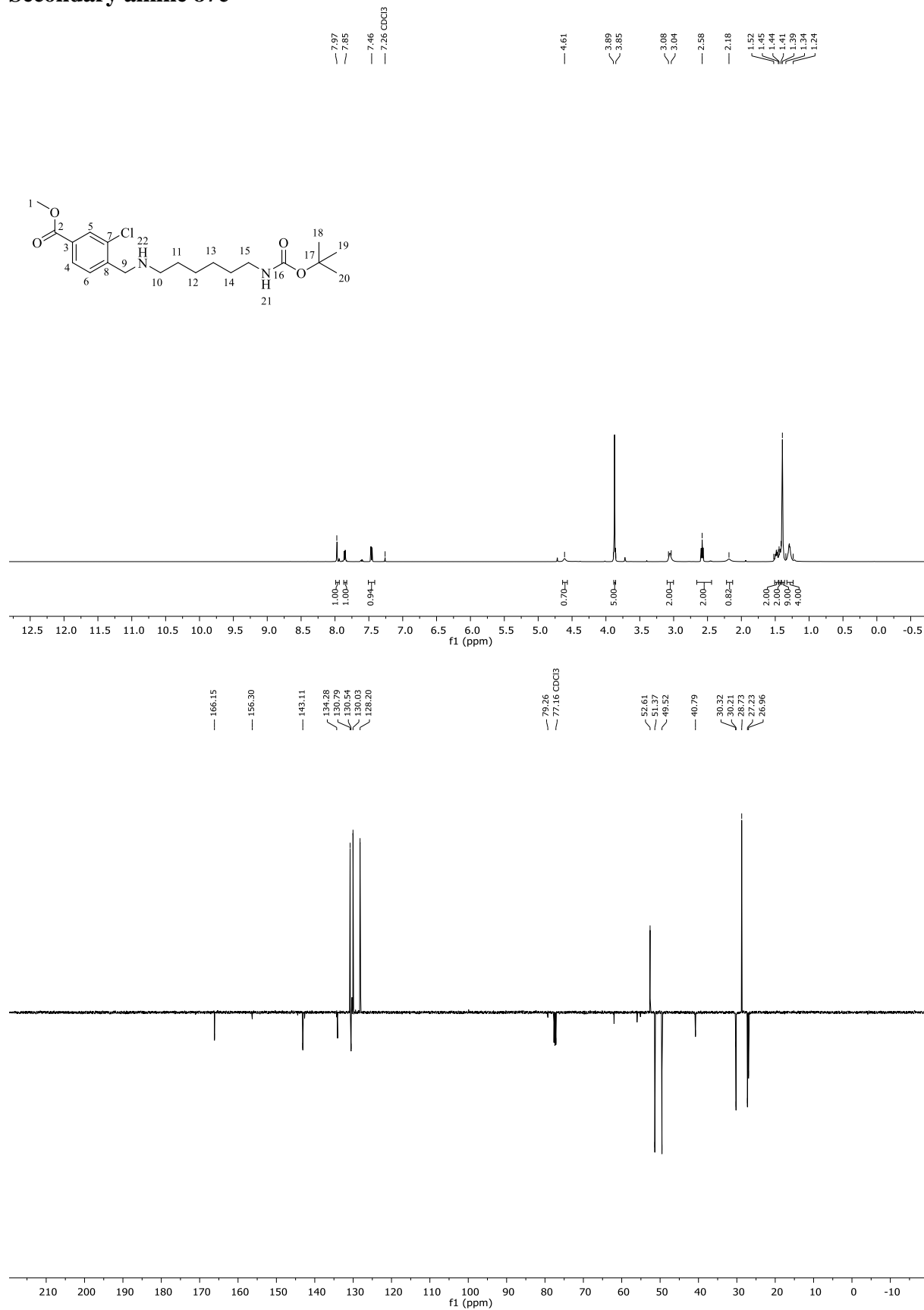
Secondary amine 87a



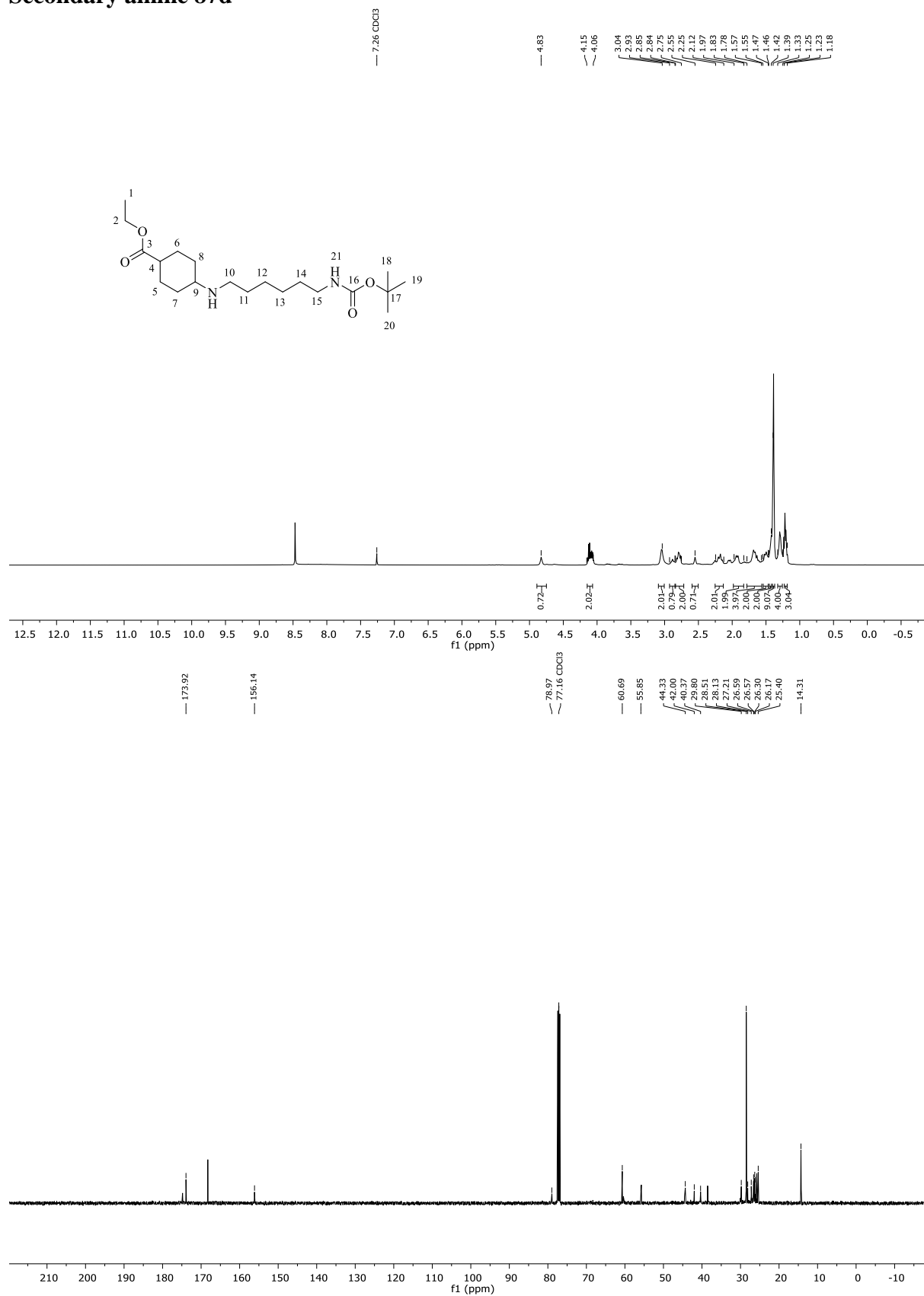
Secondary amine 87b



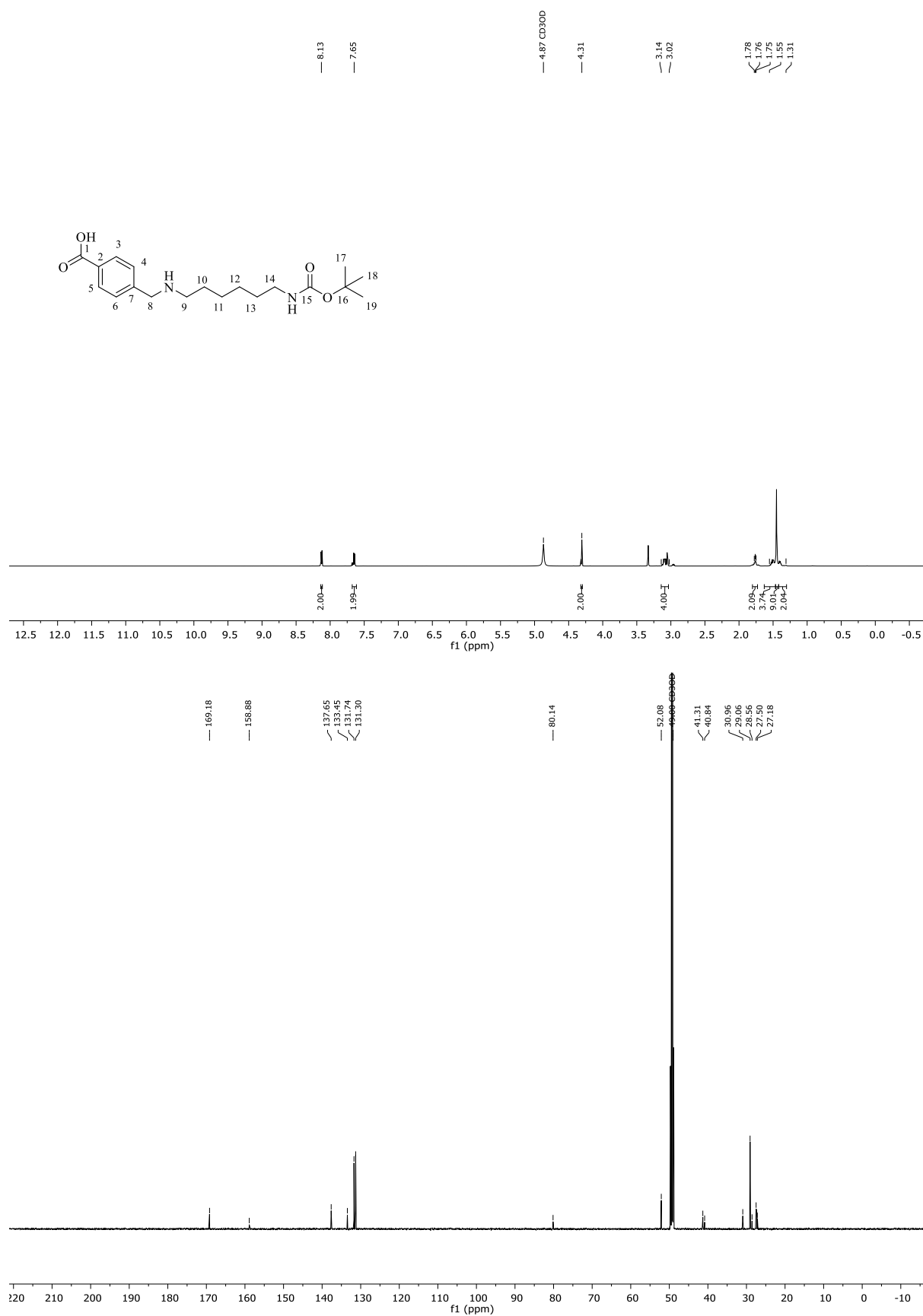
Secondary amine 87c



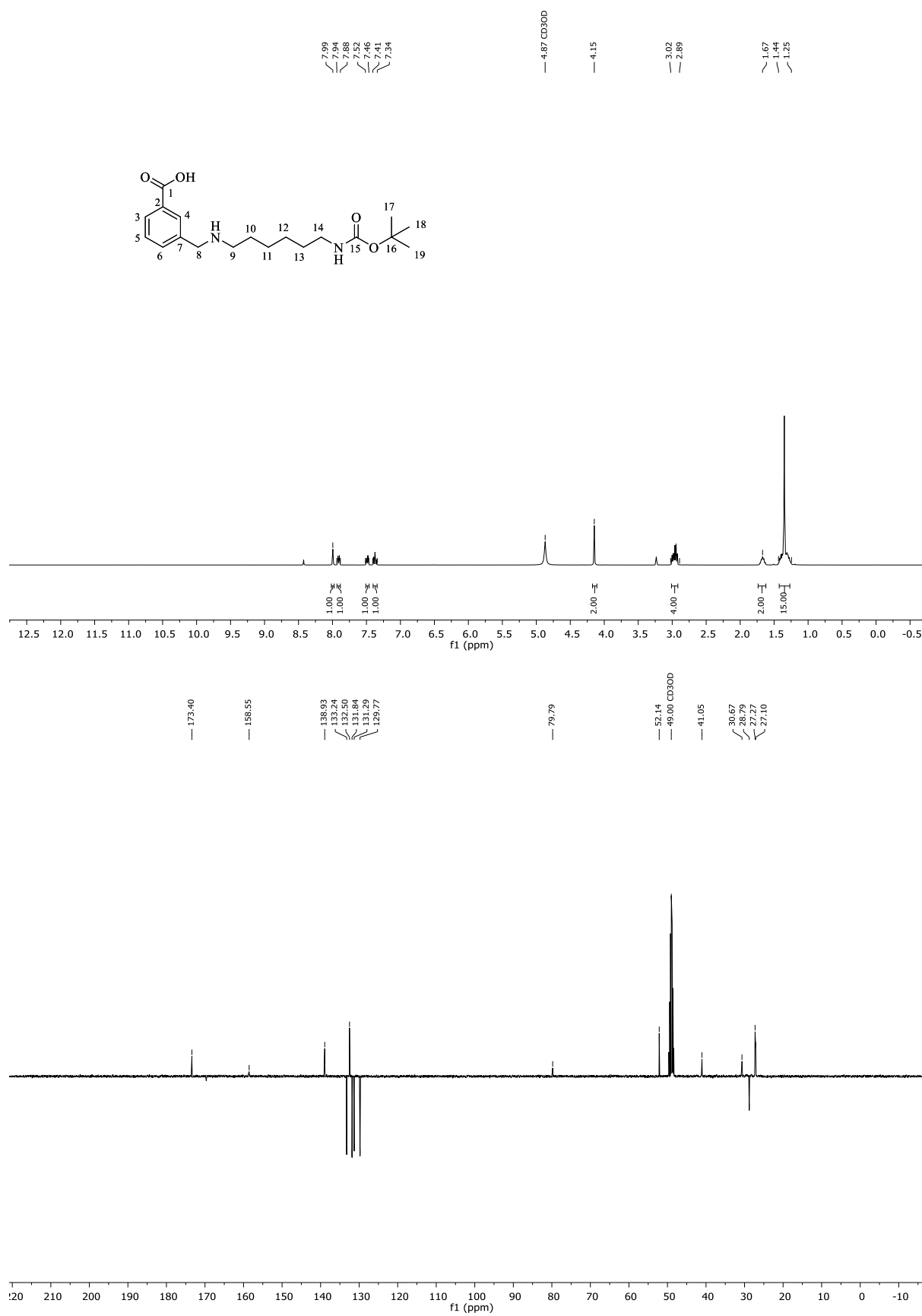
Secondary amine 87d



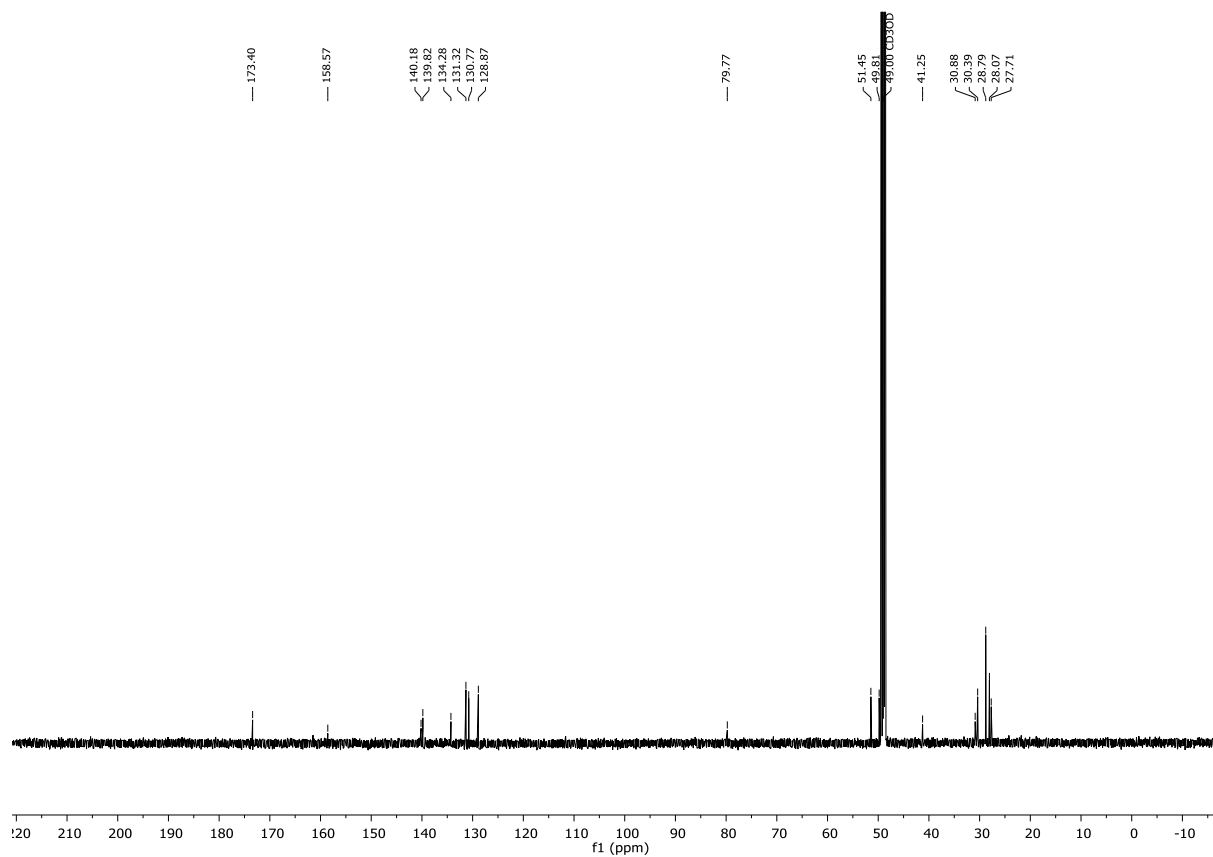
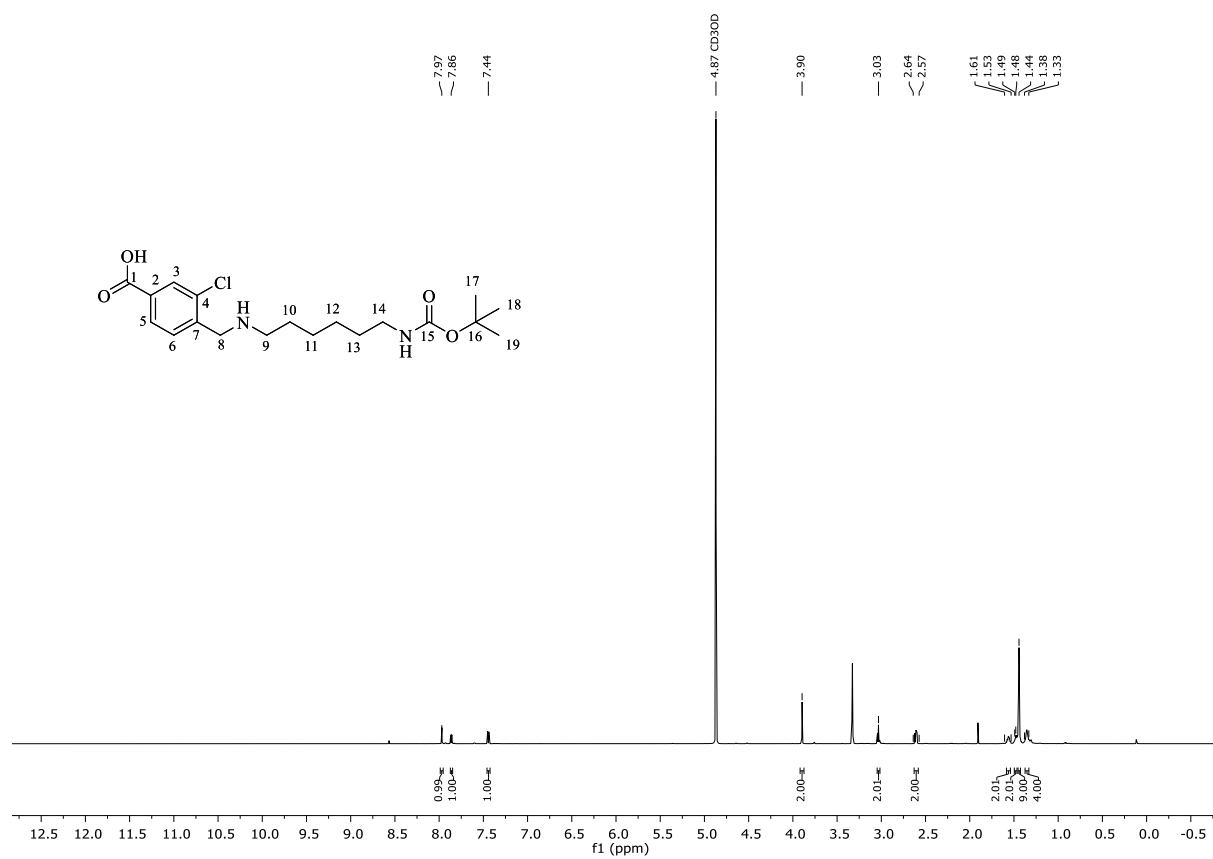
Carboxylic acid 86a



Carboxylic acid 86b



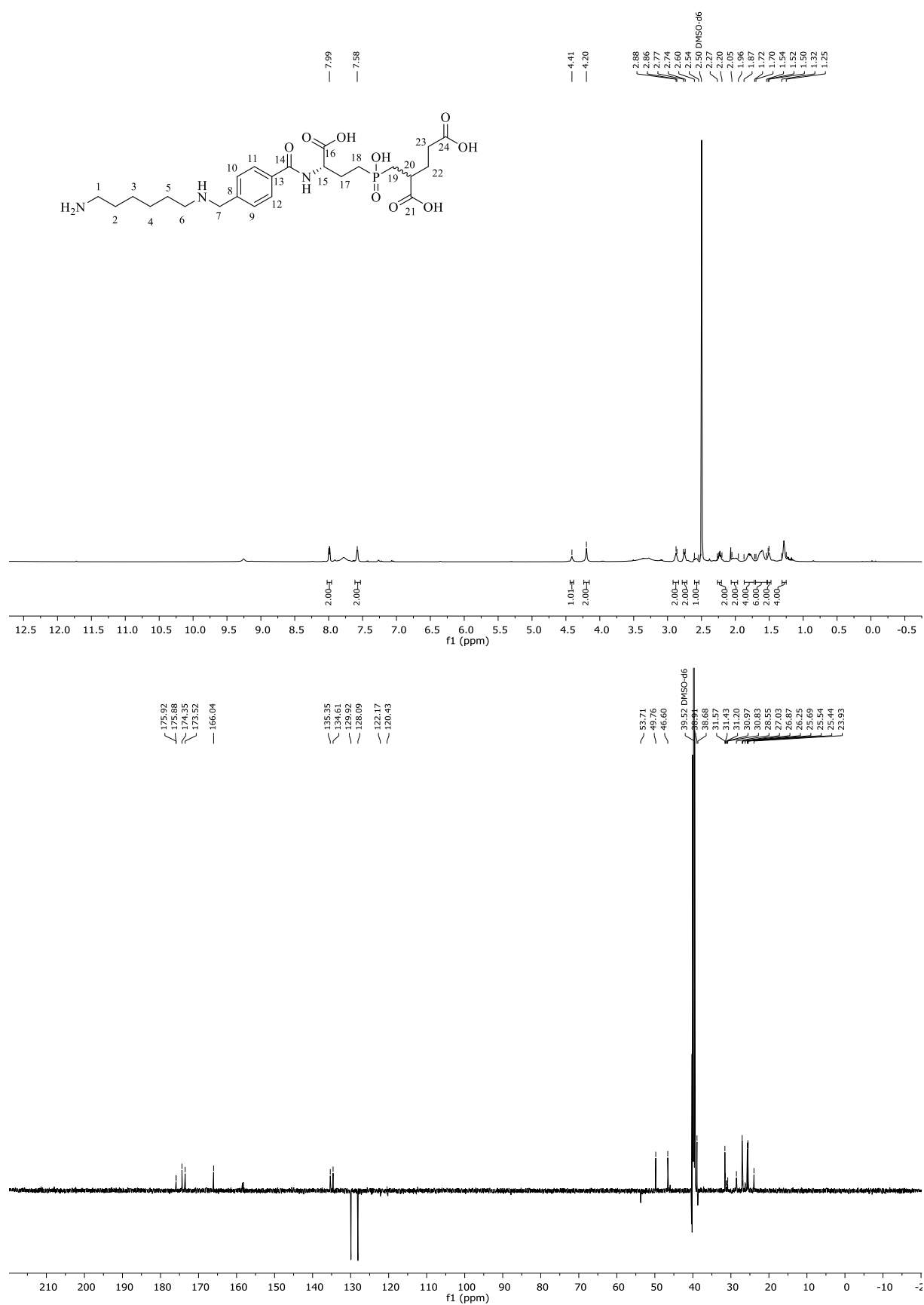
Carboxylic acid 86c



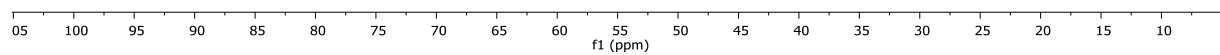
Carboxylic acid 86d



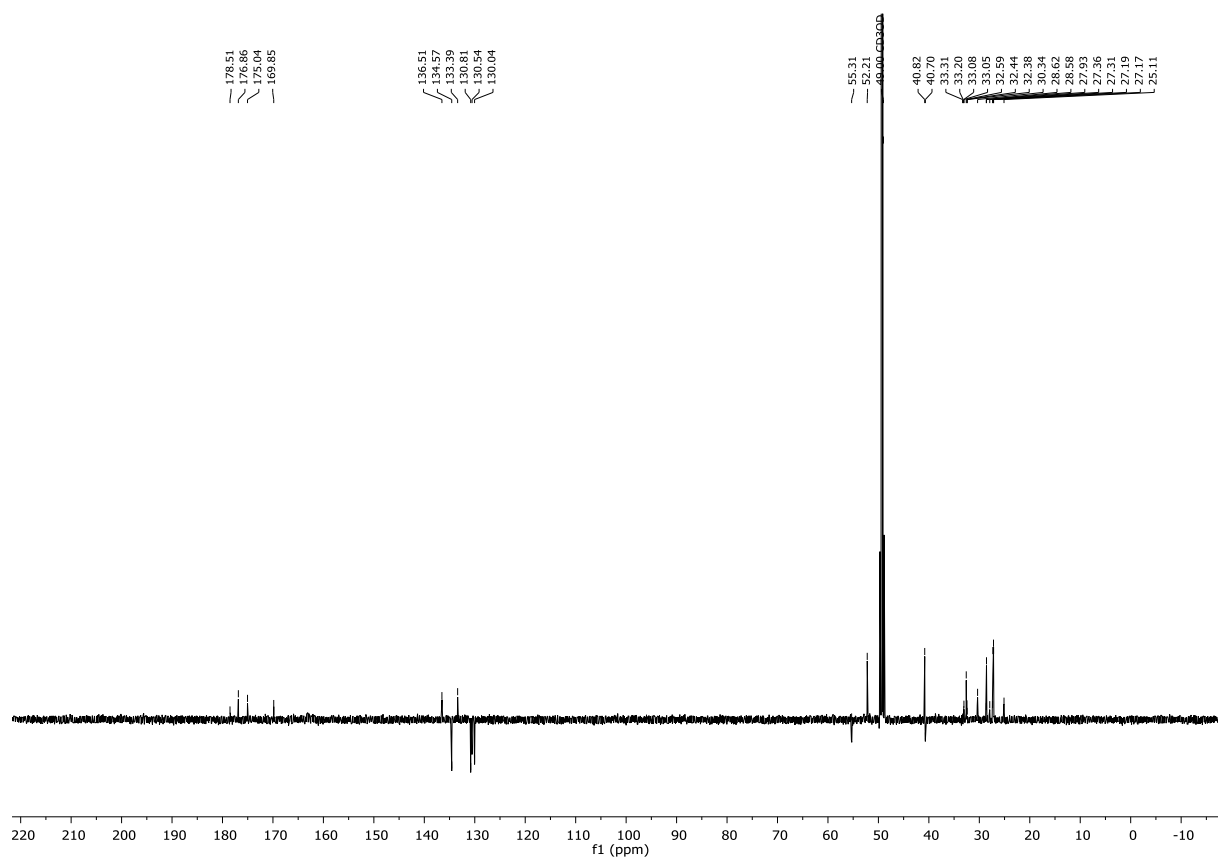
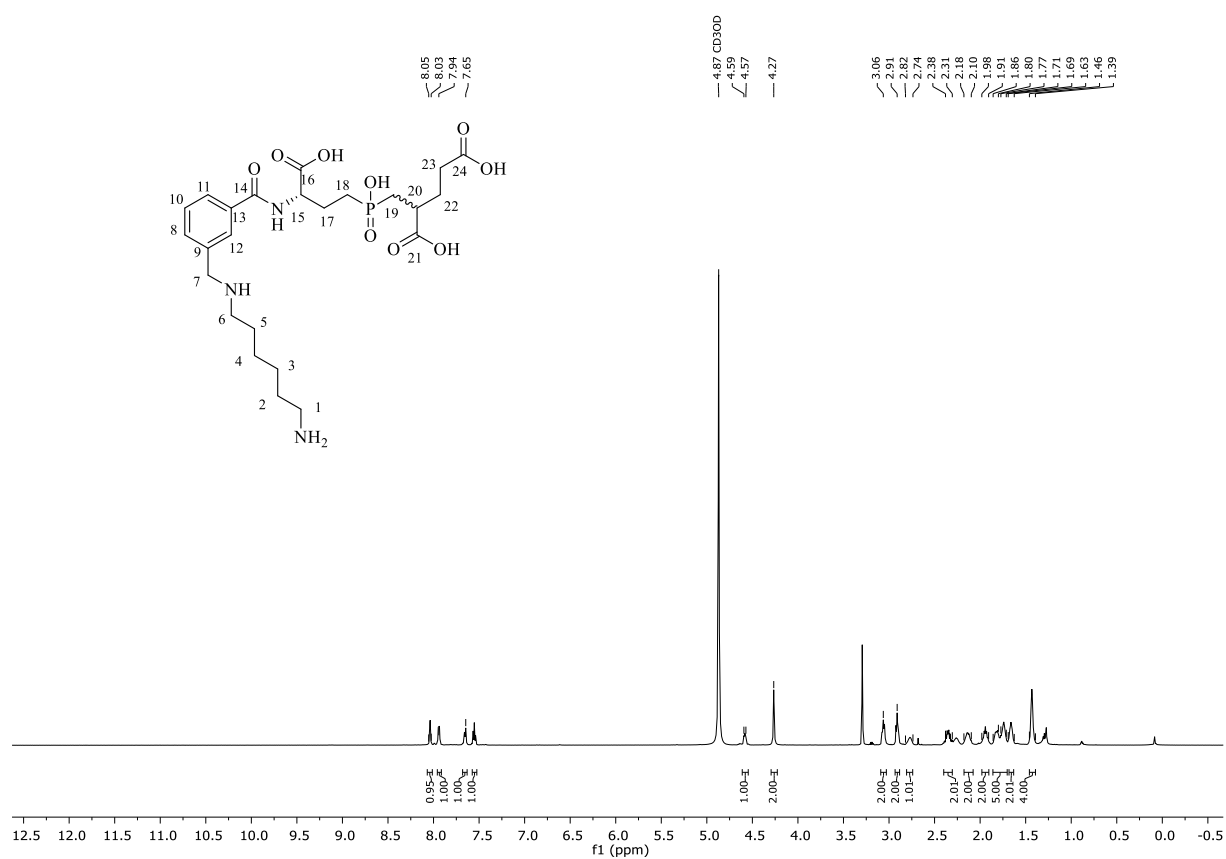
Simplified folate-GPI conjugate 85a

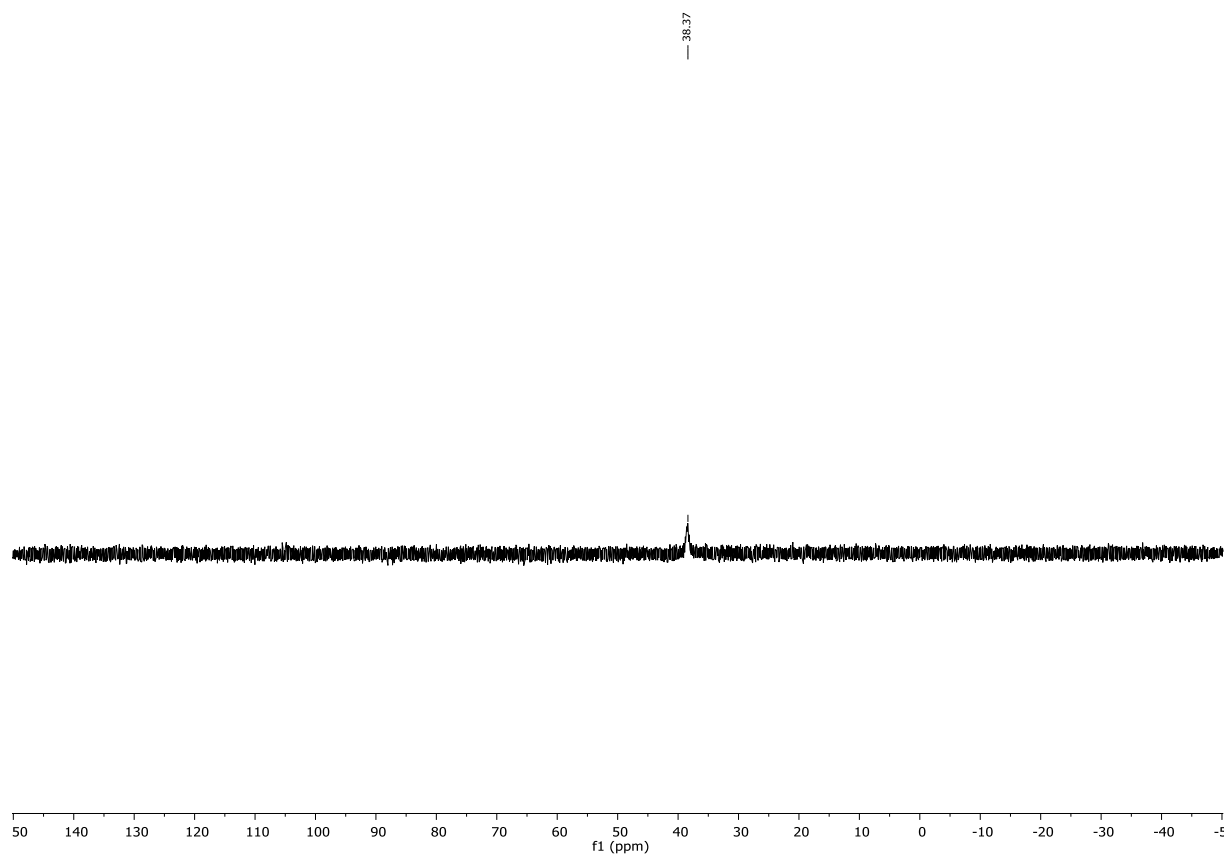


— 61.34

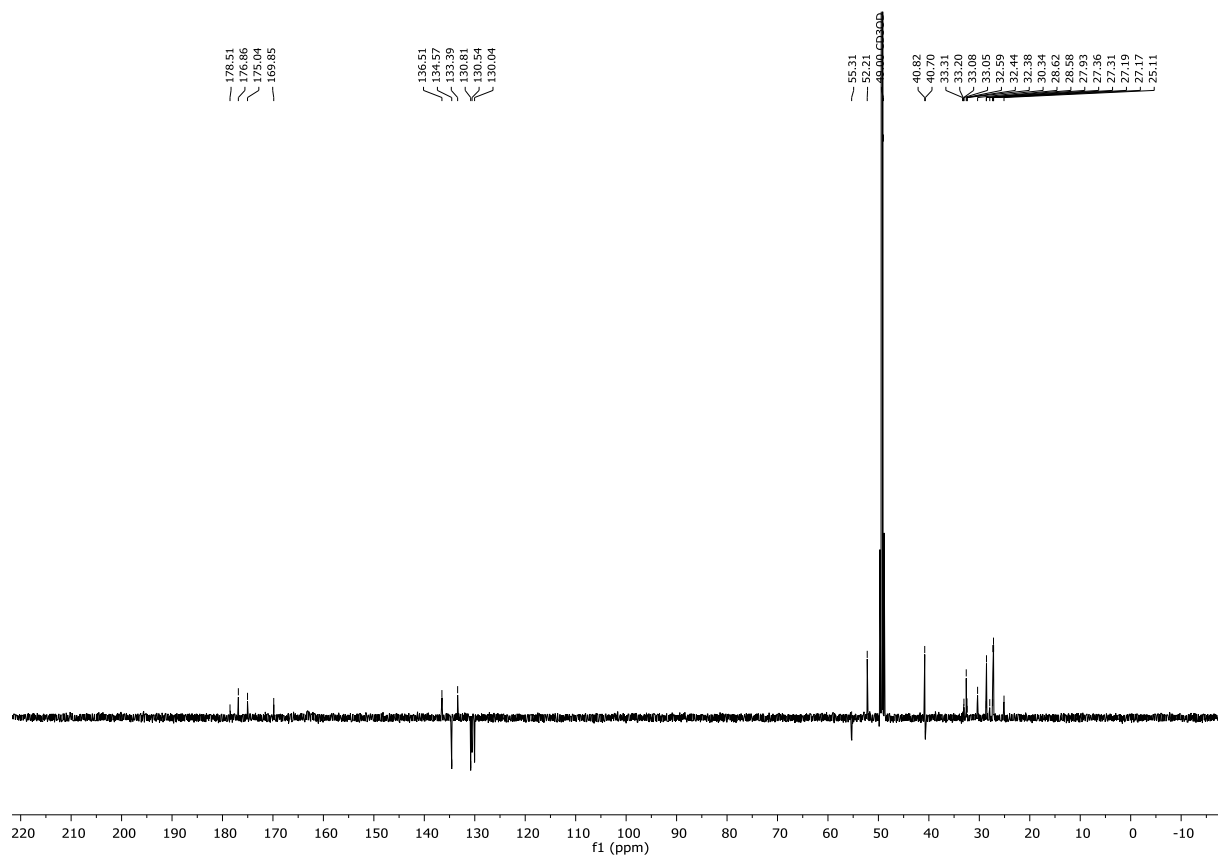
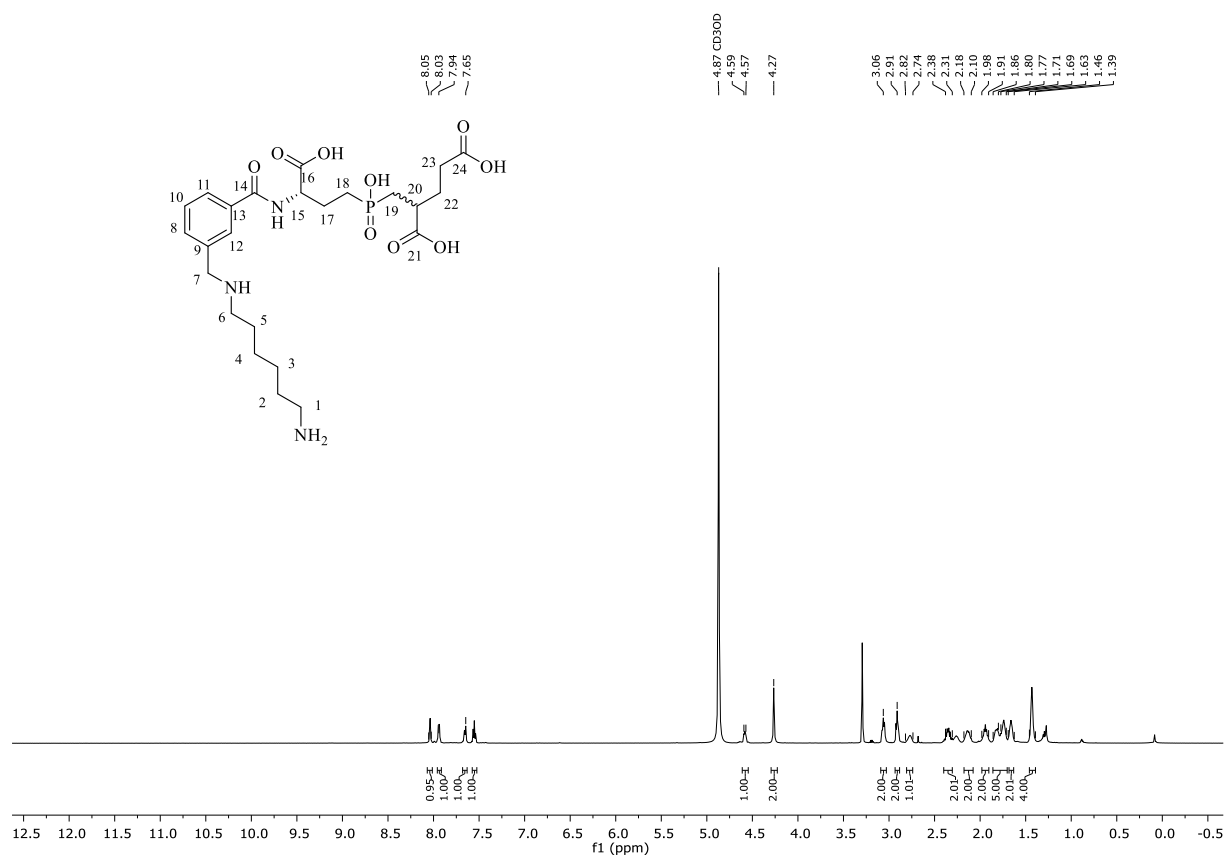


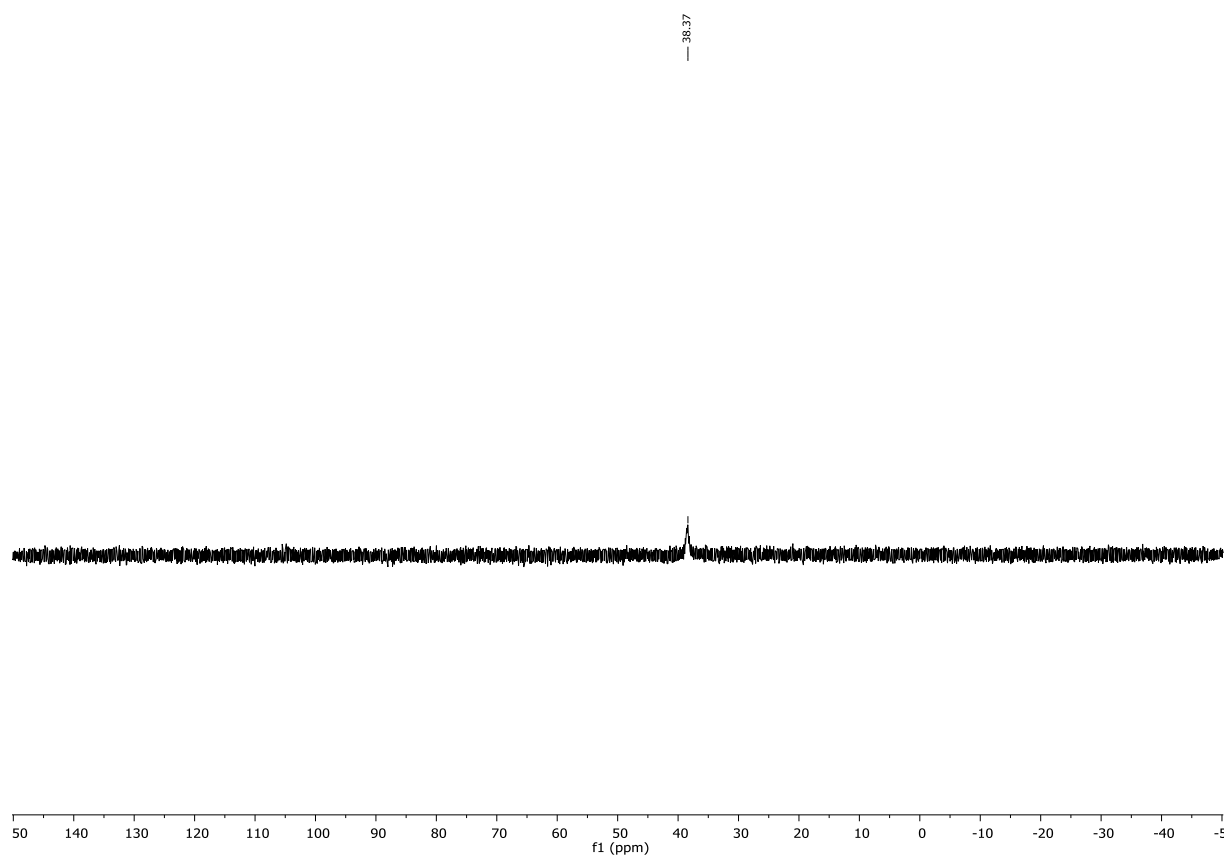
Simplified folate-GPI conjugate 85b



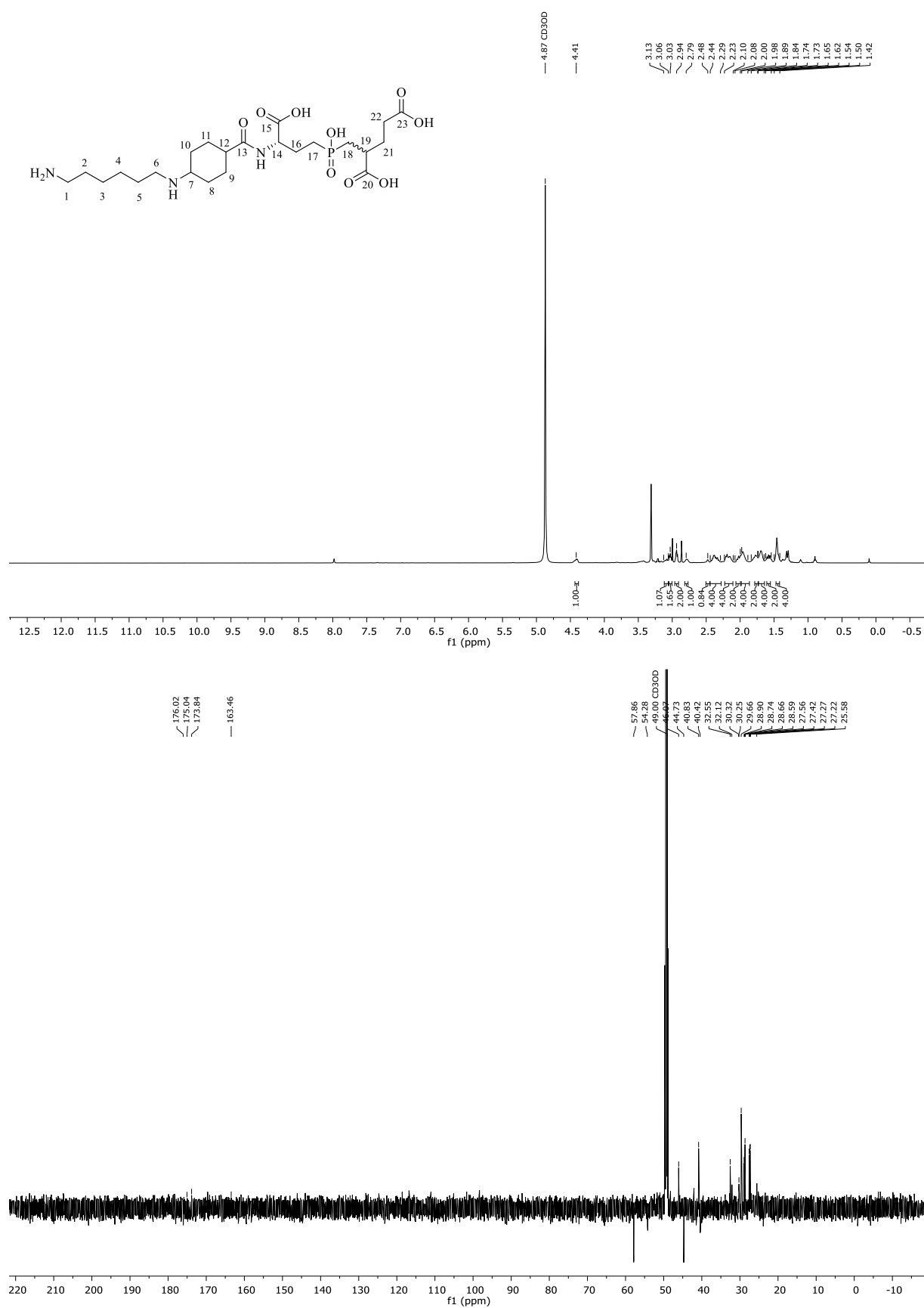


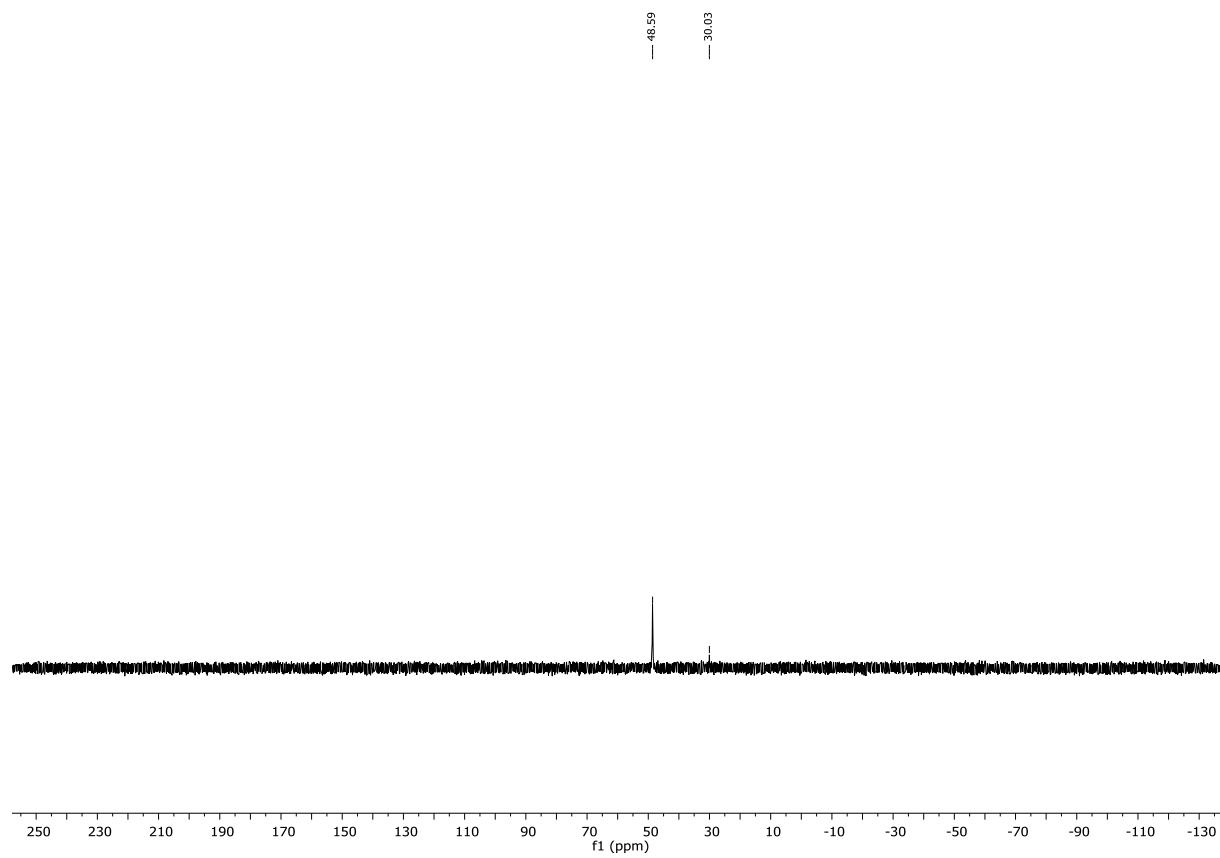
Simplified folate-GPI conjugate 85c



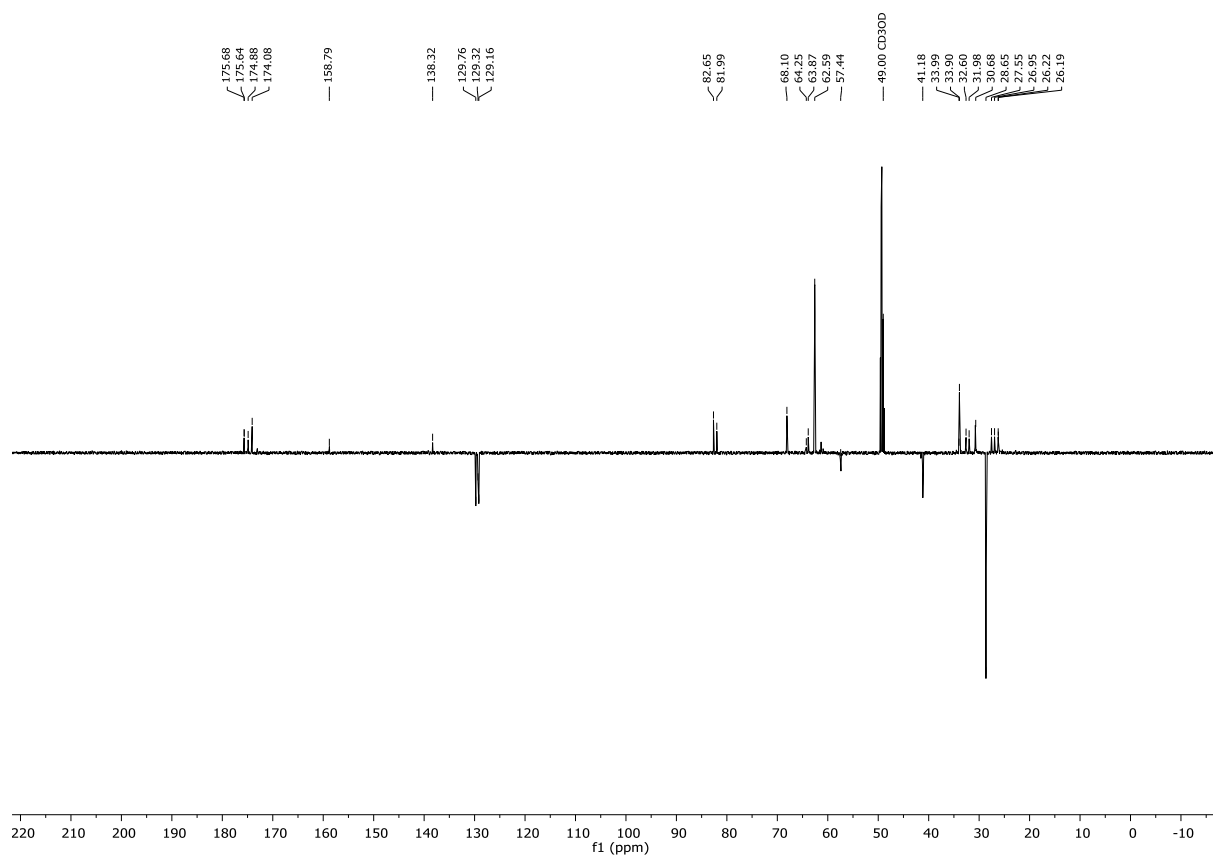
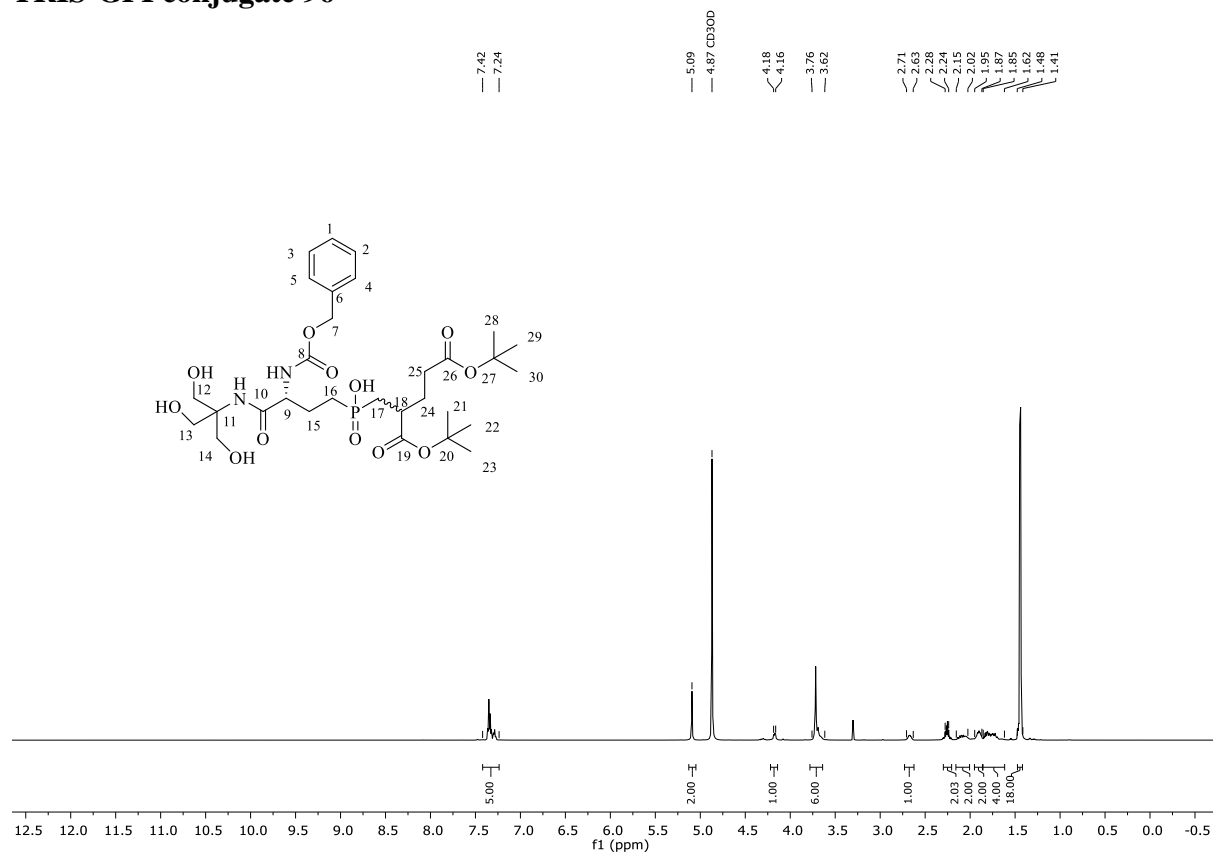


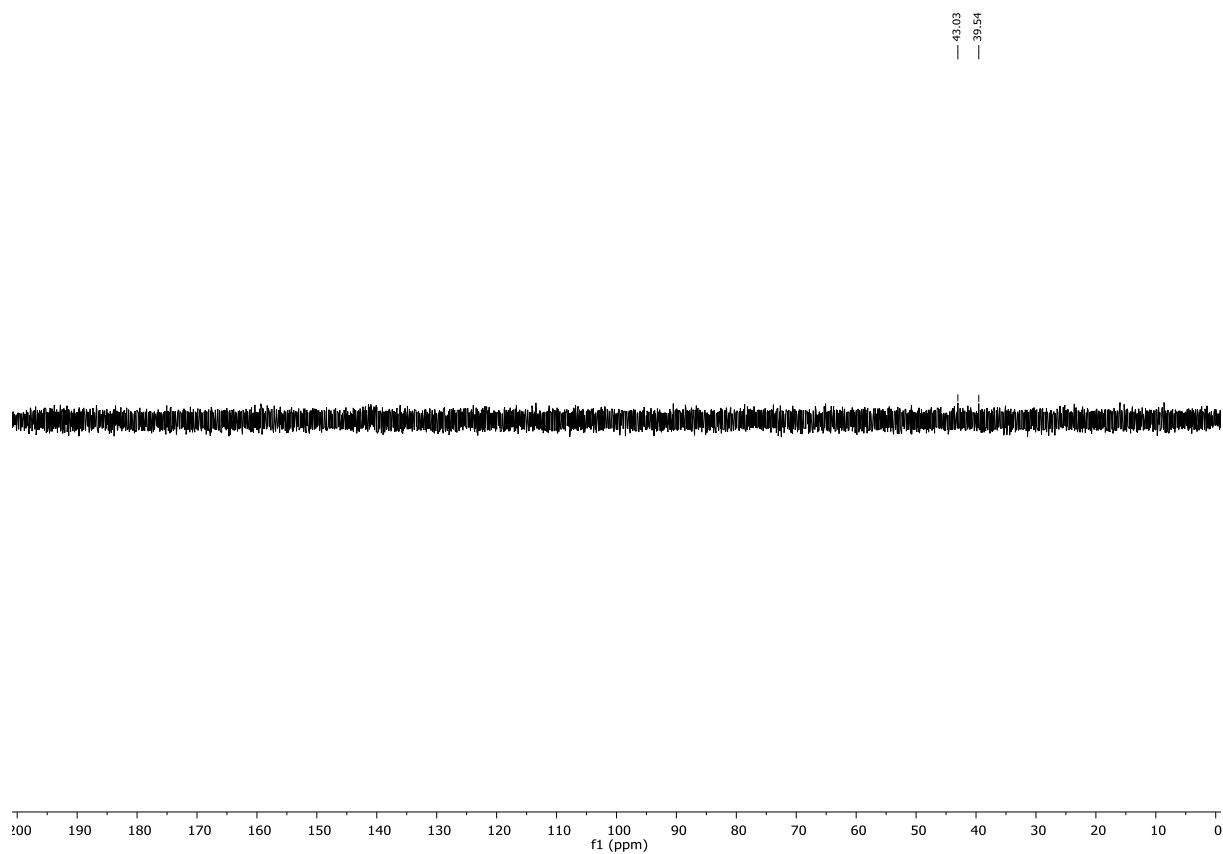
Simplified folate-GPI conjugate 85d



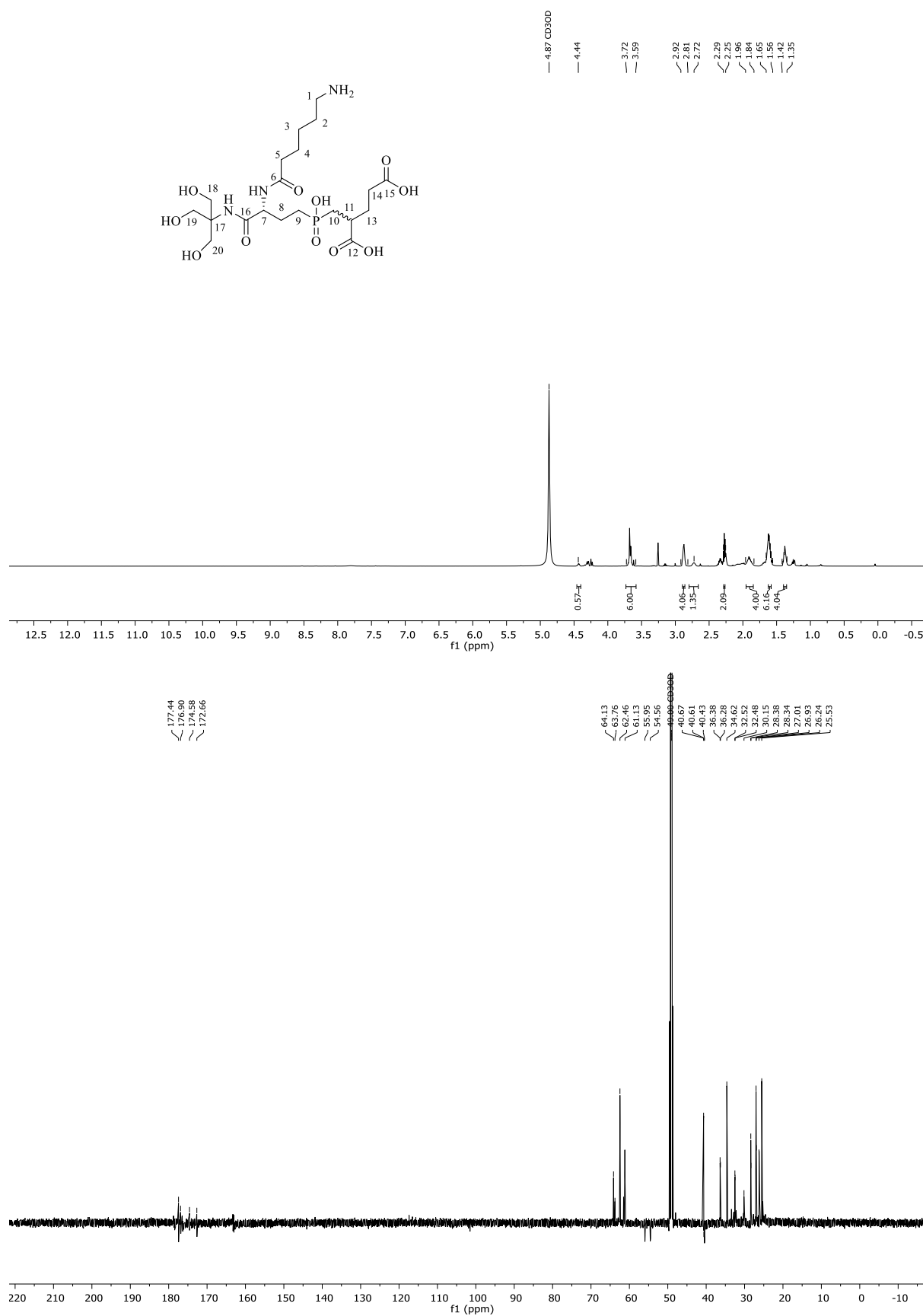


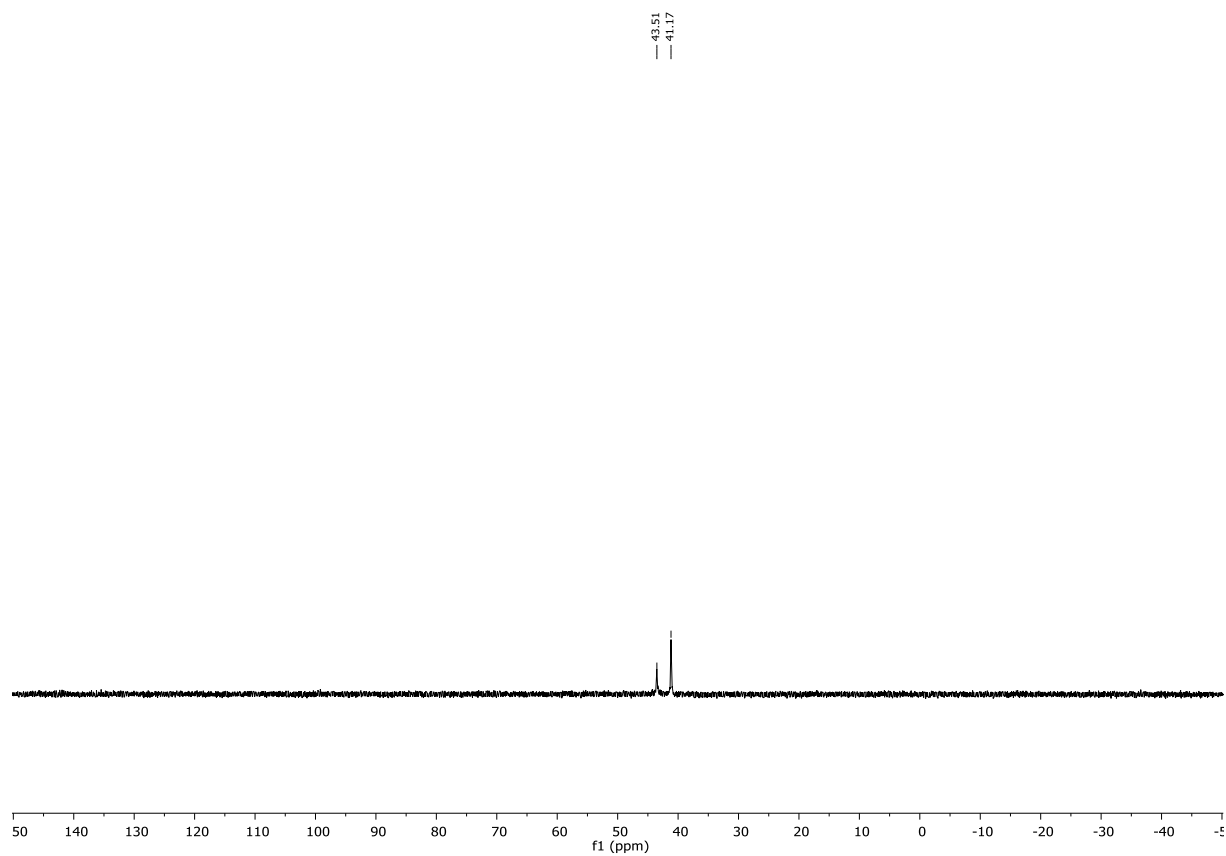
TRIS-GPI conjugate 96



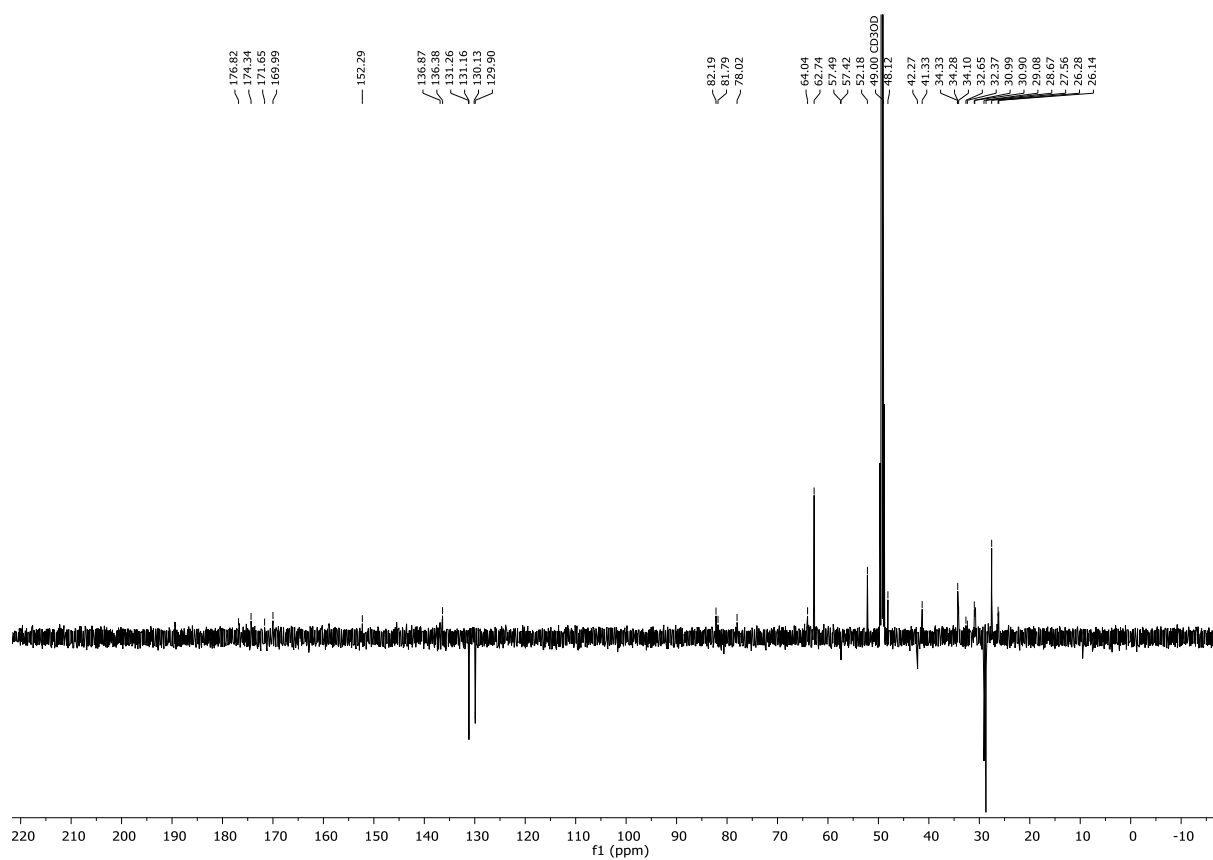
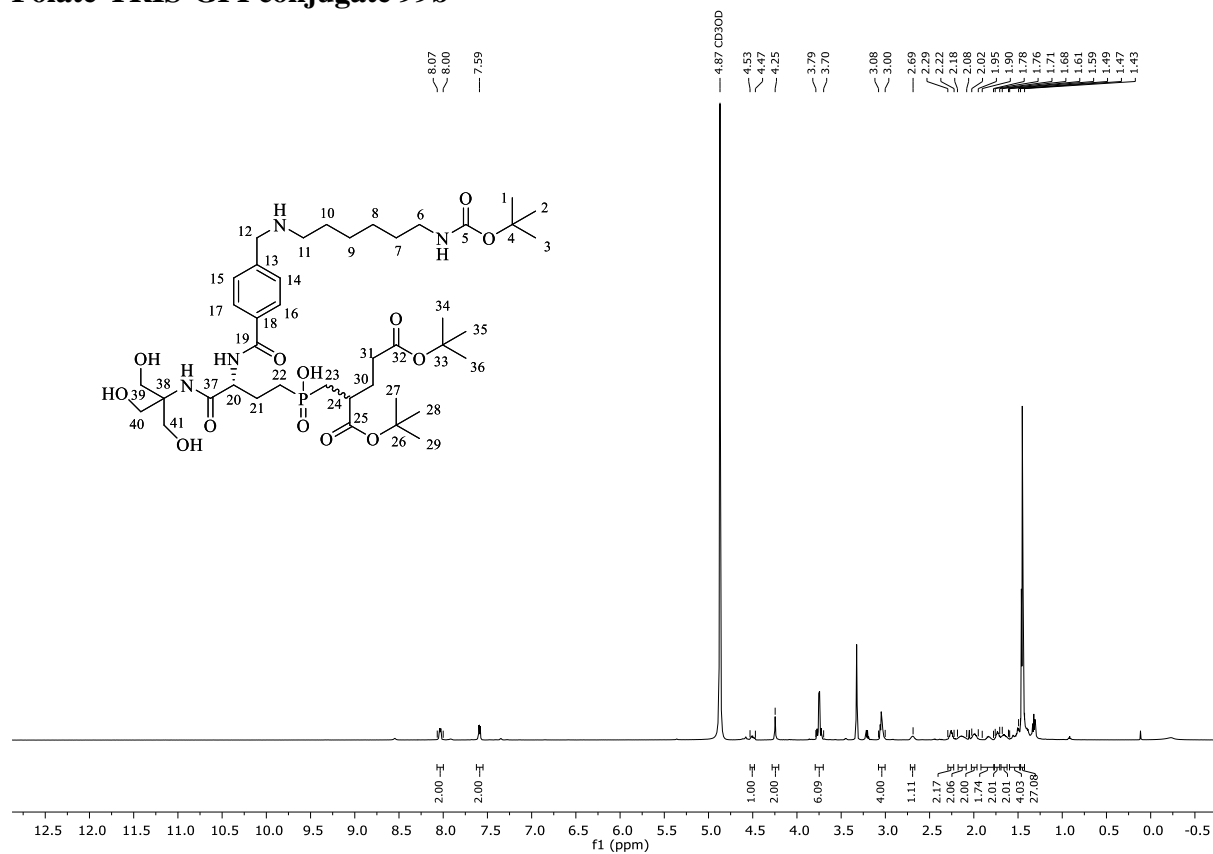


TRIS-GPI-AHX conjugate 95a

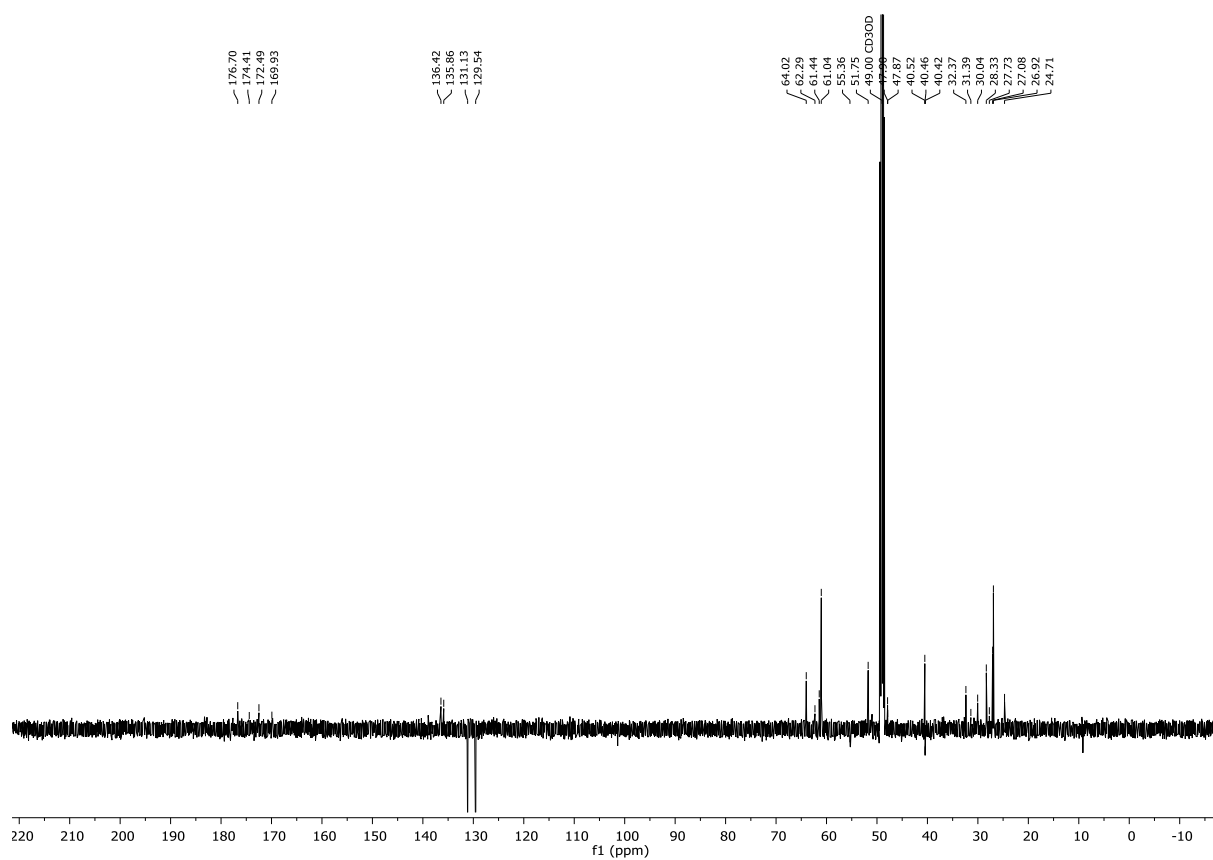
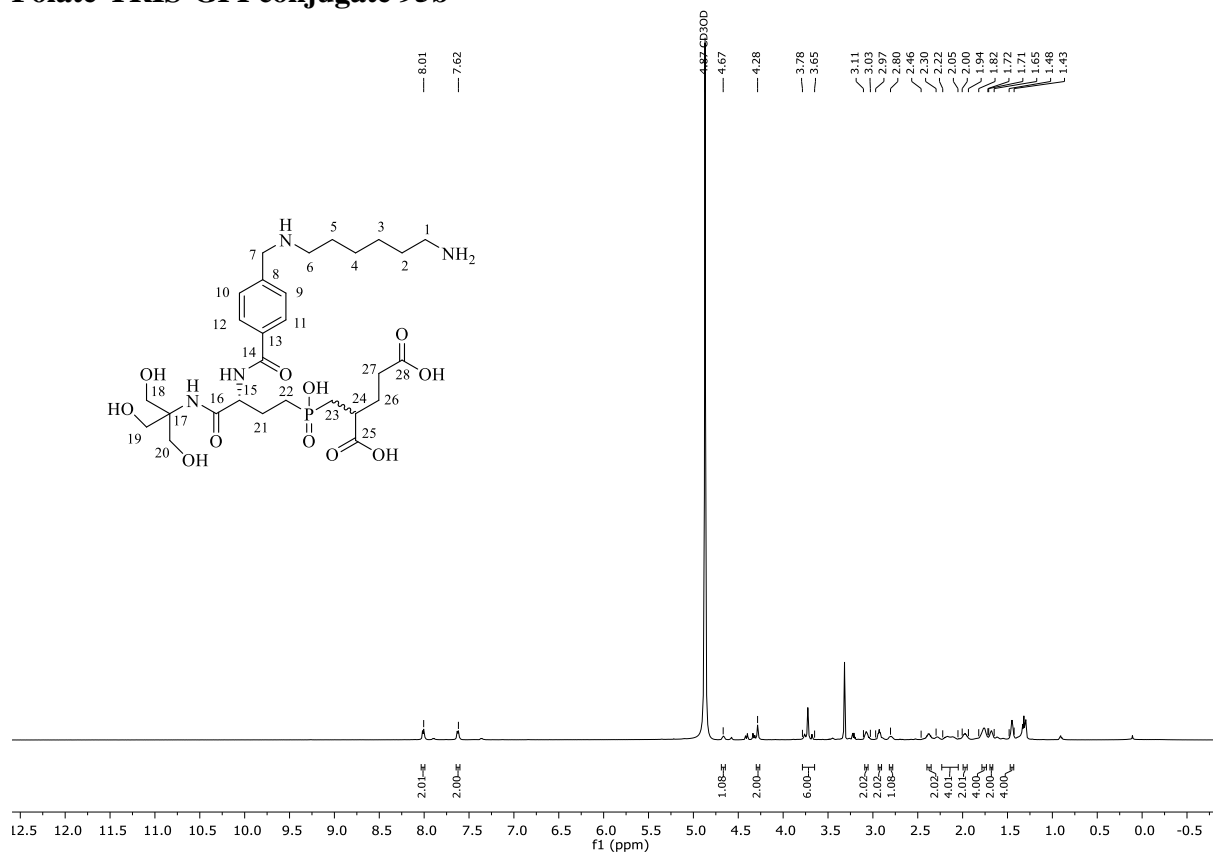


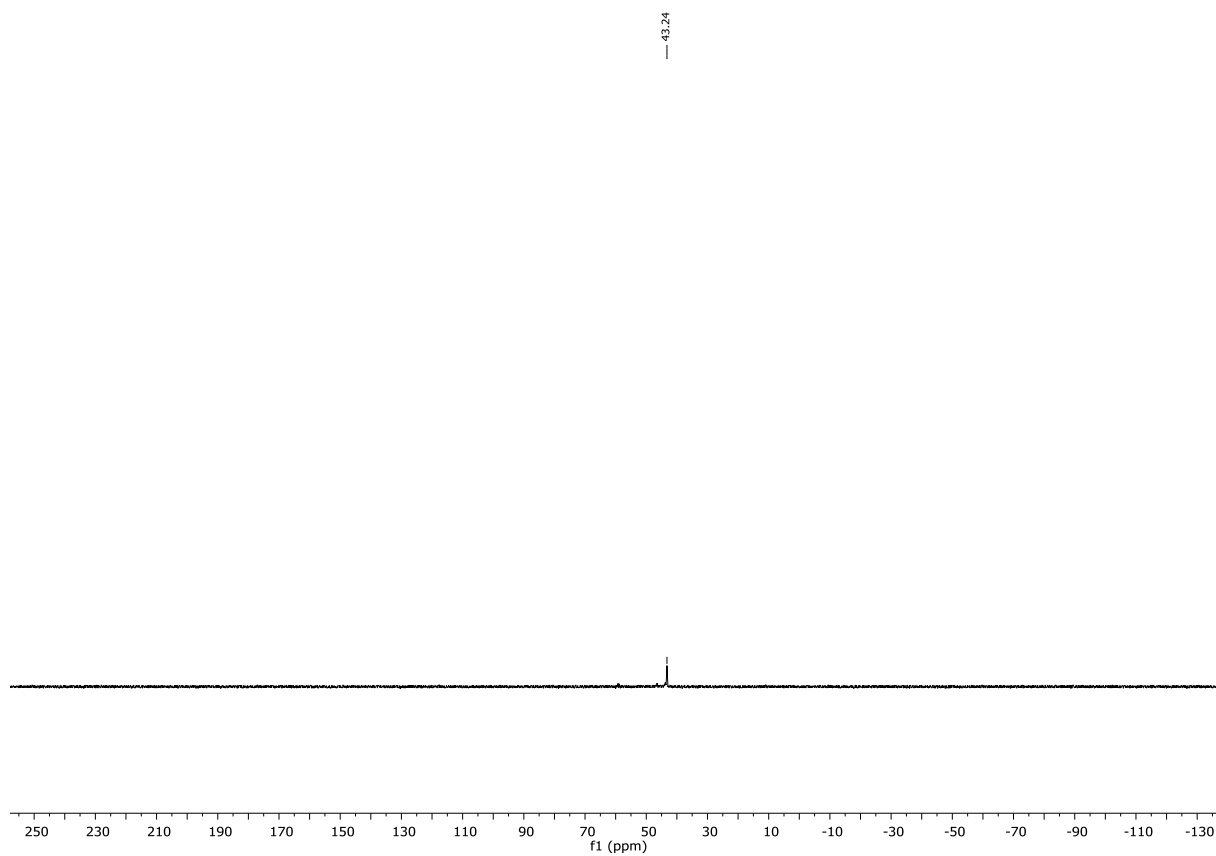


Folate-TRIS-GPI conjugate 99b



Folate-TRIS-GPI conjugate 95b





9 Literature

- (1) Bertino, J. R. *J. Clin. Pharmacol.* **1990**, *30*, 291.
- (2) Kompis, I. M.; Islam, K.; Then, R. L. *Chem. Rev.* **2005**, *105*, 593.
- (3) Crider, K. S.; Yang, T. P.; Berry, R. J.; Bailey, L. B. *Adv. Nutr.* **2012**, *3*, 21.
- (4) Stover, P. J. *Nutr. Rev.* **2004**, *62*, S3.
- (5) Gonen, N.; Assaraf, Y. G. *Drug Resist. Updat.* **2012**, *15*, 183.
- (6) Wilson, R. D.; Wilson, R. D.; Audibert, F.; Brock, J.-A.; Carroll, J.; Cartier, L.; Gagnon, A.; Johnson, J.-A.; Langlois, S.; Murphy-Kaulbeck, L.; Okun, N.; Pastuck, M.; Deb-Rinker, P.; Dodds, L.; Leon, J. A.; Lowell, H.; Luo, W.; MacFarlane, A.; McMillan, R.; Moore, A.; Mundle, W.; O'Connor, D.; Ray, J.; Van den Hof, M. *J. Obstet. Gynaecol.* **2015**, *37*, 534.
- (7) Greene, N. D. E.; Copp, A. J. *Annu. Rev. Neurosci.* **2014**, *37*, 221.
- (8) Metz, J. *Bull. W.H.O.* **1963**, *28*, 517.
- (9) Green, R.; Miller, J. W. *Semin. Hematol.* **1999**, *36*, 47.
- (10) Wang, R.; Zheng, Y.; Huang, J.-Y.; Zhang, A.-Q.; Zhou, Y.-H.; Wang, J.-N. *BMC Public Health* **2014**, *14*, 1326.
- (11) Choi, S. W.; Mason, J. B. *J. Nutr.* **2000**, *130*, 129.
- (12) Spellacy, C. J.; Northrup, H.; Fletcher, J. M.; Cirino, P. T.; Dennis, M.; Morrison, A. C.; Martinez, C. A.; Au, K. S. *PLoS One* **2012**, *7*, e51330.
- (13) Mentch, S. J.; Locasale, J. W. *Ann. N. Y. Acad. Sci.* **2016**, *1363*, 91.
- (14) Matherly, L. H.; Goldman, D. I. *Vitam. Horm.* **2003**, *66*, 403.
- (15) Zhao, R.; Diop-Bove, N.; Visentin, M.; Goldman, I. D. *Annu. Rev. Nutr.* **2011**, *31*, 177.
- (16) Cheung, A.; Bax, H. J.; Josephs, D. H.; Ilieva, K. M.; Pellizzari, G.; Opzoomer, J.; Bloomfield, J.; Fittall, M.; Grigoriadis, A.; Fignini, M.; Canevari, S.; Spicer, J. F.; Tutt, A. N.; Karagiannis, S. N. *Oncotarget* **2016**, *7*, 52553.
- (17) Ledermann, J. A.; Canevari, S.; Thigpen, T. *Ann. Oncol.* **2015**, *26*, 2034.
- (18) Miotti, S.; Bagnoli, M.; Tomassetti, A.; Colnaghi, M. I.; Canevari, S. *J. Cell Sci.* **2000**, *113 Pt 2*, 349.
- (19) Bianchi, E.; Doe, B.; Goulding, D.; Wright, G. J. *Nature* **2014**, *508*, 483.
- (20) O'Shannessy, D. J.; Yu, G.; Smale, R.; Fu, Y. S.; Singhal, S.; Thiel, R. P.; Somers, E. B.; Vachani, A. *Oncotarget* **2012**, *3*, 414.
- (21) Shia, J.; Klimstra, D. S.; Nitzkorski, J. R.; Low, P. S.; Gonen, M.; Landmann, R.; Weiser, M. R.; Franklin, W. A.; Prendergast, F. G.; Murphy, L.; Tang, L. H.; Temple, L.; Guillem, J. G.; Wong, W. D.; Paty, P. B. *Hum. Pathol.* **2008**, *39*, 498.
- (22) Crippa, F.; Buraggi, G. L.; Di Re, E.; Gasparini, M.; Seregni, E.; Canevari, S.; Gadin, M.; Presti, M.; Marini, A.; Seccamani, E. *Eur. J. Cancer Clin. Oncol.* **1991**, *27*, 724.
- (23) Shi, H.; Guo, J.; Li, C.; Wang, Z. *Drug Des. Devel. Ther.* **2015**, *9*, 4989.
- (24) Boogerd, L. S.; Boonstra, M. C.; Beck, A. J.; Charehbili, A.; Hoogstins, C. E.; Prevoo, H. A.; Singhal, S.; Low, P. S.; van de Velde, C. J.; Vahrmeijer, A. L. *Oncotarget* **2016**, *7*, 17442.
- (25) Zwicke, G. L.; Mansoori, G. A.; Jeffery, C. J. *Nano Rev.* **2012**, *3*.
- (26) Ke, C. Y.; Mathias, C. J.; Green, M. A. *Adv. Drug Del. Rev.* **2004**, *56*, 1143.
- (27) Lutz, R. J. *Targeting the folate receptor for the treatment of ovarian cancer*, 2015; Vol. 4.
- (28) van Zanten-Przybysz, I.; Molthoff, C. F.; Roos, J. C.; Verheijen, R. H.; van Hof, A.; Buist, M. R.; Prinssen, H. M.; den Hollander, W.; Kenemans, P. *Int. J. Cancer* **2001**, *92*, 106.

- (29) Majoros, I. J.; Myc, A.; Thomas, T.; Mehta, C. B.; Baker, J. R. *Biomacromolecules* **2006**, *7*, 572.
- (30) Liu, J.; Kolar, C.; Lawson, T. A.; Gmeiner, W. H. *J. Org. Chem.* **2001**, *66*, 5655.
- (31) Liang, X.; Sun, Y.; Zeng, W.; Liu, L.; Ma, X.; Zhao, Y.; Fan, J. *Biorg. Med. Chem.* **2013**, *21*, 178.
- (32) Leamon, C. P.; Reddy, J. A.; Vlahov, I. R.; Kleindl, P. J.; Vetzal, M.; Westrick, E. *Bioconj. Chem.* **2006**, *17*, 1226.
- (33) Bertino, J. R. *Best Pract. Res. Clin. Haematol.* **2009**, *22*, 577.
- (34) Farber, S.; Diamond, L. K.; Mercer, R. D.; Sylvester, R. F.; Wolff, J. A. *N. Engl. J. Med.* **1948**, *238*, 787.
- (35) Goldin, A.; Venditti, J. M.; Humphreys, S. R.; Dennis, D.; Mantel, N.; Greenhouse, S. W. *J. Natl. Cancer. Inst.* **1955**, *15*, 1657.
- (36) Matloub, Y.; Bostrom, B. C.; Hunger, S. P.; Stork, L. C.; Angiolillo, A.; Sather, H.; La, M.; Gastier-Foster, J. M.; Heerema, N. A.; Sailer, S.; Buckley, P. J.; Thomson, B.; Cole, C.; Nachman, J. B.; Reaman, G.; Winick, N.; Carroll, W. L.; Devidas, M.; Gaynon, P. S. *Blood* **2011**, *118*, 243.
- (37) Colleoni, M.; Cole, B. F.; Viale, G.; Regan, M. M.; Price, K. N.; Maiorano, E.; Mastropasqua, M. G.; Crivellari, D.; Gelber, R. D.; Goldhirsch, A.; Coates, A. S.; Gusterson, B. A. *J. Clin. Oncol.* **2010**, *28*, 2966.
- (38) Jaffe, N. *Cancer Treat. Res.* **2009**, *152*, 239.
- (39) Salliot, C.; van der Heijde, D. *Ann. Rheum. Dis.* **2009**, *68*, 1100.
- (40) Habeck, L. L.; Mendelsohn, L. G.; Shih, C.; Taylor, E. C.; Colman, P. D.; Gossett, L. S.; Leitner, T. A.; Schultz, R. M.; Andis, S. L.; Moran, R. G. *Mol. Pharmacol.* **1995**, *48*, 326.
- (41) Jackman, A. L.; Taylor, G. A.; Gibson, W.; Kimbell, R.; Brown, M.; Calvert, A. H.; Judson, I. R.; Hughes, L. R. *Cancer Res.* **1991**, *51*, 5579.
- (42) Jackman, A. L.; Harrap, K. R.; Boyle, F. T. *Invest. New Drugs* **1996**, *14*, 305.
- (43) Visentin, M.; Zhao, R.; Goldman, I. D. *Hematol. Oncol. Clin. North Am.* **2012**, *26*, 629.
- (44) Calvert, H. *Semin. Oncol.* **2003**, *30*, 2.
- (45) Adjei, A. A. *Expert Rev. Anticancer Ther.* **2003**, *3*, 145.
- (46) Adjei, A. A. *Expert Rev. Anticancer Ther.* **2003**, *3*, 145.
- (47) Norman, P. *Curr Opin Investig Drugs* **2001**, *2*, 1611.
- (48) Hanauske, A. R.; Chen, V.; Paoletti, P.; Niyikiza, C. *Oncologist* **2001**, *6*, 363.
- (49) Li, K. M.; Rivory, L. P.; Clarke, S. J. *Br. J. Cancer* **2007**, *97*, 1071.
- (50) DeGraw, J. I.; Colwell, W. T.; Piper, J. R.; Sirotnak, F. M. *J. Med. Chem.* **1993**, *36*, 2228.
- (51) Izbicka, E.; Diaz, A.; Streeper, R.; Wick, M.; Campos, D.; Steffen, R.; Saunders, M. *Cancer Chemother. Pharmacol.* **2009**, *64*, 993.
- (52) Krug, L. M.; Heelan, R. T.; Kris, M. G.; Venkatraman, E.; Sirotnak, F. M. *J. Thorac. Oncol.* **2007**, *2*, 317.
- (53) O'Connor, O. A.; Hamlin, P. A.; Portlock, C.; Moskowitz, C. H.; Noy, A.; Straus, D. J.; Macgregor-Cortelli, B.; Neylon, E.; Sarasohn, D.; Dumetrescu, O.; Mould, D. R.; Fleischer, M.; Zelenetz, A. D.; Sirotnak, F.; Horwitz, S. *Br. J. Haematol.* **2007**, *139*, 425.
- (54) O'Connor, O. A.; Horwitz, S.; Hamlin, P.; Portlock, C.; Moskowitz, C. H.; Sarasohn, D.; Neylon, E.; Mastrella, J.; Hamelers, R.; Macgregor-Cortelli, B.; Patterson, M.; Seshan, V. E.; Sirotnak, F.; Fleisher, M.; Mould, D. R.; Saunders, M.; Zelenetz, A. D. *J. Clin. Oncol.* **2009**, *27*, 4357.
- (55) Wang, E. S.; O'Connor, O.; She, Y.; Zelenetz, A. D.; Sirotnak, F. M.; Moore, M. A. *Leuk. Lymphoma* **2003**, *44*, 1027.
- (56) Gourni, E.; Henriksen, G. *Molecules* **2017**, *22*.

- (57) Ceci, F.; Castellucci, P.; Fanti, S. *Q. J. Nucl. Med. Mol. Imaging* **2018**.
- (58) Dorkin, T. J.; Neal, D. E. *Semin. Cancer Biol.* **1997**, *8*, 21.
- (59) Pomper, M. G.; Musachio, J. L.; Zhang, J.; Scheffel, U.; Zhou, Y.; Hilton, J.; Maini, A.; Dannals, R. F.; Wong, D. F.; Kozikowski, A. P. *Mol. Imaging* **2002**, *1*, 96.
- (60) Banerjee, S. R.; Pullambhatla, M.; Byun, Y.; Nimmagadda, S.; Green, G.; Fox, J. J.; Horti, A.; Mease, R. C.; Pomper, M. G. *J. Med. Chem.* **2010**, *53*, 5333.
- (61) McLeod, D. G. *Rev. Urol.* **2004**, *6*, S13.
- (62) Carter, R. E.; Feldman, A. R.; Coyle, J. T. *Proc. Natl. Acad. Sci.* **1996**, *93*, 749.
- (63) Mesters, J. R.; Barinka, C.; Li, W.; Tsukamoto, T.; Majer, P.; Slusher, B. S.; Konvalinka, J.; Hilgenfeld, R. *EMBO J.* **2006**, *25*, 1375.
- (64) Chang, S. S. *Rev. Urol.* **2004**, *6*, S13.
- (65) Luthi-Carter, R.; Barczak, A. K.; Speno, H.; Coyle, J. T. *J. Pharmacol. Exp. Ther.* **1998**, *286*, 1020.
- (66) Silver, D. A.; Pellicer, I.; Fair, W. R.; Heston, W. D.; Cordon-Cardo, C. *Clin. Cancer Res.* **1997**, *3*, 81.
- (67) Sokoloff, R. L.; Norton, K. C.; Gasior, C. L.; Marker, K. M.; Grauer, L. S. *Prostate* **2000**, *43*, 150.
- (68) O'Keefe, D. S.; Bacich, D. J.; Heston, W. D. W. *Prostate* **2004**, *58*, 200.
- (69) Troyer, J. K.; Beckett, M. L.; Wright, G. L., Jr. *Int. J. Cancer* **1995**, *62*, 552.
- (70) Leek, J.; Lench, N.; Maraj, B.; Bailey, A.; Carr, I. M.; Andersen, S.; Cross, J.; Whelan, P.; MacLennan, K. A.; Meredith, D. M. *Br. J. Cancer* **1995**, *72*, 583.
- (71) Davis, M. I.; Bennett, M. J.; Thomas, L. M.; Bjorkman, P. J. *Proc. Natl. Acad. Sci.* **2005**, *102*, 5981.
- (72) Bařinka, C.; Rojas, C.; Slusher, B.; Pomper, M. *Curr. Med. Chem.* **2012**, *19*, 856.
- (73) Jackson, P. F.; Cole, D. C.; Slusher, B. S.; Stetz, S. L.; Ross, L. E.; Donzanti, B. A.; Trainor, D. A. *J. Med. Chem.* **1996**, *39*, 619.
- (74) Navrátil, M.; Ptáček, J.; Šácha, P.; Starková, J.; Lubkowski, J.; Bařinka, C.; Konvalinka, J. *FEBS J.* **2014**, *281*, 3228.
- (75) Pinto, J. T.; Suffoletto, B. P.; Berzin, T. M.; Qiao, C. H.; Lin, S.; Tong, W. P.; May, F.; Mukherjee, B.; Heston, W. D. *Clin. Cancer Res.* **1996**, *2*, 1445.
- (76) O'Keefe, D. S.; Bacich, D. J.; Huang, S. S.; Heston, W. D. W. *J. Nucl. Med.* **2018**, *59*, 1007.
- (77) Wondergem, M.; van der Zant, F. M.; Vlottes, P. W.; Knol, R. J. J. *J. Nucl. Med.* **2018**, *59*, 1081.
- (78) Meyerhoff, J. L.; Carter, R. E.; Yourick, D. L.; Slusher, B. S.; Coyle, J. T. *Brain Res.* **1992**, *593*, 140.
- (79) Tsai, G.; Passani, L. A.; Slusher, B. S.; Carter, R.; Baer, L.; Kleinman, J. E.; Coyle, J. T. *Arch. Gen. Psychiatry* **1995**, *52*, 829.
- (80) Kwo-On-Yuen, P. F.; Newmark, R. D.; Budinger, T. F.; Kaye, J. A.; Ball, M. J.; Jagust, W. J. *Brain Res.* **1994**, *667*, 167.
- (81) Jackson, P. F.; Slusher, B. S. *Curr. Med. Chem.* **2001**, *8*, 949.
- (82) Ross, J. S.; Sheehan, C. E.; Fisher, H. A.; Kaufman, R. P., Jr.; Kaur, P.; Gray, K.; Webb, I.; Gray, G. S.; Mosher, R.; Kallakury, B. V. *Clin. Cancer Res.* **2003**, *9*, 6357.
- (83) Mesters, J. R.; Henning, K.; Hilgenfeld, R. *Acta Crystallogr. D Biol. Crystallogr.* **2007**, *63*, 508.
- (84) Lipinski, C. A.; Lombardo, F.; Dominy, B. W.; Feeney, P. J. *Adv. Drug Del. Rev.* **2001**, *46*, 3.
- (85) Paul, F. J.; Barbara, S. S. *Curr. Med. Chem.* **2001**, *8*, 949.
- (86) Chen, Y.; Foss, C. A.; Byun, Y.; Nimmagadda, S.; Pullambhatla, M.; Fox, J. J.; Castanares, M.; Lupold, S. E.; Babich, J. W.; Mease, R. C.; Pomper, M. G. *J. Med. Chem.* **2008**, *51*, 7933.

- (87) Michalska, M.; Schultze-Seemann, S.; Bogatyreva, L.; Hauschke, D.; Wetterauer, U.; Wolf, P. *Oncotarget* **2016**, *7*, 22531.
- (88) Lapidus, R. G.; Tiffany, C. W.; Isaacs, J. T.; Slusher, B. S. *Prostate* **2000**, *45*, 350.
- (89) Elsasser-Beile, U.; Reischl, G.; Wiehr, S.; Buhler, P.; Wolf, P.; Alt, K.; Shively, J.; Judenhofer, M. S.; Machulla, H. J.; Pichler, B. J. *J. Nucl. Med.* **2009**, *50*, 606.
- (90) Chen, Y.; Pullambhatla, M.; Banerjee, S. R.; Byun, Y.; Stathis, M.; Rojas, C.; Slusher, B. S.; Mease, R. C.; Pomper, M. G. *Bioconj. Chem.* **2012**, *23*, 2377.
- (91) Lutje, S.; Heskamp, S.; Cornelissen, A. S.; Poeppel, T. D.; van den Broek, S. A.; Rosenbaum-Krumme, S.; Bockisch, A.; Gotthardt, M.; Rijpkema, M.; Boerman, O. C. *Theranostics* **2015**, *5*, 1388.
- (92) Huang, S. S.; Wang, X.; Zhang, Y.; Doke, A.; DiFilippo, F. P.; Heston, W. D. *Prostate* **2014**, *74*, 702.
- (93) Alt, J.; Stathis, M.; Rojas, C.; Slusher, B. *FASEB J.* **2013**, *27*, 2620.
- (94) Valiaeva, N.; Bartley, D.; Konno, T.; Coward, J. K. *J. Org. Chem.* **2001**, *66*, 5146.
- (95) Misra, P.; Humblet, V.; Pannier, N.; Maison, W.; Frangioni, J. V. *J. Nucl. Med.* **2007**, *48*, 1379.
- (96) Benesova, M.; Schafer, M.; Bauder-Wust, U.; Afshar-Oromieh, A.; Kratochwil, C.; Mier, W.; Haberkorn, U.; Kopka, K.; Eder, M. *J. Nucl. Med.* **2015**, *56*, 914.
- (97) Eder, M.; Schafer, M.; Bauder-Wust, U.; Hull, W. E.; Wangler, C.; Mier, W.; Haberkorn, U.; Eisenhut, M. *Bioconj. Chem.* **2012**, *23*, 688.
- (98) Afshar-Oromieh, A.; Hetzheim, H.; Kratochwil, C.; Benesova, M.; Eder, M.; Neels, O. C.; Eisenhut, M.; Kubler, W.; Holland-Letz, T.; Giesel, F. L.; Mier, W.; Kopka, K.; Haberkorn, U. *J. Nucl. Med.* **2015**, *56*, 1697.
- (99) Taneja, S. S. *Rev. Urol.* **2004**, *6*, S19.
- (100) Kahn, D.; Williams, R. D.; Manyak, M. J.; Haseman, M. K.; Seldin, D. W.; Libertino, J. A.; Maguire, R. T. *J. Urol.* **1998**, *159*, 2041.
- (101) Sodee, D. B.; Malguria, N.; Faulhaber, P.; Resnick, M. I.; Albert, J.; Bakale, G. *Urology* **2000**, *56*, 988.
- (102) Liu, H.; Moy, P.; Kim, S.; Xia, Y.; Rajasekaran, A.; Navarro, V.; Knudsen, B.; Bander, N. H. *Cancer Res.* **1997**, *57*, 3629.
- (103) Vallabhajosula, S.; Kuji, I.; Hamacher, K. A.; Konishi, S.; Kostakoglu, L.; Kothari, P. A.; Milowski, M. I.; Nanus, D. M.; Bander, N. H.; Goldsmith, S. J. *J. Nucl. Med.* **2005**, *46*, 634.
- (104) Bander, N. H.; Trabulsi, E. J.; Kostakoglu, L.; Yao, D.; Vallabhajosula, S.; Smith-Jones, P.; Joyce, M. A.; Milowsky, M.; Nanus, D. M.; Goldsmith, S. J. *J. Urol.* **2003**, *170*, 1717.
- (105) Bander, N. H.; Milowsky, M. I.; Nanus, D. M.; Kostakoglu, L.; Vallabhajosula, S.; Goldsmith, S. J. *J. Clin. Oncol.* **2005**, *23*, 4591.
- (106) Holland, J. P.; Divilov, V.; Bander, N. H.; Smith-Jones, P. M.; Larson, S. M.; Lewis, J. S. *J. Nucl. Med.* **2010**, *51*, 1293.
- (107) Evans, M. J.; Smith-Jones, P. M.; Wongvipat, J.; Navarro, V.; Kim, S.; Bander, N. H.; Larson, S. M.; Sawyers, C. L. *Proc. Natl. Acad. Sci.* **2011**, *108*, 9578.
- (108) Vallabhajosula, S.; Goldsmith, S. J.; Kostakoglu, L.; Milowsky, M. I.; Nanus, D. M.; Bander, N. H. *Clin. Cancer Res.* **2005**, *11*, 7195s.
- (109) Kampmeier, F.; Williams, J. D.; Maher, J.; Mullen, G. E.; Blower, P. J. *EJNMMI Res.* **2014**, *4*, 13.
- (110) Milowsky, M. I.; Nanus, D. M.; Kostakoglu, L.; Vallabhajosula, S.; Goldsmith, S. J.; Bander, N. H. *J. Clin. Oncol.* **2004**, *22*, 2522.

- (111) Tagawa, S. T.; Beltran, H.; Vallabhajosula, S.; Goldsmith, S. J.; Osborne, J.; Matulich, D.; Petrillo, K.; Parmar, S.; Nanus, D. M.; Bander, N. H. *Cancer* **2010**, *116*, 1075.
- (112) Pandit-Taskar, N.; O'Donoghue, J. A.; Ruan, S.; Lyashchenko, S. K.; Carrasquillo, J. A.; Heller, G.; Martinez, D. F.; Cheal, S. M.; Lewis, J. S.; Fleisher, M.; Keppler, J. S.; Reiter, R. E.; Wu, A. M.; Weber, W. A.; Scher, H. I.; Larson, S. M.; Morris, M. J. *J. Nucl. Med.* **2016**, *57*, 1858.
- (113) Jain, R. K. *Adv. Drug Del. Rev.* **2012**, *64*, 353.
- (114) Kuchenthal, C. H.; Maison, W. *Chembiochem* **2010**, *11*, 1052.
- (115) Muller, C. *Molecules* **2013**, *18*, 5005.
- (116) Muller, C. *Curr. Pharm. Des.* **2012**, *18*, 1058.
- (117) Bettio, A.; Honer, M.; Muller, C.; Bruhlmeier, M.; Muller, U.; Schibli, R.; Groehn, V.; Schubiger, A. P.; Ametamey, S. M. *J. Nucl. Med.* **2006**, *47*, 1153.
- (118) Al Jammaz, I.; Al-Otaibi, B.; Okarvi, S.; Amartey, J. *J. Labelled Compd. Radiopharm.* **2006**, *49*, 125.
- (119) Ross, T. L.; Honer, M.; Lam, P. Y.; Mindt, T. L.; Groehn, V.; Schibli, R.; Schubiger, P. A.; Ametamey, S. M. *Bioconjug. Chem.* **2008**, *19*, 2462.
- (120) Al Jammaz, I.; Al-Otaibi, B.; Amer, S.; Al-Hokbany, N.; Okarvi, S. *Nucl. Med. Biol.* **2012**, *39*, 864.
- (121) Fischer, C. R.; Müller, C.; Reber, J.; Müller, A.; Krämer, S. D.; Ametamey, S. M.; Schibli, R. *Bioconj. Chem.* **2012**, *23*, 805.
- (122) Fani, M.; Wang, X.; Nicolas, G.; Medina, C.; Raynal, I.; Port, M.; Maecke, H. R. *Eur. J. Nucl. Med. Mol. Imaging* **2011**, *38*, 108.
- (123) Muller, C.; Struthers, H.; Winiger, C.; Zhernosekov, K.; Schibli, R. *J. Nucl. Med.* **2013**, *54*, 124.
- (124) Muller, C.; Zhernosekov, K.; Koster, U.; Johnston, K.; Dorrer, H.; Hohn, A.; van der Walt, N. T.; Turler, A.; Schibli, R. *J. Nucl. Med.* **2012**, *53*, 1951.
- (125) Siwowska, K.; Haller, S.; Bortoli, F.; Benesova, M.; Groehn, V.; Bernhardt, P.; Schibli, R.; Muller, C. *Mol. Pharm.* **2017**, *14*, 523.
- (126) Denmeade, S. R.; Mhaka, A. M.; Rosen, D. M.; Brennen, W. N.; Dalrymple, S.; Dach, I.; Olesen, C.; Gurel, B.; Demarzo, A. M.; Wilding, G.; Carducci, M. A.; Dionne, C. A.; Moller, J. V.; Nissen, P.; Christensen, S. B.; Isaacs, J. T. *Sci. Transl. Med.* **2012**, *4*, 140ra86.
- (127) Mhaka, A.; Gady, A. M.; Rosen, D. M.; Lo, K.-M.; Gillies, S. D.; Denmeade, S. R. *Cancer Biol. Ther.* **2014**, *3*, 551.
- (128) Bartley, D. M.; Coward, J. K. *J. Org. Chem.* **2005**, *70*, 6757.
- (129) Barinka, C.; Hlouchova, K.; Rovenska, M.; Majer, P.; Dauter, M.; Hin, N.; Ko, Y.-S.; Tsukamoto, T.; Slusher, B. S.; Konvalinka, J.; Lubkowski, J. *J. Mol. Biol.* **2008**, *376*, 1438.
- (130) Misra, P.; Humblet, V.; Pannier, N.; Maison, W.; Frangioni, J. V. *J. Nucl. Med.* **2007**, *48*, 1379.
- (131) Fisher, R. E.; Siegel, B. A.; Edell, S. L.; Oyesiku, N. M.; Morgenstern, D. E.; Messmann, R. A.; Amato, R. J. *J. Nucl. Med.* **2008**, *49*, 899.
- (132) Feng, Y.; Coward, J. K. *J. Med. Chem.* **2006**, *49*, 770.
- (133) Chen, Y.; Pullambhatla, M.; Banerjee, S. R.; Byun, Y.; Stathis, M.; Rojas, C.; Slusher, B. S.; Mease, R. C.; Pomper, M. G. *Bioconjug. Chem.* **2012**, *23*, 2377.
- (134) Benesova, M.; Bauder-Wust, U.; Schafer, M.; Klika, K. D.; Mier, W.; Haberkorn, U.; Kopka, K.; Eder, M. *J. Med. Chem.* **2016**, *59*, 1761.
- (135) Barinka, C.; Hlouchova, K.; Rovenska, M.; Majer, P.; Dauter, M.; Hin, N.; Ko, Y. S.; Tsukamoto, T.; Slusher, B. S.; Konvalinka, J.; Lubkowski, J. *J. Mol. Biol.* **2008**, *376*, 1438.
- (136) Nasr, G.; Cristian, A.; Barboiu, M.; Vullo, D.; Winum, J.-Y.; Supuran, C. T. *Biorg. Med. Chem.* **2014**, *22*, 2867.







- (137) Norcross, B. E. *J. Chem. Educ.* **1993**, *70*, A51.
- (138) Gribble, G. W.; Lord, P. D.; Skotnicki, J.; Dietz, S. E.; Eaton, J. T.; Johnson, J. *J. Am. Chem. Soc.* **1974**, *96*, 7812.
- (139) Klinkenberg, J. L.; Hartwig, J. F. *Angew. Chem. Int. Ed. Engl.* **2011**, *50*, 86.
- (140) Surry, D. S.; Buchwald, S. L. *Chem. Sci.* **2011**, *2*, 27.
- (141) Gowrisankar, S.; Neumann, H.; Beller, M. *Chemistry* **2012**, *18*, 2498.
- (142) Tajbakhsh, M.; Hosseinzadeh, R.; Alinezhad, H.; Ghahari, S.; Heydari, A.; Khaksar, S. *Synthesis* **2011**, *2011*, 490.
- (143) Hartwig, J. F. *Angew. Chem. Int. Ed. Engl.* **1998**, *37*, 2046.
- (144) Wolfe, J. P.; Buchwald, S. L. *Tetrahedron Lett.* **1997**, *38*, 6359.
- (145) Muci, A. R.; Buchwald, S. L. In *Cross-Coupling Reactions: A Practical Guide* 2002, p 131.
- (146) Hartwig, J. F. *Acc. Chem. Res.* **2008**, *41*, 1534.
- (147) Surry, D. S.; Buchwald, S. L. *Angew. Chem. Int. Ed. Engl.* **2008**, *47*, 6338.
- (148) Bruno, N. C.; Buchwald, S. L. *Org. Lett.* **2013**, *15*, 2876.
- (149) Bruno, N. C.; Tudge, M. T.; Buchwald, S. L. *Chem. Sci.* **2013**, *4*, 916.
- (150) Biscoe, M. R.; Fors, B. P.; Buchwald, S. L. *J. Am. Chem. Soc.* **2008**, *130*, 6686.
- (151) Johansson Seechurn, C. C. C.; Parisel, S. L.; Colacot, T. J. *J. Org. Chem.* **2011**, *76*, 7918.
- (152) Hadei, N.; Kantchev, E. A. B.; O'Brien, C. J.; Organ, M. G. *Org. Lett.* **2005**, *7*, 1991.
- (153) Zim, D.; Buchwald, S. L. *Org. Lett.* **2003**, *5*, 2413.
- (154) Li, H.; Johansson Seechurn, C. C. C.; Colacot, T. J. *ACS Catal.* **2012**, *2*, 1147.
- (155) Colacot, T. J.; Shea, H. A. *Org. Lett.* **2004**, *6*, 3731.
- (156) Louie, J.; Hartwig, J. F. *Tetrahedron Lett.* **1995**, *36*, 3609.
- (157) Arrechea, P. L.; Buchwald, S. L. *J. Am. Chem. Soc.* **2016**, *138*, 12486.
- (158) Satoh, T.; Inoh, J.; Kawamura, Y.; Kawamura, Y.; Miura, M.; Nomura, M. *Bull. Chem. Soc. Jpn.* **1998**, *71*, 2239.
- (159) Inoh, J.; Satoh, T.; Pivsa-Art, S.; Miura, M.; Nomura, M. *Tetrahedron Lett.* **1998**, *39*, 4673.
- (160) Burton, P. M.; Morris, J. A. *Org. Lett.* **2010**, *12*, 5359.
- (161) Niwa, T.; Yorimitsu, H.; Oshima, K. *Angew. Chem. Int. Ed. Engl.* **2007**, *46*, 2643.
- (162) Kim, B. S.; Jimenez, J.; Gao, F.; Walsh, P. J. *Org. Lett.* **2015**, *17*, 5788.
- (163) Biscoe, M. R.; Barder, T. E.; Buchwald, S. L. *Angew. Chem. Int. Ed. Engl.* **2007**, *46*, 7232.
- (164) Huang, X. H.; Anderson, K. W.; Zim, D.; Jiang, L.; Klapars, A.; Buchwald, S. L. *J. Am. Chem. Soc.* **2003**, *125*, 6653.
- (165) Tom, N. J.; Simon, W. M.; Frost, H. N.; Ewing, M. *Tetrahedron Lett.* **2004**, *45*, 905.
- (166) Bertrand, M. B.; Wolfe, J. P. *Tetrahedron* **2005**, *61*, 6447.
- (167) Küchenthal, C. H., Justus-Liebig-Universität Gießen, **2012**.
- (168) Rüping, F., University of Hamburg, **2017**.
- (169) Anderson, G. W.; Zimmerman, J. E.; Callahan, F. M. *J. Am. Chem. Soc.* **1963**, *85*, 3039.
- (170) Pavlicek, J.; Ptacek, J.; Cerny, J.; Byun, Y.; Skultetyova, L.; Pomper, M. G.; Lubkowski, J.; Barinka, C. *Bioorg. Med. Chem. Lett.* **2014**, *24*, 2340.
- (171) Zhang, A. X.; Murelli, R. P.; Barinka, C.; Michel, J.; Cocleaza, A.; Jorgensen, W. L.; Lubkowski, J.; Spiegel, D. A. *J. Am. Chem. Soc.* **2010**, *132*, 12711.
- (172) Maung, J.; Mallari, J. P.; Girtsman, T. A.; Wu, L. Y.; Rowley, J. A.; Santiago, N. M.; Brunelle, A. N.; Berkman, C. E. *Bioorg. Med. Chem.* **2004**, *12*, 4969.









- (173) Abla, M.; Durand, G.; Pucci, B. *J. Org. Chem.* **2011**, *76*, 2084.
(174) Felpin, F.-X.; Fouquet, E. *Chem. Eur. J.* **2010**, *16*, 12440.

10 Hazard materials














All used chemicals are listed with their corresponding hazard (H-) and precautionary (P-) statements and GHS-pictograms.











Table 8: Used substances with hazard classification and disposal instructions.



















Substance	GHS-Symbols	H-Statements	P-Statements
acetone	 danger	H225-H319- H336	P210-P261- P305+ P351+P338
acetonitrile	 danger	H225-H302+ H312+H332- H319	P210-P280- P305+P351+P3 38
caesium carbonate	 warning	H315-H319- H335	P261-P305 + P351 + P338
celite	 warning	H319-H335	P305 + P351 + P338
cyclohexancarbal dehyde	 danger	H226-H315- H319-H335	P261- P305+P351+P3 38
CyJohnPhos	substance not classified as harmful according to GHS		
DavePhos	substance not classified as harmful according to GHS		
dichloromethane	 danger	H315-H319- H335-H336- H351-H373	P261-P281- P305+ P351+P338
DMSO	substance not classified as harmful according to GHS		
dppf	substance not classified as harmful according to GHS		






DME		H225-H332-H360	P201-P210-P240-308+313
	danger		
DMF		H226-H312-H332-H319-H360	P201-P210-P302+P352-P304+P340-P305+P351+P338-P308+P313
	danger		
EEDQ		H302-H315	P261-P280a-P305+P351+P338-P304+P340-P405-P501a
	warning		
EDC·HCl		H314	P 280-305+351+338-310
	danger		
ethanol		H225-H319	P210-P240-P305+P351+P338-P403+P233
	danger		
ethyl 4-oxocyclohexanecarboxylate		H315-H319-H335	P26- P264 P271-P280 P302+P352
	warning		
formic acid		H226-H302-H314-H331	P210P-280-P303+P361+P353-P304+P340+P310-P305+P351+P338-P403+P233
	danger		
HCl		H290-H314-H335	P261-P280-P305 + P351 + P338-P310
	danger		

N-hydroxysuccinimid substance not classified as harmful according to GHS

kalium butoxide	<i>tert</i> -	  	H228-H251- H314	P210-P235 + P410-P280- P303 +P361+P353- P304 + P340 +P310-P305 +P351+P338
lithium bis(trimethylsilyl) amide		 	H228-H314	P210-P280- P305 + P351 + P338-P310
methanol		 	H225-H301 +H311+H331- H370	P210-P260- P280- P301+P310- P311
methyl formylbenzoate	4-		H315-H319- H335	P-305-P351- P280
methyl formylbenzoate	3-		H302	
methyl 4-formyl 3-chlorobenzoate			H302-H315- H317-H335	P261-P264- P270-P271
4-methyl- bromobenzoate			H315-H319- H335	P261-P305 + P351 + P338
Na ₂ SO ₄				substance not classified as harmful according to GHS
palladium(II) acetate			H318	P280-P305 + P351 + P338
Pd/C			H317	P261-P272— P280-P302 + P352-P333 +

	warning		P313-P303- P501
<i>n</i> -pentane	 	H225-H304- H336-H411	P210-P261- P273-P301 + P310-P331
	danger		
2-quinoline- carboxaldehyde		H315-H319- H335	P261-P305 + P351 + P338
	warning		
3-quinoline- carboxaldehyde		H315-H319- H335	P261-P305 + P351 + P338
	warning		
4-quinoline- carboxaldehyde		H315-H319- H335	P261-P305 + P351 + P338
	warning		
6-quinoline- carboxaldehyde		H315-H319- H335	P261-P305 + P351 + P338
	warning		
8-quinoline- carboxaldehyde		H315-H319- H335	P261-P305 + P351 + P338
	warning		
silicon dioxide		H373	
	warning		
sodium borohydrate	 	H260-H301- H311-H314	P223- P231+P232- P280- P301+P310- P370+P378- P422
	danger		
sodium chloride	substance not classified as harmful according to GHS		

sodium triacetoxyborohydride	 	H228-H261-H315-H335	P210-P231 + P232-P261-P422
sodium sulfate		substance not classified as harmful according to GHS	
SPhos		substance not classified as harmful according to GHS	
tetramethylguanidine	  	H226-H302-H314	P210-P280-P305+P351+P338-P310
tributylphosphine	   	H226-H250-H302 + H312-H314	P222-P231-P280-P305 + P351 + P338-P310-P422
tricyclohexylphosphine		H315-H319-H335	P261-P305 + P351 + P338
trichloromethane- <i>d</i> ₁	 	H302-H315-H351-H373	P281
triethylamine	  	H225-H302-H311+H331-H314-H335	P210-P261-P280-P305+P351+P338-P310
triethylborane	  	H225-H250-H301-H314	P210-P222-P231-P280-P301 + P310-P422

triphenylphosphine		H302-H317-H373	P280-P301 + P312 + P330-P333 + P313
	warning		
toluene	 	H225-H304-H315-H336-H361d-H373	P210-P261-P281-P301+P310-P331
	danger		
XantPhos		substance not classified as harmful according to GHS	
XPhos		substance not classified as harmful according to GHS	
TFA		H314-H332-H412	P273-P280-P305 + P351 + P338-P310
	danger		
TRIS		H315-H319-H335	P261-P305+P351+P338
	warning		

Declaration

This thesis with the title “Synthesis of modular folate derivatives for tumor targeting” was submitted in part fulfilment of the requirements for the degree of Doctor rer. nat. at the University of Hamburg. Unless otherwise stated the work described in this thesis is original and has not been submitted previously in whole or in part for any degree or other qualification. The submitted written version corresponds to that on the electronic storage medium. I do not agree to publish this thesis.

Eidesstattliche Erklärung

Hiermit erkläre ich an Eides statt, dass ich die vorliegende Dissertationsschrift mit dem Titel „Synthesis of modular folate derivatives for tumor targeting “ selbstständig und ohne fremde Hilfe verfasst habe. Andere als die angegebenen Quellen und Hilfsmittel habe ich nicht benutzt und die wörtlich oder inhaltlich übernommenen Stellen als solchen kenntlich gemacht. Ich erkläre außerdem, dass diese Dissertation weder in gleicher noch in anderer Form bereits in einem anderen Prüfungsverfahren vorgelegen hat. Die eingereichte schriftliche Fassung entspricht der auf dem elektronischen Speichermedium. Ich bin nicht einverstanden, dass die Dissertation veröffentlicht wird.

08.05.2019

Hamburg



(Unterschrift)